# GROUND IMPROVEMENT BY DEEP VIBRATORY METHODS

KLAUS KIRSCH AND FABIAN KIRSCH

Spon Press

# Ground Improvement by Deep Vibratory Methods

# Ground Improvement by Deep Vibratory Methods

Klaus Kirsch and Fabian Kirsch

Spon Press
an imprint of Taylor & Francis
LONDON AND NEW YORK

First published 2010
by Spon Press
2 Park Square, Milton Park, Abingdon, Oxon OX14 4RN

Simultaneously published in the USA and Canada
by Spon Press
270 Madison Avenue, New York, NY 10016, USA

*Spon Press is an imprint of the Taylor & Francis Group, an informa business*

This edition published in the Taylor & Francis e-Library, 2010.

To purchase your own copy of this or any of Taylor & Francis or Routledge's collection of thousands of eBooks please go to www.eBookstore.tandf.co.uk.



*British Library Cataloguing in Publication Data*
A catalogue record for this book is available from the British Library

*Library of Congress Cataloging-in-Publication Data*
Kirsch, Klaus.
Ground improvement by deep vibratory methods / Klaus Kirsch and Fabian Kirsch.
p. cm.
Includes bibliographical references and index.
1. Soil stabilization. 2. Vibratory compacting. 3. Foundations.
I. Kirsch, Fabian. II. Title.
TA749.K57 2010
624.1′51363 – dc22 2010003222

ISBN 0-203-87428-5 Master e-book ISBN

ISBN10: 0–415–55015–7 (hbk)
ISBN10: 0–203–87428–5 (ebk)

ISBN13: 978–0–415–55015–4 (hbk)
ISBN13: 978–0–203–87428–8 (ebk)

# Contents

# Preface and acknowledgements

The use of depth vibrators for the improvement of soils that are unsuitable as foundations for structures in their original state dates back over more than 70 years. Over the course of time the deep vibratory methods have become probably the most-used dynamic in-situ soil improvement methods today. They have not only experienced a continuous development of plant and equipment to carry it out in practice, but also design methods have been proposed and refined to predict the degree of soil improvement that can be achieved.

Today the importance of deep vibratory soil improvement is unrivalled among modern foundation measures; the demand for in-situ deep treatment of soils introducing, if any, only environmentally harmless materials into the ground continues to increase with the rising level of awareness for the environment. Continued development of plant and process controls has resulted in considerable increases in production rates.

When looking at the design concepts in use today the reader will realise that experience with the system in different soil conditions still plays an important role. With sand compaction this is because the relative simplicity and convincing economy of the system, together with the familiar testing methods for the estimation of settlements, has probably inhibited the development of theories that would allow the calculation of the improved properties of granular material based upon the fundamentals of soil dynamics. Recent developments show encouraging attempts to correlate the characteristic motion of the depth vibrator working in the ground with the achieved soil properties. The composite system of vibro stone columns and the surrounding cohesive soil has become a challenging field for engineers to apply finite element analyses to, particularly where the foundation of more complex structures and single foundations are concerned. This computational tool supports the designer in his endeavour to find the most economical solution by optimising the foundation system.

It was the son who encouraged the father to embark on this book project, after the latter had collected knowledge and experience in the field of ground improvement over a period of almost 35 years of his professional life. The book aims to give an insight into deep vibratory soil improvement methods,

both from the contractor's view (Klaus) and from the perspective of the consulting engineer (Fabian), whose dissertation on experimental and numerical investigations of the load-carrying mechanism of vibro stone column groups provided an interesting aspect in this context. We are grateful to our publisher, Taylor & Francis, for their support in realising the book which underlines their continued interest in ground improvement methods.

We hope that the book provides the practising engineer and the design engineer with a comprehensive insight into deep vibratory soil improvement methods. The historical development of these ground improvement methods is presented in Chapter 2, which is based on an earlier publication, Kirsch (1993) "Die Baugrundverbesserung mit Tiefenrüttlern", in Englert and Stocker (eds) *40 Jahre Spezialtiefbau 1953–1993: Technische und rechtliche Entwicklungen* (Werner Verlag, Düsseldorf). We wish to thank Werner Verlag for their kind permission to use it within this book.

We also hope that we will succeed in demonstrating the astounding versatility of these methods as reflected in a number of international case histories from recent years. The reader will hopefully also realise that vibro compaction and vibro replacement stone columns are presently fulfilling – and will continue to do so – all the requirements of sustainable construction. We will demonstrate in a separate chapter of the book that these methods require only natural materials for their execution, leaving behind only a minimal carbon footprint.

Finally, we do hope that the book will help stimulate further work and research on the subject and on those problems that are not yet satisfactorily resolved or are still the subject of controversy, to enable further plant development and to improve ground engineering.

We wish to thank Keller Group plc for their noble assistance in preparing this book, for funding the preparation of graphs and diagrams but especially for allowing access to the technical archives and for using data in preparing most of the case histories. In this context our thanks go in the first place to Justin Atkinson, the chief executive of Keller. With the publication of this book in 2010, we would like to take this opportunity to extend our best wishes for continued development and success to Keller Group plc, which pioneered deep vibratory soil improvement and which celebrates its 150th anniversary this year.

Invaluable support has also been given in discussions with former and present colleagues on technical matters. Our thanks go especially to Dr Alan Bell who has critically reviewed the manuscript based on his long experience of working in ground engineering. Thanks are also due to George Burke, Jonathan Daramalinggam, Guido Freitag, Johannes Haas, Dieter Heere, Gert Odenbreit, Dr Vesna Raju, Dr Thomas Richter, Raja Shahid Saleem, Raja Samiullah, Prof. Dr Stavros Savidis, Dr Lisheng Shao, Barry Slocombe, Dr Wolfgang Sondermann, Reiner Wegner and Dr Jimmy Wehr. Special thanks go to Christine Trolle for her patience in supporting us to organise the design of graphs for the manuscript.

In preparing case histories of recent applications of vibro compaction and vibro stone column methods we gratefully acknowledge the support of special contractors in providing valuable data and information: Keller Holding GmbH for Sections 3.6.1–4 and 4.6.4–6, Hayward Baker Inc for Section 3.6.5, Keller Limited for Section 4.6.8 and Bauer Gruppe for Section 4.6.9.

Klaus Kirsch
Fabian Kirsch
December 2009

# 1 An overview of deep soil improvement by vibratory methods

Realisation of structures always makes use of the soil on which, in which, or with which they are built. Whenever engineers find that the natural conditions of the soil are inadequate for the envisaged work they are faced with the following well-known alternatives of:

1 bypassing the unsuitable soil in choosing a deep foundation;
2 removing the bad soil and replacing it with appropriate soil;
3 redesigning the structure for these conditions;
4 improving these conditions to the necessary extent.

When the Committee on Placement and Improvement of Soils of the ASCE's Geotechnical Engineering Division published its report *Soil Improvement: History, Capabilities, and Outlook* in 1978 it concluded that "it is likely that the importance of the fourth alternative will increase in future". Indeed, in the decades since "the need for practical, efficient, economical, and environmentally acceptable means for improving unsuitable soils and sites" has increased.

Before selecting the appropriate soil improvement measures it is necessary to determine the requirements, which follow from the ultimate and serviceability limit state of design. These are:

- increase of density and shear strength with positive effect on stability problems;
- reduction of compressibility with positive effect on deformations;
- reduction/increase of permeability to reduce water flow and/or to accelerate consolidation;
- improvement of homogeneity to equalise deformation.

When leaving aside the method of exchanging the soil, ground improvement can be categorised into compaction and reinforcement methods. Table 1.1 shows a classification of the methods of ground improvement that are of practical relevance today.

*Table 1.1* Ground improvement methods (after Sondermann and Kirsch, 2009)

| *Ground improvement methods* | | | | |
|---|---|---|---|---|
| *Compaction* | | *Reinforcement* | | |
| *Static methods* | *Dynamic methods* | *Displacing effect* | *No displacing effect* | |
| | | | *Mechanical introduction* | *Hydraulic introduction* |
| • pre-loading<br>• pre-loading with consolidation aid<br>• compaction grouting<br>• influencing groundwater | • compaction by vibration:<br>  • using depth vibrators<br>  • using vibratory hammers<br>• impact compaction:<br>  • drop weight<br>  • explosion<br>  • air pulse method | • vibro stone columns<br>• vibro concrete columns<br>• sand compaction piles<br>• lime/cement stabilising columns | • MIP[1] method<br>• CMI[2] method<br>• permeation grouting<br>• freezing | • jet grouting |

*Notes:* 1 mixed-in-place; 2 cut-mix-inject (Topolnicki, 2004)

This book deals with two important soil improvement methods that utilise the depth vibrator as the essential tool for their execution. Granular soils are compacted utilising the dynamic forces emanating from the depth vibrator when positioned in the ground. The reinforcing effect of stone columns, constructed with modified depth vibrators, in cohesive soils improves their load-carrying and shearing characteristics.

Since the development of vibro compaction during the 1930s and vibro replacement stone columns in the 1970s, they have become the most frequently used methods of soil improvement worldwide due to their unrivalled versatility and wide range of application.

As we will see, deep vibratory sand compaction is a simple concept, and therefore design and quality control of compaction in cohesionless soils have remained almost entirely empirical. The development of predictive design methods based upon fundamental soil dynamics were probably inhibited by the simplicity of in-situ penetration testing for settlement and bearing capacity calculations. The study of the effect of resonance developing during compaction in granular soils surrounding the vibrator and improved mechanical and electronic controls of the compaction process have, only relatively recently, opened opportunities for significant advances in this field.

The introduction of coarse backfill during vibro compaction and the

resulting formation of a granular or stone column was a logical and almost natural development when unexpectedly cohesive or non-compactable soils were encountered. The composite of stone column and surrounding soil stimulated theoretical studies on settlements and shear resistance by applying standard soil mechanics principles.

Each of the systems, vibro compaction and vibro stone columns, has its characteristics and method of execution, and even machine types are different for the two systems of ground improvement, as are design principles, field testing and quality control.

When in motion, depth vibrators send out horizontal vibrations, and are all excellent boring machines in loose sandy and soft cohesive soils.

The horizontal motion emanating from the depth vibrator being positioned in the ground is the distinctive characteristic that distinguishes this method from all the other methods, which utilise vertical vibrations. These methods, which are in general less effective for the compaction of granular soils and which cannot be used for the improvement of fine-grained cohesive soils, are generally not recognised as true vibro compaction methods and hence are not discussed in great detail.

Depth vibrators are normally suspended like a pendulum from a standard or special crane for vertical penetration into the ground. The vibrator sinks by the desired depth, sometimes assisted by water or air flushing, additional weight when necessary, or even by downward thrust developed by special cranes with vertical leaders. In granular soils the surrounding sand is compacted in stages during withdrawal, and in cohesive soils imported backfill is employed to form a stiffening column.

The choice of technique follows from the soil and groundwater conditions given in site investigation reports. As will be explained later, the grain size distribution diagram of the soil to be improved is a valuable tool for this choice. Sand and gravel with negligibly low plasticity and cohesion can be compacted by the vibrations emanating from the depth vibrator (vibro compaction) while with an increasing content of fines vibrations are dampened rendering the method ineffective. Experience shows that the limit of vibro compaction is reached with a silt content of more than approximately 10%. Clay particles at even smaller percentages (1–2%) cause a similar effect. In these cases an improvement of the soil characteristics can only be obtained by adding granular material during the process of forming compacted stone columns (vibro replacement stone columns).

Following a historic overview of the development of these soil improvement methods, two chapters deal with the improvement of granular soils by the vibro compaction method and of fine-grained cohesive soils by the vibro replacement stone column method. The chapters include detailed descriptions of the equipment used and the specific physical processes controlling the two methods and provide state-of-the-art design principles, including methods to assess and mitigate seismic risk when applying either improvement method. Quality control procedures, the evaluation of suitable

soils and practical method limitations together with recent case histories complete these chapters.

In final three chapters, method variations and related processes will be described as well as environmental considerations and contractual implications of these ground improvement methods for the practising engineer.

# 2 A history of vibratory deep compaction

An overview of the development of ground improvement by deep vibratory compaction starts in Germany between the two world wars. The worldwide economic crisis from 1929 to 1931 had a severe impact on the German construction industry. The absence of profits prevented badly needed investment. Mass unemployment reached over 30% and paralysed economic activity. Farsighted personalities, however, looked into new working and construction methods at a time when the government under Chancellor Brüning (1885–1970) tried to mitigate the worst misery by job-generating measures such as the first programme to build highways, which was then intensified under the Hitler regime after 1933. In this context, the need to compact large quantities of concrete, sand and gravel was the motive for numerous engineers to look for better and more efficient methods.

## 2.1 The vibro flotation method and first applications before 1945

The Keller Company was particularly interested in making a dense and strong concrete by employing a completely new method, as proposed by Degen and Steuermann. Their idea was simple, but the effect novel and startling (Johann Keller GmbH, 1935).

> The basic principle of the new method is shown by two simple model tests (Figure 2.1):
>
> a) A steel box is filled with concrete aggregate which is compacted by a vibrator situated at the surface while simultaneously a cement suspension is pumped with moderate pressure through a pipe ending in the lower layer; the cement suspension rises slowly and steadily through the aggregate to the surface – an ideal concrete pulp and, after setting, a particularly strong and dense concrete is created this way, at a very economical cement consumption.
> b) The same box is filled with gravelly sand which is compacted in the same way while water is introduced from below; the sand surface

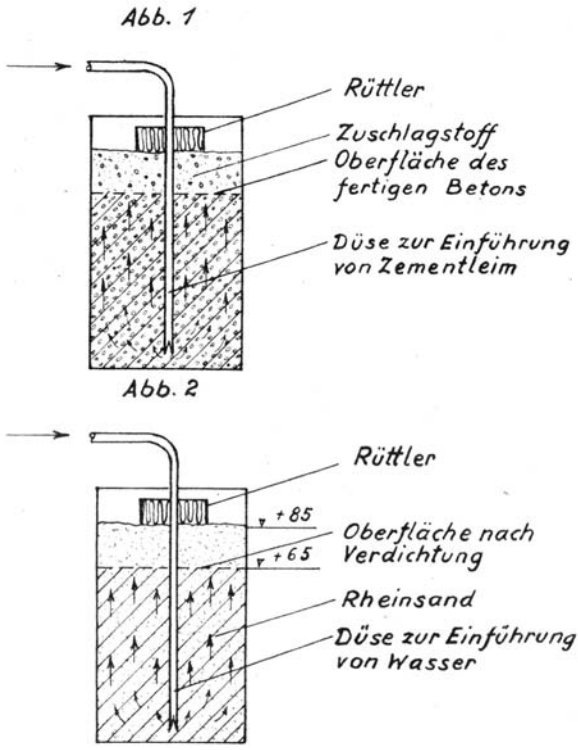


*Figure 2.1* Effect of the vibro flotation method
*Note:* Abb.1: Rüttler – vibrator, Zuschlagstoff – aggregate, Oberfläche des fertigen Betons – concrete surface after densification, Düse zur Einführung von Zementleim – nozzle to insert cement suspension; Abb.2 Rüttler – vibrator, Oberfläche nach Verdichtung – surface after densification, Rheinsand – Rhine-sand, Düse zur Einführung von Wasser – nozzle to insert water

sinks from its original thickness of 85 cm to a height of 65 cm; comparison trials show that no other compaction method achieves an equally strong compression of the sand; even with very intensive vibration, without the rising water the sand thickness is only 72 cm.

This novel method of concrete densification was, for the first and only time, tried in 1934 for the foundation of an I.G. Farbenindustrie building near Frankfurt. The system, which proved so successful even in large scale trials, failed in practice when it was applied to densifying the concrete of a bored pile foundation. The idea of concrete densification was eventually abandoned and the focus of development of this method was aimed at its possibilities of sand compaction.

The method shown in Figure 2.1 encompasses all the necessary features that today remain important for effective sand compaction: extensive annulment of internal friction, full saturation of the sand to be compacted

and complete rearrangement of the sand grains with a minimum void ratio as a result of intensive vibrations. Realisation of the method required rather complicated watering systems and, above all, powerful surface vibrators to compact the sand in sufficiently thick layers. Even the strongest surface vibrators at the time did not reach deeper than 2.50 m, which limited the new method considerably.

The compaction of sand at large depths was required for the construction of the new congress hall at Nuremberg. The designers of this gigantic project had high demands for the durability of its foundations in the light of the aggressive groundwater, and this could not be fulfilled by conventional methods. Also the dimensions of the structure were exceptional, and so were its loads: the main hall measured 260 m by 265 m; the ceiling was 65 m high with a free span of 160 m from wall to wall. The subsoil consisted of sand deposits that extended to 16 m depth where strong sandstone started.

As no proven methods existed for compacting this sand, the designer proposed a field trial to be carried out under the supervision of the Degebo (German research society for soil mechanics). Two compaction methods were to be tested and compared: a modified Franki method and the newly developed so-called Keller method. Trial compaction finally commenced in 1936.

The Keller proposal was as follows:

a To build vibrators following the principle of a bob weight connected to an electric motor in cylindrical form on a vertical axis with strong horizontal force.
b To bring the vibrator by means of a bore hole into any desired depth of the sand to be compacted. Abb. 5 (Figure 2.2) shows the fundamental arrangement of the new method: the vibrator has been lowered inside the borehole to the deepest layer of the sand to be compacted, and the casing has been pulled out to the extent that the vibrator is fully surrounded by the sand. Vibrator and casing are simultaneously extracted in this position with progressing densification. Compaction is accordingly achieved in layers progressing from below to the surface.

What had been so simply and convincingly formulated at the time, represented in reality a major technical problem: by means of a heavy wooden 23 m high gantry a 460 mm diameter drilling casing was lowered through 16 m of sand down to the Keuper sandstone employing conventional boring methods. Then the 2 m long vibrator was introduced. It should be emphasised that this was to generate horizontal vibrations in contrast to the surface vibrators generally working with vertical oscillations. Compaction was achieved by simultaneously adding water while casing and vibrator were slowly withdrawn at a rate of 8 min/m. The compaction effect was visible at the surface in a crater developing around the casing, into which

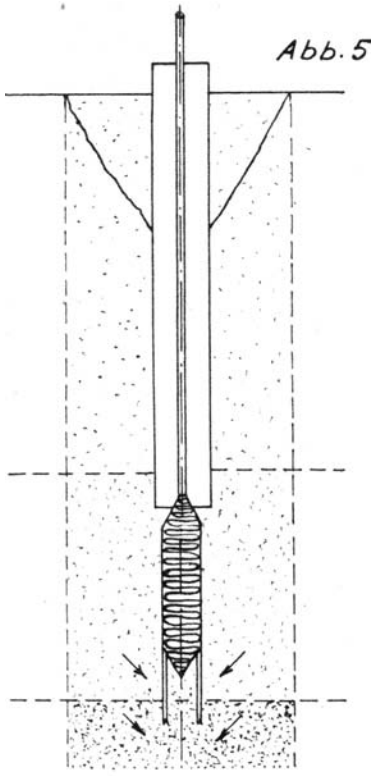


*Figure 2.2* Vibro flotation method used at the congress hall at Nuremberg

the excavation material and additional imported sand was backfilled as necessary. Compaction centres were arranged in a triangular grid at a distance of 2.16 m from each other, representing 4.05 $m^2$ per probe. Sand consumption was 5.5 $m^3$ for each compaction point, an astounding amount, exceeding all expectations. Degebo confirmed the excellent compaction and raised the allowable bearing capacity from the original 2.5–4.5 $kg/cm^2$ (250–450 kPa). The unexpectedly favourable results which were also confirmed by seismic tests could not obscure grave problems identified during execution. Not only was the method very time-consuming, but the vibrator itself, still just a prototype, could only be kept operational at considerable repair expenses. This was the reason that only a relatively minor portion of the foundation work could be performed by the novel vibro flotation method in spite of the convincing test results. The major part of the gigantic foundation totalling some 22,000 compaction centres was performed employing the Franki method compacting crushed gravel and sand backfill (Ahrens, 1941).

Even during the execution of the trial compaction, mechanical improve-

ments were made to the vibrator, extending its operational time. However, it was Rappert, then Keller's project site manager, who had the decisive idea that lead to the breakthrough with this method. To complete one compaction point took 22 hours: 8 hours for boring, 12 hours for compaction and backfilling and 2 hours to move the gantry to the next position. He proposed avoiding the extraordinarily time-consuming drilling operation by making use of the liquefaction effect of the vibrations on the in-situ sand, enabling the vibrator to sink into the ground under its own weight to the required depth from where the compaction work was to begin by extracting the vibrator slowly back up from the ground. The necessary modifications of the vibrator were made in the same year, so that by 1937 the first foundation works on loose sand with the new vibro flotation method were carried out.

Understandably little was published about the vibrator – the key precondition for the method – and little survived the war in the archives of the Keller Company. After a patent was granted on the method in 1933 the vibrator together with other additional features of the method were also patented in 1936.

Efficient work on site required the following from the vibrator:

- It should be capable of penetrating as quickly as possible to the required depth.
- It should be possible to withdraw the vibrator without problems from the ground during compaction.
- The vibratory effect should efficiently compact a zone in the soil as large as possible.

A blueprint of a depth vibrator from 1937 (Figure 2.3) shows that it consisted of a 260 mm diameter, 2.0 m long, steel tube. In its interior, two electric motors of 12.5 kW each were placed on the upper part of the vertical axis with up to three bob weights at the lower end. The upper part of the vibrator consisted of a device for channelling water to a nozzle at the vibrator point, an inlet for the electric cable for the motors and mechanical features separating the vibratory motions created by the rotating bob weights from the follower tubes carrying the vibrator and enabling its deep penetration into the ground. The motors rotated at 50 Hz resulting in 75 kN horizontal force of the eccentric weights creating a double amplitude of 10 mm. The lifetime of the bearings posed a major problem at the time, but the designers must have quickly succeeded in making the machine robust enough for its use on site, because in the following years many interesting foundations were carried out with the vibro flotation method.

The new method attracted much interest among experts, although scepticism prevailed in the early years in spite of convincing test results. Leading German ground engineering institutes were involved with trial compactions, and on sites, introducing various methods to check the densification achieved. Not everybody could be convinced of the compaction

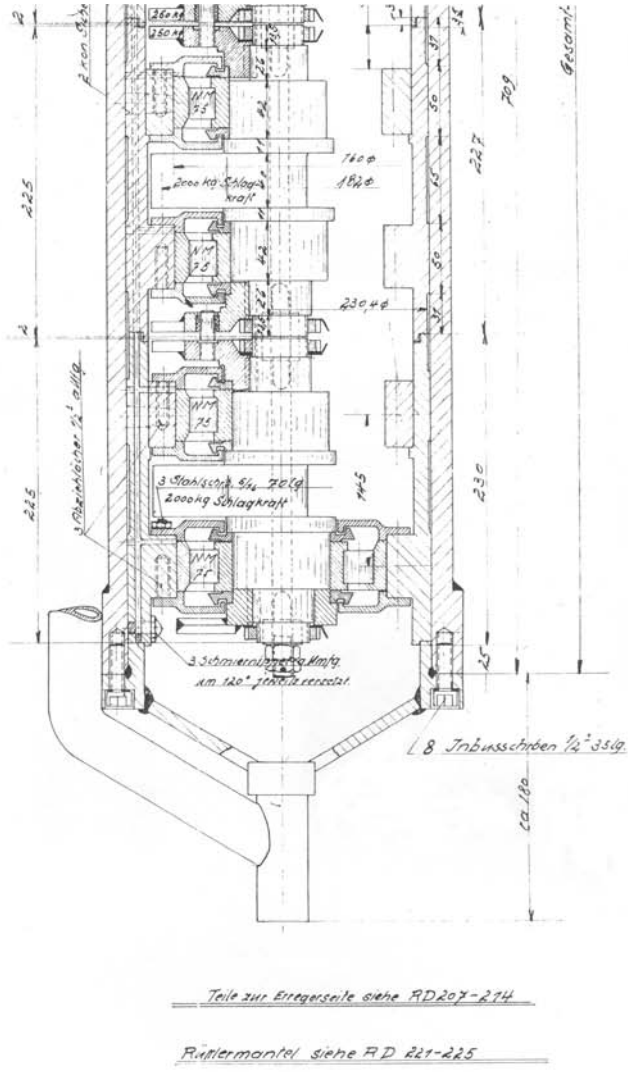


*Figure 2.3* Detail from a blueprint of one of the first Keller depth vibrators, 1937

results just on the basis of the often surprisingly large amounts of added sand material. Checking and control measures included all known in-situ testing methods at the time, such as direct density measurements, deep soundings, geophysical tests, the exact volumetric measurement of the sand added during compaction, combined with site levelling before and after compaction and full-scale load testing. As the number of successful applications of the method increased, loose sand, even when under water, lost its poor reputation as unsuitable foundation soil.

In a company catalogue, Keller (1938) summarised the advantages of sand compaction:

- Naturally deposited sand can be compacted to any depth.
- Artificial sand fill can be compacted over its full height in one operation.
- Densification achieved is complete, and void ratio can be as low as its theoretical minimum.
- The method is safe, fast and economic.

These advantages were the reason that increasingly costly pile foundations could be avoided and replaced by shallow foundations on sand with previously unheard-of bearing pressures. Of equal importance were the increased shear strength and the reduced compressibility which accompany the high density of the compacted sand. These findings helped the vibro flotation, or vibro compaction method, as it was also called, to gain an exceptionally broad recognition during the few years before and even during the war. Completed projects included warehouses and industrial plants employing the effect of sand densification at depth to increase the allowable bearing pressure, thus leading to smaller and more economical footing sizes. In connection with water structures at the North and Baltic Seas, the method was frequently also used to compact sand-fill behind walls or dredged fill. Records of some of these projects survived the war and are worth recalling, because interesting features of early vibro flotation works are included.

In 1939, a comprehensive compaction trial was carried out for the foundation of the Great Hall in Berlin. Under the supervision of the Degebo, the newly developed method was successfully used in medium sand to a depth of 20 m. Density increased considerably and bearing capacity was more than doubled. To test the capability of the vibrator to penetrate to greater depths, it was suspended from a 40 m high gantry and Degebo, 1940, observed that the vibrator sank to a depth of 35 m, where it was obviously stopped by the presence of a hard marl layer (Figure 2.4). It was not until 40 years later that modern depth vibrators achieved the same depth again in conjunction with the compaction work carried out for the foundation of the Jebba Dam in Nigeria (Solymar *et al*., 1984).

Scheidig reported in 1940 on an interesting work for the foundation of a large grain silo at Bremen, where, for the first time, the method was used to increase the bearing capacity of bored piles by compacting the sand below the toe and along the shaft of the piles.

*Figure 2.4* Vibro compaction employing wooden gantry, 1939

During the war, construction activities were increasingly directed towards military installations or for facilities closely connected with the wartime economy. Were these to be built on alluvial deposits, or in the vicinity of the shoreline, the natural density of the sands was frequently insufficient to carry substantial structural loads using normal shallow foundations without intolerably high deformations. Increasingly in these cases the vibro flotation method was used by which sand could be compacted sufficiently to carry even the highest loads. In this way it was possible to avoid expensive pile foundations for which concrete and steel were needed, an effect which was most welcome given the shortage of almost all raw materials. Also, there were major military shelters at Rotterdam and near Bremen where the in-situ or dredged sand was compacted by vibro flotation to such a degree that these heavy structures could be built using incredibly high bearing pressures. At Rotterdam, where a submarine bunker was built, Casagrande proposed an allowable bearing capacity of 15 kg/cm$^2$ (1.5 MPa) to be used, for which a spacing of the compaction centres of 4 m$^2$ was necessary. To

accelerate the work the compaction grid was widened to 5 $m^2$ per probe and the bearing pressure reduced to 10 $kg/cm^2$ (1.0 MPa). Figure 2.5 shows a cross-section through the submarine shelter.

Of much greater importance in the development of the vibro compaction method were observations made in 1942 in connection with the foundation of an I.G. Farben facility at Rolingheten in Norway. Here fine-grained, loose partially silty to very silty sand was to be compacted at high groundwater table to carry heavy structural loads. The works were supervised by Degebo (1942), who recommended a rather close spacing of 2.5 $m^2$ per compaction probe in this case. However, a satisfactory compaction of the sand was only possible through the addition of gravely medium sand as backfill material during execution (Figure 2.6). Backfill material amounted to 20% of the compacted sand volume. Site investigation carried out after compaction revealed for the first time that the core of the compaction consisted primarily of the coarse backfill material, which was compacted to 100% relative density. In the surrounding fine-grained soil between the compaction cores a relative density of 60% was measured. With today's perception this compaction work was probably for the first time close to what today is called vibro replacement, whereby, as will be shown later, the in-situ fine-grained material cannot be satisfactorily compacted by the vibratory motion alone and coarse backfill material needs to be added. In the Norwegian example, load tests carried out on, and between, the compaction probes revealed an allowable bearing pressure of 6 $kg/cm^2$ (600 kPa). The effect of

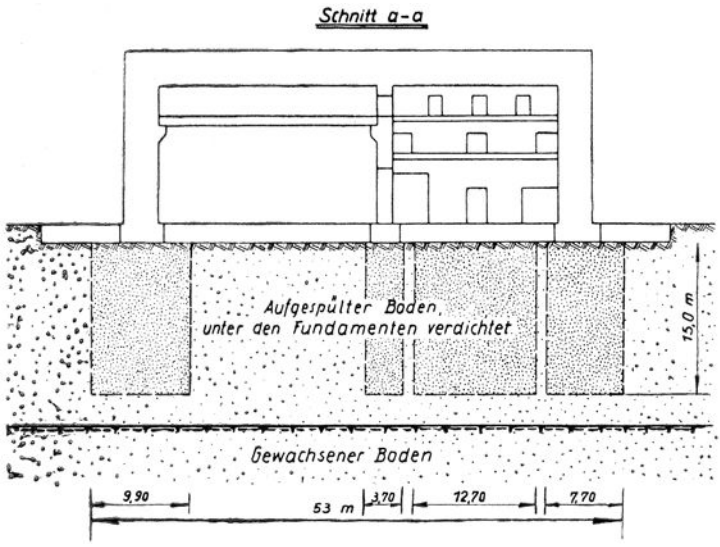


*Figure 2.5* Foundations of a submarine shelter, 1942
*Note:* Schnitt – cross-section, Aufgespülter Boden unter den Fundamenten verdichtet – dredged sand compacted below footings, Gewachsener Boden – natural ground

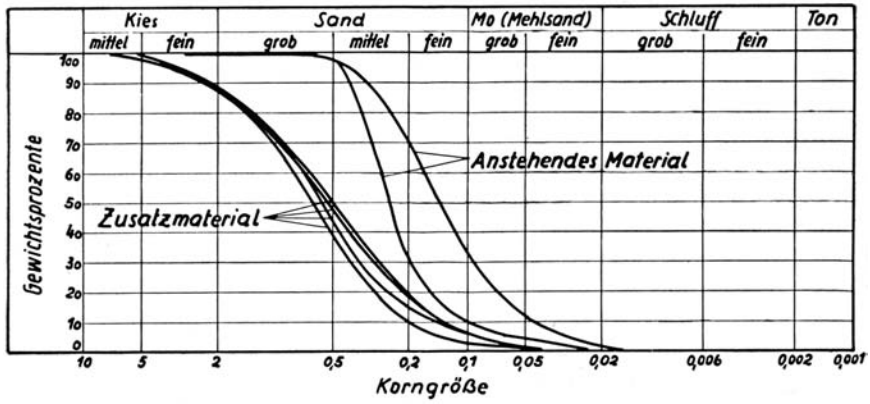


*Figure 2.6* Grain size distribution curves for vibro compaction work at Rilingheten, Norway

*Note:* Gewichtsprozente – percent by weight, Korngröße – grain size in mm, Zusatzmaterial – added material, Anstehendes Material – in-situ material

the compaction work was quite impressive: "although even light vehicles could not pass the site surface before compaction, heavy trucks could run over it after compaction without any difficulties" (Degebo, 1942).

In a relatively short time the vibro flotation method was acknowledged as an efficient foundation measure and both execution methods as well as testing procedures were continuously improved. However, even long after the war, slow-moving gantries were still in use that carried the vibrator and could only be moved on tracks. This and the time-consuming method of adding sand using wheelbarrows allowed shift productions of just 50 lin.m of compaction probe or 150–250 $m^3$ of compacted sand.

## 2.2 Vibro compaction in post-war Germany during reconstruction

By the end of the war the situation of the German construction industry and particularly specialist foundation companies was frightful. Developments that had continued and made progress even during the war came to an abrupt end. Since all efforts were concentrated now on restoring and maintaining the necessities of life, construction activity was restricted to repairing major damage and the restoration of the infrastructure. As the people regained confidence in their future after the currency reform in 1949, construction work on new buildings slowly developed again. The impressive practical results of the vibro flotation method were, however, not forgotten by engineers, consultants, the administration, the industry and the universities. The method quickly gained increasing importance during the reconstruction phase due to its astounding flexibility and adaptability in

solving different construction problems. Whenever the density of naturally deposited or filled sand was insufficient for foundation purposes the depth vibrator was a useful tool to remedy the situation. Eventually, the outdated gantries were replaced by crawler cranes which, together with other modern equipment, reduced site installation costs and increased production rates considerably.

Besides the densification effect of the depth vibrator as described above, its potential to temporarily liquefy fully saturated sand below the water table was soon realised and further developed for practical use. Prefabricated concrete piles and steel tubes as well as sheet piles could be easily lowered into the liquefied zone surrounding the depth vibrator. The process was further supported by strong water flush emanating close to the point of the vibrator. This was of significance as top vibrators and vibratory hammers did not then exist. Many such jobs were successfully executed during the 1950s including one spectacular case: a complete lighthouse Tegeler Plate was sunk 40 km northwest of Bremerhaven 18 m deep into the sandy bottom of the North Sea by means of six depth vibrators attached to its shaft (Figure 2.7).

In 1953, when the planning of a new dry dock at Emden commenced, the designers were considering a special proposal to use the ability of the depth vibrator to sink larger bodies into the ground to install anchors which were necessary for the uplift protection of the dock. Experiments were carried out to establish the optimal size of the anchor blocks together with the number of depth vibrators needed to lower the blocks to the predetermined depth. For the dry dock 500 cross-shaped concrete anchor blocks were sunk 14 m into the underlying sand layer, simultaneously using two or three vibrators for each block. The 46 mm dia. corrosion-protected steel cables, which were securely fastened in the anchor blocks, extended into the slab of the dry dock from where they were post-tensioned with 1 MN. As the sand below the dry dock was also well compacted, when the vibrators were withdrawn, the system of anchors and dense sand provided an excellent solution for the foundation of the dry dock which was more economical than a conventional gravity structure.

In 1956, at Braunschweig, similar difficulties were experienced during foundation works for an engine shed for the German railway as at the above-mentioned project in Norway in 1942, so a new soil improvement method was developed. Here, the subsoil again consisted of very fine, very silty sand that was totally liquefied by the vibratory motions, transforming the ground surrounding the vibrator into a viscous liquid. A measurable compaction effect, if at all, was only achieved after a very long time. The vibro flotation method had reached its limit of application. The solution that was finally adopted consisted of lowering the vibrator into the ground without the use of flushing water, withdrawing it completely from the ground after it had reached its final depth and filling the temporarily stable hole left behind by the vibrator with coarse material. By repeated repenetration and

*Figure 2.7* Lighthouse Tegeler Plate being set up to be vibrated into the seabed

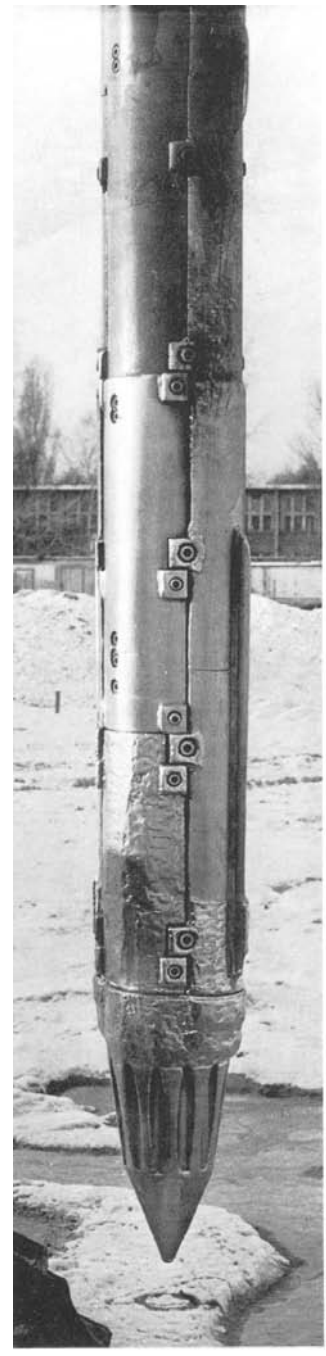

*Figure 2.8* The Keller "Torpedo" vibrator

backfilling, a stone column consisting of well-compacted coarse material was formed. The in-situ soil was displaced laterally providing, at the same time, a supporting horizontal confining pressure.

To build efficiently such a "vibro replacement stone column", as the system was soon called, the available depth vibrator proved rather unsuitable. Not only was its surface not smooth enough, and the water pipes attached to it prevented rapid penetration, but the vibrator and its extension tubes were not connected with each other rigidly enough to exercise the desired downward thrust.

## 2.3 The "Torpedo" vibrator and the vibro replacement stone column method

The new findings gathered on sites formed the basis of considerations to redesign the original vibrator which was used unaltered for over 20 years in sand compaction and make it suitable for the treatment of cohesive soils. Finally the Keller Company developed a much improved depth vibrator which was, as a result of its shape, called "Torpedo" vibrator (Figure 2.8). It was characterised by a much more powerful electric motor – 35 kW, running at 3000 rpm and developing a horizontal force of 156 kN. The double amplitude of the freely suspended vibrator measured 6 mm. Fundamentally new features were its almost smooth surface and a coupling that was capable of transmitting substantial vertical forces via the vibrator into the ground stemming from either heavy extension tubes or later from the downward thrust of the special machines carrying the vibrator. In this way, the vibrator could achieve penetration into the ground without the assistance of flushing water, provided the necessary total weight could be applied.

Relatively soon the first foundation works were carried out in only partially saturated silts by forming stone or gravel columns with the vibrator. These well-compacted stone columns were closely interlocked with the soil and acted together with the surrounding soil and other adjacent columns like a normal load-bearing soil. Initially the stone columns were exclusively constructed using crane-hung vibrators that were lowered into the partially saturated soils under their own weight without the help of water. In this way, the consistency of the soils was not negatively influenced. The vibrator was normally completely withdrawn from the ground and a specified charge of coarse fill was placed into the cylindrical hole left behind by the vibrator. Then the vibrator repenetrated and compacted the fill, squeezing it also laterally into the surrounding soil. By repetition of this sequence, a strongly compacted stone column was created.

Consequently, by the end of the 1950s, deep vibratory systems were already being utilised across almost the full range of alluvial soils. Grain size distribution curves became a prime indicator for the appropriate choice of ground treatment method (Figure 2.9). When sands and gravel with less then 10% fines were encountered, vibro compaction was the chosen method

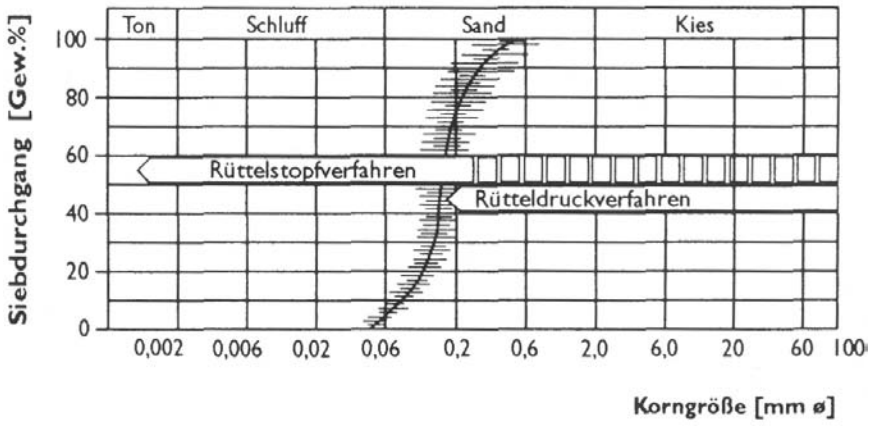


*Figure 2.9* Range of application of deep vibratory methods
*Note:* Siebdurchgang – percent passing by weight, Korngröße – grain size, Rüttelstopfverdichtung – vibro stone columns, Rütteldruckverdichtung – vibro flotation

of treatment. In all other cases, the alluvial soils would be improved by the vibro replacement method, whereby fine-grained soils with low water content would be treated without the use of water, and those with high water content with the help of flushing water. In both cases the temporary stability of the cylindrical hole created by the depth vibrator was important and decisive for building a proper stone column of moderate length. The state of the art which the deep vibratory systems had reached in Germany by the end of the 1960s is described by Lackner (1966) in his inaugural lecture at the Technical University of Hannover, underlining the versatility of the method and its economic importance for the treatment of otherwise unsuitable soils.

With the increasing usage of the method, particularly in fine-grained soils, occasional failures and setbacks forced the engineers to think more about the limitations of the stone column method. It was realised that cohesive soils with very high water contents and correspondingly low consistencies could not provide strong lateral support for the stone columns. If the stone columns were placed insufficiently closely packed to each other in these soft soils, which were frequently interspersed by peat layers, overall settlements would exceed expectations. In the absence of accepted design principles for these stone columns which would allow a reliable quantitative settlement prediction, the works on site were more closely supervised instead. Besides geometrical measurements of the stone columns the supervision of their steady and consistent build-up by control and registration of the energy used during their construction was introduced. These findings were supplemented by other standard in-situ testing methods and load tests on single columns and column groups. In this way, special contractors and consulting

engineers collected valuable information on the behaviour of stone columns in different soils which were very helpful for their further application. The lack of computational methods, however, was increasingly considered a shortcoming of this method, but at the same time it represented a challenge for the engineers. Numerous ideas for the design of soil improvement by stone columns were developed not only in Germany but also elsewhere when its use spread beyond its borders.

## 2.4 Development of vibro compaction outside Germany

Steuermann, one of the method's inventors, had already left Germany a few years before the Second World War broke out. A personal contract with the Keller Company on the usage of certain joint patent rights granted Steuermann full rights to the method in the USA where he went to live. In 1939, he published in the *Engineering News Record* an article on the experiences gained with the method of vibro flotation in compacting sands in Germany. However, it took almost ten more years before reliable compaction equipment was built in the USA and the first construction works could be carried out.

The new method was called "vibroflotation" in the USA. It only gained full recognition in the early 1950s after the Bureau of Reclamation reported vibro flotation experiments at Enders Dam (1948) and particularly after D'Appolonia (1954) had published his article "Loose sands – their compaction by vibroflotation".

The vibrator or Vibroflot, as it was called in the USA, was equipped, like its German forerunner, with an electric motor and was operated at 1800 rpm developing 30 Hz with a horizontal force of 100 kN at maximum double amplitude of 19 mm (Figure 2.10). Due to these characteristics, it was ideal for the compaction of sands. The advantages of vibro flotation were seen in the first instance in its easy and controllable working method for effectively compacting loose sands. Soon practical recommendations were developed enabling the engineer to design and supervise the compaction works. The main criterion for judging the success of the compaction became the relative density of the sand, measured initially directly, but increasingly indirectly using the Standard Penetration Test, and later on also by static Cone Penetration Testing. The general understanding that a safe foundation on sand in a seismic zone required a densification to at least 85% relative density supported the increasing popularity of the method, at first along the east coast of the USA, then in the mid west and later also in California. The range of application was from simple foundations for apartment and office buildings to rather complex structures such as numerous rocket launching pads at the Cape Kennedy Space Centre in Florida (Figure 2.11) and the extensive compaction works at the then largest dry dock at Bremerton in Washington, which the US Navy built in 1961 for the aircraft carriers of its Pacific Fleet.

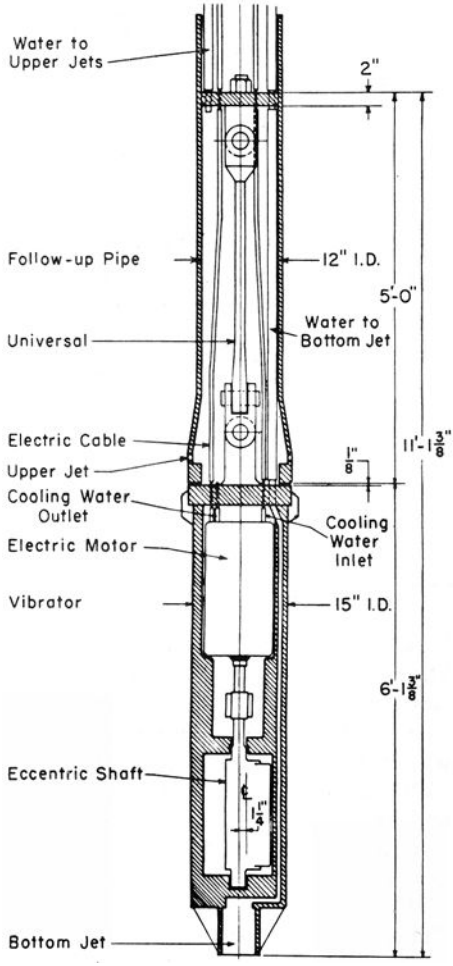


*Figure 2.10* Section through Vibroflot

All these works were exclusively for the compaction of sands before the experiences gained in Europe, and particularly in Germany, with the vibro replacement stone column method were recognised in the USA, and the first stone column foundation was carried out in 1972 for the foundation of water tanks at Key West, Florida.

As international consulting engineers gathered experience with ground improvement by means of depth vibrators the new method of vibro compaction spread beyond the borders of Germany and of the USA. British consultants with their connections within the Commonwealth played a particularly important role in this scenario. By way of licence agreements vibro flotation works were already being carried out by the late 1950s in these countries

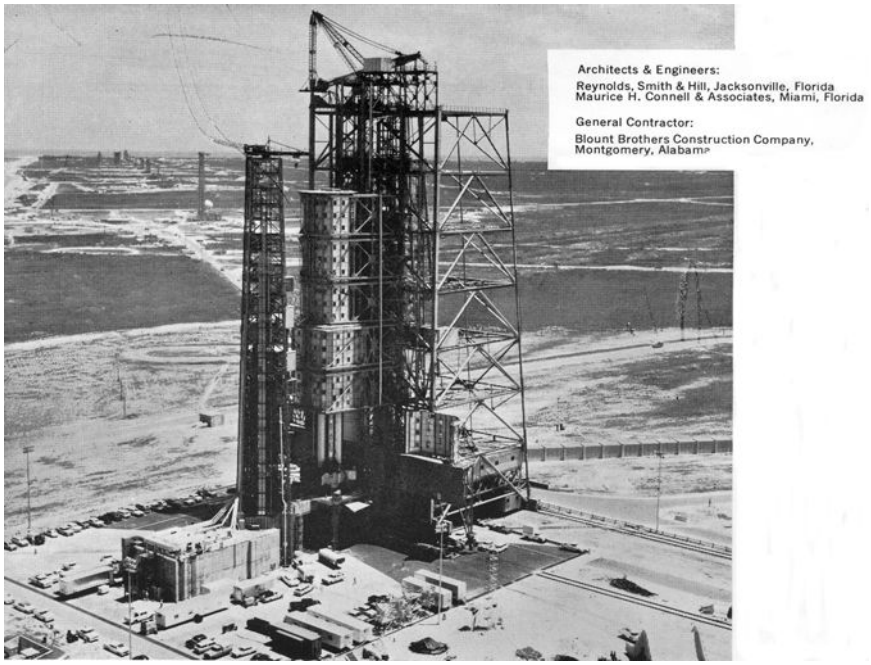


*Figure 2.11* Saturn Rocket Launching Facility at Florida (Vibroflotation Foundation Company brochure)

using vibrators from Germany and the USA. From about 1965 the Cementation Company in the UK built its own vibrators with similar features to the American equipment. However, in 1968, the electric motor was replaced by a hydraulic drive.

More important than these mechanical modifications was the fact that depth vibrators were now increasingly also used in the UK for the improvement of fine-grained cohesive soils. The application of stone columns in soft soils was accompanied by efforts to develop suitable criteria for the design of this ground improvement method (e.g. Thorburn *et al.*, 1968).

Vibro flotation foundations and, since 1968, also vibro replacement stone column foundations were carried out on some very large international projects, and this made the method known on all continents.

From 1955 to 1958 extensive compaction trials were carried out by the Keller Company to establish the design criteria for the foundation of the Aswan High Dam (Sad al-Ali) now retaining Lake Nasser in Upper Egypt. The effect of vibro flotation performed under water in hydraulically placed fine to medium dune sand was investigated and compared with the results of compaction by blasting. It was found that densification of the sand by vibro compaction was superior to that by blasting (Figure 2.12), and the Board of Consultants for the Sad al-Ali Commission, led by Terzaghi, recommended

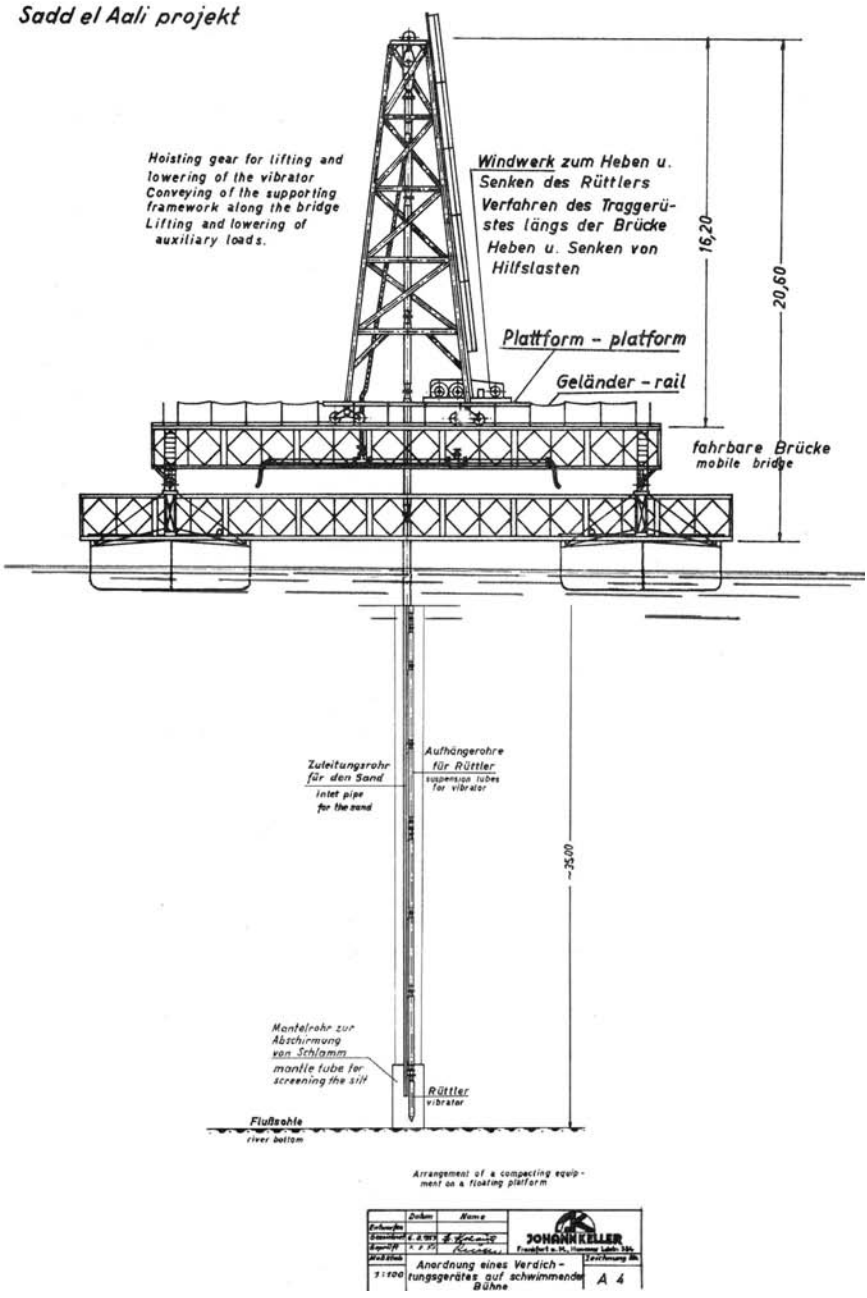


*Figure 2.12* Compaction trials equipment for the Aswan High Dam (Keller, 1958)

compacting approximately 3.4 million $m^3$ of dredged sand through 35 m of water under the core of the dam by this method. The Suez crisis of 1956 and the political tensions thereafter rendered the financing of the project difficult and prevented the contract award to an originally favoured German construction consortium. The gigantic project was finally financed and built by the Soviet Union, and purpose-built Russian vibrators were used to compact the sand from 1965 to 1967. Apart from the information that these machines were operated at 1750 rpm no other characteristics became known nor did the equipment appear again on the international market.

Of similar scale were the foundation works carried out in 1960–63 for the Usinor steel works at Dunkirk. The subsoil consisted of alluvial fine sands to a depth of up to 30 m, frequently interspersed by silt and clay layers, occasionally even peat. Stiff clay followed below requiring relatively deep embedment of an alternative piled foundation. The economical and practical advantages of a vibro compaction solution convinced the client to follow the recommendations of its foundation consultant, Kerisel, for shallow foundations on vibro-compacted sand, in preference to the piled option. The vibro approach additionally enabled detailed planning to be carried out after the whole area was first compacted, providing programme advantages for projects of this size. In less than two years, some 480,000 lin.m of compaction were carried out. Where necessary, the cohesive layers were bridged by large diameter vibro replacement stone columns built by two vibrators (in places even four) suspended 80 cm apart from each other from one crane using particularly strong water flush. The works were performed in double shifts employing up to 15 vibrators simultaneously. Compaction results were checked continually by static cone penetration tests. The settlement performance of the structure was as expected by the soil mechanics consultants. Measurements conducted over many years after the plant was put into operation showed only 2 to 3 cm of settlement even of the heaviest footings.

After India and Pakistan gained their independence in 1947 lengthy and difficult negotiations over the usage of the water from the main tributaries of the Indus flowing from India to Pakistan commenced. The agreement finally reached was laid down in the Indus Valley Plan, a project financed and controlled by the World Bank and which finally started in 1960. The plan foresaw a series of barrages built on loose sandy river deposits within deep excavations reaching deep below groundwater table. For load transfer purposes and to prevent liquefaction in case of earthquakes the in-situ sands below the barrages and distribution structures had to be compacted to depths of 20 m. At Sidnai (1963), Mailsi (1965), Marala (1966), Rasul (1966), and Chasma (1968), British and German vibrators compacted well over 2 million $m^3$ of sand. Figure 2.13 gives an impression of the considerable size of these works showing the deep excavation for the Chasma barrage at the time of the vibro compaction works.

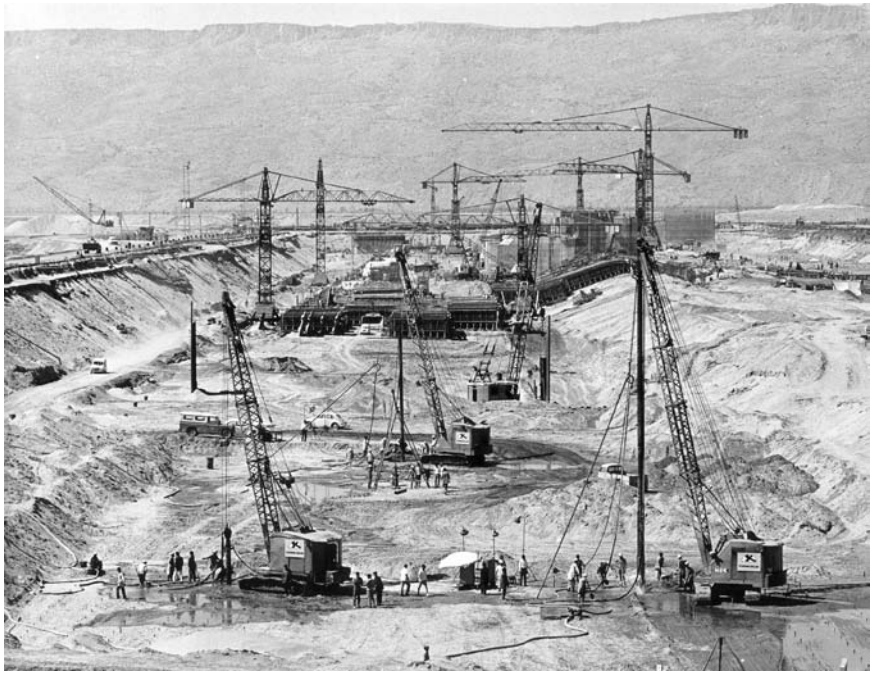

*Figure 2.13* Vibro compaction works in progress at the Chasma barrage in Pakistan

When the works in Pakistan were still in progress quite complex vibro compaction works had to be designed and carried out for an underwater tunnel that was to connect the cities of Parana and Santa Fe in Argentina. The 2400 m-long road tunnel was assembled from prefabricated concrete elements, each 10.8 m in diameter and 65.5 m long, which were placed by a lifting platform into a trench dredged out in the river bed. The double-lane tunnel at its deepest has its crown 17.7 m below water level and covered by 3.5 m of sand. To create a safe foundation and to minimise the lateral pressure, the in-situ and dredged sand below and around the tunnel was compacted. Some 125,000 lin.m of deep compaction were carried out in 1968 under difficult site conditions.

One example for the advantageous use of the deep vibratory methods in harbour construction, is the foundation works for the quay wall of Thuwwal harbour on the west coast of Saudi Arabia. About 160,000 lin.m of vibro flotation in loose coral sands were carried out in 1978 for this project from a working ship equipped with five vibrator units (Figure 2.14). Numerous and often quite extensive foundation works employing deep vibrator methods were carried out on the Arabian peninsula starting in the early 1970s for the infrastructure as it exists today: large power plants and desalination units and impressive facilities for the petrochemical, steel,

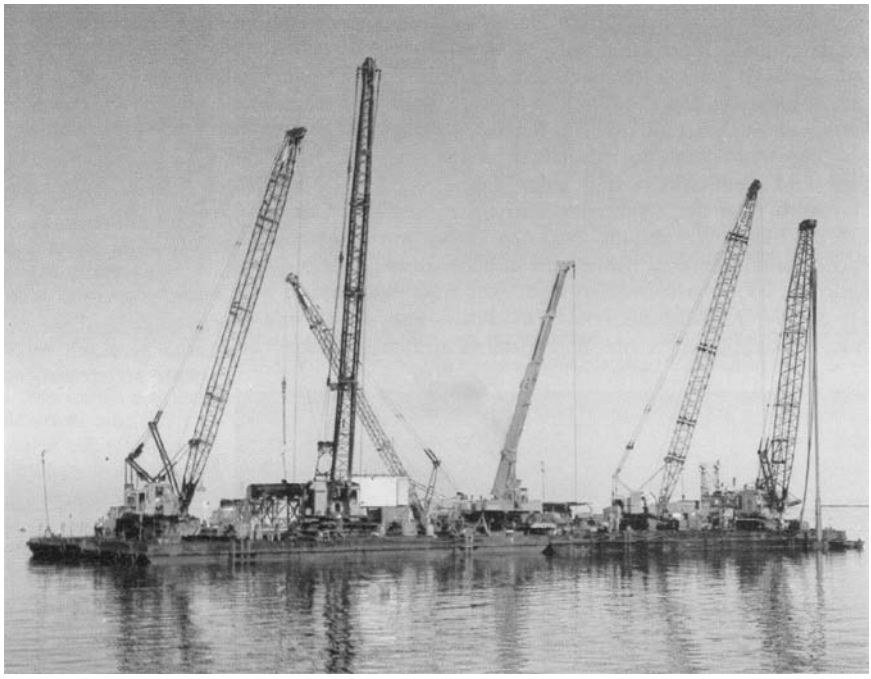

*Figure 2.14* Underwater compaction works at Thuwwal Harbour in Saudi Arabia (by courtesy of Bauer)

aluminium and cement industry. Vibro compaction was and is regularly recommended by the consulting engineers in this area when, besides the cost advantage of the system, the groundwater is particularly aggressive against concrete. This concrete attack, which is especially strong on piles, can be better controlled and indeed avoided by the choice of a shallow foundation placed on improved ground whereby the direct contact with the aggressive groundwater can be avoided or minimised.

Although the first phase of a large grain terminal at Kwinana at the west coast of Australia was founded in 1969 on driven piles, the owner opted for vibro compaction with depth vibrators for the second phase of the project. Situated near Perth, this grain terminal with its loading facilities is among the largest of its kind. The in-situ fine-grained sand was compacted to a depth of 24 m to safely carry the heavy loads of the silos, to reduce the overall settlement of the structures and to increase their safety against earthquakes. After just 14 months, some 260,000 lin.m of vibro compaction was completed in 1974. The foundation works for this impressive grain terminal won the 1974 Construction Achievement Award of the Australian Federation of Construction Contractors which helped the method of vibro compaction to gain acceptance also on the fifth continent. This was followed by some interesting works at Botany Bay Harbour south of Sidney and then

some vibro replacement works for the foundation of railway embankments on soft ground.

In 1962, the Ughelli Power Plant in Nigeria had its foundations laid using the vibro compaction method, and in 1972 the method was again used for the foundation of the Massingir Dam in Mozambique. Complex compaction work became necessary for the construction of the Jebba Dam in Nigeria in 1982 and 1983, where deep underlying non-cohesive, loose river deposits had to be compacted up to 90% relative density to fulfil earthquake design requirements. The necessary densification to depths of 45 m together with the large volume to be compacted in a relatively short time pushed the limits of the technology and the existing equipment. It was only achieved by a combination of vibro compaction to 30 m with deep blasting for the sand below.

By the end of the 1970s soil improvement using depth vibrators was already an internationally accepted foundation method, which had not only passed its acid test on all continents but enjoyed great popularity thanks to numerous publications on very different fields of application. In 1973, Breth described in a German publication on nuclear reactor safety the importance of vibro compaction to reduce the liquefaction potential of saturated sands during earthquakes. At the same time, interesting studies and field trials on vibro replacement stone columns were carried out in California in conjunction with the foundation of a sewage treatment plant (Engelhardt and Golding, 1973). The investigations were performed to study the behaviour of stone columns in a seismic environment. The findings were indeed very encouraging and extended the field of application of the method considerably. It was demonstrated that vibro replacement stone columns provide very effective drainage paths helping to reduce the excess pore water pressures that normally develop in saturated soils during a seismic event. Due to their large shear resistance, the stone columns can also safely carry the horizontal loads that develop during an earthquake as a result of the horizontal ground acceleration. Figure 2.15 shows a picture of a horizontal load test to identify the stone column's shearing resistance. Subsequently numerous foundations employing the vibro compaction and replacement methods were carried out in the seismic zones of Europe, North America, Africa and Asia and have performed successfully since.

## 2.5 Method improvements

During the first years after the war the vibro flotation method continued to use the rather ponderous wooden gantries that travelled on rails and from which the vibrators were suspended and operated by standard rope winches (Figure 2.4). Soon, however, this slow setup was replaced by standard crawler cranes and, for moderate compaction depths, by purpose-built lifting gear, the so-called vibrocats (Figure 2.16), which resulted in a considerably better output. With the increasing application of the vibro

*Figure 2.15* Preparation of a horizontal load test on vibro stone columns

replacement stone column method it was found that the vibrator would not penetrate fast enough into cohesive soil with relatively low water content. A remedy was found initially by increasing the weight of the extension tubes of the vibrator. But the additional load increment was rather limited. Only after the vibrocats were modified and improved in such a way as to allow a downward thrust to be effected on the vibrator was this handicap eliminated and satisfactory performance also achieved in these soils. This new setup provided a considerably improved process security and enhanced productivity when compared with the crane-hung method, and this was welcomed for technical reasons by supervising engineers, and for economical reasons by specialist contractors.

The construction of a stone column, using the dry top feed method, requires the vibrator to be completely withdrawn from the ground to allow the stone or gravel to be filled in scoops into the hole created by the vibrator.

*Figure 2.16* First generation vibrocats, 1956

This modus operandi reaches its limit in very soft, saturated soils when the vibrator hole tends to collapse immediately after the vibrator has been withdrawn from the ground. In these circumstances hole stability can be obtained by using water which emanates from the vibrator point creating an annular space around the vibrator, through which the backfill material can be fed into the hole. The coarse backfill sinks to the bottom of the hole where it is compacted by the vibrator which is withdrawn in stages from the ground. The flushing water is loaded with soil particles and flows back to the top of the hole from where it needs to be channelled away from the compaction point generally into a settling pond. Sludge handling and water treatment to allow its safe return into the environment can be time-consuming and expensive. However, this wet method is still being used today whenever the local conditions permit.

A major breakthrough was achieved when, in 1972, a patent was registered for the bottom feed vibrator. It allows the stone backfill to be

channelled via special piping in the extension tubes, at the outside of the vibrator, and supported by compressed air to be released directly at the vibrator point. The vibrocats were adapted for the new requirements and a special material lock was subsequently developed that allowed the stone backfill to be fed in a controlled way into the extension tubes now acting as material containers. The advantages of the improved method were soon fully realised and were so convincing that the wet method for stone column installation was almost completely replaced by the new bottom feed method. It was not only the sludge-handling problem that was responsible for this development, it was also the new concept itself, which enabled for the first time a safe – and even for critical users visible and verifiable – construction of an uninterrupted stone column. Hitherto occasionally occurring discontinuities or even interruptions in stone columns, which had caused excess settlements, were a key reservation that critics raised against the method. Not only did clients and their consultants welcome the new bottom feed method, but also the practitioners on sites, because by the new method the quality of stone columns was substantially increased without increasing the accompanying controls.

After the main patent rights to the vibrator elapsed at the end of the 1960s, other specialist contractors, especially in Germany, started designing and constructing their own vibrators. Because hydraulic motors had gained general acceptance in the design of construction equipment, it was not surprising that hydraulic drives were also used for these vibrators. Above all, it was the aim of the designers to increase the stamina and endurance of the vibrator for its rough usage on sites. Nevertheless, design and development targets for the improvement of vibrator performance were – and are still today – not at all equal among the few companies specialised in the manufacture of vibrators. And it is interesting to see that very little has been published so far about their key characteristics. It is generally accepted today that an optimal ground improvement can only be achieved by an optimal choice of the compaction equipment.

## 2.6 Design aspects

Although densification of clean sands by vibro flotation is the oldest form of deep vibratory compaction no computational design method has yet been developed. As the degree of density in a given sand achieved by vibro compaction depends on the distance between compaction centres, the vibratory energy consumed and the characteristics of the vibrator itself, it is common practice to determine the necessary probe spacing for the required density by field trials. Correlations of direct and indirect in-situ density measurements with the deformation modulus form the basis of settlement predictions. Seed and Booker (1976) and later on Baez (1995) developed certain design principles for the application of vibro compaction or stone columns to reduce the liquefaction potential of sands in seismic areas.

During the 1970s, the use of vibro replacement stone columns depended very much on the experience gained from numerous projects. As the interest in the method increased with more scientifically orientated engineers, field experience was increasingly complemented by design approaches to predict bearing capacity and deformation behaviour of stone columns. Numerous publications on the subject reflect this development during the 1980s. Stone columns improve the ground because they are stiffer than the soil that they replace. Their stiffness depends on the characteristics of both the soil and the stone column material. Although their interaction under load is very complex, reasonably accurate computational methods for predicting settlements do exist for the simple case of the infinite grid of stone columns. Priebe proposed a simple, semi-empirical method in 1976, which he then refined and adapted to better match reality in later years, for the last time in 2003, when he extended his method and formulae into extremely soft soils (Priebe, 1976, 1987, 1988, 1995, 2003). This and other methods have in common the fact that they are not applicable for small groups of stone columns, a case which is of great practical importance. We will see later in this book that this gap is being closed today by numerical methods for the calculation of the bearing capacity and settlement behaviour of stone column groups.

On site, a fully controlled and instrumented construction process of the deep vibratory method is today – more than 70 years after it was for the first time introduced in Germany – as important as is an efficient verification of the success of the soil improvement itself. The flexibility and versatility of the method has widened the spectrum of its use not only geographically but even more so from a technical point of view. It is environmentally completely neutral as it uses only inert and chemically inactive materials, and an overview of its seven decades of history is not just nostalgia but, as will be shown in the following, opens up interesting perspectives for its further development.

# 3 Vibro compaction of granular soils

## 3.1 The depth vibrator

The design principles of modern depth vibrators have little changed since the time they were invented and then further developed to suit the needs of practical use on sites. The vibrator is essentially a cylindrical steel tube with external diameters ranging between 300 mm and almost 500 mm, containing internally as its main feature an eccentric weight at the bottom, mounted on a vertical shaft which is linked to a motor in the body of the machine above. The length of the vibrator is typically between 3 m and 4.5 m and its weight ranges from 1500 kg to about 4500 kg. Figure 3.1 displays these features in a cross-sectional presentation.

When set in motion, the eccentric weight rotates around its vertical axis and causes horizontal vibrations that are needed for the vibro compaction method. The dynamic horizontal forces are thus applied directly to the surrounding soil through the tubular casing of the vibrator, with the machine output remaining constant regardless of the depth of penetration; this is the key factor distinguishing vibro compaction from other methods employing vibratory hammers with their vertical vibrations.

A flexible, vibration dampening device or coupling connects the vibrator with follower tubes of the same or slightly smaller diameter providing extension for deep penetration into the ground. These tubes contain water and power lines for the motor, occasionally also air pipes for jets located at the nose of the vibrator and at opposite sides generally just above the coupling.

Motor drive is either electric or hydraulic, powered by a generator or power pack which is generally mounted as a counterweight on the rear of the suspending crane. Common power ratings of vibrator motors are between 50 kW and 180 kW with the largest machines developing up to 220 kW. The rotational speed of the eccentric weight, which can also be split into two or more parts for structural reasons, is with electrically driven machines determined by the frequency of the current and the polarity of the electric motor. A 50 Hz power source results in a 3000 rpm or 1500 rpm rotational motion with a single or double pole drive. When operating at 60 Hz, the rotational speed is 3600 rpm or 1800 rpm respectively.

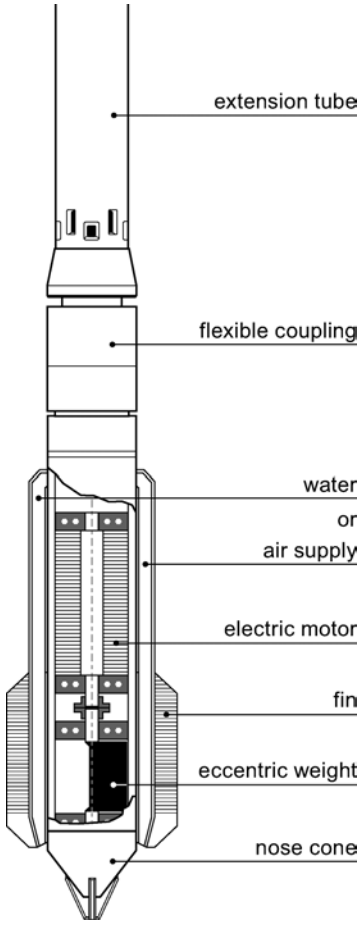


*Figure 3.1* Cross-section through depth vibrator

The width of the horizontal oscillation 2*a*, or double amplitude, is linearly distributed over the length of the vibrator (see Figure 3.2). It is zero at the vibrator coupling and reaches its maximum – typically between 10 mm and almost 50 mm – at the point or nose cone of the freely suspended vibrator when operating without any lateral confinement. This is also the point of maximum acceleration $a \cdot \omega^2$ at the vibrator surface, which can reach over 50 g.

The centrifugal force $F$ is resulting from the rotational speed $\omega$ of the eccentric weight with the mass $M$ and an eccentricity of $e$, and acts as lateral impact force on the surrounding soil causing its compaction.

$$F = M \cdot e \cdot \omega^2 \tag{3.1}$$

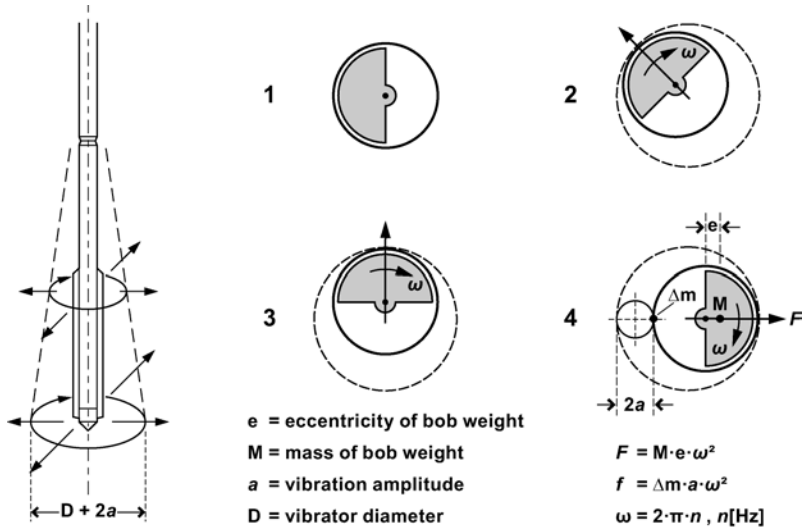


*Figure 3.2* Principle of vibro compaction and vibrator accelerations in horizontal plane

The centrifugal force $F$ ranges between 150 kN for smaller vibrators and over 700 kN for the heaviest depth vibrators. When the machine is in normal working conditions it is restrained by the ground and oscillation amplitudes and surface accelerations are much less despite the constant centrifugal force $F$.

Table 3.1 provides an overview of vibrator and motor characteristics of depth vibrators in use today. Hydraulically driven vibrator motors had until recently certain operational advantages because any desired frequency changes are relatively easily effected. However, operational faults may cause unwanted oil spills posing a potential hazard to groundwater and soil unless biologically degradable hydraulic oil is used.

When the vibrators are in operation, the ground response causes – as well as the dampening of acceleration and oscillation width – a certain reduction in operational speed of the vibrator motor. This reduction is generally less with electric motors where it reaches up to 5% corresponding with the slip in asynchronous motors. More recently, electronic control technology by frequency converters has made it possible to operate electrically driven depth vibrators at variable speeds. In order to avoid the otherwise loss of lateral impact force when reducing rotational speed, designers have developed special divisible eccentric weights that increase their eccentricity substantially when reversing the rotational direction to continue compaction at reduced speed.

One of the key objectives of machine design, besides keeping wear and tear low and repair costs within economically acceptable limits, is to

*Table 3.1* Selection of curently available depth vibrators (2009)

| *Specialist contractor* | *Machine type* | *Length (m)* | *Diameter (mm)* | *Weight (kg)* | *Power rating (kW)* | *Operating frequency (Hz)* | *Centrifugal force (kN)* | *Double amplitude (mm)** | *Special features* |
|---|---|---|---|---|---|---|---|---|---|
| Vibroflotation | V10 | 2.73 | 248 | 820 | 70 | 60 | 150 | 10 | el, c |
| Soletanche Bachy | V23 | 3.57 | 350 | 2200 | 130 | 30 | 300 | 23 | el, c |
| (Vinci Group) | V48 | 4.08 | 378 | 2600 | 175 | 25 | 472 | 48 | el, c |
| Keller | MB1670 | 3.20 | 315 | 1700 | 70 | 50–60 | 157–226 | 7 | el, v |
| (Keller Group) | MB1650 | 3.20 | 315 | 1700 | 55 | 50 | 157 | 7 | el, v |
| | S340/34 | 3.10 | 421 | 2900 | 120 | 30 | 340 | 29 | el, c |
| | S700 | 4.30 | 490 | 4400 | 180 | 25 | 742 | 50 | el, v |
| | | | | | | 38 | 690 | 15 | |
| Bauer | TR17 | 3.30 | 298 | 1400 | 112 | ≤53 | ≤193 | 5 | hyd, v |
| (Bauer Gruppe) | TR75 | 4.20 | 406 | 2580 | 235 | ≤33 | ≤313 | 11 | hyd, v |
| Pennine | HD 130 | n/a | 310 | 1850 | 98 | 50–60 | 140–202 | 16 | hyd, v |
| (Balfour-Beatty) | HD 150 | n/a | 310 | 2250 | 130 | 50–60 | 200–288 | 22 | hyd, v |
| | BD 300 | n/a | 310 | 2575 | 120 | 30–36 | 175–252 | 28 | hyd, v |
| | BD 400 | n/a | 400 | 4400 | 215 | 30–35 | 310–426 | 34 | hyd, v |

c = constant operational frequency
v = variable operational frequency
el = electric drive
hyd = hydraulic drive
* = at vibrator point

maintain substantial amplitude in the ground. This depends on the interaction of vibrator characteristics and soil response – a complex problem especially with soil constraints differing not only from site to site, and with depth on the same site, but also with compaction time at any given depth. It is therefore desirable to know as precisely as possible the operational condition of the vibrator at any time and depth during compaction. The specialists working in this field have developed registration and control devices that record a multitude of parameters as a function of time:

- depth of the vibrator;
- amperage or oil pressure as a measure of the power output;
- operational frequency;
- air or water flow pressure.

Visual display and recording of these working parameters is today essential and allows the operator to perform the compaction work in an orderly, repeatable and verifiable manner. Temperature measurements at selected locations within the vibrator motor can also serve as motor protection in extreme working conditions.

The outer surface of the depth vibrator is subjected to strong abrasive forces from the surrounding soil. They are particularly severe for broken quartz particles but less so when rounded calcareous material is encountered. Aggressive groundwater, and indeed seawater, accelerate corrosion and may require special attention. For these reasons the vibrator is generally protected by special wearing plates or other protective means on its outside.

The efficiency of the vibratory systems, when working on site, is very important and all potential problems leading to unwanted interruptions of the construction process need to be scrutinised. A special connection of the electric cable leading to the vibrator motor was therefore developed to avoid the otherwise rather time-consuming process of a vibrator change in deep penetrations where the heavy cable has to be drawn through the complete length of the extension tubes. This cable connector is of the same diameter as the depth vibrator, is capable of transmitting an electric currenct of 600 A at 400 V, is waterproof up to 10 bar and is situated just above the vibrator coupling.

The instrumentation and control systems in combination with GPS-based setting out of the compaction probes represent only a first step which eventually will lead in future to a fully automated vibro compaction process. The elements of such technology do already exist and, to some extent, are already being used on sites with modern equipment. However, current labour laws and safety regulations are still prohibitive for its practical realisation and introduction in most countries.

## 3.2 Vibro compaction treatment technique

### *3.2.1 Compaction mechanism of granular soils*

Clean sands in loose to medium dense states are densified as the particles become rearranged more closely. The resulting degree of volume reduction depends on the characteristics of the vibrations, the soil properties and the duration of the compaction process. In these soils, the practical depth of efficient surface compaction by powerful vibratory rollers is limited to about 1.5 m. When deeper sand deposits need densification, deep compaction methods using depth vibrators are normally used. In contrast to surface compactors and vibratory hammers, depth vibrators agitate the soil by horizontal vibrations.

With increasing radial distance from the vibrator the ground vibrations are attenuated by the forces acting between the soils particles. Compaction is therefore only possible when their frictional contact is broken by overcoming the residual frictional strength of the soil. Only then will the soil particles rearrange themselves to find a state of lower potential energy, i.e. from loose to dense. For this purpose a minimum dynamic force is required with a dependent acceleration sufficiently high to break the soil strength. Where, despite continuing transmission of attenuated weak vibrations, the resisting forces within the soil prevent further compaction there is a limit to how far from the vibrator effective vibrations reach.

It has been found that the stability of the structure of granular soils is destroyed by dynamic stresses when a critical acceleration of over 0.5 g is reached. With increasing accelerations the shear strength of the sand decreases until it reaches a minimum between 1.5 g and 2 g. At this point the soil is fluidised, and a further increase of acceleration causes dilation. Figure 3.3a shows the idealised relation between shear strength of the soil and the induced acceleration.

In a stage of fluidisation, the shear strength of the soil is reduced but not eliminated completely. Therefore vibrations, although of course dampened, can be transmitted through this zone where particle contacts are continuously broken and remade. As the acceleration transmitted from the vibrator decreases with increasing distance from its source several annular density zones surrounding the vibrator can be defined as is shown in Figure 3.3b.

In water-bearing soils, fluidisation occurs principally when the rate of the pore water pressure increase that is induced by the vibrations exceeds the rate of dissipation, until this pressure overcomes the normal pressure acting between the particles. It may also occur in dry soils by the action of water jetting or when the upward-directed vertical component of acceleration exceeds gravity. As modern machines easily produce accelerations in excess of 10 g fluidisation is induced in the vicinity of the vibrator normally as a combination of the two effects. Soil instability directly caused by the action

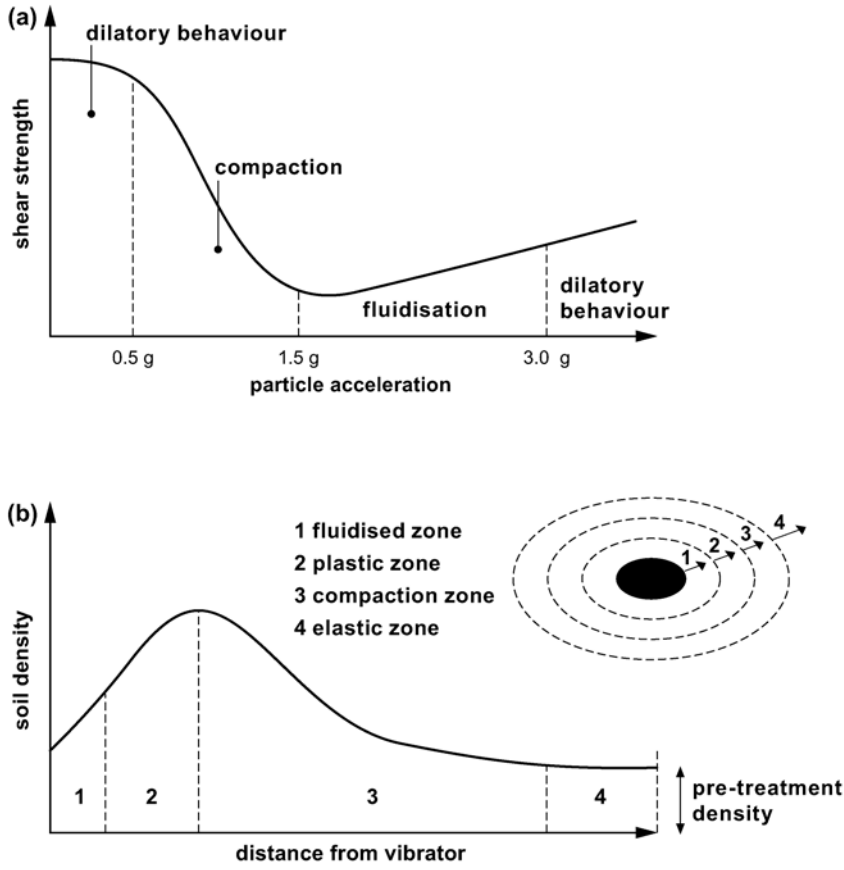


*Figure 3.3* Idealised response of granular soils to vibration (after Rodger, 1979)

of acceleration in dry soils is referred to as fluidisation, whereas in saturated soils the vibrator-induced oscillations cause liquefaction depending on pore fluid pressure.

Soil properties that influence the vibro compaction process are:

- initial density
- grain size
- grain shape and grading
- specific particle gravity
- depth (influencing inter granular and normal stress level)
- permeability.

Essential vibrator characteristics influencing compaction are frequency, amplitude and acceleration of the induced oscillations and out-of-balance

force. And finally the duration of the vibration also influences the degree of compaction achieved.

Interpretations suggest that the fluidised zone, which is characterised by minimum shear strength, is a measure of the soil's transmissibility of vibrations and thus is responsible for the radius of influence of the vibratory treatment. In the transitional or plastic zone, the dynamic forces are not sufficient to fluidise the soil but still strong enough to shear the soil particles from each other at such a rate that they can find a closer packing. From the point of maximal achievable density (Figure 3.3b) attenuation of vibration occurs until it reaches certain threshold shear strength in the ground where any further compaction is inhibited. Water saturation reduces the effective stresses and therefore increases the radius of the compaction zone. It is for this reason that in dry soils the use of flushing water and even flooding of the whole site extends the radius of compaction.

Practical experience gained from construction sites, where depth vibrators with different compaction frequencies were working side by side, has shown that sand can generally be most effectively compacted by vibrating frequencies that are close to what we might call their natural frequency. For this reason, specialist contractors have developed vibrators capable of compacting granular soils using frequencies as low as 25–30 Hz. Occasionally the accompanying reduction of centrifugal force with frequency was found to be advantageous in optimising the compaction effect.

Theoretical study of these observations – both surface and deep compaction – that treat vibro compaction as a "plastic–dynamic problem", confirm some fundamental findings that have been acquired in practice under operational conditions: i.e. at constant impact force the effective range of the vibrations increases with decreasing vibrator frequency, whereas the degree of compaction increases with an increasing impact force. The studies generally aim to develop some kind of on-line control of the vibro compaction by continuously evaluating information obtained from the vibrator movements during compaction. Fellin (2000) suggested making simultaneous measurements of horizontal acceleration in two orthogonal directions at the vibrator tip and coupling. These would, together with the phase angle $\Phi$ of the rotating mass completely describe the vibrator motion when working in the ground. This information could indeed eventually provide the operator with valuable information to better control and direct the compaction work on site. So far, this additional vibrator instrumentation has only been realised in exceptional cases to support special investigations and scientific research programmes.

The study of surface compaction using vibratory rollers also shows an optimal compaction of the soil at its resonance frequency which will generally be between 13 Hz and 27 Hz. These findings compare favourably with the experience obtained from vibro compaction projects indicating that sand and gravel are compacted best by using agitating frequencies of below 30 Hz which are close to their natural frequency.

Model tests carried out in saturated sand also indicate that resonance of the vibrator–soil-system could lead to optimal compaction of the surrounding soil. However, in practice, the control of resonance at any point and time during compaction requires sophisticated on-line measurement of vibrator data such as the phase angle $\Phi$ between the position of the rotating mass and the vibrator movement and its control during compaction by changing the vibrator frequency $f$. Figure 3.4 gives the principle of the slip angle measurement, which would form the basis of this control mechanism, with $\Phi = \pi/2$ at resonance. The complexity of such an undertaking in practice becomes evident when remembering the interdependency of vibrator performance characteristics and soil properties with time during compaction.

Today, numerical simulations of the vibro compaction process can also help to better understand this method. It is a well-established fact that granular soils can be better compacted by repeated shearing rather than by compression, and that the degree of compaction achieved depends in the first place on the shear strain amplitude. If the induced strain is too low the minimum density cannot be reached even with very large numbers of load cycles; conversely with large strain amplitudes optimal densification may not be obtained owing to the effects of dilatancy of the sand.

Based on these principles, a three-dimensional finite element model was

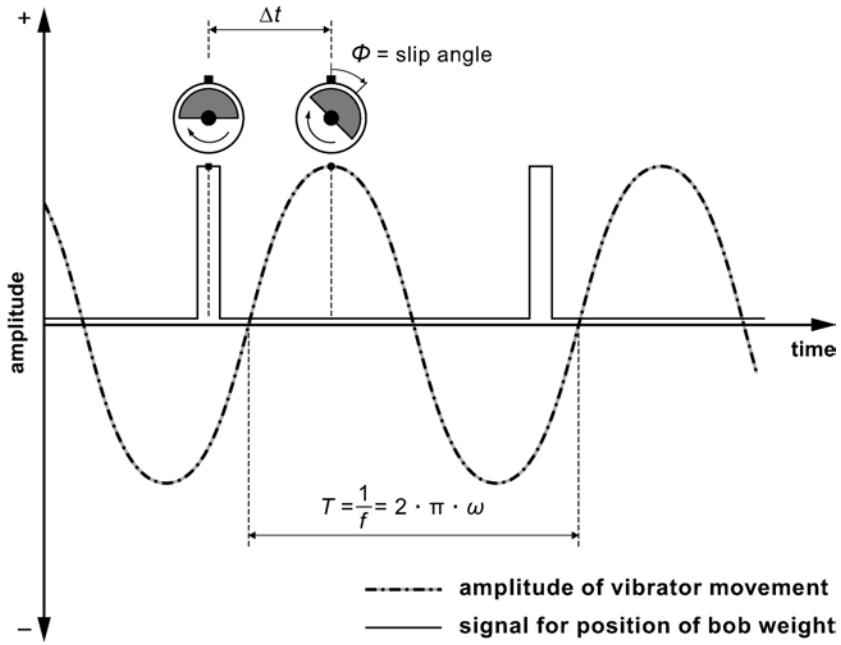


*Figure 3.4* Principle of slip angle measurement for resonance control (after Nendza, 2006)

recently developed using quartz sand with an initial void ratio of 0.85, a dry density of 1.43 g/cm$^3$ and a particle density of 2.65 g/cm$^3$. A disc-shaped element, 0.5 m high and with a radius of 15 m, at a depth of 15 m below surface was modelled. The movement of the vibrators (both a depth vibrator and a top vibrator or vibratory hammer) were simulated using boundary conditions at the surface of a cylindrical hole in the centre of the disc. The frequency was chosen as 30 Hz with amplitudes of 7.5 mm, horizontal for the depth vibrator and vertical for the vibratory hammer. By observing the evolution of the void ratio with increasing numbers of strain cycles, three zones were distinguished surrounding both types of vibrators. In the first zone, immediately surrounding the vibrator – radial distance $r$ smaller than 0.5 m – compaction was finished after a few cycles without reaching the minimum void ratio. It is believed that, owing to the relatively large strain amplitudes prevailing within in this zone, dilatancy and contractancy balance each other, resulting in a relatively small volumetric change or densification. In the second zone, which extends from 0.5 m to 3 m the compaction works best. Strain amplitudes are too small to create dilatancy, allowing the soil to compact. However, with increasing distance from the

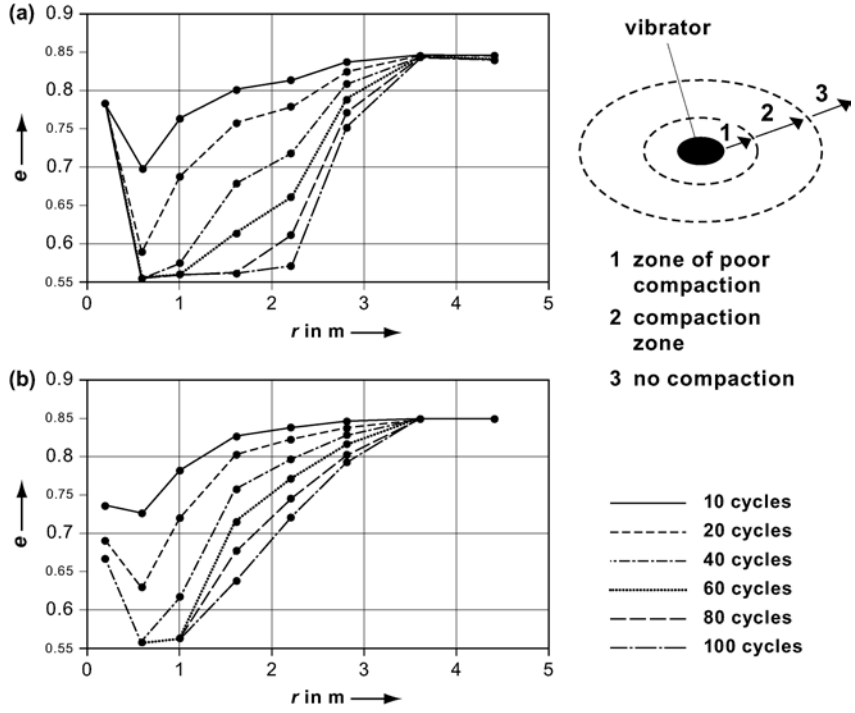


*Figure 3.5* Development of void ratio $e$ as a function of the distance $r$ from the source of vibrations (a) for a depth vibrator, (b) for a top vibratory hammer (from Arnold *et al.*, 2008)

vibrator, more stress cycles are required to achieve measurable densification before, in zone 3, at a distance of more than 3 m, the strain amplitudes are too small to overcome the inter-granular stress level, so no compaction is achieved.

The numerical model not only supports the qualitative findings described above and as shown in Figure 3.3, it also ties in well with the experience gained on site, particularly that compaction time plays an important role in extending the radius of influence of this zone. Figure 3.5 shows the void ratio development with increasing strain cycles as a function of the distance from the vibrator axis. Although the model predicts too fast a compaction rate when compared with field application, probably due to simplifying assumptions of the model, it highlights the importance of multidirectional shearing in achieving an optimal compaction. While with the depth vibrator the minimum void ratio in zone 2 extends from 0.5 m to 2.2 m after 100 cycles, this zone reaches only 0.5–1 m for vibratory hammers, simply because the depth vibrator compacts the soil by multiaxial shearing, while the vibratory hammer compaction turns out to be a completely radial symmetric phenomenon resulting in much less multidirectional shearing; this explains the known superiority of depth vibrators in the practice of deep soil compaction.

It is hoped that the findings of newer research work to better understand the complexity of the compaction of granular soil will eventually help to further modernise this technology particularly by obtaining information on the compaction process achieved directly from certain vibrator parameters measured during compaction.

### *3.2.2 Vibro compaction in practice*

With the machine running, if the lower water jets are switched on this assists penetration under the weight of the vibrator and its extension tubes. At this stage, the jetting water needs to be only at moderate pressure albeit relatively high volume, sufficient to transport loosened sand to the surface through the annulus between the vibrator and the surrounding soil. This material flow allows the vibrator to sink. It is advantageous to maintain a balanced outflow at the surface. Any temporary excess pore water pressure is quickly reduced, again as a result of the high permeability of the granular material in which the compaction work is being carried out. In dry sand any existing local effective stresses or even slight consolidations from cementation are quickly released and overcome by water saturation and by the shear stresses emanating from the vibrator.

For very deep compactions in excess of 20 m (Figure 3.6) it may be necessary to attach additional water lines with jets at intervals along the extension tubes, or to apply compressed air to maintain or to support the upward water velocity within the annulus against the water losses by seepage from the hole. Should no flushing medium be used in dry sand

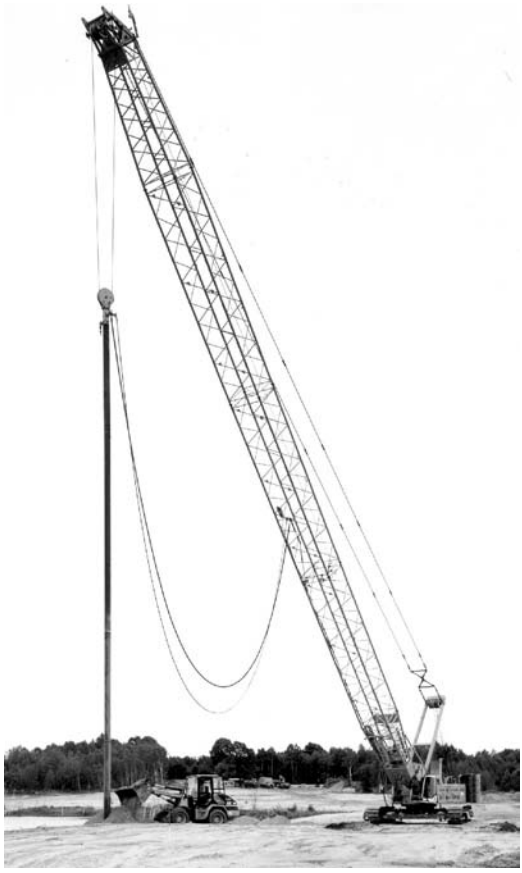

*Figure 3.6* Crane-hung depth vibrator, rigged up for 40 m compaction depth (by courtesy of Keller Group plc)

during the penetration phase, compaction of the material surrounding the vibrator will eventually tighten the soil to such an extent that penetration is stopped. This phenomenon depends – besides the soil properties – mainly on the characteristics of the vibrator. Sinking or penetration rates are generally 1–5 m/min. It is during this penetration stage that the vibrator tends to twist to a certain extent, although fins are generally attached to the vibrator (Figure 3.1) to prevent or at least reduce this behaviour, which is the result of the rotational movement of the eccentric mass. Twist, if necessary, can be adjusted by removing the vibrator completely out of the ground or, with certain vibrator types, by changing the rotational direction upon reaching the final penetration depth.

When the vibrator attains the design depth, the penetration aids (water and air) are usually switched off or reduced considerably. High pressure, low volume horizontal water jets situated near the vibrator coupling are

now switched on with the aim of undercutting the sand at the sides of the bore and at making it to fall to the vibrator tip, thereby providing a sufficient volume of sand to be compacted. Ideally the water flow should also be strong enough in terms of volume to maintain a stable bore, balancing any water losses along the bore and at the surface.

Compaction occurs as the vibrator is slowly withdrawn from the ground. It is important at this stage that the vibrator maintains a good and permanent contact with the surrounding soil. When this contact is lost the vibrator motions may become irregular resulting in insufficient compaction. For better operational control, compaction is normally done in stages of 0.3–1.0 m maintaining the machine steady at each level either for a predetermined time or until monitored vibrator data indicate sufficient compaction having taken place (i.e. power consumption of the electric motor or oil pressure of the hydraulic engine). These time intervals are generally between 30 to 90 seconds depending on the characteristics of the soil, the required degree of compaction and the characteristics of the vibrator used.

Whatever the individual operational modes of the specialist contractors may be, it should be remembered that effective compaction requires time and that the unwanted lowering of the machine during the compaction stage may give rise to increased power demand and to a false indication of satisfactory compaction. Densification of the sand surrounding the vibrator causes a reduction of the pore volume, which must be compensated either by extracting it from the material to be compacted, or by introducing imported suitable backfill into the bore from the surface. When no imported sand fill is used and the sand surface is allowed to settle as a result of densification, the surface settlement may reach up to 15% of the compaction depth depending on the original density and the degree of compaction achieved. Independent of the operational mode, an effective regulation of the water flow in the annulus is important. Falsely arranged side jets and badly controlled jetting volumes often lead to the wrong assumption that only by the addition of coarse backfill, which tends to sink more rapidly, can too slow compaction be avoided.

When the cycle of lowering the vibrator to design depth and subsequent stage-by-stage compaction is completed, a new compaction probe can be commenced by repeating the procedure described. The compaction process so carried out leaves behind a compacted sand column of enhanced density, with a dense core followed by material of decreasing density as the distance from the centre increases. The diameter of such a column ranges typically between 3 m and 6 m depending on the characteristics of vibrator and soil. By arranging the individual compaction points in a grid-like fashion, almost any surface configuration can be treated to the desired depth, both from the dry and off shore.

The distances between compaction points in an equilateral triangular pattern are normally 2.5–5.0 m, and this can cover areas of up to 15 $m^2$ for each compaction probe. In this way, up to 20,000 $m^3$ of sand of a favourable

grading (zone B in Figure 3.11) can be compacted within a 10-hour shift with a single vibrator operation. When double vibrators (Figure 3.7) can be employed, the production output can be almost doubled.

Typically, for large compaction volumes the depth vibrators would be suspended from a heavy crawler crane, which also carries an electric generator at its rear. For economic reasons it may be advantageous to operate more than one vibrator from one base machine. In this way, up to six vibrators have been used simultaneously, carried by a specially designed frame for compaction over water. However, this kind of operation is restricted for practical reasons to a compaction depth of about 25 m. This depth range also represents the maximum depth for the majority of applications. Only in particular circumstances – as were prevailing during the rehabilitation of the derelict open pit brown coal mining areas in Lusatia, Germany – might deeper compaction, in excess of 50 m, become necessary.

*Figure 3.7* Crane-hung twin vibrators for underwater compaction (by courtesy of Keller Group plc)

As a result of both the vibrator shape and the much-reduced lateral soil pressure close to ground level, densification by the vibro compaction method is generally less effective in the upper 1–2 m below working grade level. If required by the foundation level, this layer therefore needs additional compaction by standard surface compactors before construction work commences.

## 3.3 Design principles

### *3.3.1 General remarks*

The foundation of structures on sand was, for centuries, regarded as a treacherous undertaking, and even today any constructor who intends to build on sand should also beware of sudden settlement of foundations caused by ground vibrations which may be activated by reciprocating man-made and natural impacts from such effects as traffic, vibrating machinery, earthquakes and even wave action. A sufficient knowledge of the characteristics and behaviour of the sand – a clean free-draining granular soil – is prerequisite of any design attempt aiming to describe its compressibility under load, its shear strength or its permeability.

Granular soils are characterised by distinctive features that determine their behaviour under load. Vibratory deep compaction is mainly concerned with the improvement of the mechanical characteristics of sand. According to the Unified Soil Classification System (USCS) sands contain over 50% of coarse-grained particles of diameters larger than 0.074 mm, with more than half of the coarse fraction being smaller than 4.75 mm. Clean sand should not contain more than 5% of material which is finer than 0.074 mm. Further subdivisions are made with regard to the nature (silt or clay) of the fine-grained material with grain sizes below 0.074 mm as is shown in Figure 3.8.

Sand is the product of mechanical abrasion of larger stones and boulders during its transport and redeposit. Its geological origin is generally alluvial or glacial, transported by rivers and streams or melt waters flowing from glaciers, sometimes followed by secondary transport process by wind, and finally deposited as sediment. Its most frequent mineral is silica, $SiO_2$, crystallised as tetrahedron, forming quartz and having a grain density typically of 2.65 g/cm$^3$. It is of some importance whether or not the sand deposit was subjected to glacial loading after its sedimentation, since most mechanical properties of the sand are a function of loading stage or stress history.

The mechanical properties of the sand deposit are also influenced by its grain characteristics such as size, shape and surface of the particles. Depending on the length of their transportation, sand grains are more or less intensely rounded. In sand, all particles are in contact with each other without any bond or cohesion. Grain packing measured by the relative amount

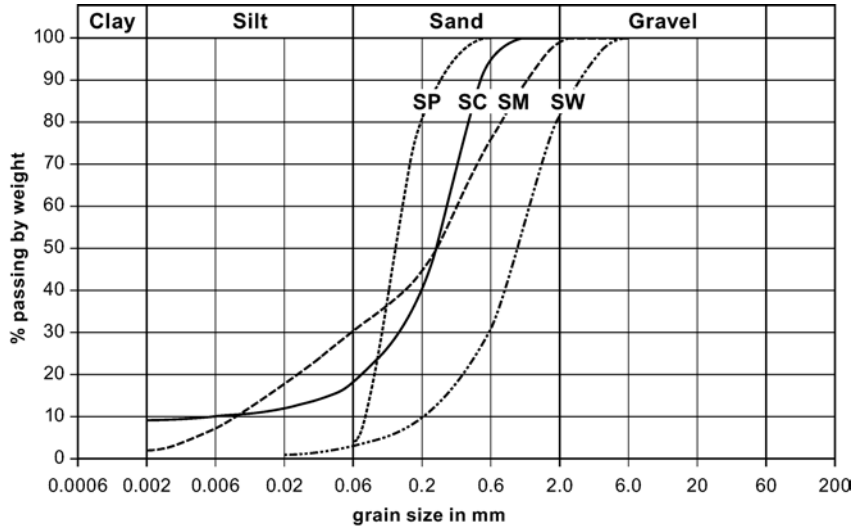


*Figure 3.8* Grain size distribution curves of sands (SW, well graded, clean sand, fines content <5%), SP (poorly graded, clean sand, fines content <5%), SM (silty sand, fines content >12% is mainly silt) und SC (clayey sand, fines content >12% is mainly clay)

of voids influences the strength and compressibility, the key mechanical properties of the sand. Two different ratios, the porosity $n$ and the void ratio $e$, describe the volume of voids, $(V - V_s)$, in relation to the total volume, $V$, and to the volume of solids, $V_s$, respectively. The following equations (3.2) describe this relationship.

$$n = (V - V_s)/V \qquad e = (V - V_s)/V_s$$
$$n = e/(1+e) \qquad e = n/(1 - n) \tag{3.2}$$

An idealised sand material consisting of spherical grains of equal diameter can be deposited in two extreme arrangements having a porosity of between $n_{min} = 0.259$ and $n_{max} = 0.476$ or void ratios of $e_{min} = 0.352$ and $e_{max} = 0.924$. These boundaries mark what is called the densest and the loosest packing stage of the deposit. All intermediate stages with porosities $n$ or void ratios $e$ are characterised by their density $D$ or relative density $D_r$:

$$D = \frac{n_{max} - n}{n_{max} - n_{min}} \qquad D_r = \frac{e_{max} - e}{e_{max} - e_{min}} \tag{3.3}$$

$D_r$ values are slightly larger than $D$, but describe substantially the same thing.

Accordingly the loosest and the densest stages are defined by a relative density of $D_r = 0\%$ and $D_r = 100\%$ respectively. In reality, sand deposits consist of a variety of grain mixtures with boundaries for the loosest and the densest stages falling into the following ranges:

$$n_{max} = 0.39 \ldots 0.46 \qquad e_{max} = 0.64 \ldots 0.85$$

$$n_{min} = 0.25 \ldots 0.33 \qquad e_{min} = 0.33 \ldots 0.49$$

Minimum and maximum void ratios of sand are determined by well-defined laboratory tests. The loosest stage of density is achieved by carefully filling a cylinder with dried sand; to achieve the densest stage, the same cylinder is filled with sand while subjecting it to vibrations and static loading. Unavoidable imperfections of the testing procedures, plus the fact that the maximum compaction achievable in the laboratory is sometimes below that achieved by vibro compaction in the field, may result in relative densities $D_r$ in excess of 100%.

It is important to understand that all mechanical parameters describing the behaviour of sand, such as stiffness and strength or permeability, are directly related to its relative density. The modulus of elasticity of the quartz grain itself, for example, is about 1000 times higher than sand, even at its densest stage.

All forces acting on the soil such as gravity or additional loading are transferred by grain contacts. The contact points themselves are able to transfer normal and shear forces, the latter depending on the surface characteristics of the grains. If an idealised sand material is considered to consist of spherical grains of equal diameter, the loosest arrangement is hexahedral whereby each sphere has six contact points with its neighbouring spheres. In the densest stage the spheres form an arrangement which is characterised by 12 contact points with their neighbouring spheres, allowing considerably higher stresses per unit volume to be transferred with much less deformations.

As already mentioned the stiffness of a sand deposit depends on the prevailing stress level and therefore rises generally with depth and the relative density as shown in Figure 3.9.

*Table 3.2* Density and relative density of sand

| *Relative density $D_r$ (%)* | *Density D (%)* | *Description* |
|---|---|---|
| 0–15 | 0–15 | very loose |
| 15–35 | 15–30 | loose |
| 35–65 | 30–50 | medium |
| 65–85 | 50–80 | dense |
| 85–100 | 80–100 | very dense |

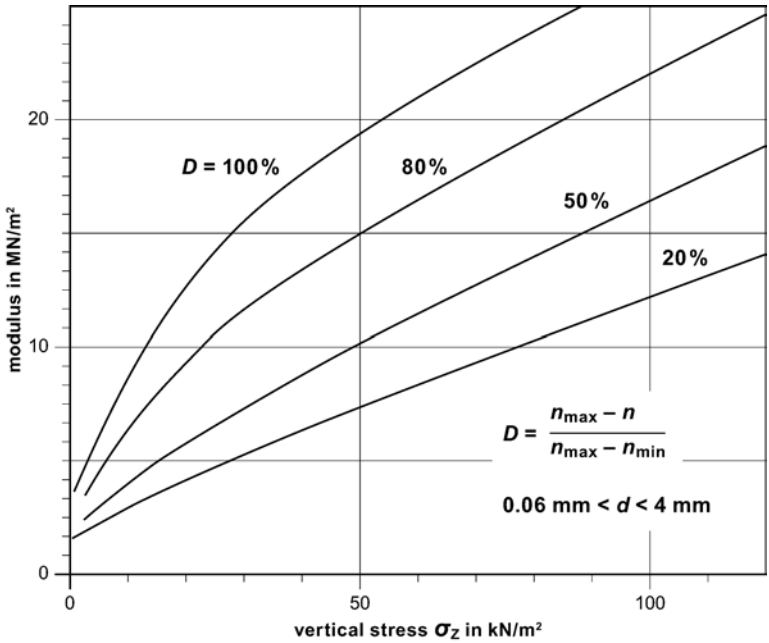


*Figure 3.9* Relationship between density $D$, vertical stress $\sigma_z$ and constrained modulus of sand (after Smoltczyk, 1966)

Beyond a certain threshold, all additional stresses acting on a granular soil are accompanied by a rearrangement of its grains and a non-reversible (plastic) deformation. Unloading of the soil leads to a stress relief and occurs without rearrangement of the grains and with considerably reduced reversed (elastic) deformations. Since this grain rearrangement requires the contact forces between the grains to be overcome, this process can be supported by the lubrication effect of water and by vibrations.

Whenever granular soils are subjected to shear stresses – and practically all loading contains a certain amount of shearing – the grains are forced to rearrange and to find a new stage of equilibrium that is best characterised by their relative density. Depending on the initial density, the applied shear strain can result in compaction or loosening of the sand specimen. This non-linear deformation behaviour of sand is shown in Figure 3.10.

As can be seen from Figure 3.10, dense sand tends to expand under shear stresses, an effect that is called *dilatancy*. We know from Coulomb's theory of friction that the transmissible shear force is a function of the normal force acting on the contact surface. Whenever this volume increase, or dilatancy, is restricted in the shear zone – for example by the adjacent soil – the normal stresses are higher thereby increasing the necessary shear forces.

Dilatancy of sand has considerable practical importance. It is, for example, responsible for the greater characteristic values of shaft friction to

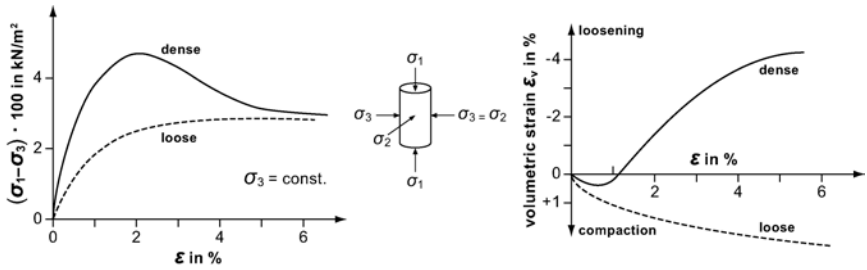


*Figure 3.10* Shear stresses in sand ($\varepsilon$ = plain strain, $\varepsilon_v$ = volumetric strain)

be used in the design for grouted micro piles in sand as compared with the relevant values for bored piles. In general, it is therefore of great economic benefit for almost all geotechnical problems where granular soils are involved to increase the density of natural and man-made sand deposits at least to a medium dense stage.

The design of structures on sand is therefore often concerned with one or a combination of the following features:

- reduction of settlement by increasing the deformation modulus;
- increase of bearing capacity by increasing the shear strength;
- decrease of liquefaction potential by increasing the density and/or the permeability.

Table 3.3 depicts the main characteristics influencing the density of sand that ultimately determine the key properties – modulus, friction angle and permeability – necessary for design. The direct or indirect measurement of the density therefore plays a decisive role in determining the need or otherwise for sand compaction and in any quality control measures.

*Table 3.3* Physical properties of saturated sand (guideline values)

| | *Very loose* | *Loose* | *Medium dense* | *Dense* | *Very dense* |
|---|---|---|---|---|---|
| Relative density $D_r$ (%) | <15 | 15–35 | 35–65 | 65–85 | 85–100 |
| $N_{SPT}$ (blows/30cm) | <4 | 4–10 | 10–30 | 30–50 | >50 |
| CPT $q_c$(MPa) | <5 | 5–8 | 8–15 | 15–20 | >20 |
| $N_{DPH}$ (heavy) (blows/10cm) | <5 | 5–10 | 10–15 | 15–20 | >20 |
| Unit weight (wet, above GWT) (MN/m³) | <14 | 14–16 | 16–18 | 18–20 | >20 |
| Constrained modulus $E_{oed}$ (MPa) | 15–30 | 30–50 | 50–80 | 80–100 | >100 |
| Friction angle $\varphi$ (°) | <30 | 30–32.5 | 32.5–35 | 35–37.5 | >37.5 |
| Shear wave velocity $v_s$ (m/s) | | <150 | 220 | 350 | 450 |

### *3.3.2 Stability and settlement control*

Natural sand deposits and artificially placed sand fill are likely to have a considerable variation of their key characteristics depending on the nature or method of placement, geological history and, as already explained, the distinctive features of the sand grains (mineralogical origin, size, shape, hardness and roughness). As we have seen, the potential increase of the fines content inhibits densification, and Figure 3.11 shows the broadly accepted range of grading suitable for vibro compaction as will be further discussed in Section 3.5.

Compressibility, shear strength and to some extent permeability depend primarily on the density of the sand, which is generally described by its relative density $D_r$ in terms of the void ratio or of the dry unit weight of the soil in the loose (L), dense (D) or natural (N) state. Figure 3.12 shows how the settlement of a sand deposit can be assessed based upon the principle of minimum and maximum void ratios.

What appears at first glance to be so simple a procedure turns out to be rather more difficult in practice, because the laboratory work involved in measuring minimum and maximum dry densities of the sand, and then collecting an undisturbed sand sample in the field, and the subsequent determination of its natural dry density, in the laboratory are subject to experimental errors. Not only is this procedure very much dependent upon the experience and accuracy of the soils engineer, it is also very time-consuming and comparatively expensive, particularly in water-bearing soils at greater depths. The direct measurement of relative density in greater depth is therefore today almost completely replaced by indirect methods

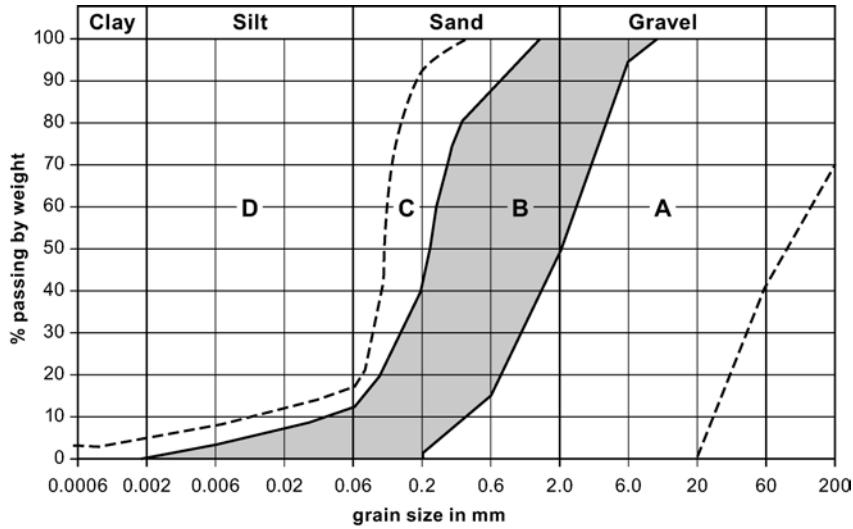


*Figure 3.11* Soil grading suitable for vibro compaction (after Degen, 1997b)

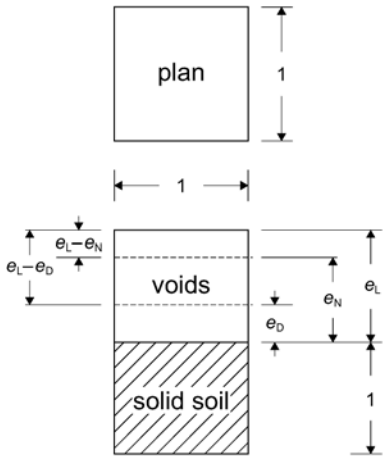


settlement of layer with thickness $H$:

$$s = \frac{e_L - e_N}{1 + e_L} \cdot H$$

total possible settlement of layer $H$:

$$s_T = \frac{e_L - e_D}{1 + e_L} \cdot H$$

$$\frac{s}{s_T} = \frac{e_L - e_N}{e_L - e_D} = D_r \text{ in \%}$$

$D_r$ = relative Density

*Figure 3.12* Settlement of sand (after D'Appolonia, 1954)

such as the various available penetration tests that can be approximately related to relative densities.

Table 3.3 gives approximate values for the strength properties of clean, predominantly silica sand, which can be useful for design purposes. However, it must be remembered that sand deposits, natural and artificial, generally vary widely in their properties both in depth and horizontal extension. Thorough site investigations together with precise and non-contradictory specifications for the densification of the sand are therefore indispensable.

Experience shows that a compacted free-draining granular soil has a relative density of at least 70% throughout, which is sufficient for foundation purposes under normal conditions and that any subsequent ground motions other than earthquakes are generally not strong enough to cause additional settlement. In the case of seismic events and exceptionally strong impacts from explosions or similar events the induced energies can be extremely high and a detailed study of the required density, which will often need to be in excess of 85% relative density, becomes necessary (see Section 3.3.3).

As we saw earlier the effectiveness of the vibro compaction process decreases with increasing distance from the centre of compaction, depending on a number of variables (vibrator characteristics, soil properties, operational modes). Figure 3.3b shows an idealised density profile for a single vibro compaction point at a selected depth. The decrease from a maximum in the neighbourhood of the centre is rather rapid at first, before it lessens in an exponential way as the distance increases and the original density is met. By arranging additional compaction points in regular patterns, practical experience shows that the density at the "weakest" point

within any chosen pattern increases broadly by the density increases of the adjacent probes for single probe behaviour at that distance. As it is common practice today that the specified minimum density for a project is to be met also at the weakest point of the pattern, this procedure generally provides an additional safety margin because, by definition, all other areas away from this point are then characterised by higher densities (see Figure 3.13).

The prime objective of vibro compaction treatment is to provide a zone of improved ground sufficiently dense beneath surface spread foundations. The settlements of spread footings such as individual pads, strips or smaller rafts are primarily controlled by the compactness of the ground immediately below the footings. Compaction points are therefore arranged beneath them as shown in Figure 3.14. Depth of treatment is very much dependent upon the development of the pressure bulb, according to elastic theory, generally about two or three times the minimum plan dimension of the footing. For

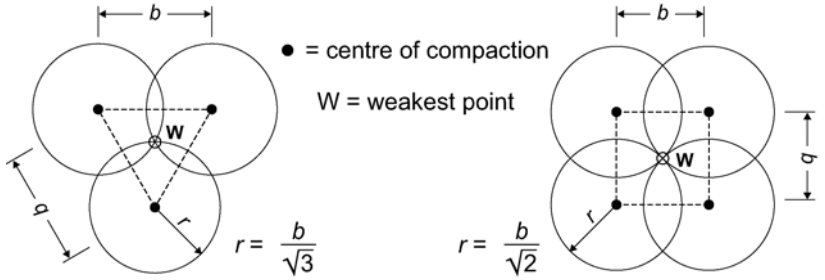


*Figure 3.13* Triangular and square compaction patterns

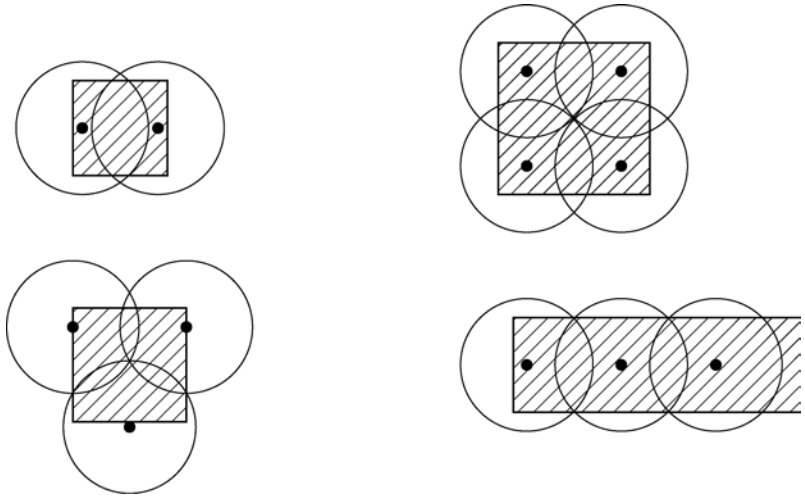

*Figure 3.14* Typical arrangements of compaction probes below isolated and strip footings

smaller rafts and closely spaced smaller footings the required depth may be somewhat deeper and may often need to reach 8–10 m. Determination of the vibro compaction probe spacing is either by experience from similar cases or by field trials. In view of today's diversity of available depth vibrators, design charts, as have been proposed and widely used in the past (D'Appolonia, 1954; Thorburn, 1975), are not to be recommended anymore. With modern machines, probe spacing can be increased to well over 3.0 m for clean sand, allowing safe bearing pressures in excess of 500 kN/m$^2$ with settlements less than 25 mm (see also Greenwood and Kirsch, 1984). One should always remember though that the main objective of settlement control is in most cases to reduce differential settlement. This aim normally does not require compaction to maximum density. Very often, equalisation by a moderate widely spaced compaction may be sufficient whereby the sand deposit receives an equally distributed density and stress history for its loaded areas.

Considerably greater depths may become necessary for large raft foundations as well as for dams, embankments or tanks, or where compaction is required to prevent liquefaction or settlement of deeper deposits due to earthquakes or other artificial vibrations. In these cases it is necessary to ensure that the stress levels induced into the soil by vibro compaction exceed those which might occur under design conditions.

We have seen earlier that the radius of influence of vibro compaction depends, for given sand, primarily on the characteristics of the depth vibrator and the chosen mode of operation. It generally varies between 2 m and 4 m and it is therefore impracticable and not advisable to specify the necessary spacing of the probes together with the required density criterion. Since the latter is determined by the requirements of the overall design of the project, the necessary spacing follows the choice of machine, and is generally established by experience and, for larger projects, by field trials. Figure 3.15 shows a typical test arrangement of such a trial. If the chosen method of testing is the cone penetration test (CPT) the comparison of pre- and post-cone penetration test results with the desired or specified criterion then determines the necessary compaction probe spacing. Field observations show that modern machines with a grid spacing of over 10 m$^2$ per probe in clean compactable medium sand can obtain 80% relative density.

Numerous researchers have studied the behaviour of sand and have proposed useful correlations of the various dynamic and static deep penetration tests, in particular the Standard Penetration Test (SPT) and the Cone Penetration Test (CPT), with relative density, compressibility and friction angle. However, the use of these tables and charts (Figures 3.16 and 3.17, Table 3.3) requires a careful validation and interpretation of their applicability in any specific case.

Figure 3.16 provides the possibility of estimating the peak friction angle $\varphi'$ as a function of the relative density $D_r$ and the gradation characteristics of normally consolidated, predominantly silica sands for a given stress level

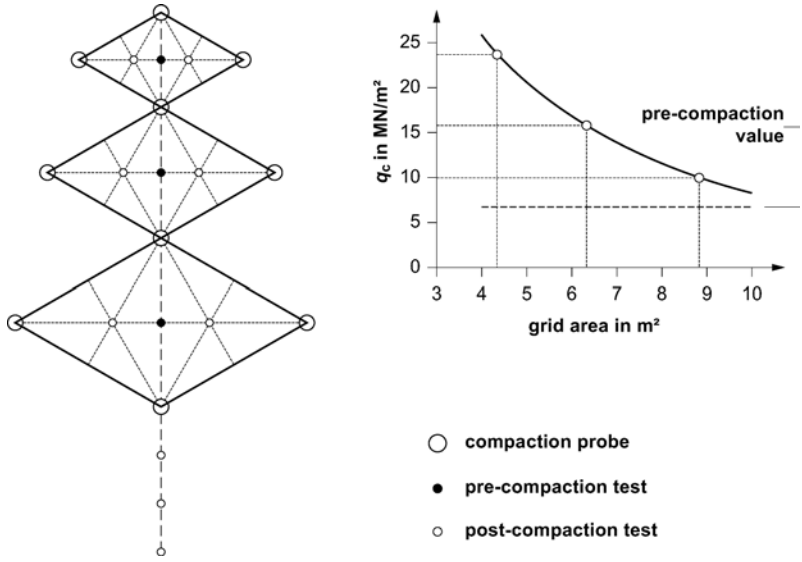


*Figure 3.15* Typical arrangement of a vibro compaction field trial to establish probe spacing (after Moseley and Priebe, 1993)

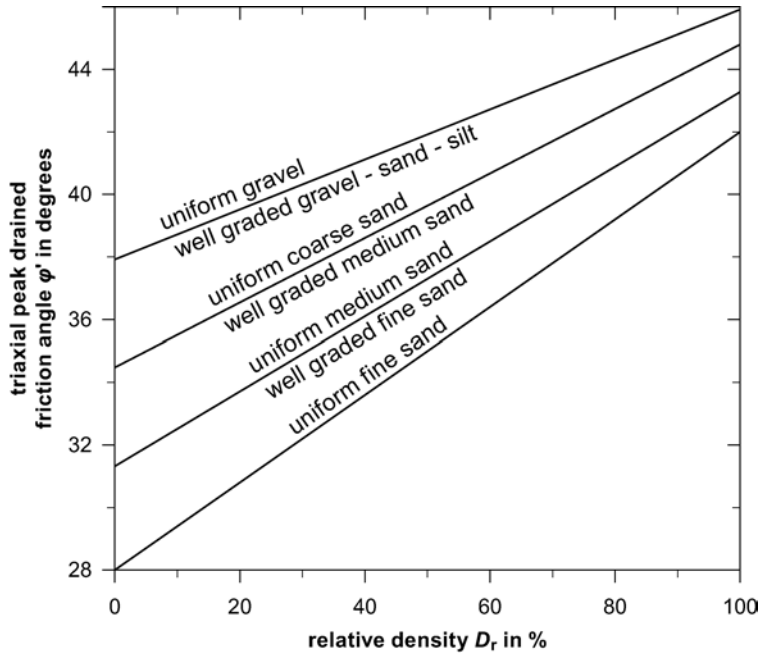


*Figure 3.16* Relationship between friction angle $\varphi'$ and relative density $D_r$ (from Lunne *et al.*, 1997, after Schmertmann, 1978)

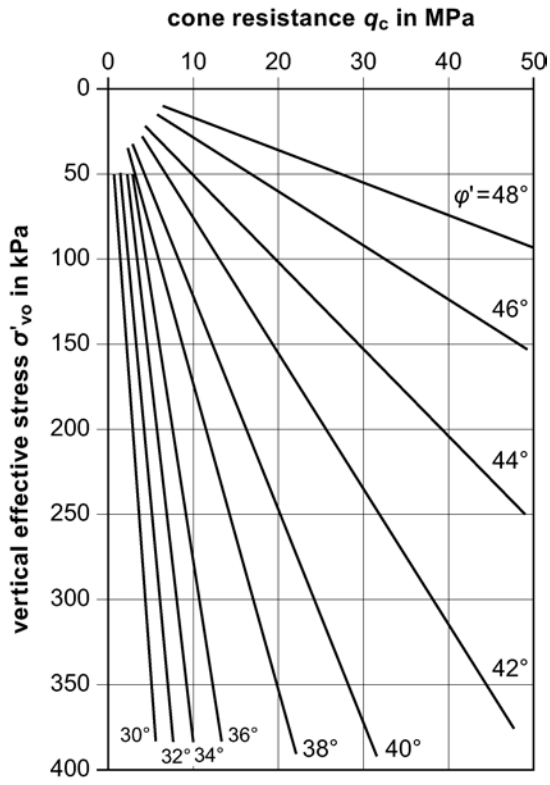


*Figure 3.17* Relationship between $\sigma'_{vo}$, $q_c$ and $\varphi'$ (from Lunne *et al.*, 1997, after Robertson and Campanella, 1983)

in the range of 150 kPa. A similar relationship is shown in Figure 3.17 for uncemented moderately incompressible, predominantly silica sands, indicating that the cone resistance increases linearly with the vertical effective stress for constant friction angles.

For foundations on sand with a smallest width of over 1.5 m, settlement is normally the key criterion for the design rather than bearing capacity. A reliable in-situ determination of the sand stiffness is of great importance because of the difficulties of measuring the deformation modulus in the laboratory on undisturbed samples obtained from the field as they are extremely difficult to retrieve from granular soils. However, to determine stiffness data for sand from in-situ penetration tests is also rather complex because of their dependence on stress levels, stress history, drainage and sand characteristics.

For normally consolidated, unaged and uncemented predominantly silica sands, the constrained modulus $M$ can be obtained from the following relations based on CPT results after Lunne and Christophersen (1983):

$$\begin{aligned} M &= 4 \cdot q_c && \text{for } q_c \text{ below 10 MPa} \\ M &= 2 \cdot q_c + 20 \text{ (MPa)} && \text{for } q_c \text{ between 10 MPa and 50 MPa} \\ M &= 120 \text{ MPa} && \text{for } q_c \text{ above 50 MPa} \end{aligned} \quad (3.4)$$

For over-consolidated sand, the same researchers recommend as a rough guideline:

$$\begin{aligned} M &= 5 \cdot q_c && \text{for } q_c \text{ below 50 MPa} \\ M &= 250 \text{ MPa} && \text{for } q_c \text{ above 50 MPa.} \end{aligned} \quad (3.5)$$

When Standard Penetration Test results are considered or specified in a project, Table 3.4 provides a useful guideline for the translation of *N*-values into equivalent $q_c$ values of the Cone Penetration Test (see also Figure 3.26).

As we have seen, correlations between in-situ measured penetration resistances and relative density provide well-established means for the design where silica sands are concerned. However, special care is necessary where sands with high carbonate content are concerned. Calcareous soils with carbonate contents below 50–70% generally behave similar to non-calcareous soils. Where higher carbonate contents are encountered, these soils often contain up to 100% $CaCO_3$, and the engineering properties are much more difficult to assess. Their coarse grains all derive from shell particles which are subject to grain fracturing during cone penetration and, in addition, very often high cone penetration resistances above the water table are the result of particle cementation due to precipitation, a phenomenon which predominantly occurs in arid countries.

It has been observed that an increasing shell content at first leads to an increase of the cone penetration resistance $q_c$ until grain fracturing becomes a dominant mechanism and the $q_c$ values start to decrease again. Grain fracturing during testing will increase in these sands with increasing shell content, effective overburden pressure and density. For these sands, measured $q_c$ values tend to grossly underestimate relative density when compared with the results in silica sands which can be up to three times higher at the same density (University Karlsruhe, 2006; Wehr, 2007). When

*Table 3.4* Proposed translation of *N* into $q_c$ values for design purposes independent of depth, relative density and water conditions (after Schmertmann, 1970)

| *Soil type* | $q_c$ *(kg/cm²)* /$N_{SPT}$ *(blows/30 cm)* |
|---|---|
| Silt, sandy silt, slightly cohesive silt–sand mixtures | 2 |
| Clean, fine to medium sands and slightly silty sands | 3.5 |
| Coarse sands and sands with little gravel | 5 |
| Sandy gravels and gravel | 6 |

conditions prevail as described above, the performance of load tests or direct density measurements and their evaluation and correlation with CPT values are more appropriate and therefore recommended (see also Section 3.5).

We will see later, in Section 3.3.3, that densification of saturated loose sand represents the key improvement measure to prevent liquefaction during an earthquake, although it is accompanied by a certain decrease in permeability. Consequently, this is apparently counterproductive; however, with density playing the prime role in controlling liquefaction, the method is very effective for this purpose. Conversely in saturated fine-grained sand and silty sands in which densification is difficult to achieve, if at all possible, liquefaction can most effectively be controlled by increasing the overall permeability of the soil mass. To this end permeable granular vibro replacement stone columns can be installed which shorten the drainage paths considerably, leading to an accelerated pore water pressure relief (see Section 4.3.4).

The above-mentioned effect of permeability reduction by vibro compaction is occasionally used for groundwater control by reducing seepage through existing flood protection dykes or for reducing the ingress of groundwater into deep excavation pits. Sidak (2000) reports on interesting case histories that indicate that vibro compaction reduced the permeability of sand by up to two orders of magnitude, an effect that can often be achieved only by less environmentally acceptable methods.

In addition to the usual application of decreasing the void ratio of granular soils to allow higher bearing pressures and reducing settlement, vibro compaction methods are well suited to resolving a large variety of geotechnical problems. For the design of retaining structures vibro compaction can be used to reduce the lateral earth pressure acting on them. The method can also be used below and around piles and caissons to increase their load-bearing capacity, and as the method can also be effectively executed offshore, it is particularly important in harbour construction and similar work (Kirsch, 1985, and Sections 3.6 and 4.6).

As we have seen, density represents the key characteristic of sand, which needs to be measured in situ to establish most of the other parameters necessary for the design. The flow chart in Figure 3.18 provides soil-inherent (internal) characteristics influencing the density of sand together with external measures by which they can be influenced.

### *3.3.3 Mitigation of seismic risks*

#### *3.3.3.1 Evaluation of the liquefaction potential*

It is well known that saturated medium-to-fine-grained sand may lose its strength during an earthquake. The phenomenon is called soil liquefaction and occurs primarily in saturated, cohesionless, fine- to medium-grained soils. In an attempt to explain liquefaction of sand Casagrande (1936) used

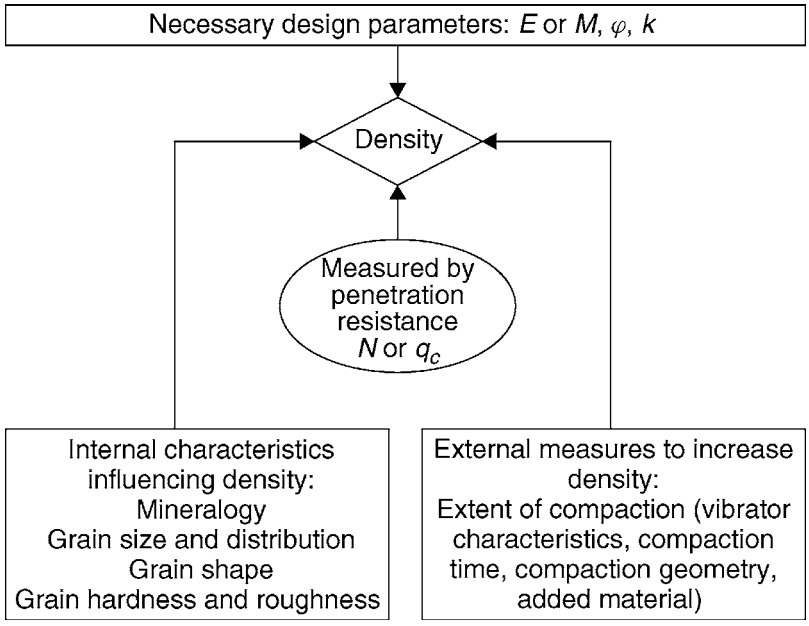


*Figure 3.18* Interdependences for the design of structures on sand

the concept of the critical void ratio – dense sand tends to dilate under shear, whereas loose sand undergoes a volume decrease under the same loading condition. The density at which no volume change occurs in the sand under shear load is called the critical density (critical void ratio).

Sands having a density below the critical density will therefore settle when subjected to earthquake motions. If drainage is prohibited, the pore water pressure $u$ will increase until it equals the overburden pressure and the resulting effective stress $\sigma'$ becomes zero. At this point, the sand has lost its strength completely and has become a liquid.

$$\sigma' = \sigma - u \tag{3.6}$$

$\sigma'$ = effective stress
$\sigma$ = total stress
$u$ = pore water pressure

The disastrous earthquakes at Niigata, Japan and in Alaska, both in 1964, triggered studies and investigations on liquefaction caused by earthquakes to better understand the principles and parameters controlling this phenomenon.

Today, the state of the art is best described in the publications of the National Center for Earthquake Engineering Research (NCEER) at the State University of New York.

The "simplified procedure" to assess the liquefaction potential of soils was first developed by Seed and Idriss (1971) and was subsequently periodically corrected and updated with new developments and findings. It deals with level or gently sloping sites over Holocene alluvial or fluvial sediments at relatively shallow depths not exceeding 15 m. The procedure defines the cyclic stress ratio (*CSR*) that would result from a design seismic event and compares it with the cyclic resistance ratio (*CRR*), also called liquefaction resistance, which the soil is able to mobilise during the earthquake.

CSR is equationted in the following equation:

$$CSR = \frac{\tau_{av}}{\sigma'_{v0}} = 0.65 \cdot \left(\frac{a_{max}}{g}\right) \cdot \left(\frac{\sigma_{v0}}{\sigma'_{v0}}\right) \cdot r_d \tag{3.7}$$

with $a_{max}$ representing the peak horizontal acceleration at ground level resulting from the design earthquake, $g$ the gravity acceleration, $\sigma_{v0}$ and $\sigma'_{v0}$ the total and effective vertical overburden pressure, respectively, and $r_d$ the stress reduction coefficient. *CSR* represents the ratio of the average horizontal shear stress $\tau_{av}$ developed by the design earthquake to the initial vertical effective stress before the cyclic loading occurred. Figure 3.19 shows the $r_d$ versus depth curves that are recommended for non-critical projects. The spread of the curves indicates the uncertainty of the method, particularly at depths greater than 15 m.

The simplified procedure replaces the unevenly distributed cyclic shear stresses of an earthquake by an equivalent average uniform shear stress that is equal to 65% of the maximum cyclic shear stress.

Equation (3.7) allows us to calculate the cyclic stresses at different depths and to determine the respective cyclic stress ratios. The magnitude of an earthquake determines the duration of the ground shaking and thus the significant number of stress cycles $N_c$ necessary to generate maximum shear stresses. Table 3.5 provides representative numbers.

By comparing the shear stresses induced by the design earthquake (determining the *CSR* value) with those shear stresses that are necessary to cause liquefaction under the prevailing site conditions, zones in the soil profile can be identified where liquefaction is likely to occur. Therefore the next step is to evaluate the liquefaction resistance of the soil or cyclic resistance ratio (*CRR*) taking into account the actual soil characteristics that are responsible for this phenomenon.

The costs for retrieving undisturbed samples from water-bearing granular soil are prohibitive for most projects. Only in exceptional cases and with specialised sampling techniques can sufficiently undisturbed specimens be collected; these are subsequently tested in the laboratory, where the seismic loading conditions can be modelled adequately. Instead, field tests have replaced this procedure and are widely used for routine liquefaction investigations. NCEER recommends four methods: the standard penetration test (SPT), the cone penetration test (CPT), shear wave velocity measurements

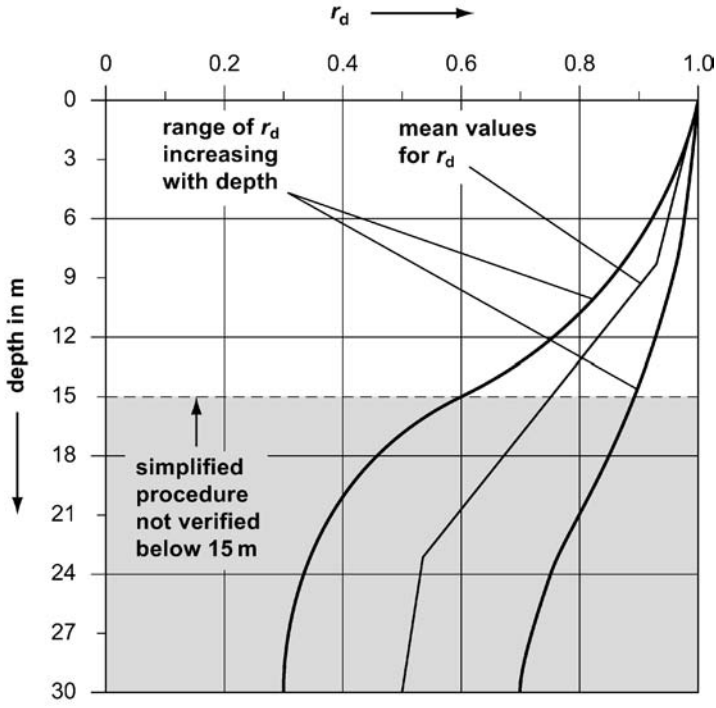


*Figure 3.19* Stress reduction coefficient $r_d$ as a function of depth (after Seed and Idriss, 1971)

*Table 3.5* Earthquake magnitudes and number of significant stress cycles (after Seed and Idriss, 1971)

| *Earthquake magnitude M* | *Number of significant stress cycles* $N_c$ |
|---|---|
| 7 | 10 |
| 7.5 | 20 |
| 8 | 30 |

and the Becker penetration test. Since, for the latter two, only limited or sparse test results from liquefactions sites are available, the following deals only with the *CRR* value measured by SPT and CPT methods.

Figure 3.20 depicts the *CRR* values as a function of the corrected blow count of the standard penetration test $(N_1)_{60}$ developed by Seed *et al.* (1985) from empirical data as recommended by the NCEER for 5%, 15%

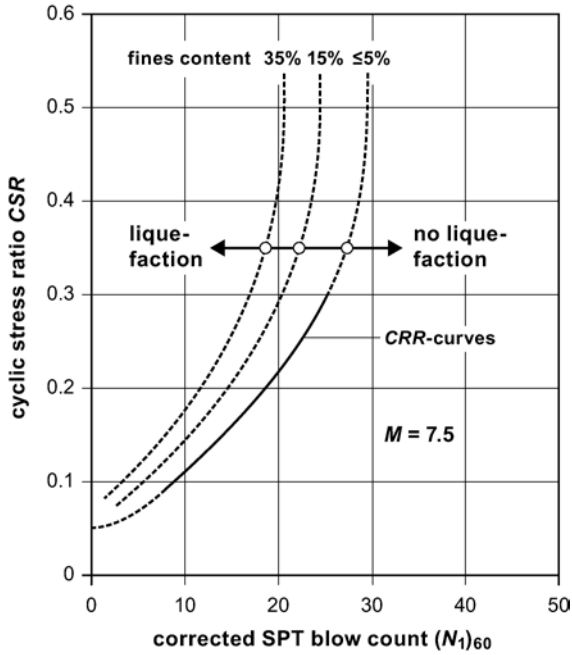


*Figure 3.20* Recommended base curve for calculation of CRR from SPT data (proposed by NCEER, 1997)

and 35% fines in the sand. However, these are only valid for magnitude 7.5 earthquakes. The blow count $(N_1)_{60}$ is the measured blow count $N_m$, corrected to account for the influencing factors, overburden pressure ($C_N$), energy ratio ($C_E$), borehole diameter ($C_B$), rod length ($C_R$) and sampling method ($C_S$) by the following equation:

$$(N_1)_{60} = N_m \cdot C_N \cdot C_E \cdot C_B \cdot C_R \cdot C_S \tag{3.8}$$

Suggested ranges of correction factors can be taken from Table 3.6. To account for the overburden pressure, the $C_N$ factor is calculated by using the effective overburden pressure $\sigma'_{v0}$ in equation (3.9) that acted at the time that the SPT test was carried out,

$$C_N = (p_a/\sigma'_{v0})^{0.5} \tag{3.9}$$

with $p_a$ representing the atmospheric pressure of 100 kPa.

The SPT-based method of computing the cyclic resistance ratio *CRR* has the advantage that the number of test measurements at liquefaction sites is

*Table 3.6* Corrections to SPT values (proposed by NCEER, 1997)

| *Factor* | *Equipment variable* | *Term* | *Correction* |
|---|---|---|---|
| Overburden pressure | | $C_N$ | $C_N = (p_a/\sigma'_{v0})^{0.5}$<br>$C_N \leq 2$ |
| Energy ratio | Donut hammer | $C_E$ | 0.5 to 1.0 |
| | Safety hammer | | 0.7 to 1.2 |
| | Automatic-trip donut type hammer | | 0.8 to 1.3 |
| Borehole diameter | 65–115 mm | $C_B$ | 1.0 |
| | 150 mm | | 1.05 |
| | 200 mm | | 1.15 |
| Rod length | 3–4 m | $C_R$ | 0.75 |
| | 4–6 m | | 0.85 |
| | 6–10 m | | 0.95 |
| | 10–30 m | | 1.0 |
| | >30 m | | >1 |
| Sampling method | Standard sampler | $C_S$ | 1.0 |
| | Sampler without liners | | 1.1 to 1.3 |

abundant and that disturbed soil samples can easily be collected during testing to establish fines content and other grain characteristics.

Figure 3.21 shows a similar graph that was developed from empirical data but was based on the relationship between the corrected CPT tip resistance $q_{c,1N}$ and the cyclic stress ratio, showing *CRR* curves for clean sands with fines contents below 5% and valid for a 7.5 magnitude earthquake. Normalisation of the measured cone penetration resistance $q_c$ is achieved by correcting it for the effective overburden pressure $\sigma'_{v0}$ by:

$$q_{c,1N} = C_Q \cdot (q_c/p_a) \tag{3.10}$$

with $C_Q = (p_a/\sigma'_{v0})^n$ and $p_a = 100$ kPa, the atmospheric pressure, and $n$ ranging from 0.5 for clean sands to 1 for clays.

In Figure 3.22 a soil behaviour type chart is shown as developed by Robertson (1990) identifying different soil types as a function of their cone resistance and their friction ratio. The CPT friction ratio (sleeve resistance $f_s$ divided by cone tip resistance $q_c$) increases with increasing fines content and plasticity of the soil. The boundaries between the different soil types of the graph can be approximated by concentric circles of the radius $I_c$, referred to as the soil behaviour type index:

$$I_c = \sqrt{(3.47 - \log Q)^2 + (1.22 + \log F)^2} \tag{3.11}$$

with $Q$ and $F$ representing the normalised cone resistance and the normalised friction ratio as follows:

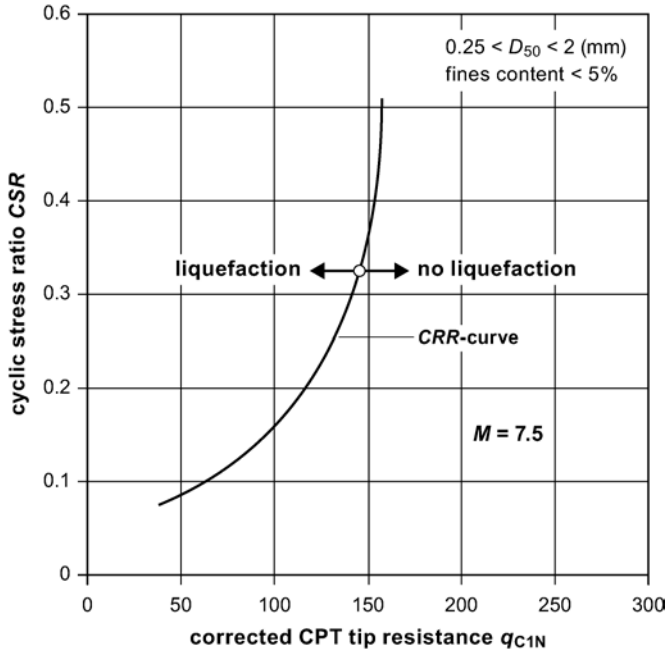


*Figure 3.21* Curve for calculation of *CRR* from CPT data (proposed by NCEER, 1997)

$$Q = [(q_c - \sigma_{v0})/p_a] \cdot (p_a/\sigma'_{v0})^n \tag{3.12}$$

$$F = [f_s/(q_c - \sigma_{v0})] \cdot 100\% \tag{3.13}$$

$I_c$ is calculated in an iterative process starting with $n = 1$ as exponent for clayey soils in equations (3.11), (3.12) and (3.13). If the calculated $I_c$ value is above 2.6 the soil is generally considered too cohesive to liquefy. For safety reasons the NCEER recommends these soils to be sampled and laboratory tested for confirmation. If the computation arrives at $I_c$ values less than 2.6 the soil is more likely granular, and calculations of $Q$ and $I_c$ should be repeated with $n = 0.5$ for sand. If $I_c$ then falls below 2.6 the soil is considered non-plastic and granular and $I_c$ can be used to determine the liquefaction potential for sand with fines contents as explained below. However, should $I_c$ be again greater than 2.6, the soil is likely to be cohesive and plastic and $I_c$ should be recalculated with the intermediate value of $n = 0.7$. The intermediate $I_c$ is then used to establish the liquefaction potential of this soil, which should also be sampled and tested for verification purposes according to NCEER recommendations. Soils with a soil behaviour index $I_c$ above 2.6 would generally not liquefy but would be rather soft (region 1 in Figure 3.22) and could therefore suffer considerable deformation during an

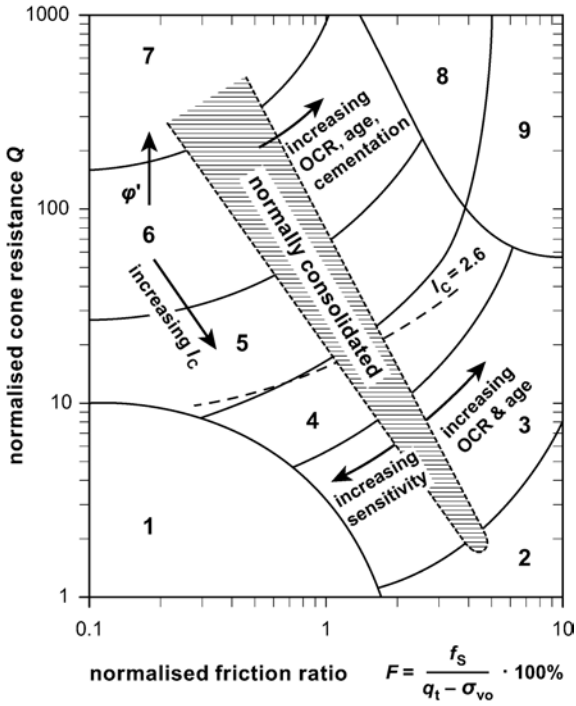


*Figure 3.22* CPT-based soil behaviour type chart after Robertson, 1990 (proposed by NCEER, 1997) 1 = sensitive, fine-grained, 2 = organic soils – peat, 3 = clays – silty clay to clay, 4 = silt mixtures – clayey silt to silty clay, 5 = sand mixtures – silty sand to sandy silt, 6 = sands – clean sand to silty sand, 7 = gravelly sand to dense sand, 8 = very stiff sand to clayey sand*, 9 = very stiff, fine-grained*
(*heavily over-consolidated or cemented)

earthquake. These soils would also be considered non-liquefiable according to the so-called Chinese criteria by which liquefaction would only occur if all three of the following criteria were met (after Seed and Idriss, 1982):

1 The clay content is less than 15%.
2 The liquid limit is less than 35%.
3 The natural moisture content is less than 0.9 times the liquid limit.

Correction of the normalised cone penetration resistance $q_{c,1N}$ of these silty sands to an equivalent clean sand value (index cs) for determining the liquefaction resistance *CRR* from Figure 3.21 is by the following relationship:

$$(q_{c,1N})_{cs} = K_c \cdot q_{c,1N} \tag{3.14}$$

where $K_c$ represents the grain characteristics correction factor, which can be taken from Figure 3.23 as a function of the soil behaviour type index $I_c$ as defined by equation (3.11).

To correct the $CRR_{7.5}$ values, which are only valid for 7.5 magnitude earthquakes, as taken from Figure 3.20, as a function of normalised corrected SPT blow counts, or from Figure 3.21, for normalised corrected CPT tip resistances, this value is multiplied by the magnitude scaling factor for stresses $MSF_M$ as proposed by the NCEER and as taken from Figure 3.24, and as given in equation (3.15):

$$CRR_M = MSF_M \cdot CRR_{7.5} \tag{3.15}$$

The factor of safety FS against liquefaction can now be written as a function of the cyclic stress ratio *CSR*, the cyclic resistance ratio for 7.5 magnitude earthquakes $CRR_{7.5}$ and the magnitude scaling factor *MSF* as follows:

$$FS = (CRR_{7.5}/CSR) \cdot MSF \tag{3.16}$$

We have seen from Figure 3.19 that the *CRR* values, as developed from Figure 3.20 and 3.21 are only valid for depths not exceeding 15 m. A correction factor $K_\sigma$ for overburden pressures greater than 100 kPa was

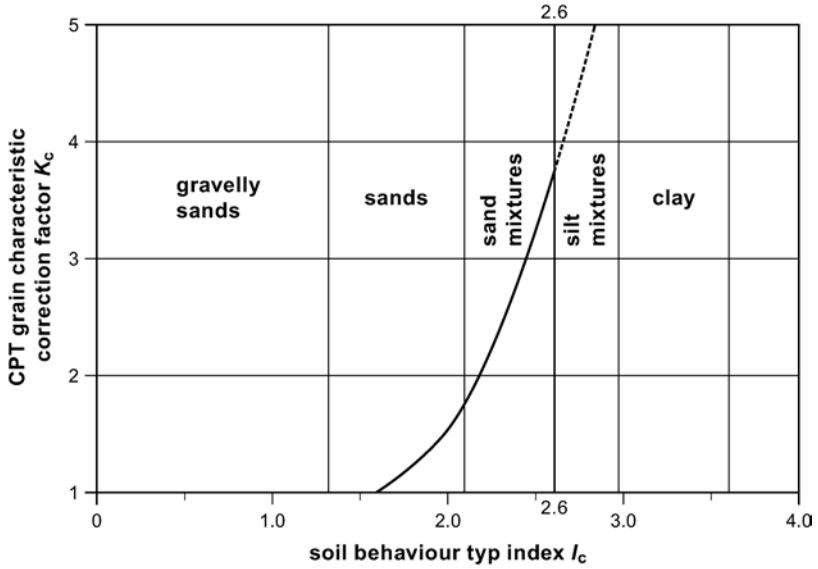


*Figure 3.23* Grain-characteristic correction factor for determination of clean-sand equivalent CPT resistance (recommended by NCEER, 1997)

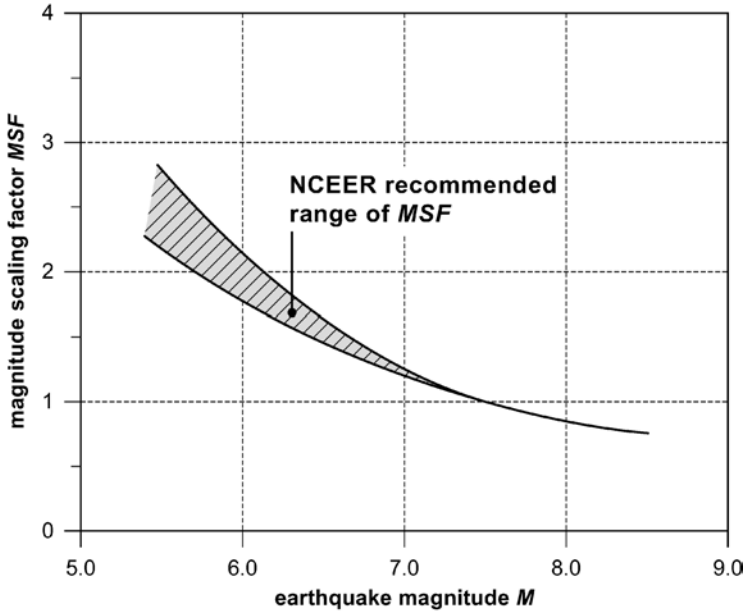


*Figure 3.24* Magnitude scaling factor (recommended by NCEER, 1997)

therefore developed. While the liquefaction resistance generally increases with increasing confining pressure, cyclic triaxial compression tests revealed that the resistance in terms of the cyclic stress ratio decreases in a non-linear form with depths greater than 15 m. To account for this effect, the NCEER recommends the $K_\sigma$ factor according to Figure 3.25 for clean and silty sands and for gravel.

For an in-depth study of the liquefaction phenomenon of saturated sand, the reader is referred to the NCEER (1997) publication and numerous other publications referenced therein.

The computational method described and proposed by the NCEER needs to be carried out for all layers of a given soil profile that are likely to liquefy during an earthquake. Factors of safety against a design earthquake can be calculated in this way, and safety profiles can be developed to establish the eventual need of soil improvement. To facilitate the calculation, particularly to avoid the cumbersome iteration procedure to find the correct soil behaviour type index $I_c$, professional software has been developed based upon these NCEER recommendations (i.e. LiquefyPro, 2008; Shake, 2000).

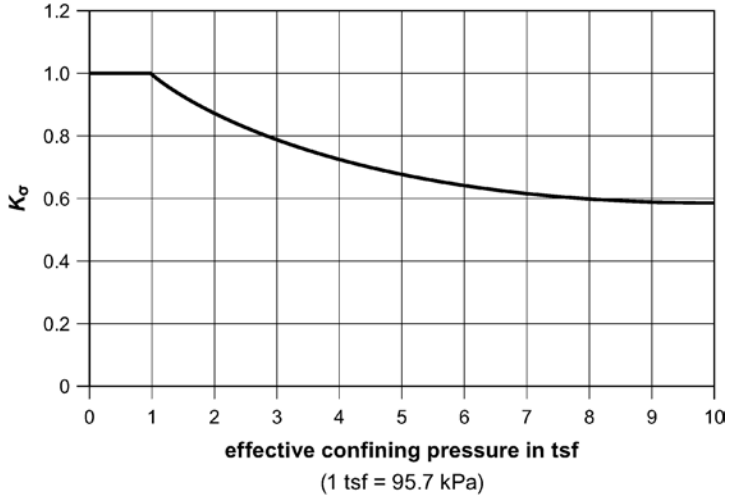


*Figure 3.25* $K_\sigma$ factor as a function of confining pressure (recommended by NCEER, 1997)

### *3.3.3.2 Settlement estimation of sands due to earthquake shaking*

Besides the potential catastrophic effects of liquefaction to structures, and their possible avoidance by soil improvement measures, the foreseeable extent of earthquake-induced deformations in granular soils is of particular interest in seismic zones. It is well known that sand tends to compact and settle when subjected to earthquake shaking. The degree of deformation depends, of course, primarily on the initial density of the sand deposit and the earthquake magnitude, and ranges generally between less than 1% volumetric strain for dense sand and up to 5% for very loose sand.

To estimate the probable settlement as a result of earthquake shaking Tokimatsu and Seed (1987) proposed that the calculations be divided into *saturated sand settlement* below groundwater, where generally liquefaction would occur, and *settlement for dry or unsaturated sand* above, with the sum of both representing the total earthquake-induced settlement.

It is recommended to base these calculations on SPT values and to convert any other in-situ density measurements, such as CPT results, into normalised $(N_1)_{60}$ values by using equation (3.10) and Table 3.4 above. For this purpose, Figure 3.26 also provides a useful relationship (after Robertson *et al.*, 1983) between the mean grain size $D_{50}$ and the $q_c/(100{\cdot}N)$ ratio for different types of sand.

If the soil behaviour type index $I_c$ is known, the conversion can also be done based upon the following relationship:

$$q_{c1}/(N_1)_{60} = 8.5 \cdot (1 - I_c/4.6) \tag{3.17}$$

with $q_{c1}$ in tsf (1 tsf = 95.7 kPa)

The primary effect of the shaking of saturated sand is the generation of excess pore water pressure with settlement occurring as it dissipates. The time for the settlement to develop depends on the length of the drainage path and the permeability of the sand. In highly permeable sand, it may occur immediately, but in less permeable sand only after many hours.

It has been found that volume deformation decreases with increasing density of the sand and decreasing induced strain. Accordingly the volumetric strain $\varepsilon_v$ in saturated sand developing after liquefaction as proposed by Tokimatsu and Seed (1987) is presented in Figure 3.27 as a function of the cyclic stress ratio and corrected normalised SPT blow count $(N_1)_{60}$. The abscissa uses a conversion between relative density $D_r$ and SPT $N$-values proposed by the same researchers, which is based upon an empirical expression which Meyerhof had presented in 1957 as follows:

$$D_r = 21 \cdot \sqrt{\frac{N}{\sigma'_0 + 0.7}} \tag{3.18}$$

with the effective overburden pressure $\sigma'_0$ in kg/cm$^2$ (1 kg/cm$^2$ = 100 kPa).

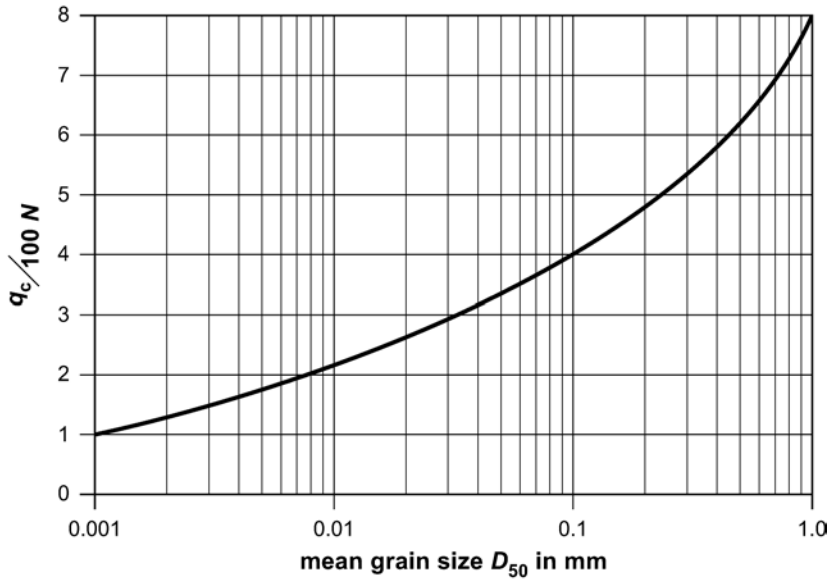


*Figure 3.26* Relationship between $D_{50}$ and $q_c/(100{\cdot}N)$ ratio, $q_c$ in kPa (after Robertson *et al.*, 1983)

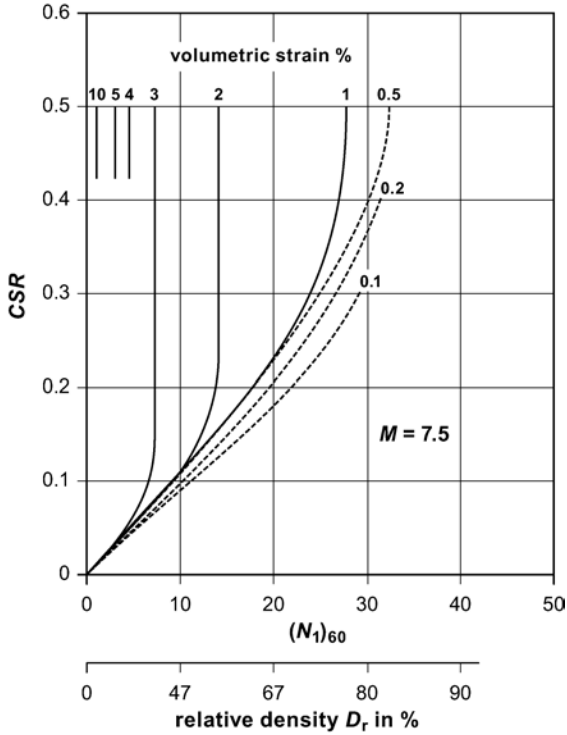


*Figure 3.27* Relationship between cyclic stress ratio, $(N_1)_{60}$, and volumetric strain in saturated sand (Tokimatsu and Seed, 1987)

As can be seen in Figure 3.27, the earthquake-induced volumetric strain can range well over 3% in loose sand and is insignificant when dense conditions prevail. To use this figure also for earthquakes other than $M = 7.5$, the values of the cyclic stress ratio have to be multiplied by the magnitude scaling factor *MFS* as obtained from Figure 3.24 and using:

$$\left(\frac{\tau_{av}}{\sigma'_0}\right)_{M=M} = \left(\frac{\tau_{av}}{\sigma'_0}\right)_{M=7.5} \cdot MSF \tag{3.19}$$

The studies of Tokimatsu and Seed also revealed that, for conditions of incomplete liquefaction, only small amounts of settlements will occur, which are generally represented by volumetric strains well below 1% (dashed lines in Figure 3.27). Figure 3.28 gives the relationship between volumetric strain and normalised stress ratios below 1 (i.e. for stress levels below liquefaction stage) for saturated clean sand, resulting in a volumetric strain of just 0.1% for a stress level of 80% of that causing liquefaction.

The liquefaction induced settlement $\Delta s$ of a soil layer with the thickness $h$

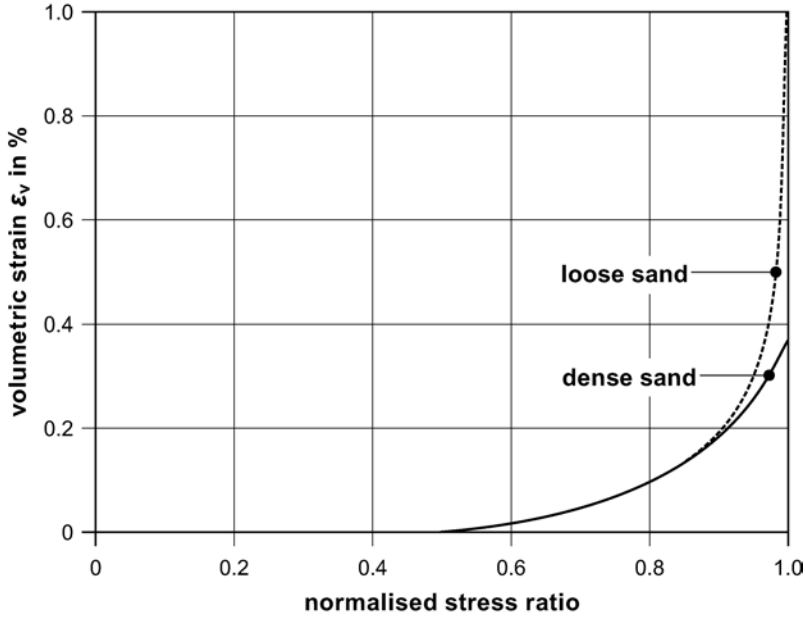


*Figure 3.28* Relationship between volumetric strain and normalised stress levels for non-liquefied saturated clean sand (Tokimatsu and Seed, 1987)

is then calculated by multiplying it with the representative volumetric strain value $\varepsilon_v$ (%) of this layer:

$$\Delta s_{sat} = \frac{\varepsilon_v}{100} \cdot h \tag{3.20}$$

For the *dry soil settlement*, investigations by Silver and Seed (1971) revealed that it is a function of the relative density of the sand, the magnitude of the cyclic shear strain and the number of strain cycles. It is insignificantly affected by the degree of the vertical stress. At a given depth in the soil the effective shear strain $\gamma_{eff}$ can be written as:

$$\gamma_{eff} = \frac{\tau_{av}}{G_{eff}} = \frac{\tau_{av}}{G_{max}\,(G_{eff}/G_{max})} \tag{3.21}$$

with $G_{max}$ the shear modulus at low strain level, $G_{eff}$ the effective shear modulus at the induced strain level and $\tau_{av}$ the average cyclic shear stress at that depth. According to equation (3.7) the average cyclic stress ratio is

$$\tau_{av} = 0.65 \cdot \frac{a_{max}}{g} \cdot \sigma_{v0} \cdot r_d \tag{3.7a}$$

leading with (3.21) to

$$\gamma_{\text{eff}} \cdot \frac{G_{\text{eff}}}{G_{\max}} = \frac{0.65 \cdot a_{\max} \cdot \sigma_{\text{v0}} \cdot r_{\text{d}}}{g \cdot G_{\max}} \tag{3.21a}$$

with

$$G_{\max} = 1000 \cdot (K_2)_{\max} \cdot \sqrt{\sigma'_{\text{m}}} \qquad \text{in psf-units} \tag{3.22}$$

and

$$(K_2)_{\max} = 20 \cdot (N_1)^{1/3} \tag{3.23}$$

In this way, the product $\gamma_{\text{eff}} \cdot G_{\text{eff}}/G_{\max}$ can be determined for any given sand layer which is plotted as abscissa in Figure 3.29 as a function of the shear strain $\gamma_{\text{eff}}$ with the confining pressure $\sigma'_{\text{m}}$ as parameter valid for an $M = 7.5$ (15 cycles) earthquake. Tokimatsu and Seed then use the cyclic shear strain in Figure 3.30 to determine the volumetric strain $\varepsilon_{\text{v}}$ for this layer.

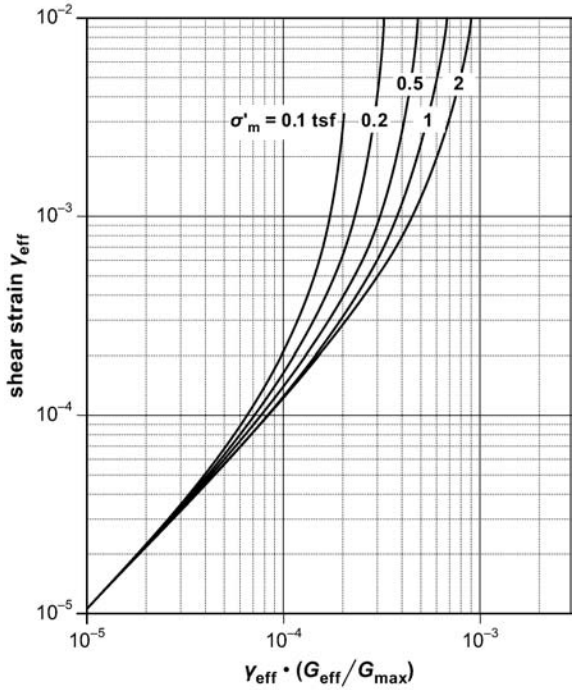


*Figure 3.29* Plot to determine the induced strain in sand deposits (after Tokimatsu and Seed, 1987)

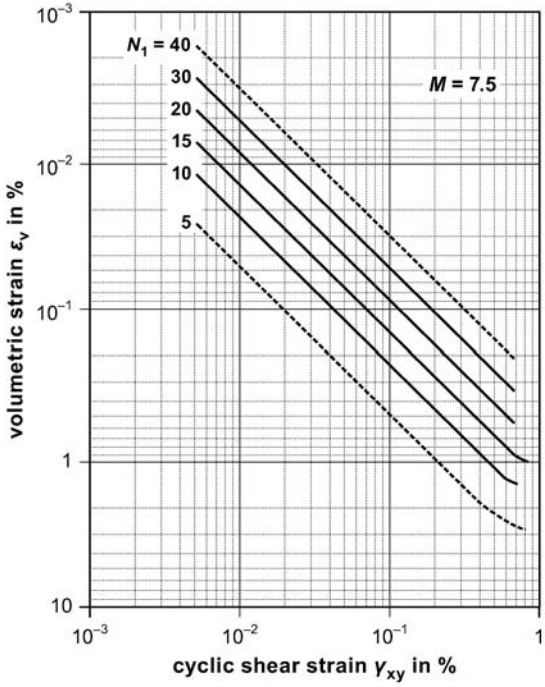


*Figure 3.30* Relationship between volumetric strain, shear strain and penetration resistance for dry sands (Tokimatsu and Seed, 1987)

*Table 3.7* Magnitude scaling factors for stress ratios causing liquefaction in saturated sand (third column) and for strain ratios in dry sand (fourth column) (after Tokimatsu and Seed, 1987)

| *Magnitude M* | *Representative stress cycles at 0.65* $\tau_{max}$ | *Scaling factor MSF1 for stress ratios* | *Scaling factor MSF2 for strain ratios* |
|---|---|---|---|
| 8.5 | 26 | 0.89 | 1.25 |
| 7.5 | 15 | 1.0 | 1.0 |
| 6.75 | 10 | 1.13 | 0.85 |
| 6 | 5 | 1.32 | 0.6 |
| 5.25 | 2–3 | 1.5 | 0.4 |

For different earthquake magnitudes, the volumetric strain values thus developed need to be multiplied by the relevant magnitude scaling factor for strain ratios *MSF2* from the fourth column in Table 3.7.

Figure 3.30 is valid for one-directional shear conditions and the $\varepsilon_v$ values have to be multiplied by 2 to reflect multidirectional shear conditions, which normally prevail in an earthquake. The dry soil settlement of the soil layer with a thickness $h$ is then

$$\Delta s_{\text{dry}} = \frac{2 \cdot \varepsilon_{\text{v}}}{100} \cdot h. \tag{3.24}$$

The total earthquake-induced settlement in a sand deposit is the sum of the settlements of layers below the water table and the settlements of the layers above:

$$s_{\text{total}} = \Sigma\, \Delta s_{\text{wet}} + \Sigma\, \Delta s_{\text{dry}}. \tag{3.25}$$

## 3.4 Quality control and testing

Once the design of the vibro compaction project has determined the geometrical extent of the treatment, together with the probe spacing necessary to obtain the required density using the method as described in Section 3.3.1, a suitable quality assurance programme needs to be developed. The aim is to ensure that the operating parameters so obtained are observed when executing the works by repeating it for each vibro compaction probe. Such a programme will have to include all elements that are essential for a well-organised special foundation site. For the vibro compaction process water management is a very important issue. It has to be channelled away from the work position into settling ponds before it is released, normally without further treatment, into the available recipient. Similarly important is the well-organised transportation of the backfill material to the working area and its stockpiling on site, when necessary. Continuous measurement of the added material, together with site surface level measurements before and after compaction, will help to evaluate compaction success after its execution.

The latest monitoring devices record – as a function of real time for each vibro compaction probe – penetration depth, energy consumption of the vibrator motor, execution time and, if found necessary, pressure and quantity of the flushing medium used. As the ground to be compacted is in general a natural deposit, variations in its granular composition from the location of the trial compaction area are likely to occur. An accompanying post-compaction test programme will normally reveal any deviations from the specified requirements, deriving from variations in the compaction method or the soil properties.

Suitable testing methods for the measurement of the compaction result, such as the standard penetration test (SPT), the cone penetration test (CPT), the Menard pressure meter test (MPT), the shear wave velocity measurement (Vs), the full-scale load test (LT) and the direct density measurement (DDM), are listed out in Table 3.8 together with their specific advantages or disadvantages of their application in sand deposits. Under special circumstances, and when specific knowledge exists, other in-situ testing methods may also be used.

*Table 3.8* Suitable testing methods to measure compaction results in sand (partially following NCEER, 1997)

| *Type of test* | *Available data* | *Repeatability* | *Depth range* | *Measures index or property* | *Can test provide soil sample?* | *Detection of soil variability* | *Cost* |
|---|---|---|---|---|---|---|---|
| SPT | abundant | poor to good | deep | index | yes | good | low |
| CPT | abundant | very poor | deep | index | no | very good | low |
| MPT | sparse | poor | medium | property | no | fair | moderate |
| Vs | limited | good | deep | property | no | fair | low |
| LT | limited | very good | low | property | no | poor | high |
| DDM | limited | poor | low | property | yes | very good | very high |

SPT – standard penetration test
CPT – cone penetration test
MPT – Menard pressure meter test
Vs – Shear wave velocity measurement
LT – load test
DDM – direct density measurement

Before starting a project it is important to select the appropriate testing method and to agree not only on the frequency of pre- and post-compaction testing but also any remedial measures and procedures should the specified density not have been met (see also Chapter 7). Engineering judgement is required to determine the need and extent of recompaction that generally follows only after the deficiency was verified by a second test in the vicinity of the failed test.

It is also very important that all pore water pressure increases created by the vibratory motion in the treated soil are allowed to fully dissipate before any post-compaction testing commences. Full relief of the excess pore water pressure in the soil has normally occurred about one week after compaction. In cases of doubt, it is better to wait for a longer period or to measure the pore water pressure development over time directly. To avoid any adverse influence on the post-compaction testing this criterion should be adhered to for a zone of about 30 m around the testing area where no simultaneous compaction work should be carried out.

In special, not yet fully understood, circumstances a so-called aging effect can occur in sand whereby the strength properties of the compacted sand continue to increase significantly for up to several weeks after compaction (Mitchell *et al.*, 1984; Schmertmann, 1991; Massarsch, 1991). It is therefore recommended to perform field trials at the beginning of larger projects with in-situ testing to start at different time intervals after compaction. By this way, the significance of any potential time effect on the post-treatment test results can be assessed, and the appropriate conclusions may be drawn. Increases in cone resistance $q_c$ of up to 100% have been reported 10 weeks after the first post-compaction test performed 1 week after completion of deep compaction.

According to an analysis made by Charlie *et al.* (1992, from Lunne *et al.*, 1997), covering projects that represent a wide range of geological and climatic conditions, the variation of the cone resistance $q_c$ with time can be expressed by an empirical relationship as follows:

$$(q_c)_N = (1 + K \log N)(q_c)_1 \tag{3.26}$$

with

$N$ = number of weeks
$K$ = an empirical constant, dependent on average air temperature $T$ measured in °C according to equation (3.27) below

$$K = 0.04 \cdot 10^{0.5 \cdot T} \tag{3.27}$$

$(q_c)_1$ = normalised $q_c$ after 1 week
$(q_c)_N$ = normalised $q_c$ after $N$ weeks

The temperature-dependent relationship indicates that chemical reactions may support inter-granular chemical bonds developing with time between particles and being responsible for this strength increase.

## 3.5 Suitable soils and method limitations

It can be regarded a prerequisite that the need for compaction of loose soils or soils with varying density is established by a site investigation. As a rule, soils suitable for vibro compaction should be granular in nature with a negligibly low cohesion or plasticity. For a quick assessment of the suitability of granular soils for treatment by vibro compaction Degen (1997b) has proposed a first approach based upon the Unified Soil Classification System (USCS) together with useful comments on the compaction method as shown in Table 3.9. Accordingly suitable soils are generally sand and gravel. Ideally their silt content (grain size below 0.06 mm) should be below 10%. Larger percentages of silt, and any clay content, will considerably obstruct the compaction process, if not prevent it totally.

Figure 3.11 shows application limits in a grain size distribution graph where area B represents soils that are ideally suited for vibro compaction with content of fines below 10%. The soils represented by area A are very well compactable, but an increasing amount of coarse gravel and cobbles also increases permeability leading to a total loss of water at about $k = 10^{-2}$ m/s. This may obstruct penetration of the depth vibrator to such an extent that the desired depth cannot be reached in some or all parts of the site. In cases like this, where the process may become uneconomic or even impossible, to execute a pre-contract trial is recommended.

Such trials may also be advisable for soils falling into area C, where vibro compaction is still possible but only with considerably extended compaction time. Speed and effectiveness of the vibro compaction process depend largely on the permeability, $k$, of the sand. At a permeability below $10^{-3}$ m/s, penetration of the vibrator will increasingly be slowed down. While for soils lying in areas A and B the necessary backfill material for compensation of the surface settlement resulting from the compaction process itself can be

*Table 3.9* Suitability assessment of granular soils for vibro compaction (modified after Degen, 1997b)

| *Soil type* | *USCS* | *Comment on suitability for vibro compaction* |
|---|---|---|
| Gravel, well graded | GW | Well suited for vibro compaction, potential penetration difficulties with less powerful machines |
| Gravel, poorly graded | GP | If $D_{60}/D_{10} \leq 2$ compaction only marginal (trial compaction recommended) |
| Gravel, silty or clayey | GM, GC | Compaction not possible if clay content >2% and silt content >10% |
| Sand, well graded | SW | Ideally suited |
| Sand, poorly graded | SP | If $D_{60}/D_{10} \leq 2$ compaction only marginal (trial compaction recommended) |
| Sand, silty | SM | Compaction inhibited if silt content >8% |
| Sand, clayey | SC | Compaction inhibited if clay content >2% |

taken from the surface, imported coarser (i.e. more suitable) backfill material is necessary when the soils to be compacted fall into area C. Soils falling completely or partially in area D cannot be compacted by the deep vibratory process. Vibro replacement stone columns (see Chapter 4) or other foundation measures may become necessary in such a case.

The boundaries described above have all been established empirically over many years of application, and it must be kept in mind that specialist contractors often rely on considerable knowledge and experience when it comes to borderline applications. In this context, the choice of the appropriate vibrator with specific characteristics can be decisive for the execution of vibro compaction. A vibrator with particularly good penetration characteristics may be advisable for soils in area A, while vibrators compacting at lower frequencies (below 30 Hz) will perform better in conditions of area C – hence the development of depth vibrators with variable frequency that combine both characteristics within one machine.

In addition to the particle size distribution of the soil, static cone penetration tests may also be used to establish compaction suitability of soils. Figure 3.31 shows an empirical relationship proposed by Massarsch (1994) between cone penetration resistance and friction ratio, and defines the zone of compactable soils to fall within friction ratios below 1% at a point resistance of at least 3 MPa. It indicates also a zone for soils that are only marginally compactable with friction ratios between 1% and 1.5% at $q_c$ values between 1 MPa and 3 MPa.

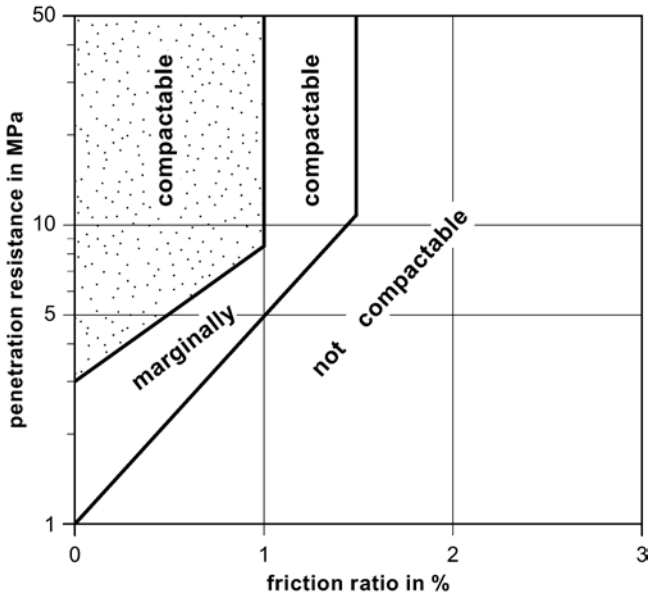


*Figure 3.31* Compactable soils as a function of cone penetration resistance and friction ratio (after Massarsch, 1994)

A suitability number *SN* based on grain size distribution has been proposed by Brown, 1977 according to the following equation:

$$SN = 1.7\left(\frac{3}{D_{50}{}^2} + \frac{1}{D_{20}{}^2} + \frac{1}{D_{10}{}^2}\right)^{0.5} \tag{3.28}$$

$D_{50}$, $D_{20}$ and $D_{10}$ are grain size diameters in millimetres at 50%, 20% and 10% passing in a grain size distribution curve. It is suggested that a low suitability number is better suited for vibro compaction than a high number of 40 to 50, above which the ground is unsuitable, and that quicker compaction is achieved with lower numbers.

Very steep grain size distribution curves, with $D_{60}/D_{10}$ below 2, are a strong indicator that vibro compaction may only be marginally possible if not inhibited completely. A compaction test in the laboratory, or a field trial, will determine the suitability of such soils when no local experience exists.

The above approaches provide reasonable guidelines, but permeability plays an important role in speed and effectiveness of vibro compaction. With decreasing permeability below $k = 10^{-5}$ m/s, compaction is increasingly inhibited, while very high permeability in excess of $10^{-2}$ m/s may slow penetration of the vibrator as a result of the loss of water. In this instance, where jetting water is normally of limited use, more powerful machines operating at higher frequencies, in excess of 50 Hz, are more suited and are capable of penetrating even highly permeable gravel and cobble. In this category are applications where brick demolition rubble is regularly compacted dry in regenerating derelict industrial city centres in the North of England to at least the depth of the former basements.

Where shallow treatment depths below 1.5 m are concerned, standard surface compaction methods such as vibratory roller compaction or heavy tamping tend to be more economical. This is especially so since the upper 1.0 m of sand is generally not well enough compacted by vibro compaction requiring either removal or subsequent surface densification by standard methods.

Very deep compactions, well in excess of 50 m, are known to have been executed successfully in exceptional cases, either to mitigate earthquake risks, to improve stability hazards of slopes or in other similar cases. In these instances, besides very heavy cranes, considerable experience is required in safely operating the extended depth vibrators. Although deep vibratory compaction is a very versatile method, in-situ trial compactions may be advisable when unknown territory is entered.

The need to compact newly dredged sand in reclamation areas for the safe foundation of quay walls, berths and similar structures often requires densification of the foundation soils through deep water. This can be achieved from floating barges and pontoons or, in shallower water, from special platforms. In offshore applications, the critical problem will always be the accurate setting of the compaction locations, which can today be

mastered by satellite-supported positioning and inclinometer measurements. As a result of the complex surveying problems, the use of multiple depth vibrators (up to four units have been used) may be advisable. It is only heavy seas or swells and strong water currents that may prevent a safe, secure performance of the vibro compaction process until a friendlier environment prevails again.

Deficiencies in the material grading can also affect penetration of the vibrator and successful compaction of sandy soils. A layer of cobbles or gap-graded material of fine uniform sand with floating cobbles may prove difficult for the compaction process; the cobbles can accumulate in front of the vibrator point and obstruct further penetration. The use of air as the flushing medium or changing the vibrator frequency can help to alleviate the situation.

However, particle size distribution, in-situ density measurement and permeability are not always sufficient to define the suitability for vibratory deep compaction nor are the in-situ measurements always easy to interprete. The mineral composition and specific gravity of the sand deposit can greatly influence the result of indirect density measurements. In this context, and in contrast to silica sand, in carbonate sands containing considerable amounts of shell debris the evaluation of cone penetration test results cannot be translated easily into relative densities.

Various researchers have found that even relatively small percentages of shell debris (10–20%) (Vesic, 1965; Cudmani, 2001) in silica sand have a considerable influence on the CPT point resistance at the same density. Bellotti and Jamiolkowski (1991) found a linear relationship between the $q_c$(silica)/$q_c$(shell) ratio and the relative density $D_r$ as given in equation (3.29). Ratios between 1.5 and 3 have been reported in special publications.

$$\frac{q_c\,(\text{silica})}{q_c\,(\text{shells})} = 1 + 0.015(D_r - 20) \tag{3.29}$$

It is therefore recommended to correlate the cone penetration test results with direct in-situ density measurements or to conduct special laboratory calibration tests between density and penetration resistance, whenever the carbonate content resulting from shell debris is in excess of 10%, unless enough experience and data exist for the referenced soil.

Wehr, 2005a, presented a shell correlation factor $f_s$ as a function of the relative density $D_r$ for Dubai sand (carbonate content in excess of 90%, $D_{60}/D_{10}$ = 3) by which the cone penetration test results measured in the calcareous sand need to be multiplied to arrive at corresponding values for silicate sand:

$$f_s = \frac{q_c\,(\text{silica})}{q_c\,(\text{shell})} = 0.0046\,D_r + 1.3629 \tag{3.30}$$

The study revealed that the influence of the in-situ density was in all tests so dominant compared with the overburden pressure that the latter could be neglected. Accordingly this correlation factor ranges between 1.4 and 1.8 and amounts to 1.64 for a relative density of 60%. It was stated that the values found represented lower limits since all shell particles larger than 4 mm in diameter where removed from the test specimens representing ~8% of the total weight.

In general it is always recommended to also consider the measured surface settlement after vibro compaction as an indicator and as supporting evidence of the increase in density achieved comparing the pre- and post-compaction volumes.

When interbedded sand layers with cohesive soils above and below require compaction it is often found that the result of the standard deep compaction is below expected levels. The reduced compaction is especially noticeable at the upper and lower interface in the granular soil with the cohesive material. It is surmised that the vibratory motions are dampened to a certain extent by these cohesive layers. The proper functioning of the sand backfill is important in these cases to compensate the volume reduction in the sand layer which will come to the fore at the upper interface. An extended compaction time and, if necessary, also reduced compaction probe spacing will help to avoid this problem.

Natural cementation of sand can be found in many parts of the world. It occurs predominantly in arid climatic conditions in calcareous sand deposited above the water table. Cementation can also occur when hydrous silicates or iron oxides act as a kind of glue at the contact point between the sand particles. Cementation may indicate a greater density or strength than actually exists and in-situ density measurements and their standard correlation may result in misleading interpretations. Weakly cemented soils with actual low relative densities may respond to vibratory compaction by collapsing and yet producing lower post- than pre-treatment test results although the compacted material is now in a much more stable condition. Strong cementation may also be an obstacle that cannot be overcome by the vibratory treatment without the help of pre-boring. To conclude, it is important to know if particle cementation exists at a site where vibro compaction is envisaged. Only then can appropriate measures be designed for its in-situ improvement.

## 3.6 Case histories

### *3.6.1 Vibro compaction for a land reclamation project*

In early 2000, the island state of Singapore embarked on another major reclamation project, for which it is renowned and by which it seeks to overcome the chronic land scarcity, a major obstacle for the development of the country. Led by the Jurong Town Corporation (JTC) much needed

industrial space was developed at Tuas, which is located towards the western tip of Singapore Island.

The vibro compaction method was chosen to safeguard the stability of the hidden dyke that defines the boundaries of the reclamation area (Figure 3.32). It is composed of a well-graded, gravelly, fine to coarse sand with an in-situ relative density after dredging of only 35% (Figure 3.33).

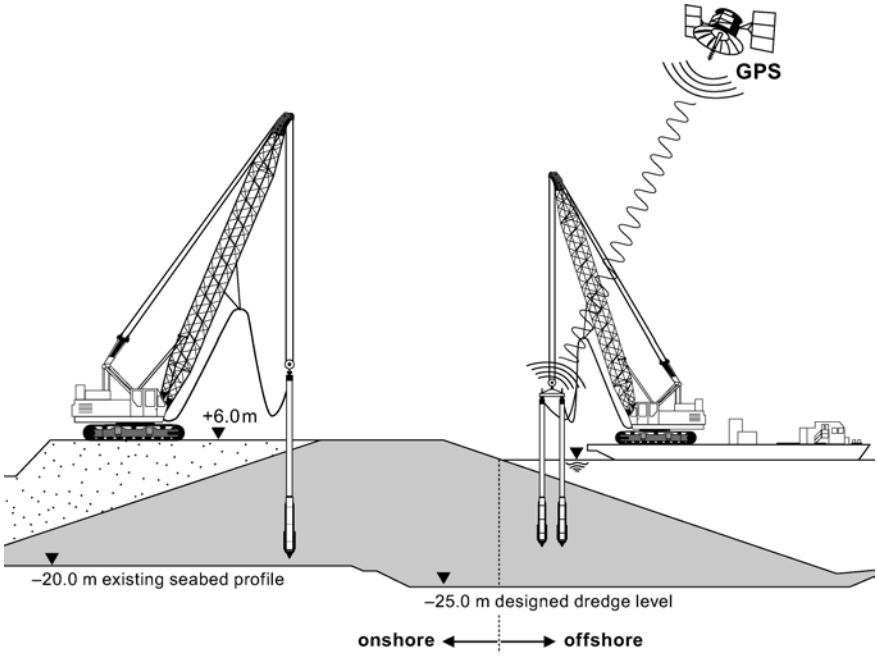


*Figure 3.32* Vibro compaction at hidden dyke (by courtesy of Keller Group plc)

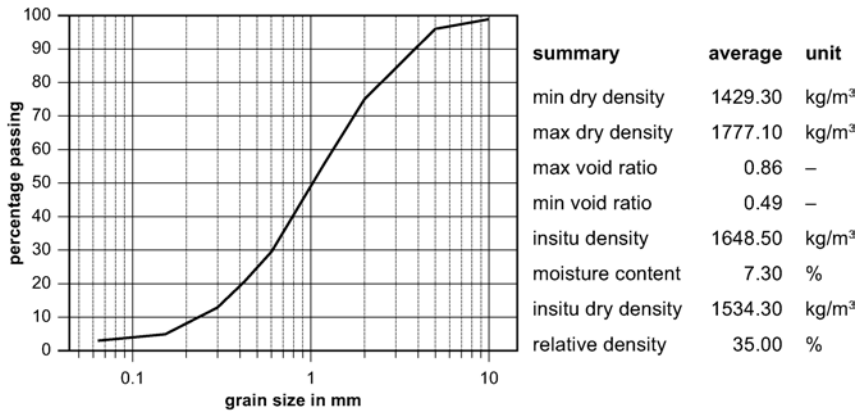


*Figure 3.33* Typical grain size distribution and properties of sand

Specifications required a minimum cone tip resistance measured by the CPT method of 4 MPa between 0 and 2 m depth, of 6 MPa between 2 m and 8 m and of 8 MPa below. Vibro compaction had to be carried out up to a maximum depth of 35 m.

The chosen compaction grid pattern, an equilateral triangular grid of 4 m, was established together with other operational details, such as the amount of water used and compaction time, in a field trial. In total, 22.4 million $m^3$ of sand were finally compacted, 67% on the dry from the land side, 33% offshore as a marine operation. Two heavy crawler cranes were used on land each carrying a single S300 Keller depth vibrator with characteristics according to Table 3.1. For the marine work a 200 ton crane with twin S300 vibrators was mounted on a barge to carry out the compaction work. In such a configuration, work was conducted in day and night shifts for six days a week, compacting approximately 1 million $m^3$ of sand per month. To locate the compaction points with sufficient accuracy over water the GPS was used with antennas mounted directly on top of the vibrator extension tubes.

Quality control was by cone penetration testing carried out seven days after the completion of a specific section of the works. Figure 3.34 shows typical pre- and post-compaction test results. Surface settlement measured after vibro compaction averaged around 1.5 m, which is equivalent to 6% of the average compaction depth of 25 m.

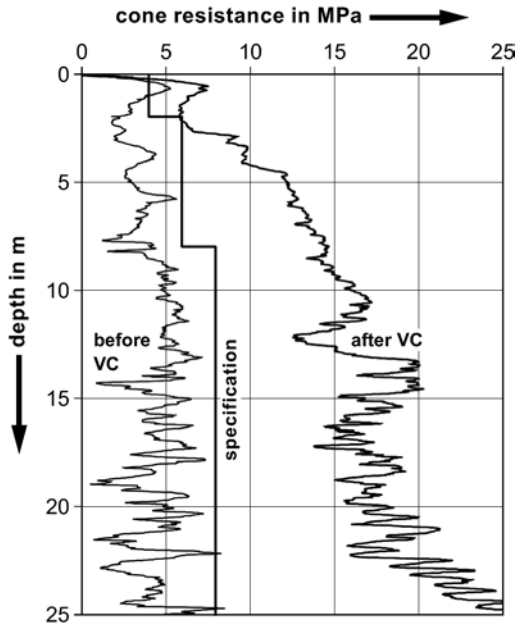


*Figure 3.34* Pre- and post-compaction test results (by courtesy of Keller Group plc)

### *3.6.2 Ground improvement treatment by vibro compaction for new port facilities*

The versatility of the vibro compaction process in solving special foundation problems is particularly appreciated where harbour construction is concerned. The need to increase the density of dredged sand fill behind or below quay walls or inside and outside coffer dams is a typical requirement that can best be achieved by this method (Figure 3.35).

The quayside unloading and breakwater facilities of the Merak harbour in West Java, Indonesia, serving the delivery of material for a pulp and paper manufacturing plant, are shown in Figure 3.36 with a typical cross-section through the quay wall. The fill material is a fine to medium sand with basically no fines with a $D_{60}/D_{10} = 4$. About 50% of its grains are silica sand, 20% shells and 30% other fragments with an overall specific gravity of 2.82.

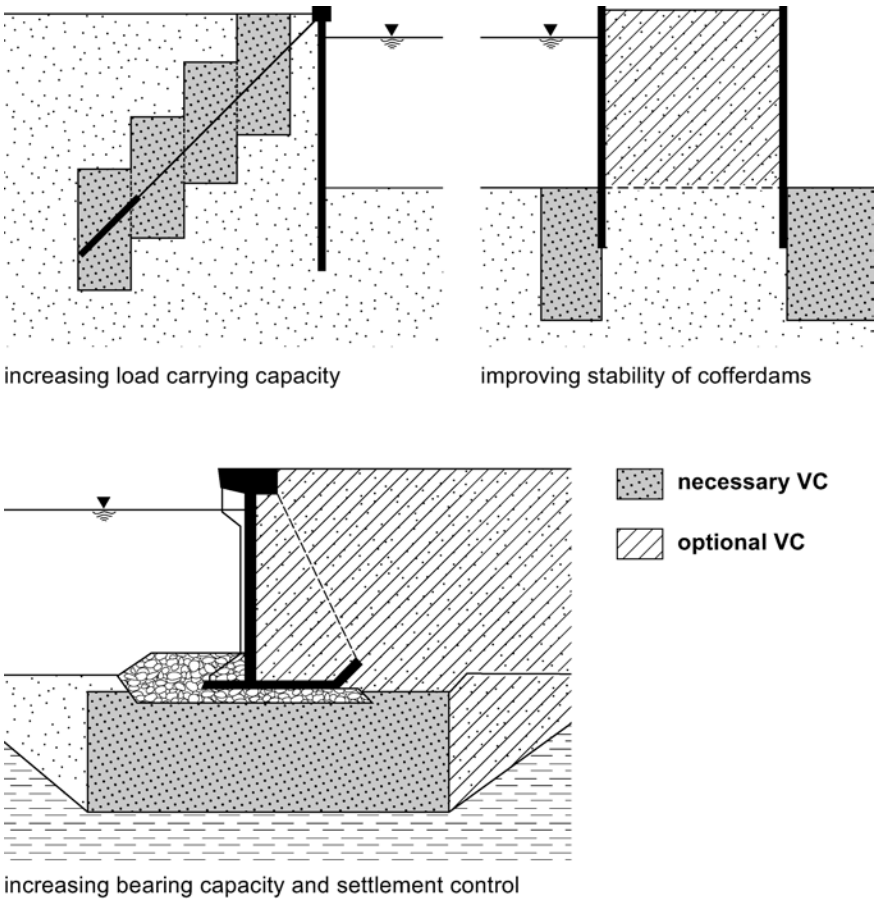


*Figure 3.35* Typical examples for ground improvement by vibro compaction in harbour construction

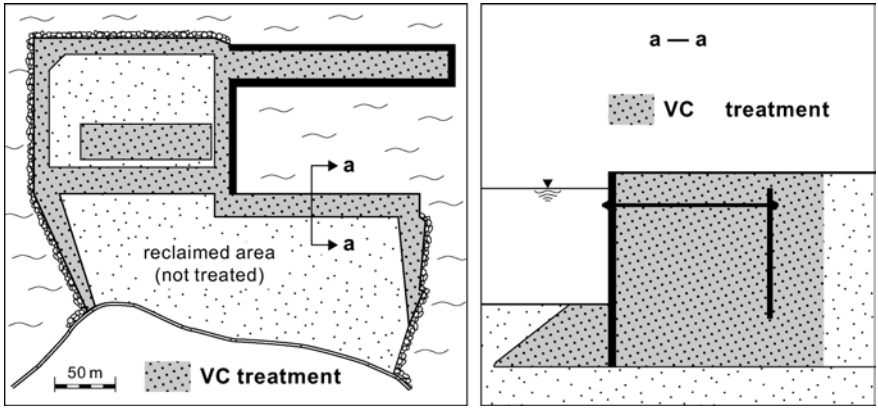


*Figure 3.36* Plan of quay walls and breakwater with treatment area and cross-section through quay wall (by courtesy of Keller Group plc)

Structural stability and the reduction of the liquefaction potential required the hydraulic sand fill in the areas shown to be compacted to a relative density of 70%. In total some 1.3 million $m^3$ of sand fill needed treatment to up to 25 m depth. The layout of the compaction probes was chosen after a trial compaction before the start of the works as a 3 m square grid.

Quality control consisted of continuous measurement and recording of vibrator motor curent over depth as a function of real time, together with post-compaction tests carried out as cone penetration tests (CPT) ten days after completion of a defined section of the works not exceeding 750 $m^2$. The specified density criterion of 70% relative density was generally exceeded in this well-compactable sand material. In addition, surface settlements induced by the compaction were measured for each works section. They reached on average 7% of the compaction depth with maximum values in areas of particularly clean sand of well over 10%.

### *3.6.3 Vibro compaction field trial in calcareous sand*

On a major prestigious development project in the Middle East that was realised between 2006 and 2009 different specialist contractors were engaged to allow the developer to follow a very tight time schedule for his project, in particular for the dredging operation and the following compaction works. Consequently, a variety of depth vibrators were employed which were all tested on site prior to the start of any contractual work. The tests were designed to establish the required vibro probe grid spacing to achieve the specified density as was laid down in a CPT target curve according to Figure 3.39 below. Accordingly ground improvement had to be designed and conducted to ensure an allowable bearing pressure of

150 kN/m$^2$ at 1 m below ground surface, total settlement (from static loads and liquefaction induced) not to exceed 25 mm at a maximum distortion of 1:500, and to eliminate the liquefaction risk of a design earthquake not exceeding a magnitude of 6 with a maximum ground acceleration of 0.15 g at bed rock level.

The dredged sand material was a light brownish grey to grey, shelly to very shelly, fine to medium carbonate sand (its $CaCO_3$ content was over 90%) with many broken shell fragments smaller than 20 mm. The sand was generally only loose to medium dense. The average depth of the man-made deposit was about 16 m, which is followed by the natural ground, consisting of cap rock and weathered limestone. Ground surface was ~3 m above mean water level of the adjacent sea. Figure 3.37 gives the band of grain size distribution curves which is representative of the project area. Its fines content (grain size less than 0.063 mm) was generally less than 10% and its clay content below 2%. The mean grain size $D_{50}$ was 0.1–0.5 mm with a maximum grain size of 10 mm.

The following describes the details of field trials using twin Keller S700 vibrators with characteristics according to Table 3.1. The total weight of the 32.1 m-long set-up, consisting of a tandem beam, 500 kN pulley head, extension tubes, water and power inlets and vibrators, was 31.1 tons. The safe operation of this special equipment required the use of a 90-ton crawler crane with a boom length of ~37 m (see Figure 3.38).

Vibro compaction probes were installed in four trial areas of 30 × 30 m each, using triangular grid spacing of 4.2 m, 4.5 m, 4.7 m and 5.0 m respectively. The following working sequence was adopted during the trials, ultimately also forming the method for the construction work.

Probe penetration started with placing the vibrators over the probe location and opening the bottom water jets. In this phase, the depth

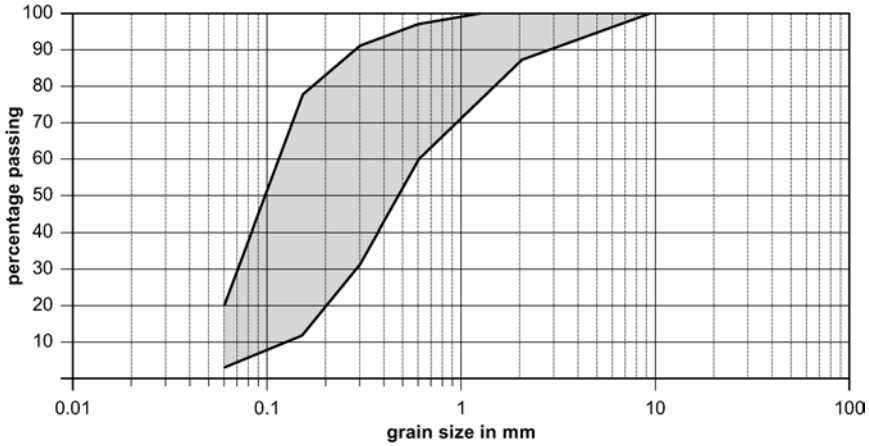


*Figure 3.37* Representative grain size distributions

*Figure 3.38* Vibro compaction equipment set up for S700 twin vibrator operation (by courtesy of Keller Group plc)

vibrators were set to rotate at 2000 rpm. During penetration into the ground, the upper side jets were opened at a depth of about 4 m. The bottom jets were generally closed again just before reaching final depth. Now the vibrators were switched to compaction mode with an operating frequency of 1300 rpm and were held in this deepest position for 1 minute or until a current consumption of 420 A was reached, whichever occurred first. The vibrators were then withdrawn in lifts of 0.75 m. After each lift the vibrators were held for 40 seconds or until 420 A was reached. The craters that developed around the vibrators as compaction proceeded were filled with sand collected at ground level whenever the crater depth reached about 2 m. When approaching ground surface, the vibrators were switched back to penetration mode at ~4 m to avoid twisting of the hanger slings. Table 3.10 gives further details of the trials performed.

*Table 3.10* Trial compaction details to obtain necessary grid spacing

| *Area* | | *A* | *B* | *C* | *D* |
|---|---|---|---|---|---|
| Number of probes | | 60 | 50 | 46 | 42 |
| Grid spacing (triangular) | m | 4.2 | 4.5 | 4.7 | 5.0 |
| Depth (average) | m | 13.96 | 13.82 | 13.90 | 13.91 |
| Penetration time | min | <4 | <4 | <6 | <4 |
| Compaction steps of 0.75 m | nos. | 18 | 18 | 18 | 18 |
| Total compaction time | min | 16 | 17 | 17 | 19 |
| Completion time pre probe | min | 20 | 21 | 23 | 23 |
| Subsidence | m | 1.170 | 1.050 | 0.925 | 0.906 |
| Relative subsidence | % | 8.4 | 7.6 | 6.6 | 6.5 |

Post-compaction ground levels were also taken to calculate the soil subsidence resulting from deep compaction as an additional indicator of soil densification. After a minimum of two weeks, cone penetration testing started to measure the densities achieved, for comparison with the post-compaction criteria of the contract. As explained in Chapter 7, a special procedure was adopted – in this case reflecting the calcareous nature of the sand – consisting of a pair of post-compaction CPTs at the one-third and at the mid point of the triangular grid, as shown in Figure 7.1 with the weighted, rolling average calculated according to equation (7.1). From the comparison of the post-compaction CPT curves thus established for the different grid patterns with the CPT target curve, the 4.5 m grid was finally chosen for the contract (see Figure 3.39).

As can be seen from Figure 3.39 the specified cone resistance was not always achieved in the upper 2–3 metres. It was therefore decided to perform a surface compaction employing the novel impact rolling compaction method at least two weeks before contract verification testing was allowed to commence. Figure 3.40 shows an impact roller in operation. According to Avalle (2007), impact rolling is an efficient and highly productive surface compaction method requiring a careful design before, and a high degree of quality control during, its execution.

From the total compacted volume of 141 million $m^3$, over 30 million $m^3$ of sand fill was compacted using Keller S700 depth vibrators by adopting the method described. On average, a shift production of 14,500 $m^3$ was achieved for twin vibrator operation. The specified compaction criterion was achieved without the need for retesting and recompaction for 68% of the total area. For 17% of the area the performance line was met after retesting. For 9%, recompaction was necessary to achieve the specified density, while for only 6% of the total area, verification of the density had to be done by a liquefaction analysis based on the local conditions encountered.

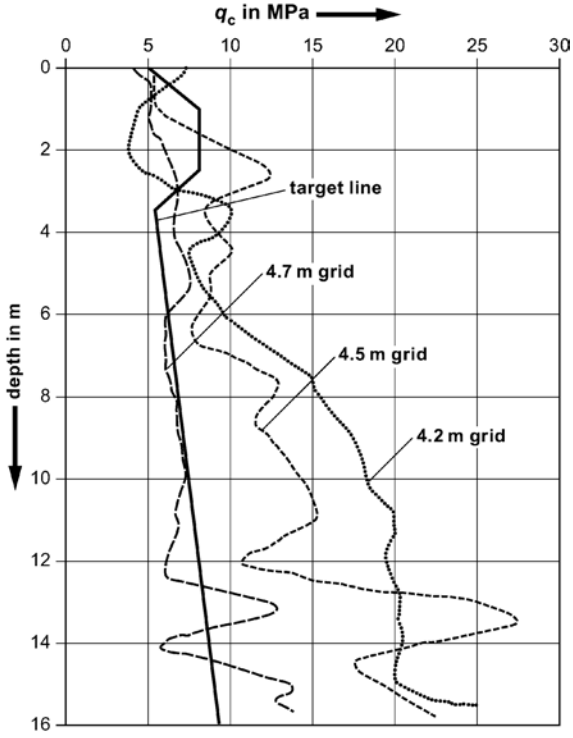


*Figure 3.39* Comparison of average post-CPT results for different grid patterns with target curve

*Figure 3.40* Impact roller in operation (by courtesy of Keller Group plc)

### *3.6.4 Foundation of a fuel oil tank farm*

For the extension of a large power and desalination plant in the Middle East 16 fuel oil storage tanks were to be constructed in 2008. The soil conditions at the site typically consist of an approximately 10 m thick layer of sand which rests on relatively incompressible bedrock made up of silt and limestone. The sand deposit consists of calcareous material of loose to medium density, generally clean to slightly silty, in places also gravelly, but its density was not sufficient to carry the high load of 250 kN/m$^2$ of the steel tanks of equal diameter of 39 m which were of the fixed roof type.

Foundation design required densification of the sand layer below the tanks together with a 5 m wide strip outside to 80% relative density, as represented by specified cone resistance target curve with $q_c$-values of up to 10 MPa at 3 m depth, of 15 MPa between 3 m and 5 m, and 20 MPa between 5 m and 7 m. Maximum settlements were restricted to 50 mm at the centre of the tanks and 25 mm below the ring beam supporting the tank shell.

Trial compactions were carried out at a representative location within the future tank farm using Keller S300 vibrators on three different triangular grids with probe spacings of 2.20 m, 2.50 m and 2.75 m. Generally all grids showed a significant increase of the CPT cone resistance after vibro compaction, and a considerable ground surface subsidence of about 8%. Although all grids met the target curve within the upper 7 m, CPT tip resistance fell below in a layer situated just a few metres above bedrock of about 1 m thickness where the friction ratio rose generally above 0.5% at a cone resistance below 5 MPa, representing the presence of silty sand, which generally can only be marginally compacted (cf. Figure 3.31). Therefore conservatively the 2.20 m grid was chosen for the vibro compaction work for all tanks. In addition, a row of 0.90 m diameter vibro replacement stone columns were installed below the tank shell at centre-to-centre distances of 2 m. These columns extended to 6.50 m in compacted sand.

Settlement performance of the chosen design was demonstrated by a finite element analysis based upon the constraint modulus of the sand as developed from the post-compaction cone penetration test results. For the maximum settlement in the tank centre 44 mm were computed, and below the tank shell 24 mm. About 10% of these settlements derived from the bedrock material below the zone of soil improvement.

Contract vibro compaction work was carried out using a pair of S300 vibrators suspended from a standard crawler crane. The stone columns construction followed, employing the wet vibro replacement method using the same depth vibrator. Surface subsidence was measured after vibro compaction for each tank ranging between 6.7% and 13.3% depending on the presence of silty sand layers, with an average of 8.5%. Contract conditions required the relatively large number of 21 post-compaction

CPTs to be carried out for each tank for quality control purposes, which is equivalent to one test for every 100 $m^2$ of compacted ground. Figure 3.41 shows average CPT curves developed for each tank, which indicate that the 80% relative density target was generally met, except in cases where the presence of a high silt content in the sand in zones close to bedrock reduced or hampered the effect of vibro compaction and where vibro stone columns were additionally installed.

In addition to the cone penetration tests three zone load tests were also

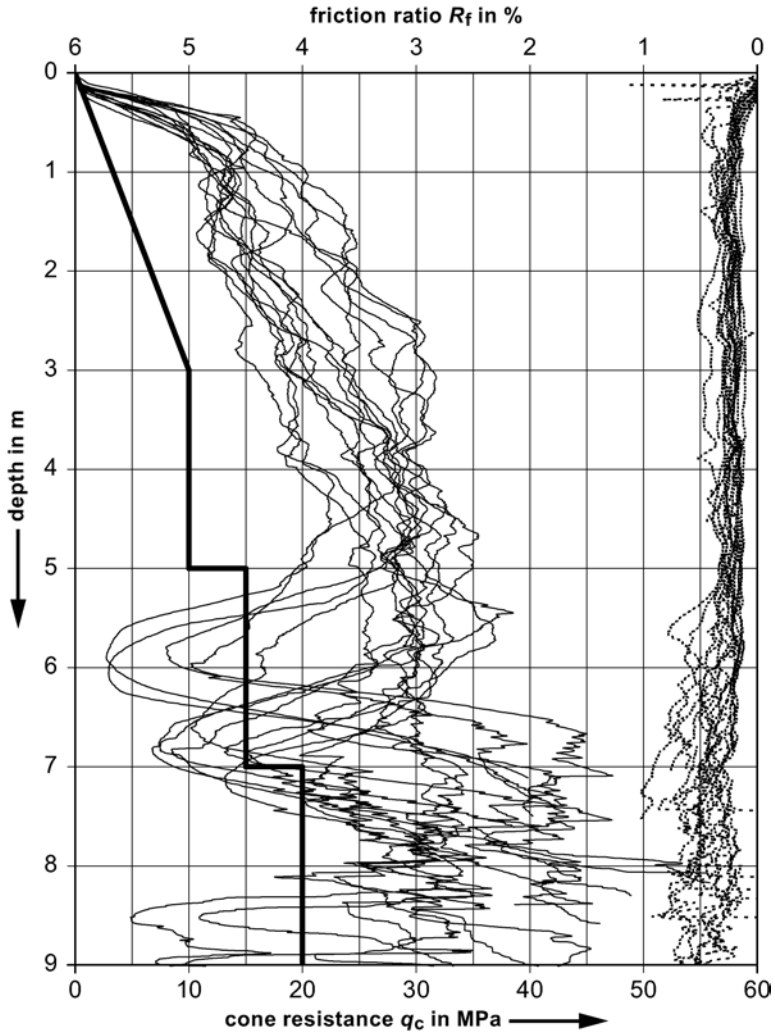


*Figure 3.41* Post-treatment cone penetration tests (each curve representing the average of 21 CPTs) and CPT target line

carried out using a prefabricated reinforced concrete footing measuring 2 × 2 × 0.6 m placed in the centre of four vibro compaction probes. The load tests were set up and performed in accordance with ASTM D1194, employing a loading platform with a total dead load of 2200 kN consisting of concrete blocks. The load was applied in equal increments of 25% of the design footing pressure of 250 kPa up to maximum load equal to 500 kPa. Figure 3.42 gives the pressure versus settlement curve for one of the load tests, and Table 3.11 shows the recorded settlements at design and twice design bearing pressure for all three load tests.

The relatively high stiffness as derived from the load tests indicates a better compaction than expected. When using a constrained modulus of 145 MN/m$^2$, which was measured for load test 1, for a settlement calculation, the tank centres will settle less than 20 mm which compares favourably with the finite element analysis mentioned above in which the stiffness employed was derived from a correlation with post-CPT tip resistances.

*Table 3.11* Settlements and moduli as obtained from load tests

| | *p = 250 kN/m$^2$* | | *p = 500 kN/m$^2$* |
|---|---|---|---|
| *Load test* | *Settlement s in mm* | *Modulus* E in MN/m$^2$* | *Settlement s in mm* |
| 1 | 3.06 | 145 | 13.27 |
| 2 | 2.54 | 173 | 9.44 |
| 3 | 2.55 | 173 | 6.81 |

* E = 0.88·p·B/s with footing width B = 2 m

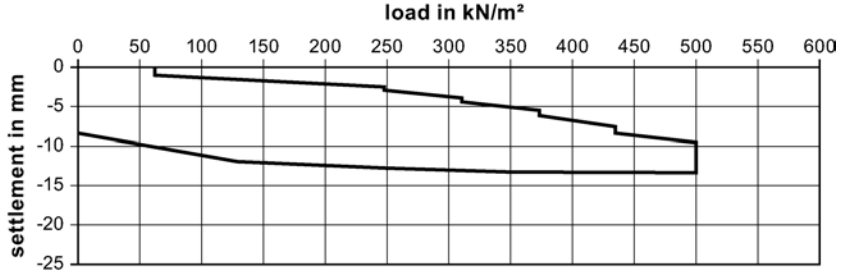


*Figure 3.42* Typical pressure–settlement curve for a 2 × 2 m footing on vibro compacted sand (by courtesy of Keller Group plc)

### *3.6.5 Liquefaction evaluation of CPT data after vibro compaction and stone column treatment*

The ground improvement programme for a Southern California church building was completed in late 2007 and addressed the liquefaction-induced settlement under the site design earthquake. To accomplish the site liquefaction mitigation, the soils were densified, drained and reinforced. In general, procedures for the liquefaction mitigation with vibro stone columns were in accordance with the methods presented by Baez and Martin (1993) and Baez (1995). The stone column programme consisted of a primary spacing of 19 ft (5.8 m) centre to centre and secondary columns at the mid point of the square grid to achieve a replacement ratio of 14.1%. Figure 3.43 shows a typical soil profile and the stone columns. Totally 416 primary stone columns and 380 secondary columns were installed at the site with an average column diameter of 3 ft (0.9 m) and a maximum column length of 48 ft (14.6 m).

A liquefaction evaluation was performed on the post-treatment CPT

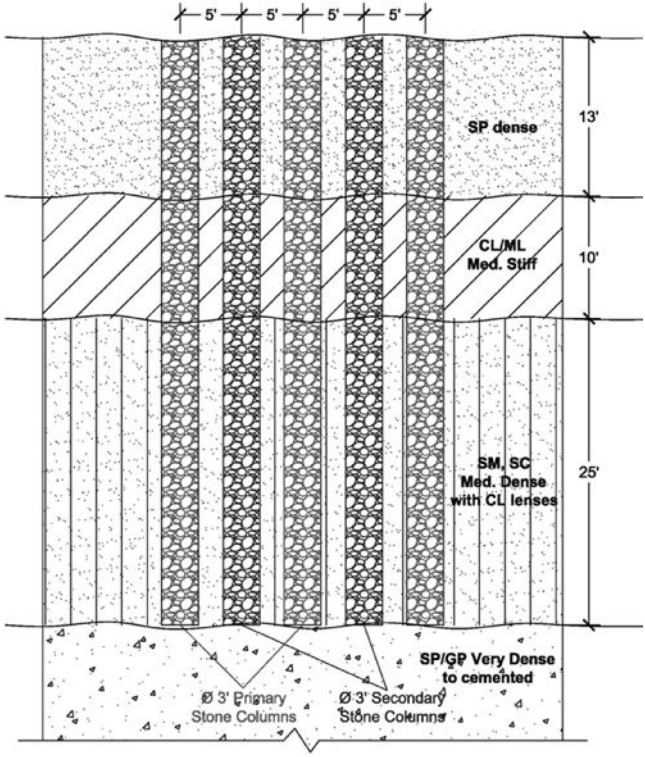


*Figure 3.43* Typical soil profile with stone columns under the church building (by courtesy of Hayward Baker Inc)

data for this project. The following outlines the analytical approach and compares CPTs before and after the stone column treatment.

Liquefaction-induced settlement analyses were based on Tokimatsu and Seed (1987) procedures and NCEER (1997) for site liquefaction evaluation. To be conservative, the soil thin layer connection was not used. The site is very close to an active fault and has a design earthquake magnitude of 6.6 and a peak ground surface acceleration of 0.69 g. The site design water table depth is 12.5 ft (3.8 m) below ground surface. A factor of safety of 1.1 was used in the liquefaction analysis and its settlement calculation. The stated procedures were developed as a function of the penetration resistance. Results of the calculations at location of pre-CPT and post-CPT are plotted in Figure 3.44. As shown, the stone column treatment significantly increased the cone tip resistance. However, the increase of the tip resistance caused the soil behaviour type index $I_c$ to decrease when compared with pre-treatment values.

Because of the decrease of the post-treatment $I_c$ value, the fines content calculated from post-CPT seems lower than the pre-CPT, therefore causing higher post-treatment liquefaction-induced settlement based on the Tokimatsu–Seed procedure.

Obviously, the vibro stone column treatment can not reduce the soil's fines content. To correct the fines content calculation error, the calculation was modified, maintaining a similar fines content as the pre-CPT data (shown in Figure 3.45) and the liquefaction-induced settlement was calculated accordingly. This $I_c$ correction reduced about 1 inch (25 mm) calculated liquefaction-induced settlement, compared with these before $I_c$ correction. The post-treatment CPTs were performed two weeks after stone column installation at the ground surface elevation 4.5 ft (1.4 m) below original grade. In Figures 3.44 and 3.45 the CPT depths are therefore adjusted to match the pre- and post-CPT elevations.

Based on the local building code, the site liquefaction analysis should be based on a 200 years flood water table depth, which is 12.5 ft (3.8 m) below the ground improvement working elevation. The real groundwater table depth during production was about 32.5 ft (9.9 m). To assist the bottom feed S300 vibro probe penetration through the unsaturated medium stiff to very stiff clay layers present on site, a Bauer BG-24 drill rig was used to pre-drill the top 30 ft (9.1 m) with a 2 ft (0.6 m) diameter auger.

The effectiveness of vibro compaction is directly related to the soil type. Figure 3.46 shows the comparison of normalised CPT tip resistance between pre- and post-treatment as a function of $I_c$ and the calculated soil's fines content, with the $I_c$ values being the corrected values according to Figure 3.45.

It must be emphasised here that the soil liquefaction and vibro compaction share the same mechanism, i.e. the sand densification under cyclic shear stress. The soils near the vibrator experienced an extremely strong "artificial earthquake". Therefore, the soil liquefaction screening criteria can be used

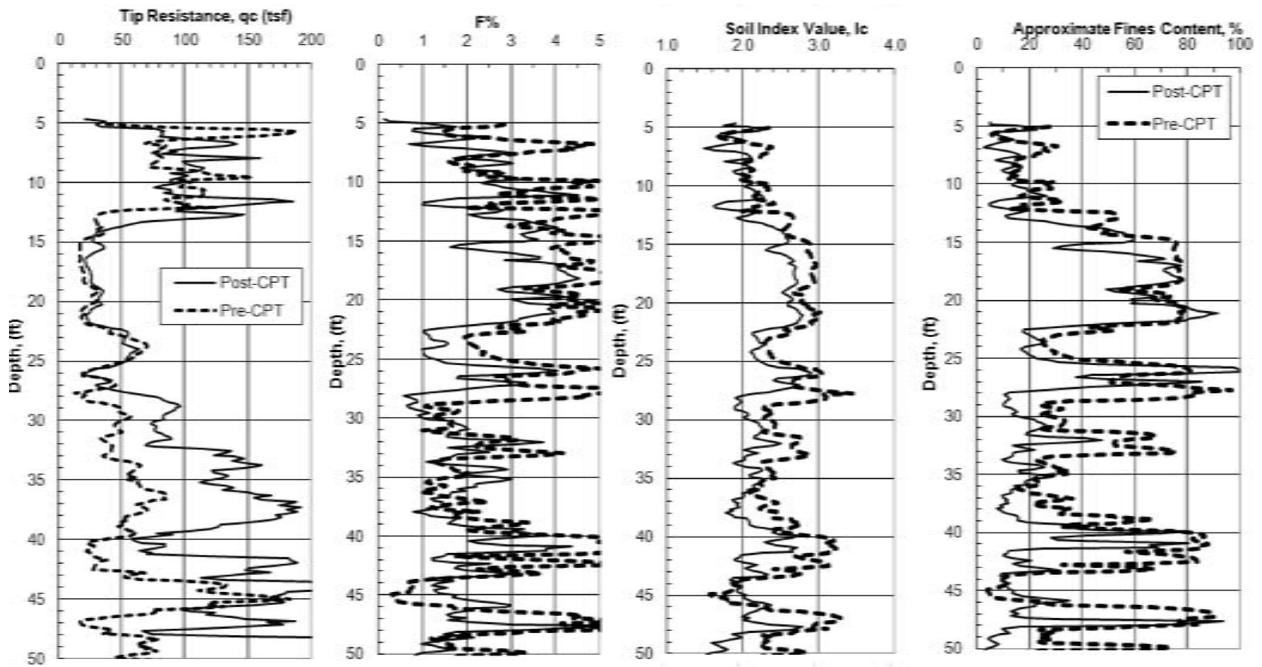


*Figure 3.44* Comparison between pre- and post-treatment CPT before $I_c$ correction (by courtesy of Hayward Baker Inc)

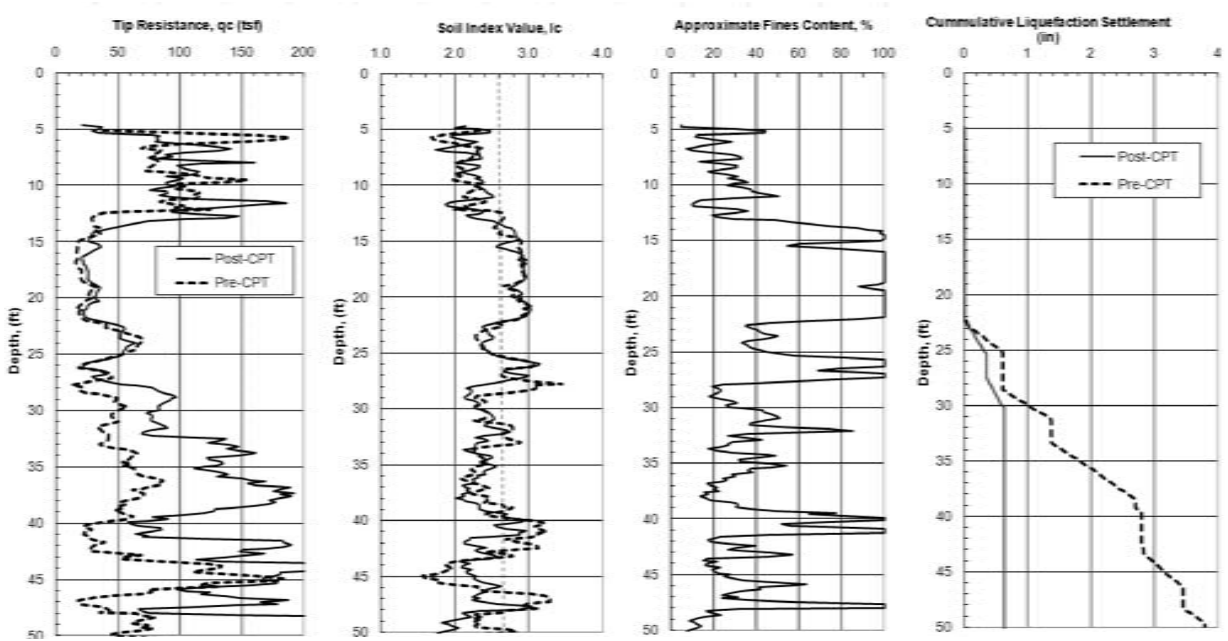


*Figure 3.45* Post-treatment CPT liquefaction analysis after $I_c$ correction (by courtesy of Hayward Baker Inc)

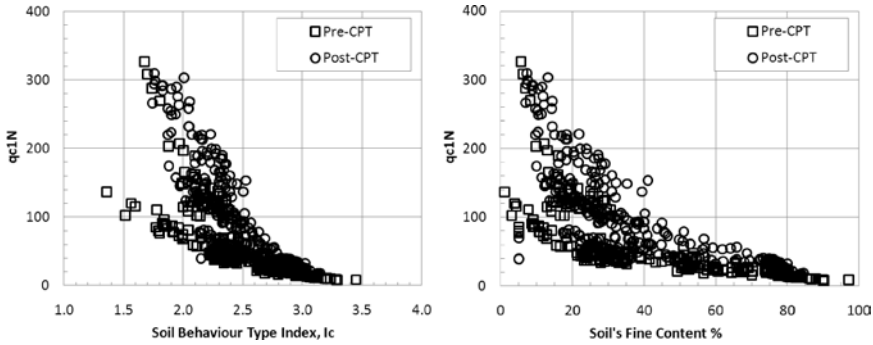


*Figure 3.46* The effectiveness of vibro densification (a) related to $I_c$ and (b) the soil fines content (by courtesy of Hayward Baker Inc)

directly to evaluate the vibro densification effectiveness. In soils with a soil behaviour type index $I_c$ in excess of 2.6 and considered as non-liquefiable, the vibro stone column treatment only has minimal effect in terms of post-CPT tip resistance, as shown in Figure 3.46(a).

Traditionally, geotechnical engineers use the soil's fines content as an indicator of its suitability for vibro compaction, especially in silty sands with SPT sampling and laboratory gradation test results. However, the clay content in sands has more impact on their densification and liquefaction behaviour than the mere percentage of fines passing the 200# sieve (0.07 mm). Although less expressive, Figure 3.46(b) indicates that sands with a soil fines content interpolated from CPT in excess of 30% do not respond anymore to vibratory compaction.

# 4 Improvement of fine-grained and cohesive soils by vibro replacement stone columns

## 4.1 Vibro replacement stone column technique

We have seen from the description of the development of the deep vibratory processes that vibro stone columns extend the limits of application of these ground improvement methods from predominantly non-cohesive into fine-grained cohesive soils. With regard to the grain size distribution of the soils to be improved, vibro replacement stone columns are used when conditions prevail as represented by areas outside of zone B in Figure 3.11. In the following, it will be shown that the load-carrying capability of soils so improved depends primarily from the interaction of the stone columns with the surrounding soil. The columns are supported by the soil which they replace and which requires therefore a certain minimum strength.

With increasing fines content in the grain size distribution of sands, the spacing between compaction probes needs to be decreased to obtain sufficient compaction when using the vibro compaction technique, as discussed in Chapter 3. At the same time, the addition of coarse backfill material helps to achieve the desired density. However, when the fines content exceeds about 10% the vibrations emanating from the depth vibrator can no longer separate the soil particles from each other to achieve a closer density, owing to their cohesive forces. Improvement of such soils, which are generally relatively soft and impervious, can be effected by introducing stone columns. Two methods are currently being distinguished by the strength range of the soils to be improved, generally in terms of their undrained shear strength $c_u$.

The *vibro replacement wet method* is employed only in water-bearing soft soils within a strength range of around $c_u$ = 10–30 kN/m$^2$. In these soils the depth vibrator normally sinks by its own weight, and that of the extension tubes, to the desired depth, helped only by the low pressure, large volume bottom jets. Collapsing soil from the side walls of the hole is transported in the water flow to the surface where an effective sludge and water management has to take care of it. To avoid pollution, only water that has been largely freed from soil particles is allowed to be disposed of into available recipients. The water can contain significant amounts of suspended silt and

clay which require proper handling in settling ponds and standing pools before the water can be reused for the stone column production or before it is released. These procedures need to be well organised to avoid disruption of the work or slowing down of production. In this context it is, however, necessary to remember that sufficient water volume is an integral part of the wet vibro replacement stone column method to guarantee stability of the hole and its diameter.

On reaching the desired depth, the vibrator is often completely withdrawn from the bore before it is allowed to repenetrate rapidly – sometimes a few times – to full depth, in this way allowing the bore to be cleaned from loosened soil material and its diameter to increase. In most cases the bore created is at least temporarily stable, and coarse backfill can now be filled, preferably in small doses, into the bore hole. The vibrator is then lowered again to full depth and the vibrations, together with a slight up-and-downward motion with amplitude of generally not more than a metre, cause the backfill to be compacted and rammed into the sides of the bore. With increasing density of the backfill, vibrations are also transmitted to the surrounding soil. The resulting shear stresses may cause the soil to collapse leading to a further increased bore diameter as the continuing water flow, movement of the vibrator and of the backfill transports this fine material to the surface. When equilibrium is reached, column building begins as further stone is added as described or through the annulus around the vibrator remaining in the bore hole. Rising resistance indicated by slowing down the sinking rate of the machine, accompanied by increased power consumption of the vibrator motor, is a sign that column building is completed at this level and that repetition of this procedure should start at the next higher level.

In this manner, a stone column is formed up to ground surface in a self-compensating way with diameters of about 0.8–1.2 m, depending on the soil resistance and the shearing and flushing action over the time of the build-up (Figure 4.1(a)).

It is evident that this replacement process causes only relatively little disturbance to the surrounding native soil, without apparent smear damage (Greenwood, 1976), allowing, under loading conditions, the pore water to freely drain into the columns, resulting in a considerably accelerated consolidation process (see Section 4.3.4).

In more stable insensitive cohesive soils with strength values $c_u$ = 30–50 kN/m$^2$ the *dry vibro displacement method* is applied whereby the depth vibrator penetrates by vibratory impact and by its own weight, sometimes increased by that of the heavy extension tubes, and always helped by compressed air emanating through the bottom jets of the machine. When the design depth is reached, it is always necessary to extract the vibrator completely from the ground to allow coarse backfill material to be introduced in small quantities into the bore. The compressed air is used primarily to prevent the bore from collapsing as a result of the suction developing when the vibrator is withdrawn, as it is generally in a tight fit in the ground. The

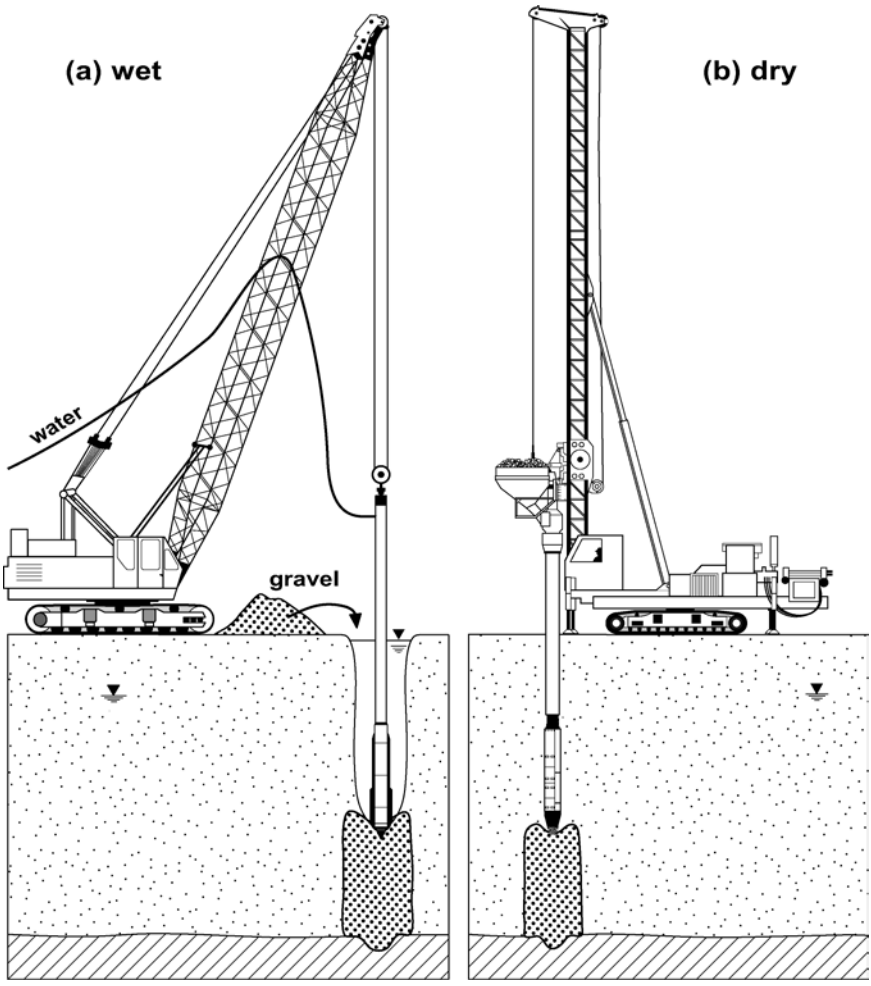


*Figure 4.1* Stone columns built (a) by the wet vibro replacement method and (b) by the dry displacement bottom feed method

column is built by tipping the backfill into the bore hole and by lowering the machine back into it in lifts of about half a metre. By the action of the depth vibrator, the coarse backfill is compacted and displaced laterally and downwards forming in this way a tightly compacted stone column of about 0.5–0.6 m diameter which is well interlocked with the surrounding sheared soil. To safeguard column verticality and to assist penetration into stiff soil, custom-built cranes with leaders were developed, replacing the standard cranes as base machines.

As this method has its downsides with deeper penetration, it being relatively slow and requiring well-supervised workmanship, a special depth

vibrator was developed avoiding the need to remove it from the ground for material backfilling and at the same time ensuring column continuity for deeper columns in much softer soils ($c_u$ = 10 kN/m$^2$). With this *dry displacement bottom feed method* the backfill is discharged directly at the point of the vibrator through a pipe that is fitted to its outside and which is fed by a backfill container with an airlock situated on top of the extension tubes. The system is best used with dedicated cranes for the depth of less than 20 m; These are called vibrocats and develop considerable pull-down forces to compensate the increased depth vibrator cross-section (Section 4.2). For greater depths standard crawler cranes can be used. A continuous column is formed by pulling the vibrator in steps of 0.5–1.0 m within the ground, in this way allowing the backfill to flow into the bore hole, helped by a moderate flow of compressed air. By repenetrating until resistance is met, the coarse material is compacted and laterally displaced into the soil. This procedure is repeated leaving behind a well-compacted stone column of about 0.5–0.8 m in diameter upto working grade level. The method is to a certain degree self-compensating since in softer soils column diameters tend to be larger than in stiffer soils. Figure 4.1(b) shows typical plant while forming vibro stone columns with the dry bottom feed method.

It is evident that the wet system primarily replaces native soil by coarse backfill with relatively little lateral displacement; the dry system is, in contrast, in the first place a displacement method. Nevertheless both methods are today generally named vibro replacement stone column methods, but we will see later that displacement of the surrounding soil can add extra strength to columns of otherwise equal dimensions.

The grading of backfill stone for the vibro stone columns differs slightly between the different methods of construction:

- For the replacement wet method rounded or subangular stone or gravel 30–60 mm in size and comparatively uniformly graded is used which passes easily through the annulus around the machine. It is always found, on excavation of a stone column, that the voids between the stones, which are in close contact with each other, are always found to be filled with the coarser particles (sand and coarse silt) from the native soil ensuring a relatively compact stone column. The finer parts of the native soil are transported to the ground surface with the flushing water.
- For the bottom feed method finer gravel or crushed stone of 10–40 mm is necessary to pass through the delivery system including the feed pipe to the vibrator point. Well-graded sand can also be used should no coarser backfill be available, but this will forfeit a considerable amount of column strength in comparison to the coarser stone backfill (Section 4.3).

The material of the stone backfill should be environmentally acceptable and can be taken either from natural gravel deposits, crushed natural stone,

or from recycled concrete or brick debris. The material itself should be of sufficient hardness and strength to resist the strong abrasive forces resulting from the vibratory action of the depth vibrator. It should not contain any organic and other deleterious material. It should be chemically inert and should resist – in cases of aggressive groundwater conditions – any potential ion attack during the lifetime of the foundations.

Regardless of the method, whether suspension from crawler cranes, or guided by leaders, vibrators are always applied in the vertical orientation. The vibrator forms a vertical hole largely by displacement, sometimes enlarged by water flushing, ultimately hanging as a pendulum in the bore hole. While crane-hung vibrators receive no guidance when penetrating and during column construction, the special rigs (Section 4.2) are generally equipped with vertical leaders providing excellent guidance to the vibrator in all working phases. Varying soil strengths during penetration, and obstructions, may cause the vibrator to depart from its vertical position. It is very important that these deviations are detected and corrected in good time in order to ensure the verticality of the stiffening columns.

Vibro stone columns improve the foundation ground because they are stiffer and of higher strength than the soil which they have replaced. The reinforcing effect depends primarily on the column diameter and the distance between adjacent columns. They are generally installed with centre spacing of 1.5–3.5 m, in rows below strip footings and in triangular or square patterns below single footings and widespread loaded areas. As with vibro compaction, the upper 0.3–0.5 m of a stone column are generally less well compacted as a result of vibrator shape and missing lateral support from the surrounding soil. Therefore, before concreting work begins, the foundation area is excavated to the required level, about 0.3 m of well-graded coarse gravel is placed on top of the treated area and the whole surface prepared in this way is well compacted with a standard surface compactor.

Production rates depend, in the main, on the stiffness of the ground needing improvement but also on the stone volume consumed for the stone columns, on the characteristics of the vibrator and on the efficiency of the working crew. Rates generally range between 150 m and 450 m of stone columns for a 10-hour shift per vibrator unit.

## 4.2 Special equipment

For the construction of vibro replacement stone columns employing the wet method, essentially the same equipment is needed as for the vibro compaction process and as described in Sections 3.1 and 3.2. When working in cohesive soils, the water management and sludge handling on site requires special attention. Silt and clay particles in suspension cannot be completely or easily removed from the water before it is released into natural or artificial recipients. If this shortcoming is environmentally acceptable, the

construction of stone columns with diameters in excess of 0.6 m can best be achieved employing vibrators with larger diameters (see Table 3.1) and high volume, low pressure water pumps. Very often when soil conditions prevail where layers of sand alternate with cohesive soils, the use of high-amplitude, low-frequency vibrators is advisable as these machines allow both efficient compaction of the sand layer and forming of stone columns in one operation.

With the dry vibro displacement method, vibrators with higher frequencies and smaller diameters are used which generally penetrate more effectively into the ground. The water pipes are replaced by smaller diameter air pipes also leading to the vibrator point. Compressed air generated by standard compressors (9 $m^3$/min, 5 bar), often mounted together with the electric generator or hydraulic power pack on the rear of the crawler crane, produces a moderate airflow, just strong enough to avoid suction developing when the vibrator is withdrawn from the ground, and sufficient to keep the stone backfill flowing in the stone supply system when the bottom feed method is used. Too strong an airflow at too high pressure should be avoided as it often does more damage to the fabric of soft soils than helping to remove the vibrator from the bore hole (Greenwood and Kirsch, 1984). It can also cause unwanted heave of the ground.

Today, we mainly use purpose-built machines with vertical leader and on-board generator and compressor. Since these machines are generally mounted on crawlers they are often called vibrocats. A special gravel container at its front allows the stone backfill to be funnelled into the bore hole, generally in small quantities just enough to form about 1.0 m of stone column length. As effective penetration aids, these machines develop a pull down force of up to about 200 kN. When obstructions or stiff layers prevent the vibrator from reaching the design depth, a more powerful vibrator can resolve the problem or preboring with continuous flight augers might become necessary, preventing uneconomical slow production and unnecessary wear and tear on the depth vibrator.

The special bottom feed equipment both for crane-hung and vibrocat operation is today the standard setup for dry stone column construction. Figure 4.2 shows a vibrocat rig with a special depth vibrator whose extension tubes have been transformed into gravel containers, feeding the stone backfill through a half-moon-shaped gravel pipe to the point of the depth vibrator.

The construction details of a bottom feed vibrator are shown in Figure 4.3 in a schematic mode. Since its cross-section is substantially increased as a result of the attached gravel pipes, penetration resistance of the soil increases considerably, requiring much more pull-down capability of the vibrocat – hence the need for the strong activating forces available in modern machines. As can also be seen from Figure 4.3, the cross-section through the vibrator and gravel pipe is of oval shape, no longer circular. The stone columns so constructed are of an oval shape and need to be transformed

*Figure 4.2* Vibrocat with bottom feed vibrator (by courtesy of Keller Group plc)

into circular columns of equal cross-sectional area in relevant design calculations.

As already mentioned, the vibrocat carries generator and compressor and is equipped with a gravel hopper which is filled with stone backfill at ground level and which slides up the vertical leader to the top of the extension/gravel container pipe. The hopper is emptied via an airlock into the gravel container with a capacity of approximately 0.1 $m^3$/m of extension tube, allowing the stone column construction to continue, usually without any interruption. With modern machines this process can be carried out in an automated way, whereby the vibrator lifts, including stone filling, repenetration and compaction are predetermined at the beginning of the site and repeated in the same manner for all stone columns of any given project. Feeding of the stone container is equally automated, to allow the operator to concentrate on the process controls displayed in front of him in the cabin of

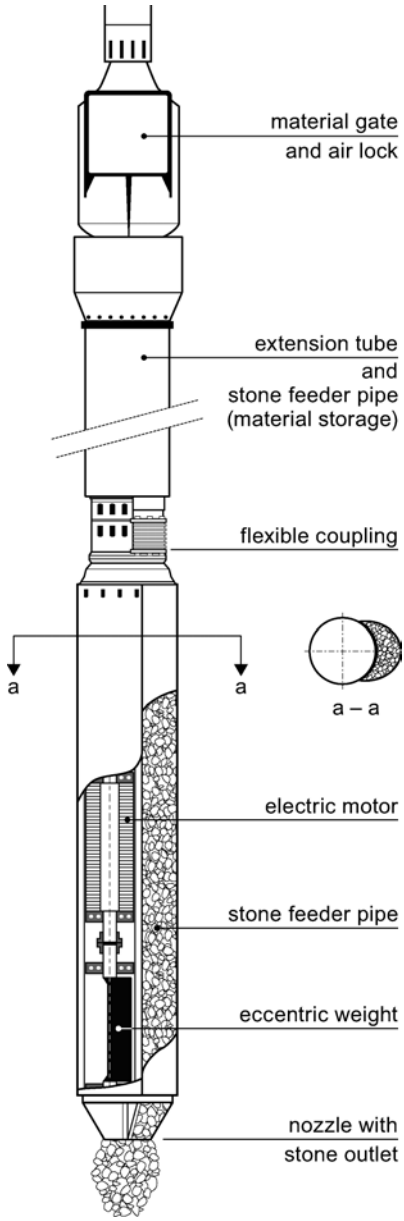


*Figure 4.3* Special features of a bottom feed vibrator

the rig. The need to refill the gravel container is indicated to the operator via a level control inside the gravel container. All process data as displayed to the operator are stored as a function of time and can be plotted for each individual stone column in real time or at the end of the shift. These data

include for each stone column: time of execution, depth, power and stone consumption over depth, total stone consumption, verticality of the leader and optionally also the pressure of the air flow.

Modern data acquisition systems controlling both column building and operational parameters of the equipment employed will eventually, together with GPS systems, allow the contractor to construct large numbers of stone columns of uniform quality and in a fully automated way. Telemetric systems are already used to transmit not only service and machine performance indicators (fuel consumption, oil pressure, etc.) but also machine location, and all relevant process data as compiled by the control and data acquisition unit employed.

Modern vibrocats are designed to install stone columns to depths of up to 20 m. To expedite setting up of the vibro replacement equipment on site special rigs were developed for shorter, more frequently used columns of up to 10 m, which represents the depth range of the majority of sites, allowing the complete bottom feed depth vibrator to remain on the rig when being transported. Figure 4.4 shows such a special vibro rig when transported on a low bed.

For stone columns deeper than 20 m, and for columns to be constructed over open waters, the crane-hung bottom feed method can be used. Base machines for this purpose are generally heavy crawler cranes that carry the depth vibrator with standard extension tubes and welded-on gravel pipes.


*Figure 4.4* Minicat on low bed (by courtesy of Keller Group plc)

A gravel container capable of carrying about 2 $m^3$ of stone backfill is situated on top of the extension tube. Gravel is filled at ground level by pay-loaders into a hopper, which is pulled upwards and delivers its contents via a receiving mechanism into the gravel container, from where it is released by special controls into the gravel pipe. Figure 4.5 shows the feeding mechanism of a crane-hung bottom feed assembly for constructing deep stone columns.

When stone columns need to be built through deep water, supply of the backfill stone to the machine is often rather difficult to achieve. For such applications special pneumatic or hydraulic transport systems for the gravel were developed which replace mechanical stone delivery by hoppers. Figure 4.6 shows such an arrangement by which the gravel is transported hydraulically via special pumps and hoses into the receiving tank from where stone supply takes place through the gravel pipe in an uninterrupted

*Figure 4.5* Crane-hung dry bottom feed system for deep stone columns (S-Alpha system) (by courtesy of Keller Group plc)

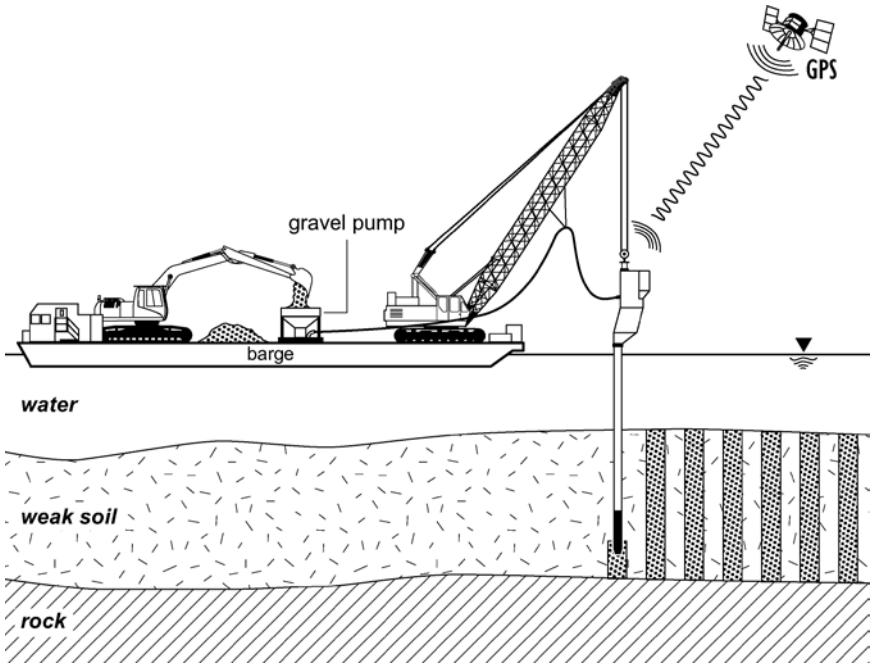


*Figure 4.6* Crane-hung bottom feed system with gravel pump for stone supply

manner under constant air pressure until it is released at the vibrator nose cone into the soil. Up and down movements compact the stone and displace it into the soil, thus forming a stone column up to the sea bottom or ground level.

## 4.3 Principal behaviour of vibro stone columns under load and their design

### *4.3.1 Overview and definitions*

Vibro stone columns are in general used to improve characteristics such as the strength and compressibility of fine-grained cohesive soils that are deemed insufficient for the geotechnical purpose. These soils are predominantly water-bearing silty and clayey sands, sandy silts and silt and clay mixtures. Their main characteristics, water content, consistency and shear strength, are shown in Figure 4.7. These soil properties, together with those of the stone columns, influence the behaviour of the composite soil–stone column matrix.

Certain definitions and some of the terminology used in conjunction with ground improvement by vibro replacement stone columns now follow. The terms “vibro replacement stone column”, “vibro stone column” and “stone

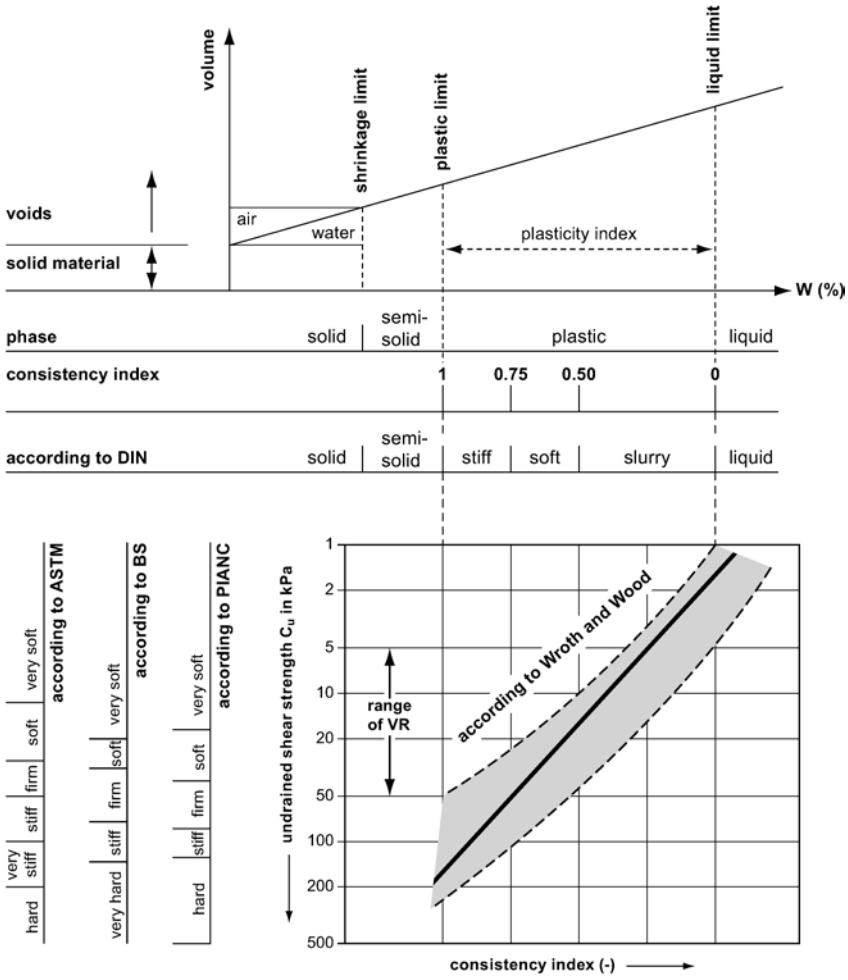


*Figure 4.7* Water content, consistency and shear strength of fine-grained cohesive soils (from CUR, 1996)

column" are used synonymously. In contrast to a single stone column, a group of stone columns is represented by a certain number of stone columns that are arranged in such a way that they influence each other in the ground when loaded and this is described as the "group effect". In contrast to the isolated stone column and the column group, large numbers of regularly arranged stone columns of equal diameter and equal separating distance are normally referred to as an "infinite grid pattern of stone columns". Their behaviour under load can be described by the unit cell concept, whereby – irrespective of the position of the column within the grid – all columns behave equally, and the description of the mechanical model of a single

column is representative for the whole grid. Figure 4.8 gives the geometry of the unit cell for triangular and square grid patterns.

The equivalent diameter of the circular unit cell $d_e$ as a function of the column distance $b$ can be calculated as

$$d_e = C \cdot b \tag{4.1}$$

with

$C = 1.05$ for the triangular pattern
$C = 1.13$ for the square pattern.

Another important parameter of the infinite grid pattern is the area replacement ratio $a_c$ calculated as ratio of column area $A_c$ and total unit cell area $A$:

$$a_c = \frac{A_c}{A} = \frac{1}{C^2} \cdot \left(\frac{d}{d_e}\right)^2 \tag{4.2}$$

Because the unit cell is symmetric by geometry, a uniform load evenly distributed over the infinitely extended area and applied by a rigid raft will not cause any shear stresses or horizontal deformations to develop at its outside boundaries. Consequently the uniform loading will remain within the unit cell. Because the stone column is stiffer than the surrounding soil, vertical stresses are concentrated in the stone column material with an accompanying stress reduction in the less stiff soil surrounding the column. This stress distribution between column and soil within the unit cell is generally called stress concentration $n$ and is represented by the ratio of the vertical stresses $\sigma_c$ in the column and the vertical stress $\sigma_s$ in the soil:

$$n = \frac{\sigma_c}{\sigma_s} \tag{4.3}$$

Equilibrium with the acting vertical stress $\sigma$ is given by the relationship

$$\sigma = \sigma_c \frac{A_c}{A} + \sigma_s \left(1 - \frac{A_c}{A}\right) = a_c \cdot \sigma_c + (1 - a_c) \cdot \sigma_s \tag{4.4}$$

which leads to expressions for $\sigma_c$ and $\sigma_s$ as follows:

$$\sigma_c = \sigma \cdot \frac{n}{(1 + (n-1) \cdot a_c)} = n_c \cdot \sigma \qquad \text{with } n_c = \frac{n}{(1 + (n-1) \cdot a_c)} \tag{4.5)/(4.6}$$

$$\sigma_s = \sigma \cdot \frac{1}{(1 + (n-1) \cdot a_c)} = n_s \cdot \sigma \qquad \text{with } n_s = \frac{1}{(1 + (n-1) \cdot a_c)} \tag{4.7)/(4.8}$$

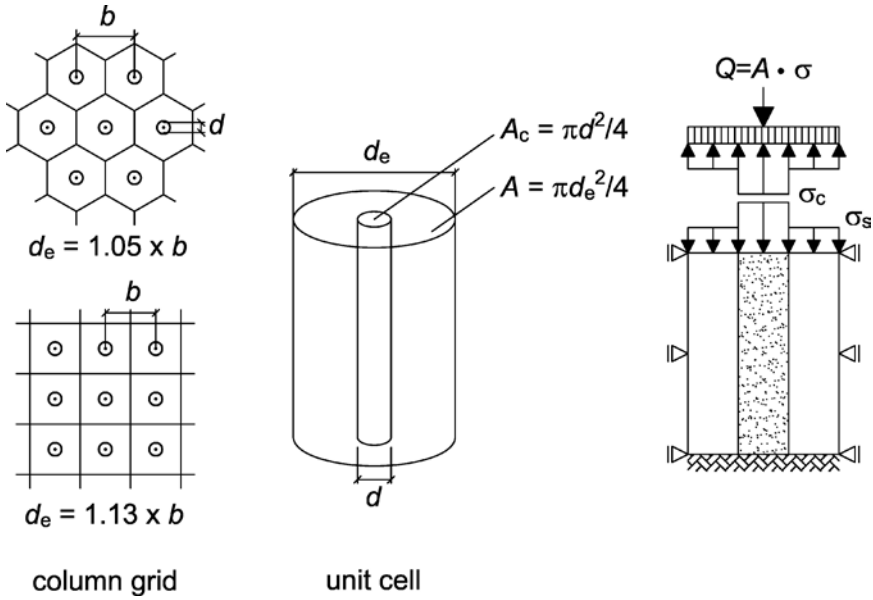


*Figure 4.8* Column grid patterns and unit cell concept

The expressions $n_c$ and $n_s$ represent the ratio of stresses in the stone column and the soil, respectively, to the average stress $\sigma$ acting on the unit cell and are connected with each other and the stress concentration factor $n$ by the expression:

$$n_c = n \cdot n_s \tag{4.9}$$

Equation (4.7) can be rewritten for the ratio of the acting stress $\sigma$ with the soil stress $\sigma_s$:

$$\frac{\sigma}{\sigma_s} = 1 + (n - 1) \cdot a_c \tag{4.7a}$$

The unit concept stipulates equal settlements for stone column and tributary soil:

$$s_s = s_c \tag{4.10}$$

Priebe (1976) was the first to define the settlement improvement $\beta$ as the ratio of the settlement $s$ of the untreated soil and the settlement $s_i$ of the improved soil. Using the assumption that settlements behave directly proportionally with their stresses, based on equation (4.10), an expression for

the settlement improvement factor $\beta$ can be derived from the unit cell concept:

$$\beta = \frac{s}{s_i} = \frac{\sigma}{\sigma_s} = 1 + (n - 1) \cdot a_c \tag{4.11}$$

In reality when other conditions generally prevail, the stress concentration factor $n$ depends not only on variables such as the area replacement ratio $a_c = A_c/A$, but also on the length of the stone column and particularly on the relative stiffness of column and soil. Values of $n$ measured in the field are about 1.5–5.0, usually taken close to foundation level. As Barksdale and Bachus (1983) have already pointed out, $n$ will increase with consolidation time and will not decrease below its value at the end of the primary settlement.

The expressions according to equations (4.6) and (4.8) are helpful in both settlement calculations and stability analyses for cases where the unit cell concept can be applied and where the stress concentration $n$ can be estimated with sufficient accuracy from equation (4.11). With decreasing numbers of stone columns in large groups the accuracy of the method decreases.

The main effect of a ground improvement measure is settlement reduction expressed by the improvement factor $\beta$ as the ratio of the settlement without stone columns and the settlement after ground improvement. The different behaviour of a stone column within a group is governed by its relative position within it and influencing its overall performance. With increasing numbers of columns, group behaviour approaches that of the infinite column grid. It is difficult to define the number of stone columns that no longer behave as a column group since other factors such as improvement depth, size and rigidity of the foundation have an influence. For practical reasons, more than 50 stone columns regularly arranged below a foundation slab may be addressed as an infinite pattern of columns when the ratio of foundation width to column depth is at least 3.

The effect of stone columns on the ground to be improved is manifold. The higher stiffness of the column material in relation to that of the soil leads to load concentrations on the columns thereby reducing the settlement. Because the column material is considerably more permeable than the soil, stone columns act as drains when constructed and loaded in water-bearing soils, reducing consolidation time substantially. The fill material also has a much higher shear strength compared to the original soil therefore also increasing its bearing capacity. The improvement effect is increased by the load concentration on the columns also leading to increased stability of structures when supported by vibro stone columns. In saturated soils, the existence of stone columns reduces the liquefaction potential of silt and sand deposits during dynamic loading or earthquakes. The combination of densification, drainage and increased shear strength prevents total loss of

strength during a seismic event. To summarise, the main effects of the vibro replacement method are:

- reduction of settlements
- reduction of consolidation time
- increase of bearing capacity
- reduction of liquefaction potential.

In parallel to the large variety of applications of vibro stone columns, and as a result of the technical development and better understanding of ground improvement in general, various computational and design methods have been proposed. These can be distinguished from each other by the computation approach, by the column geometry that is being considered and by the design objective, which could be bearing capacity, settlement reduction or acceleration, or earthquake risk mitigation. Some of these methods are exclusively based on empirical findings, while others use analytical approaches of the cylindrical half space or introduce empirical parameters into their design concept. A more recent group of methods develops design diagrams that are based on numerical calculations.

Most design methods deal with isolated column or the infinite grid of vibro stone columns. Almost all methods apply the principle of the circular unit cell (Figure 4.8). Only a few methods consider the behaviour of column groups.

Settlement reduction is of particular practical importance for the design of vibro stone columns, where the allowable bearing pressure needs to be secured in a separate step by also determining the ultimate bearing capacity of the system. In addition, consolidation time or the reduction of the liquefaction potential may also have to be determined.

A selection of the commonly used design methods can be found in Table 4.1 together with their key design targets. The table also gives the parameters necessary for the design calculation. These methods are empirical and analytical, purely analytical or analytical and numerical.

Ideally, the design models should reflect the interactions between load application, stone columns and surrounding soil as will be discussed in the following sections. In particular, the elastic–plastic behaviour and the dilatancy of the stone column material are important features for the model, and the model is not only valid for the two special cases of the isolated column and for the infinite column grid, but it also governs the column group behaviour. However, such high demands are not yet state-of-the-art in designing stone columns, since all methods are still based on far-reaching simplifying assumptions (Soyez, 1987; Bergado *et al.*, 1994; Kirsch, 2004).

### *4.3.2 Load-carrying mechanism and settlement estimation*

Principal loading situations for stone column foundations are shown in Figure 4.9. Foundation stresses acting on the improved soil lead to a stress

*Table 4.1* Necessary design parameters for commonly used computation methods

| | *Priebe* | *Goughnour / Bayuk* | *Hughes / Withers* | *Brauns* | *Van Impe / Madhav* | *Balaam / Booker* |
|---|---|---|---|---|---|---|
| **Column** | | | | | | |
| unit weight | • | • | | | | • |
| friction angle | • | • | • | • | • | • |
| cohesion | | | | | | |
| stiffness | • | • | | | • | • |
| Poisson's ratio | • | • | | | • | • |
| angle of dilatancy | | | | | • | • |
| **Soil** | | | | | | |
| unit weight | • | • | | | | • |
| friction angle | | • | | | | |
| cohesion | | | | | | |
| undrained shear strength | | | • | • | | |
| stiffness | • | | | | • | • |
| Poisson's ratio | • | | | | • | • |
| initial stress state | | • | | | | |
| loading | | • | | | | |

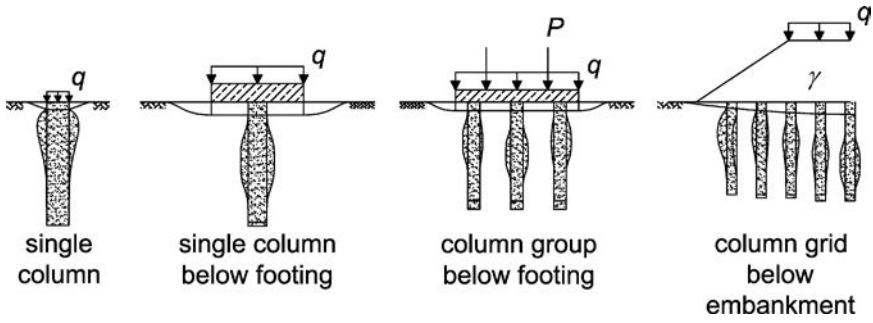


*Figure 4.9* Different loading scenarios for stone columns

concentration in the material of higher stiffness, i.e. in the stone columns, which results in a stress relief of the soft surrounding soil. From the assumption that vertical deformations of stone column and soil are equal in horizontal planes, with the reduced load on the native soil, follows the settlement reduction of this ground improvement system. Various researchers have confirmed this assumption in the laboratory (Nahrgang, 1976), by numerical calculations (Balaam and Poulos, 1983) and by in-situ measurements (Gruber, 1994; Kirsch, 2004).

In contrast to the load-carrying mechanism of a rigid foundation element, such as a pile, where the load transfer into the ground is by toe resistance and friction at the pile perimeter, stone columns transmit their load into the soil by stimulating its horizontal earth pressure without relative displacement between column and soil. In this state of contained compression, the stone column, which is characterised by high density and stiffness, will ultimately fail by bulging as a result of the high column load and the minimal supporting capacity of the surrounding soil. Owing to its high density, the column yields locally in its upper part under the shearing forces by lateral bulging, counteracted by the surrounding soil, depending on its stiffness and strength. This horizontal deformation is further increased by the dilatancy of the column material. This volume increase was measured to about 9%, albeit that there is considerable axial column compression (Kirsch, 2004).

The hypothesis that a column is triaxially loaded in confined compression leading to the peculiar horizontal deformation, as described, has been verified by numerous researchers (Greenwood, 1970; Hughes and Withers, 1974; Hughes *et al.*, 1975; Brauns, 1980; Barksdale and Bachus, 1983; Kirsch, 2004). This has been done theoretically, in model tests and in field tests on excavated columns. Figure 4.10 shows such a model test to investigate column group behaviour. The different behaviour of a centre column in comparison to one at the edge is clearly visible.

As column bulging is followed by lateral support, triggering soil deformation which in response further increases the horizontal stresses, the over-

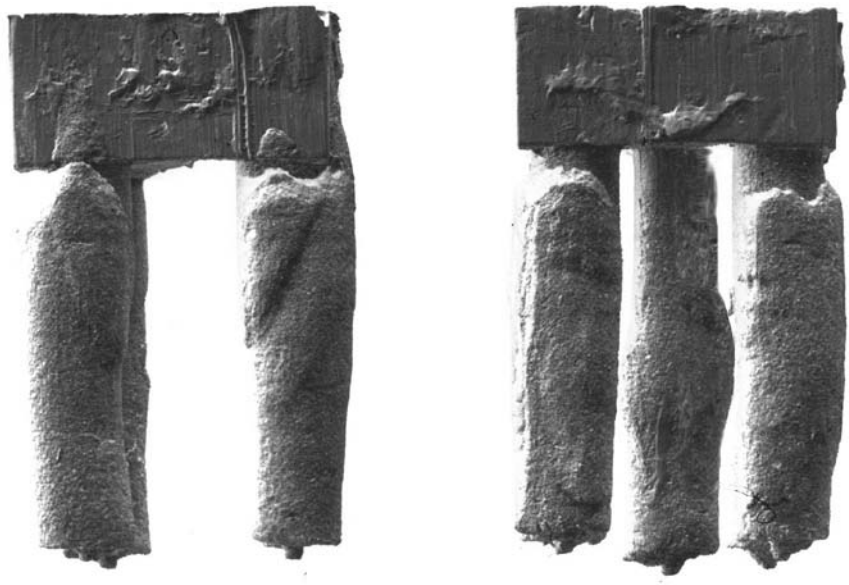

*Figure 4.10* Model tests on four and five stone columns to study column group behaviour

all load-carrying mechanism is controlled by the interaction of the load application with columns and native soil. Figure 4.11 shows the different features of this interaction of the composite of column and soil with the load application.

In most applications of the vibro replacement method the column heads are not in direct contact with the applied load, which is almost always transferred via a load distribution layer. Occasionally, horizontal load-

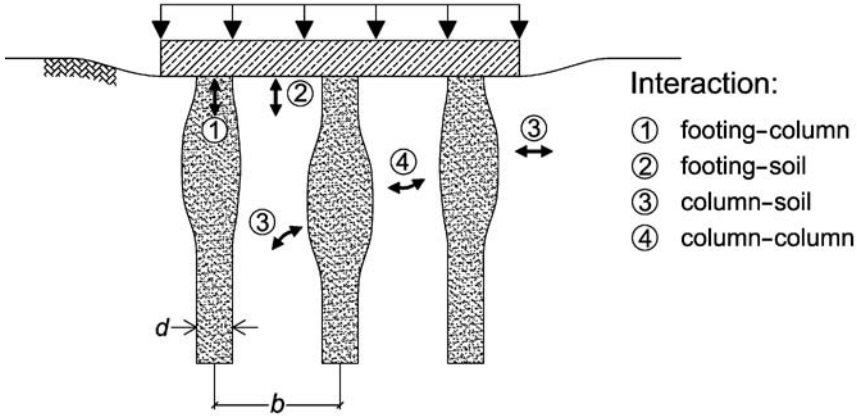


*Figure 4.11* Interaction of load application with stone columns and soil

carrying layers consisting of a combination of coarse granular material and special geotextiles are used, particularly below embankments and similar structures, where horizontal forces need to be controlled. These load-transfer layers can provide an additional load concentration at the column head when they are thick enough in relation to column diameter and distance for an arching effect to develop. This is beneficial for the design of the foundation slab, but the load distribution has no significant effect on the overall settlement (Figure 4.12).

Almost all approaches to calculating the settlement reduction by the use of vibro stone columns are based on the infinite column grid. Few deal with the quantitative behaviour of column groups, and all make major simplifying assumptions. Investigations of the settlement behaviour of isolated columns are rare and of little practical use. Frequently, however, single-column load testing is performed as a quality control measure and to predict settlement performance of structures, a method requiring particularly careful evaluation (see Section 4.4).

Greenwood (1970) was the first to propose a design chart for the infinite column grid providing a relationship for the reciprocal improvement factor $1/\beta$ as a function of the column distance in the grid for cohesive soils with strengths between $c_u$ = 20 kPa and $c_u$ = 40 kPa (Figure 4.13). From the context of the paper the column diameter can be assumed as 0.9 m to 1.0 m for wet and as 0.6 m to 0.7 m for dry column construction.

Of the many design methods, only two are of practical importance today – the Priebe method and the Goughnour and Bayuk method – which will be presented in the following. The Priebe method is widely used in Europe and was presented for the first time in 1976, with improvements and alterations made to it later (Priebe, 1976, 1988, 1995, 2003). The method uses the unit cell concept as shown in Figure 4.8 describing the stress situation of an infinite grid pattern of stone columns loaded with the vertical stress $\sigma$ via a rigid foundation raft. The deformation of the stone column is approximated by the cylindrical cavity expansion method, which was proposed by Gibson and Anderson (1961), for describing the pressure meter deformations.

From equal settlements for stone column and tributary soil within the unit

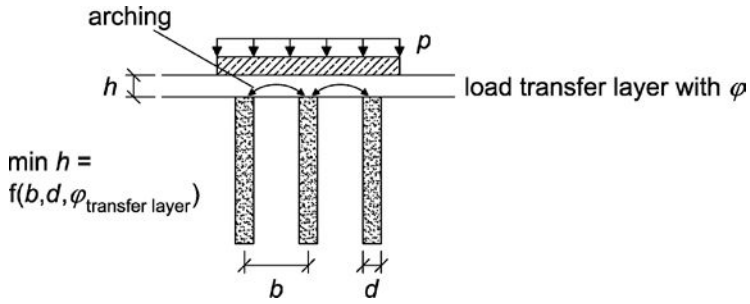


*Figure 4.12* Load-transfer layer and arching effect

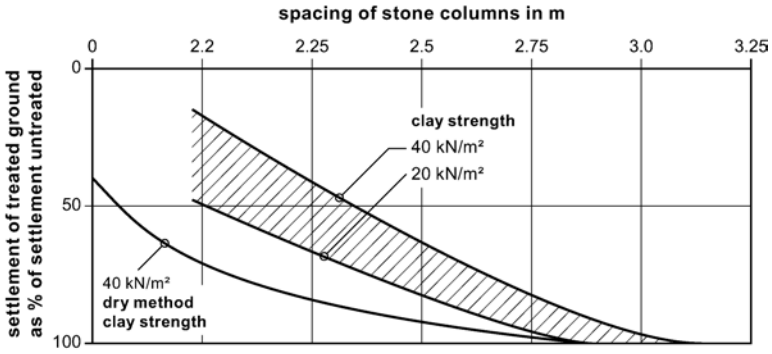


*Figure 4.13* Settlement diagram for stone columns in soft uniform clay (after Greenwood, 1970)
*Note:* Curves neglect immediate settlement and shear displacement. Columns assumed resting on firm clay, sand or harder ground

cell, and equilibrium between foundation load and the loading shares of column and soil, comes an expression for the improvement factor $\beta$ as the ratio of the settlement of the untreated ($s$) and the improved ground ($s_i$):

$$\beta = \frac{s}{s_i} = 1 + \frac{A_c}{A} \cdot \left[ \frac{1/2 + f(\mu_s, A_c / A)}{K_c \cdot f(\mu_s, A_c / A)} - 1 \right] \tag{4.12}$$

with

$$f(\mu_s, A_c / A) = \frac{1 - \mu_s^2}{1 - \mu_s - 2\mu_s^2} \cdot \frac{(1 - 2\mu_s) \cdot (1 - A_c / A)}{1 - 2\mu_s + A_c / A} \tag{4.13}$$

and

$$K_{ac} = \tan^2 (45° - \varphi_c / 2) \tag{4.14}$$

In these equations the notations of the unit cell from Figure 4.8 are used, with $\varphi_c$ representing the friction angle of the column material and $\mu_s$ the Poisson's ratio of the soil.

For easy use of the method, Priebe developed a diagram for the improvement factor $\beta$ for the infinite column grid as a function of the ratio $A/A_c$ (total grid area $A$ to column area $A_c$) with friction angle $\varphi_c$ of the column material as sole parameter. In Figure 4.14, this diagram is presented with the area replacement ratio $a_c = A_c/A$ as abscissa for the practically relevant range of $a_c$ between 0.10 and 0.35. The graph was also extended to column material friction angles in excess of 45°.

In practice, the method requires a conventional settlement calculation to be carried out for the untreated ground, usually by the summation of settle-

ment contributions from layers of differing depths, properties and stresses. This settlement $s$ without soil improvement is then divided by the improvement factor $\beta$ as taken from Figure 4.14 for the respective replacement ratio $a_c$ and the column friction angle $\varphi_c$. The settlement with soil improvement $s_i$ follows accordingly:

$$s_i = \frac{s}{\beta} \tag{4.15}$$

Stress concentration factors $n$ after Priebe range between 5 and 11 for area replacement ratios $a_c$ between 0.1 and 0.4 and for friction angles of the stone column material between 35° and 45°. These $n$ values overestimate the effect of the stone columns to a certain extent when compared with field measurements in which $n$ was found to be between 1.5 and 5, as already mentioned.

Priebe assumes that the stress state in the soil surrounding the stone column will be influenced by its installation in such a way that hydrostatic stresses develop. Consequently, he sets the earth pressure coefficient to $K = 1$. Other key assumptions initially made in this simplified calculation procedure are that the stone columns are based on a competent bearing stratum and that the column material is incompressible. In addition, both column and soil density are neglected, which has the consequence that the lateral support provided by the surrounding soil would not increase with depth, resulting in a column expansion that would be constant over its full length. Subsequent revisions of the method (Priebe, 1995, 2003) consider the positive influence of the compressibility of the column material, of the

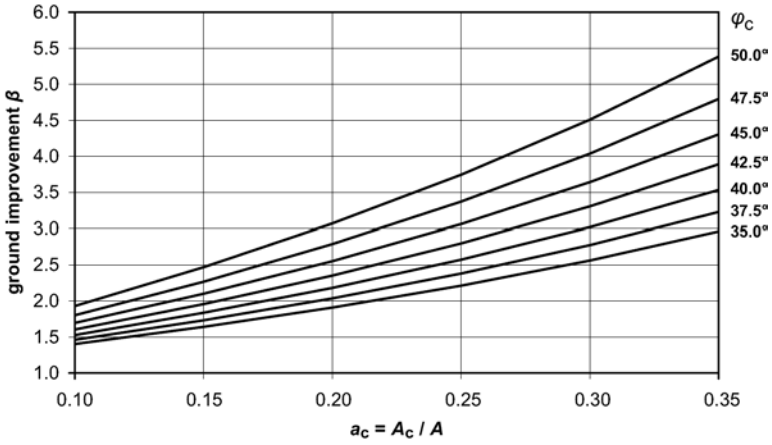


*Figure 4.14* Basic ground improvement design chart after Priebe, 1976 for infinite column grid patterns with $a_c$ between 0.1 and 0.35 and extended range of $\varphi_c$

bulk weight of column and soil, and allow for an estimate of the additional settlement of "floating" stone columns that are not founded on a load-carrying stratum. One of these revisions (Priebe, 1988) also includes charts for computing the settlements of single and strip footings. Unfortunately, the settlement computations with these refinements are somewhat more cumbersome, as can be seen in Section 4.6.1, where a case history demonstrates the use of the revised Priebe method. The method has also been frequently adapted to spreadsheet programs and ready-made software solutions. For a quick assessment of the expected settlements of a structure, the standard method is, however, considered adequate.

Goughnour and Bayuk (1979b) and Goughnour (1983) propose an incremental solution, based on the unit cell concept, for the settlement calculation of an infinite column grid. The unit cell is divided into slices of the thickness $\Delta h$ for which the vertical deformation is independently calculated, based on elastic and elastic–plastic analysis, with the larger of the two being the relevant deformation. Computation starts with the incremental slice at the column head and is carried on to the bottom of the column. Figure 4.15 shows a flow chart of the necessary computational steps. The method is, however, rather unsuitable for a conventional hand calculation because of the iterative calculation approach necessary for the solution of its set of equations. Computer programs were therefore developed instead.

Key assumptions of this method are that shear stresses are zero at the unit cell perimeter, that they are also zero at the surface and bottom of each incremental slice, and that no relative deformation occurs between column and soil. In Section 4.6.1 a sample calculation of this method in comparison with the Priebe method is presented.

From the relatively large number of methods proposed for the estimation of settlements of soft soil improved by stone columns, those have been proposed that are widely used today, delivering reasonable results within the normal accuracy bound of settlement calculations, provided that reasonable assumptions are made with regard to the shear strength of the column material and in particular to the area ratio of the column grid.

Numerical calculations adopting the finite element method are recommended for major projects and in the presence of particularly soft soils, say below $c_u = 20$ kPa, provided that the elastic–plastic behaviour of the unit cell and the shear zones in the stone column can be modelled with sufficient accuracy. For large foundations, two-dimensional calculations may suffice, but other foundations may require the use of three-dimensional approaches.

### *4.3.3 Failure mechanism and bearing capacity calculations*

The bearing capacity of a foundation on vibro replacement stone columns is governed by a number of possible failure mechanisms. For isolated columns these are

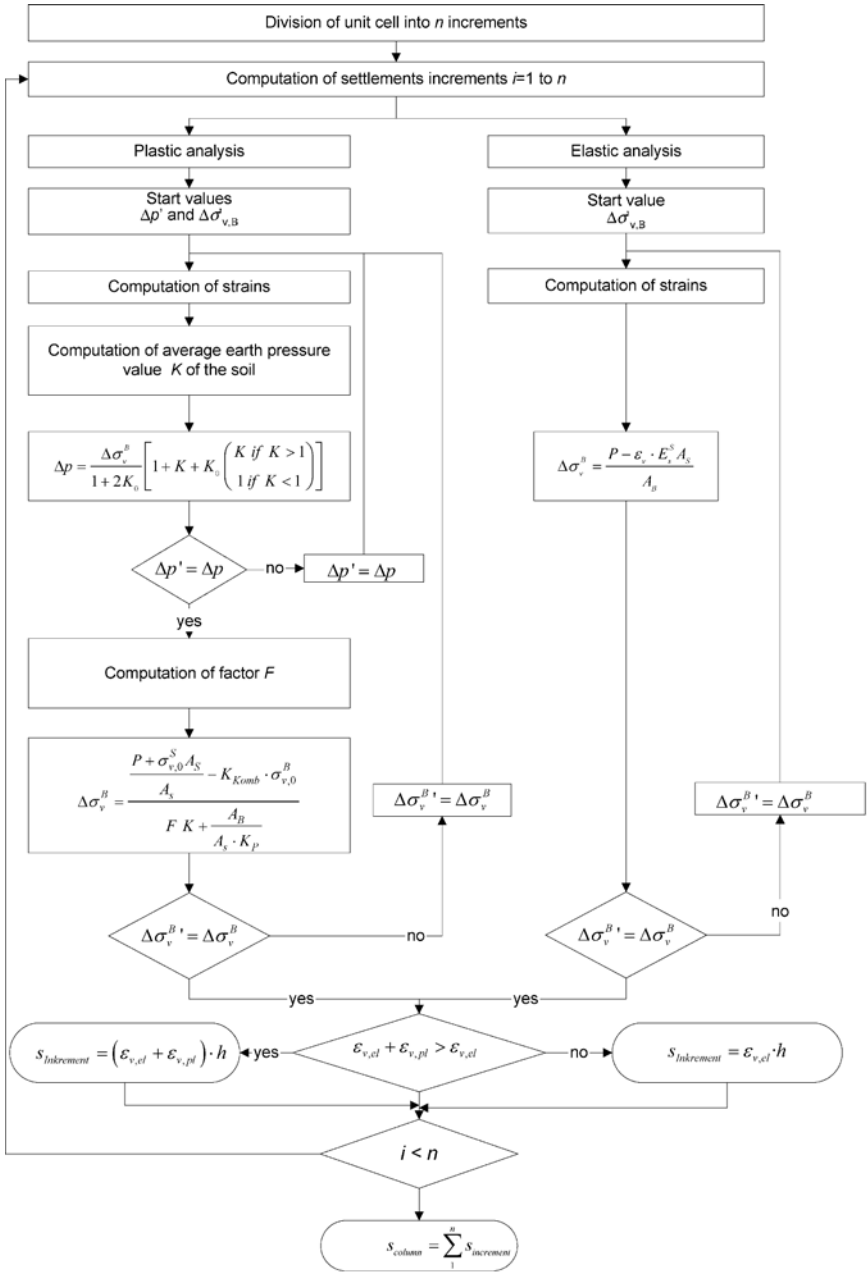


*Figure 4.15* Computational steps of the Goughnour and Bayuk method

- bulging of long, supported columns
- shearing of short, supported columns
- punching failure by sinking of short, floating columns
- bulging in deeper layers

as demonstrated in Figure 4.16.

Bulging of the column is the main load-carrying mechanism of a stone column, which will fail when the surrounding soil cannot lend any further lateral support. In homogeneous soil conditions, bulging is concentrated within a region between the column head and a depth of about four times the column diameter. Short columns with lengths below four column diameters may fail by sinking into the soil. However, if these columns are placed on a reliable bearing stratum and the lateral support by the soil is sufficient, failure surfaces will develop through the column head and the adjacent soil close to grade. The described failure mechanisms are idealised. Failure may also occur at greater depths than four column diameters in the presence of particularly soft soil layers that are thick enough (say in excess of two column diameters) to allow bulging to develop as shown in Figure 4.16(d).

Column groups show basically similar failure mechanisms, which are however less simple due to the complexity of the interaction between load application, soil and columns, and their geometrical parameters. Figure 4.17 displays failure mechanisms for column groups that can develop with rigid concrete foundations.

When looking at the infinite stone column pattern, the behaviour of the

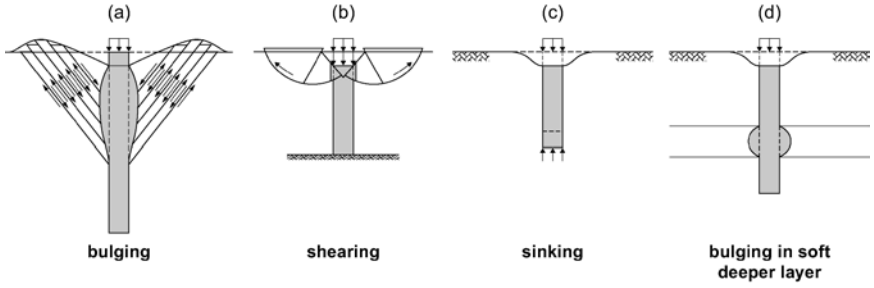


*Figure 4.16* Failure mechanisms of isolated stone columns

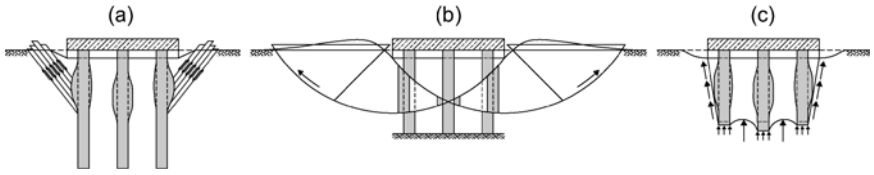


*Figure 4.17* Failure mechanisms for column groups

circular unit cell under load has to be analysed. In this symmetrical state of contained compression, no shearing will occur in the soil. Initially, soil and column will settle by elastic deformation and consolidation. However, the column is already under relatively low stresses, and will shear, dilate and bulge, but it will be contained in plastic equilibrium, with the internal stresses corresponding with their plastic state. Typically, such infinite grids of stone columns are used for the foundation of storage tanks and embankments. To avoid uneconomical stone column patterns, design load on the unit cell needs to be high enough for the columns to pass through their maximum stiffness, rendering sufficient settlement reduction for the structure (Greenwood and Kirsch, 1984).

Similar conditions prevail for vibro stone columns below embankments where, besides reducing the overall settlement, they act predominantly to enhance slope stability. As will be shown later, the approaches that do not consider the stress concentration in the stone columns and that rely only on the higher shear resistance of the column material in relation to the native soil lead to over-conservative factors of safety, and uneconomical designs. Design is generally based on conventional slip circle analyses and must take into account that, in order to fully mobilise the high column shear strength, substantial overburden pressure is required.

The easiest estimate of the ultimate bearing capacity of an isolated stone column makes use of a plane failure surface as defined by Bell (1915), and defines the equilibrium of a soil element at the column perimeter. The estimate is only valid for plane strain conditions and thus underestimates the capacity when applied to the axis-symmetric stone column. The maximum horizontal stress within the soil is governed by its undrained shear strength $c_u$ and the vertical stresses $q$, which represents the loading on the soil next to the column when the soil itself is assumed to be weightless.

$$\sigma'_{s,h} = q + 2c_u \tag{4.16}$$

The maximum vertical loading $\sigma'_{c,v,max}$ on the column can then be calculated using the passive earth pressure coefficient for the horizontal equilibrium as follows:

$$\sigma'_{c,v,max} = \sigma'_{s,h} \cdot \tan^2\left(\frac{\pi}{4} + \frac{\varphi_c}{2}\right) = (q + 2c_u) \cdot \tan^2\left(\frac{\pi}{4} + \frac{\varphi_c}{2}\right) \tag{4.17}$$

Based upon the hypothesis of Greenwood (1970) that loaded single columns are in triaxially confined compression, all respective computational methods use the following relationship:

$$\sigma_{ult} = \sigma'_{c,v,max} = \tan^2\left(\frac{\pi}{4} + \frac{\varphi_c}{2}\right) \cdot (\sigma'_{s,h} + k \cdot c_u + u) \tag{4.18}$$

with

| | |
|---|---|
| $\sigma'_{c,v,max}$ | maximum vertical column stress in kPa |
| $\varphi_{c'}$ | friction angle of column material |
| $\sigma_{s,h}$ | horizontal soil stress before column construction in kPa |
| $k$ | factor of influence |
| $c_u$ | undrained shear strength of soil in kPa |
| $u$ | pore water pressure at column perimeter in kPa. |

The equation describes the failure state in a column according to Figure 4.16(a), bulging, when the maximum horizontal stress in the column cannot be balanced anymore by the resisting horizontal soil stress. According to Brauns, 1978 the factor of influence $k$ can be computed by

$$k = 1 + ln\left(\frac{E_{oed,s}}{3 \cdot c_u}\right) \tag{4.19}$$

with $E_{oed,s}$ being the oedometric, or constraint, modulus of the soil.

Brauns also proposes a relationship for the shear failure of a vibro stone column according to Figure 4.16(b) which may occur near the column head as

$$\sigma'_{c,v,max} = \left(q + \frac{2 \cdot c_u}{\sin(2 \cdot \delta)}\right) \cdot (1 + \frac{\tan\left(\frac{\pi}{4} + \frac{\varphi_c}{2}\right)}{\tan \delta}) \cdot \tan^2\left(\frac{\pi}{4} + \frac{\varphi_c}{2}\right) \tag{4.20}$$

with

| | |
|---|---|
| $q$ | surcharge at ground surface in kPa |
| $\delta$ | angle of the assumed failure cone in the column. |

The minimum value of $\sigma'_{c,v,max} = \sigma_{ult}$ needs to be found by variation of the slip angle $\delta$, with $\delta = 65°$ being a reasonable starting value.

Since no bearing capacity failure can occur with the infinite column grid, we look now at the failure of column groups under load as shown in Figure 4.17. The complexity of an analytical problem solution requires simplifying assumptions to be made with all methods available to date (Aboshi *et al.*, 1979; Priebe, 1995), which are not always physically justifiable. It is therefore proposed to utilise the method after Barksdale and Bachus (1983), assuming planar failure surfaces within the column group.

The failure load $q_{ult}$ is calculated as follows, utilising the notations of Figure 4.18:

$$q_{ult} = \sigma_3 \cdot \tan^2 \delta + 2 \cdot c_{avg} \cdot \tan \delta \tag{4.21}$$

with

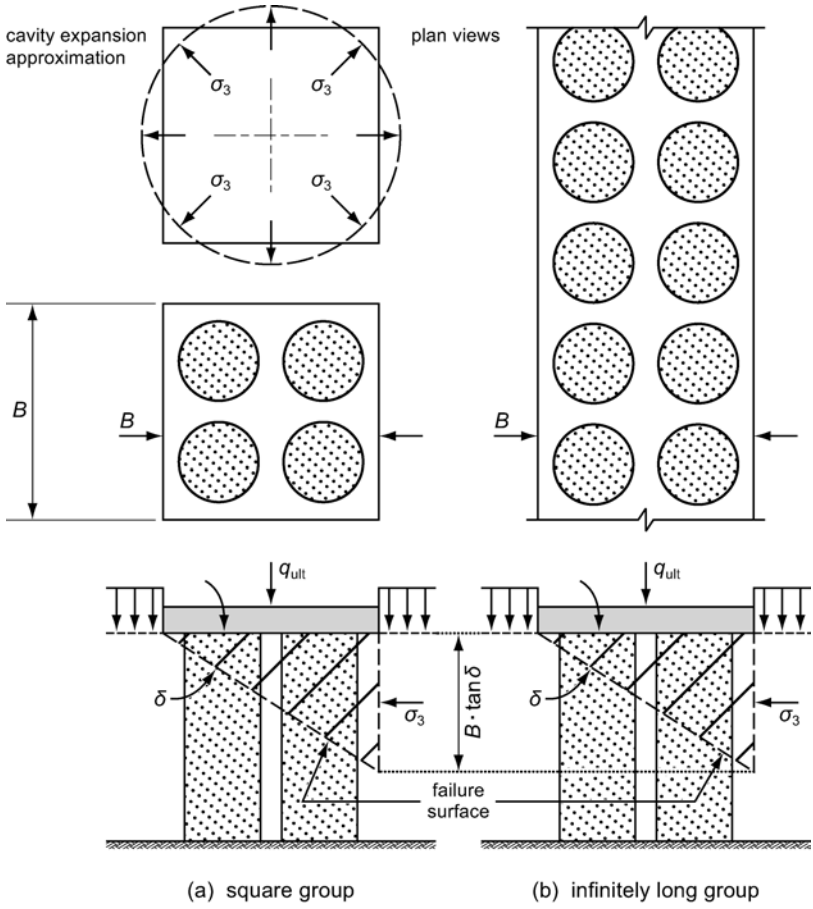


*Figure 4.18* Bearing capacity of vibro stone column groups (a) below square footings and (b) long strip footings (according to Barksdale and Bachus, 1983)

$\sigma_3$ average horizontal soil pressure in kPa
$\delta$ inclination of failure plane of the composite soil
$c_{avg}$ average cohesion in kPa.

In this consideration, quick loading conditions are assumed with the undrained shear strength $c_u$ prevailing in the soil ($\varphi_s = 0$) and with no cohesion for the stone column material. For the composite material of soil and stone column, an average friction angle $\varphi_{avg}$ and a composite cohesion $c_{avg}$ can be calculated using the equations (4.25) and (4.27) below with $n_c$ representing the stress concentration in the column. For simplicity, the stress concentration may be neglected with $n_c = 1$ and tan $\varphi_{avg}$ calculated as the weighted average of the stone column and soil areas. However, this leads

to conservative ultimate bearing capacities. With the improvement factor, $\beta$, developed with the Priebe method at the average depth of $\frac{1}{2} \cdot B \cdot \tan \delta$, the stress concentration factor $n$ can be calculated using equation (4.11) and introduced into equation (4.26).

The lateral average earth pressure $\sigma_3$ is calculated by the classical earth pressure theory for the long strip foundation using equation (4.22) and according to the cylindrical cavity expansion approximation after Vesic (1972) for the square foundation with equation (4.23).

$$\sigma_3 = \frac{\gamma_s \cdot B \cdot \tan \delta}{2} + 2 \cdot c_u \tag{4.22}$$

$$\sigma_3 = c \cdot F'_c + q \cdot F'_q \tag{4.23}$$

with

| | |
|---|---|
| $c$ | cohesion |
| $q$ | mean stress $1/3 \cdot (\sigma_1 + \sigma_2 + \sigma_3)$ at failure depth |
| $F'_c$, $F'_q$ | cavity expansion factors according to Figure 4.19 |
| $I_r$ | rigidity index $E_s/(2(1 + \mu)(c + q \cdot \tan \varphi_s))$ |
| $E_s$ | Young's modulus of the soil |
| $\mu$ | Poisson ratio in soil |
| $\varphi_s$ | friction angle in soil |
| $\gamma_s$ | unit weight of soil. |

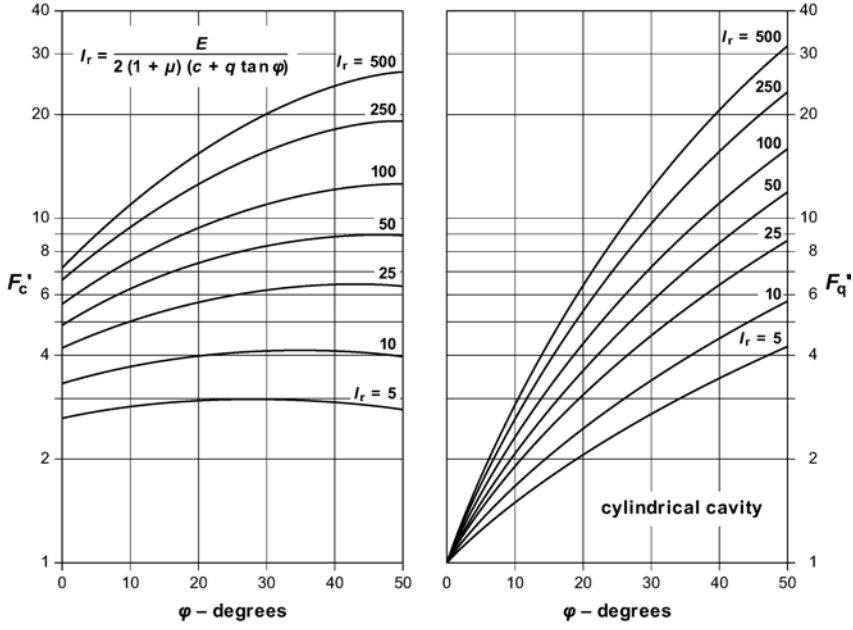


*Figure 4.19* Cylindrical cavity expansion factor after Vesic (1972) for soils with friction angle $\varphi_s$ and cohesion $c$

The relevant slip angle $\delta$ can be calculated from equation (4.24):

$$\delta = 45° + \frac{\varphi_{avg}}{2} \tag{4.24}$$

with

$$(\tan \varphi)_{avg} = \frac{n \cdot \tan \varphi_c}{\frac{A}{A_c} + n - 1} = n_c \cdot a_c \cdot \tan \varphi_c \tag{4.25}$$

and

$$n_c = \frac{n}{(1 + (n-1) \cdot a_c)} \tag{4.26}$$

The average cohesion of the composite soil follows from

$$c_{avg} = (1 - a_c) \cdot c \tag{4.27}$$

A sample calculation of this method is shown in Section 4.6.3.

We have seen that a bearing capacity failure of an infinitely distributed, evenly loaded grid of stone columns cannot occur. However, at the edge of large column groups (below tanks and embankments), the general rotational or linear type shear failure resistance needs to be investigated. The design is generally based on conventional slip circle analysis and it is evident that, for a significant improvement of the safety factor, it is necessary to consider the stress concentration on the columns to fully mobilise their superior friction strength together with a substantial overburden pressure. Barksdale and

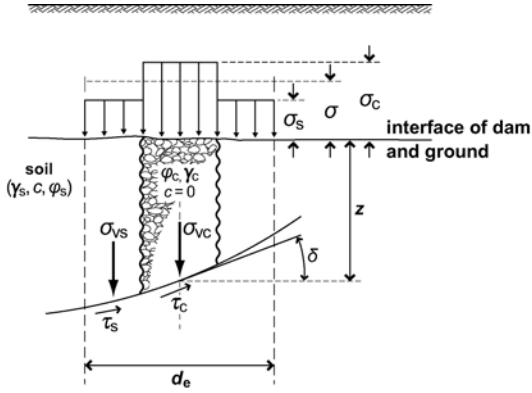


*Figure 4.20* Unit cell concept for slope stability analysis (after Barksdale and Bachus, 1983)

Bachus (1983) have proposed for this purpose how to make use of the stress concentration $n$ in hand calculations when adopting the unit cell concept.

Figure 4.20 shows such a unit cell at a depth where it intersects with the assumed failure line. The vertical effective stress $\sigma'_{v,c}$ resulting from the column weight and the applied stress $\sigma$ can be expressed by

$$\sigma'_{v,c} = \gamma_c \cdot z + n_c \cdot \sigma \tag{4.28}$$

with $n_c$ representing the stress concentration factor in the stone column at the depth $z$.

The shear strength of the stone column follows then as

$$\tau_c = (\sigma'_{v,c} \cdot \cos^2\delta) \tan \varphi_c \tag{4.29}$$

Vertical effective stress $\sigma'_{v,s}$ and shear stress $\tau_s$ in the soil surrounding the column are calculated from

$$\sigma'_{v,s} = \gamma_s \cdot z + n_s \cdot \sigma \tag{4.30}$$

and

$$\tau_s = c + (\sigma'_{v,s} \cdot \cos^2 \delta) \tan \varphi_s \tag{4.31}$$

The weighted average unit weight $\gamma_{avg}$ of the reinforced unit cell is used to calculate the acting moment.

$$\gamma_{avg} = a_c \cdot \gamma_c + a_s \cdot \gamma_s \tag{4.32}$$

With the known stress distribution factors $n$ which have to be estimated or which can be calculated relatively easily by the Priebe method using the relationship between $n$ and $\beta$ according to equation (4.11) and taking $\beta$ from the diagram in Figure 4.14, the slope stability analysis can be carried out with known standard methods. Calculating $n$, $n_c$ and $n_s$ for different depths $z$ from equations (4.6), (4.8) and (4.9) using Priebe's graphs for the improvement factor $\beta$ can be avoided by opting for an average depth $z_{avg}$ taken as representative of the slip circle or plane considered, and establishing in this way the average stress concentration factors. An example calculation of the stability of an embankment founded on stone columns is shown in Section 4.6.2.

When comparing results of slope stability analyses carried out by three-dimensional finite element methods (Kirsch and Sondermann, 2003) – with a good reproduction of the depth-dependent stress distribution between column and soil with conventional methods using homogenisation of the shear parameters by the weighted area average or the Barksdale and Bachus method with the $\beta$ and $n$ values developed after Priebe – it can be concluded

that the weighted area method underestimates safety considerably, that the combined Barksdale and Bachus/Priebe methods overestimate safety, and that a safety factor obtained from a calculation with the average of both methods represents a reasonable result close to reality.

### *4.3.4 Drainage, reduction of liquefaction potential and improvement of earthquake resistance*

It is obvious that stone or gravel columns installed in fine-grained and cohesive soils represent elements of considerably greater permeability than the surrounding native soils. In water-bearing soils their beneficial effect of accelerating consolidation settlement and reducing the liquefaction potential of sandy soils (Seed and Booker, 1977) is generally appreciated.

As with sand drain construction, the wet installation of vibro replacement stone columns is superior to the displacement dry methods because it avoids the development of smear zones along the column perimeter. For standard, non-seismic applications, the choice of the grading of the stone column material installed by the wet process in sand, silty sand and sandy silt is unproblematic even when using uniformly graded coarse backfill, since the voids are generally filled with the remaining coarser particles of the native soil which were not washed out during column installation, in this way precluding material entry from the surrounding area.

When looking at the gradation of the column material for vibro replacement stone columns installed by the dry method – which is generally quite uniform as we have seen in Section 4.1 – the question of filter stability is occasionally raised. It is suggested that the uniform grading of the column material would allow surrounding cohesive material to be transported with the seepage flow into their voids, thereby not only clogging them up but also leading to additional settlement. This effect has never actually been observed in practice, and dry vibro replacement stone columns generally show similar load settlement behaviour to wet columns. When analysing this problem, the Terzaghi filter rule cannot be used as it is only applicable for non-cohesive soils. Stability of the boundary between the granular column material and the cohesive soil is governed instead by the relevant void diameter of the filter, the tensile strength of the cohesive soil and the prevailing hydraulic gradient. It appears from a recent study of this question that these hydraulic gradients, measured in practice, are too small to cause material transport into the stone columns (Boley, 2007).

In water-bearing non-plastic silts that generally behave like granular soils, the choice of method (dry or wet) and column material deserves more careful consideration. Modern dry bottom feed systems allow the use of well-graded gravel and even sand as column material to avoid any transport of fines into the columns as a result of seepage flow. However, this choice would result in a distinct reduction of the friction angle of the column material.

In water-bearing fine-grained soils under load, that are improved by stone columns, pore water moves towards columns and drainage layers above or below. The curved flow paths can be divided into vertical and radial components, and the seepage flow rules adopted accordingly. Equation (4.33) describes the degree of consolidation $U$ in the stone column reinforced layer as the combined effect of the vertical consolidation $U_v$ and the radial consolidation $U_r$.

$$U = 1 - (1 - U_v) \cdot (1 - U_r) \tag{4.33}$$

The settlement $s_t$ at the time $t$ is in direct proportion with the degree of consolidation $U$ and the final settlement $s$.

$$s_t = U \cdot s \tag{4.34}$$

The time factor for vertical flow $T_v$ is given by equation (4.35) as a function of the elapsed time $t$, the length of the drainage path $h$ and the coefficient of vertical consolidation $c_v$. The time factor $T_r$ for radial flow is given by equation (4.36). Figure 4.21 gives the notations used for vertical and radial flow conditions, in the latter case utilising the unit cell concept. Figure 4.22 provides the degree of consolidation $U_v$ and $U_r$ as a function of the time factor $T_v$ and $T_r$ for vertical (v) and radial (r) flow conditions with stone column grid parameters $d_e/d$ = 3, 5 and 10.

$$T_v = \frac{c_v \cdot t}{h^2} \tag{4.35}$$

$$T_r = \frac{c_h \cdot t}{d_e^2} \tag{4.36}$$

$$\frac{c_h}{c_v} = \frac{k_h}{k_v} \tag{4.37}$$

with

$k_v$, $k_h$ vertical, horizontal permeability of the soil
$c_v$, $c_h$ coefficient of vertical, horizontal consolidation.

With known parameters for the above expressions, the consolidation time $t$ can be calculated for different degrees of consolidation of the composite layer of soil and stone columns. In practice, it is helpful to remember that horizontal drainage is dominant in this scenario. Not only is the length of the flow path within an infinite stone column pattern in radial direction very often considerably shorter than in the vertical direction, but also horizontal permeability in clays is generally up to 15 times larger than in vertical

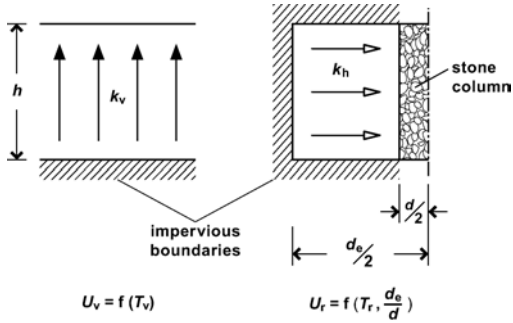


*Figure 4.21* Vertical and radial drainage flow characteristics

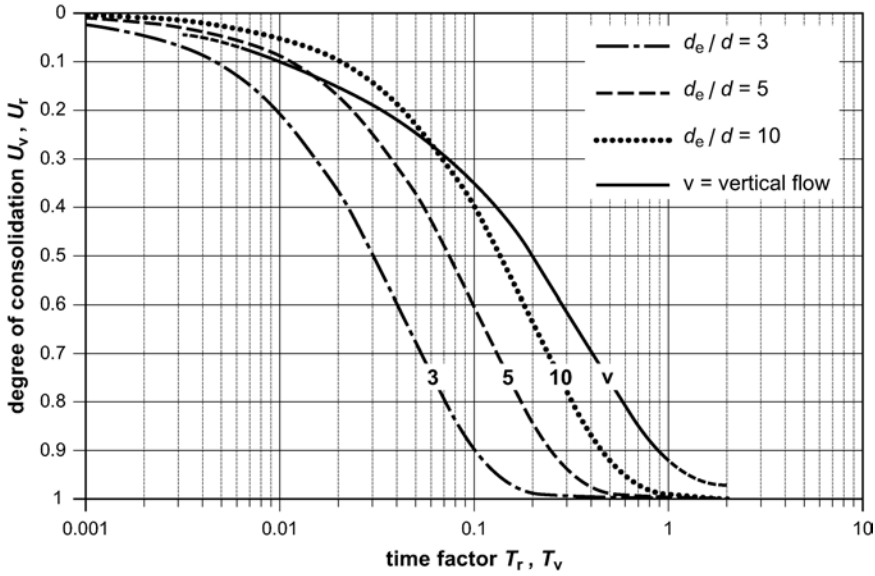


*Figure 4.22* Time factors $T_v$ and $T_r$ for vertical and radial seepage flow (according to Terzaghi and Peck, 1961 and Barron, 1948)

direction. Consequently it is sufficient to assess the consolidation time by neglecting the effect of vertical consolidation and to rely only on radial consolidation.

The relevance of this proposal can easily be verified by the following consideration. Let us assume that an infinite pattern of stone columns with diameter $d$ = 1 m is placed in a triangular grid with distances of $a$ = 3 m, yielding the unit cell diameter $d_e$ = 3.15 m. Column length is 10 m, equal to the vertical drainage path length. Let us calculate the degree of combined consolidation at the time $t$ when the vertical consolidation $U_v$ has reached just 10%. Assuming conservatively a ratio of 1 for horizontal to vertical

permeability, and using equations (4.35) and (4.36) at the time $t$, we get an expression for the time factor of radial consolidation $T_r$ as follows:

$$T_r = \left(\frac{h}{d_e}\right)^2 \cdot \left(\frac{c_h}{c_v}\right) \cdot T_v \tag{4.38a}$$

and with (4.37)

$$T_r = \left(\frac{h}{d_e}\right)^2 \cdot \left(\frac{k_h}{k_v}\right) \cdot T_v = \left(\frac{10}{3.15}\right)^2 \cdot T_v = 10.08 \cdot T_v \tag{4.38b}$$

From Figure 4.22, we obtain, for $U_v = 10\%$, the time factor $T_v = 0.01$ for vertical consolidation, which when used in equation (4.38) leads to $T_r = 0.1$. From Figure 4.22 follows now with $d/d_e = 3.15 = \sim 3$ the degree of radial consolidation $U_r = 90\%$. With equation (4.33) the combined consolidation ratio is then $U = 91\%$. Accordingly, at the chosen time $t$, the contribution of vertical consolidation represents only 1% of the combined total consolidation.

$$U = 1 - (1 - 0.1) \cdot (1 - 0.9) = 0.91 \tag{4.39}$$

This example was used to demonstrate that the vertical drainage flow can be neglected under normal conditions since radial consolidation generally governs the rate of combined consolidation of soil improved by stone columns. This also shows that this simplification is a safe assumption.

When adopting the dry bottom feed method for the stone column construction, a zone of reduced column permeability may develop at its perimeter as a result of mixing of disturbed soil with the column material. In order to account for this "smear effect", as it is called, it is recommended to reduce the column diameter by 5% and to use this effective diameter in the relationships presented above. Regardless of the construction method, it is important to ensure the vertical flow of water in the stone columns, and this requires a permeable granular blanket to be placed over the column heads on ground surface that has good horizontal drainage characteristics.

When stone columns are installed in non-liquefiable cohesive soils, they can take considerable horizontal earthquake loads. These horizontal loads are generally transferred by friction from the load distribution layer placed below the foundation into the heads of the stone columns. When considering only the shear capacity of the stone column, i.e. neglecting the higher shear resistance of stone column and tributary soil, a safety factor against earthquake-induced shear failure can be defined for the infinite stone column pattern with the notations from Figure 4.23 according to:

$$SF = \frac{\tau_c \cdot A_c}{a_h \cdot \sigma_v \cdot A} = \frac{\sigma_c \cdot \tan \varphi_c \cdot A_c}{a_h \cdot \sigma_v \cdot A} = \frac{n_c \cdot a_c \cdot \tan \varphi_c}{a_h} \tag{4.40}$$

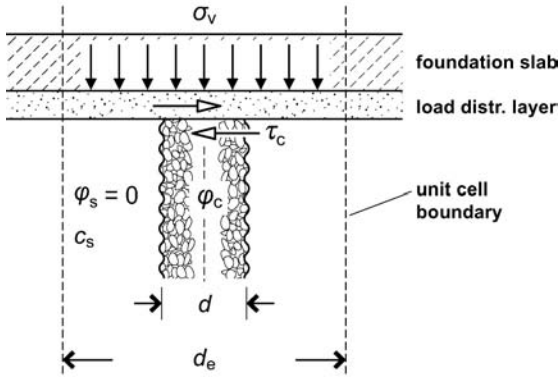


*Figure 4.23* Shear forces acting on unit cell as a result of earthquake motions

with

- $\tau_c$ shear resistance which can be mobilised in the stone column
- $a_h$ horizontal design earthquake acceleration factor
- $\sigma_v$ acting normal foundation stress
- $a_c$ area replacement factor
- $n_c$ stone column stress concentration factor.

The allowable shear stress $\tau_c$ developed by the stone column can either be verified by a direct shear test executed on an actual column on site (see Figure 2.15 and Section 4.4), or can be estimated from the relationship for $n_c$ in which the area replacement factor $a_c$ and the stress concentration factor were introduced:

$$\tau_c = \sigma_c \cdot \tan \varphi_c = n_c \cdot \sigma_v \cdot \tan \varphi_c \tag{4.41}$$

When introducing equation (4.41) into equation (4.40), the safety factor can be rewritten as a function of the angle of internal friction $\varphi_c$ of the stone column material and the horizontal design earthquake acceleration factor $a_h$. In cases where the vertical component $a_v$ of the ground acceleration also needs to be considered, the resisting normal stresses in the stone column $\sigma_c$ would have to be reduced by the vertical design earthquake acceleration $a_v$ accordingly and the expression in equation (4.40) would then be

$$SF = \frac{a_v \cdot n_c \cdot a_c \cdot \tan \varphi_c}{a_h} \tag{4.42}$$

The column stress concentration factor $n_c$ is in the order of 2 close to foundation level. It can also be estimated with the assumptions of the Priebe method by first taking the improvement factor $\beta$ from Figure 4.14 for $a_c$ and

$\varphi_c$, then calculating $n$ and $n_c$ with equations (4.11) and (4.6). However, as previously indicated, the Priebe method seems to overestimate the effect of the stone columns leading to $n_c$ values of about 3 for the infinite grid with $a_c = 0.25$ and $\varphi_c = 45°$. Unfortunately, only few data from field measurements exist for $n$ and $n_c$ but they indicate $n_c$ values between 1.5 and 2.0 only (Kirsch, 2004). It is therefore recommended to conduct field shear tests in critical cases to establish the allowable shear force that can be mobilised under actual conditions. In Section 4.6.4 a detailed discussion of the stress concentration factors can be found which will help to provide a better understanding of the variation of this parameter with depth $t$ and relative column length $\lambda$.

Provided that sufficient compaction time is allowed, the stone column installation will also significantly increase the relative density of loose, clean sand layers, which could be imbedded in the soils to be improved, and which might liquefy. To ensure that sufficient density was achieved to prevent liquefaction, the methods described in Section 3.3.3.1 need to be applied with the earthquake-induced settlements to be estimated according to Section 3.3.3.2.

However, in silty sands that can only marginally be compacted by vibro compaction, the stone columns will act as gravel drains and will help to prevent the detrimental pore water pressure build-up occurring in cohesionless soils during an earthquake. Seed and Booker (1976) have developed design principles for stone or gravel columns acting as drains by which the necessary drain spacing and diameter can be evaluated to avoid liquefaction. Figure 4.24 gives useful design charts allowing determining the necessary relative stone column pattern spacing $d/d_e$ as a function of the maximum allowable pore water pressure increase $r_g$, a ratio for the earthquake severity $N_{eq}/N_l$ and the time factor $T_{ad}$ according to the following expressions:

$r_g = u_g/\sigma'_v$ greatest pore water pressure ratio allowed in the design
$N_{eq}$ equivalent numbers of uniform stress cycles causing a stress ratio $\tau_{av}/\sigma'_v$ during time $t_d$ (see also Section 3.3.3.1)
$N_l$ number of stress cycles causing initial liquefaction in the laboratory with $\tau_{av}$

$$T_{ad} = \frac{k_h}{\gamma_w} \cdot \frac{t_d}{m_{v3} \cdot d_e^2} \tag{4.43}$$

with

$k_h$ horizontal permeability of the soil
$\gamma_w$ unit weight of water
$t_d$ duration time of earthquake
$d_e$ diameter of unit cell
$m_{v3}$ coefficient of volume compressibility.

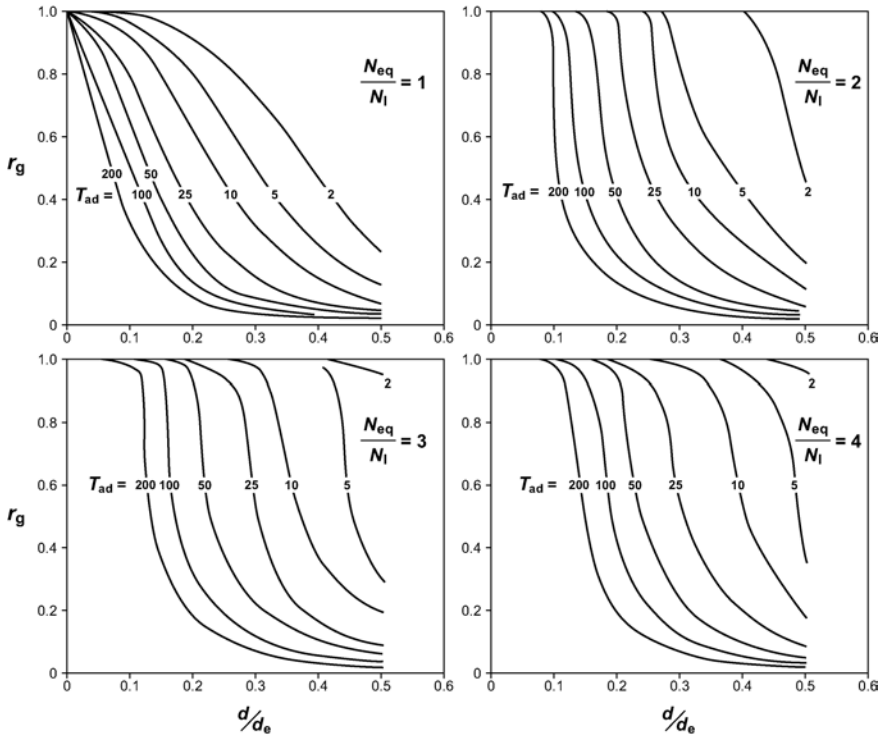


*Figure 4.24* Design charts for the relative stone column spacing $d/d_e$ as a function of the greatest design pore water pressure ratio $r_g$ for different time factors $T_{ad}$ and earthquake severities $N_{eq}/N_l$ (after Seed and Booker, 1976)

The above design assumes an infinite permeability for the stone column material but it is also valid for stone column permeability in excess of $200 \cdot k_h$ of the soil. In addition to the soil permeability $k_h$, the computation requires the following parameters, which need to be determined specifically for each project:

- the number of equivalent stress cycles $N_{eq}$ and the duration $t_d$ of the design earthquake;
- the liquefaction resistance of the soil expressed by the number of stress cycles $N_l$ causing liquefaction;
- the allowable pore water pressure ratio $r_g$ chosen for the design.

With the calculated time factor $T_{ad}$, the relative stone column spacing can be determined from Figure 4.24 for various earthquake severities.

The selection of an adequate grading of the stone column material for seismic applications requires special considerations. It is important that the high permeability of the vibro stone column is maintained during the

earthquake by a proper choice of the grading of the backfill material. Saito *et al.* (1987) have presented a particle size selection standard for the use of gravel in vertical drains as a countermeasure for sand liquefaction. The proposed filter criterion, which was developed for dynamic loading conditions with less restrictive lower limits for $D_{15}$ of the filter material when compared with Terzaghi's filter rule is given by equation (4.44).

$$20 \cdot d_{15} < D_{15} < 9 \cdot d_{85} \tag{4.44}$$

The notations $D_{15}$ and $d_{15}$ signify that 15% by weight of smaller grain diameters of the filter material and the natural soil, respectively, are passing the sieve. Vrettos and Savidis (2004) describe an interesting case history of the successful improvement of liquefiable silty sand by stone columns for the foundation of an immersed road tunnel in Greece. The marine stone column installation used gravel with a grain size distribution according to the Saito criteria for highly permeable, choke-free drains. In total over 130,000 lin.m of stone columns with a diameter of 600 mm and a nominal length of 15 m were executed from a barge to depths of up to 42 m applying the wet method.

Ground improvement to increase the liquefaction potential of cohesionless soils by vibro replacement stone columns constructed using the dry bottom feed method has become a standard method in the USA. This method not only utilises the compaction effect of the depth vibrator, but also combines it with the enhanced drainage capacity of the stone columns placed within the less permeable sand material around. Stone backfill used in these instances generally consists of sufficiently hard, durable, clean, crushed rock, free of vegetable matter and other deleterious substances. The stone should have a sufficiently high durability index – over 40 measured by the California Test 229 as specified by the State of California, Department of Transportation. The gradation of the backfill suitable for the bottom feed gravel system and designed for an SW sand would be reflected by 100% passing the 50 mm sieve, 90% to 100% passing the 25.4 mm sieve, and 10% to 80% passing the 12.7 mm and up to 5% passing the 4.75 mm sieve. Should higher sand contents be required for economic or technical reasons, up to 30% passing the 4.75 mm sieve can be used. Typically for these projects a maximum distance of the stone columns (generally in the range of 3 m) together with their required diameter of about 800–900 mm would be specified. The sand between the columns would have to be compacted to certain equivalent clean sand CPT tip resistance values, in general normalised and corrected for overburden pressure in accordance with the seismic risk evaluation (see Section 3.3.3 and the case history in Section 3.6.5).

### *4.3.5 Recommendations*

The various steps in designing a vibro replacement foundation will generally commence with an assumed and preliminary arrangement of the stone columns, which will have to be verified by the assessment of bearing capacity and deformation under load. These assumptions primarily concern attributable load per column (generally between 200 kN and 500 kN), distance between column axis (generally between 2 and 5 column diameters), stone column diameter (ranging between 0.5 m and 1.2 m) and column depth ranging normally between 2 m and 25 m. The choice will have to take into account the prevailing soil conditions, the available coarse backfill material and the chosen depth vibrator and the method of installation. In water-bearing soils of low plasticity (sandy silts to clayey silts) depth vibrators with larger diameters will be used in general, and column construction will be either by the wet or the bottom feed dry method, always creating columns in excess of 0.8 m. Conversely, in stiffer cohesive soils, smaller diameter, high frequency depth vibrators will ensure penetration to the required depth and will generally form columns with diameters below 0.8 m.

As we have seen when discussing the design principles, essential parameters controlling the performance of the stone column foundation are their diameter and the distance between each other, expressed by the area replacement factor $a_c$, together with the angle of internal friction $\varphi_c$ of the column material. The gravel material which is normally used is generally coarse grained alluvial deposits or crushed rock. Its stress dependent friction angle usually decreases with increasing normal pressure, with $\varphi_{c,max}$ corresponding with $\sigma_{c,min}$ and vice versa. The friction angle of gravel is, as with other granular material, also directly proportional to its density. Installation methods generally guarantee that the column material is very well compacted by the vibratory motions of the depth vibrator with void ratios in general close to minimum values as field measurements have shown (Herle *et al.*, 2007). Their shear parameter $\varphi_c$ can be taken from a $\sigma$–$\tau$ diagram, which can be determined relatively easily by shear box tests in the laboratory. Maximum friction angles can be as high as 60° (generally measured at moderate pressures of ~50 kN/m$^2$) with minimum values of about 50° measured at normal pressures of over 200 kN/m$^2$. Herle *et al.* (2007) have also noted that conventionally used friction angle values of only 40° appear too conservative when designing vibro replacement stone columns.

Table 4.2 shows stress-dependent peak friction angles of dense gravel and provides useful guidelines for selecting the appropriate friction angle of the stone column material, where its physical properties can be considered and also the prevailing stress regime. We remember that a loaded stone column tends to bulge under load generally within its upper part. In this plastic state of equilibrium it appears appropriate to use the residual friction angles in any settlement or slip failure calculation. It is therefore recommended to

*Table 4.2* Stress dependent friction angles of dense gravel to be used as stone column material (selected from Herle *et al.*, 2007)

| *Type of gravel* | $\varphi_{c,max}$ *(degrees)* | $\sigma_{c,min}$ *(kN/m²)* | $\varphi_{c,min}$ *(degrees)* | $\sigma_{c,max}$ *(kN/m²)* | *Remarks* |
|---|---|---|---|---|---|
| Crushed lime stone | 63.1 | 50 | 53.8 | 200 | DS |
| River gravel | 58.8 | 50 | 51.9 | 200 | DS |
| River gravel, sub-round | 57.1 | 50 | 50.9 | 200 | DS, $d_{60}/d_{10} = 2.6$ |
| River gravel, sub-round | 59.2 | 50 | 53.2 | 200 | DS, $d_{60}/d_{10} = 2.1$ |
| River gravel, crushed | 60.4 | 50 | 55.2 | 200 | DS |
| Basalt | 71.8 | 8 | 45.6 | 240 | TX, $D_{50} = 30$ mm |
| Basalt | 70.0 | 8 | 51.1 | 120 | TX, $D_{50} = 39$ mm |
| Basalt | 64.2 | 27 | 45.6 | 695 | TX |
| Sandstone | 60.1 | 27 | 37.4 | 695 | TX |
| Dolomite | 64.0 | 15 | 43 | 500 | TX, $\gamma = 1.7$ g/cm³ |
| Dolomite | 54.0 | 15 | 40 | 500 | TX, $\gamma = 1.5$ g/cm³ |

TX = triaxial test, DS = direct shear test, $d_{60}/d_{10}$ = uniformity coefficient

reduce the peak friction values in Table 4.2 by 5–7% to obtain approximate residual values. Whenever backfill material with unknown shear characteristics have to be used it is strongly recommended to perform suitable laboratory tests for determining their friction angle for design purposes.

The material chosen for constructing the stone columns needs to be chemically inert to resist aggressive groundwater, and physically strong enough to endure the abrasive forces emanating from the vibrator during column installation. Their grain size distribution should enable the formation of a dense column and guarantee sufficiently high and permanent permeability for effective drainage. The European standards EN 14731 on deep vibratory methods and EN 1097–2 and EN 13450 on physical properties of crushed rock provide useful guidelines for specifying sufficiently durable stone backfill for use in stone column construction. Whenever recycled material is foreseen for this purpose its abrasion resistance and its chemical characteristics require special consideration.

When adopting the displacement method of constructing stone columns the horizontal stresses increase in the soil adjacent to the stone columns during their installation. This stress increase is permanent and results also in an elevated modulus in those soils that are sufficiently stiff and do not tend to creep. Kirsch (2004) has measured this effect in a field test on two groups of 25 stone columns each in silty clay and sandy silt, respectively. Column diameter was $d = 0.8$ m and column depth 6 m to 9 m. Figure 4.25(a) shows the effective horizontal stresses after column installation in relation to the initial stresses before, expressed as the ratio of the earth pressure factors at rest $K_0$ after and before (index i) column installation, with a maximum of 150% at a distance of between $4{\cdot}d$ and $5{\cdot}d$ from column

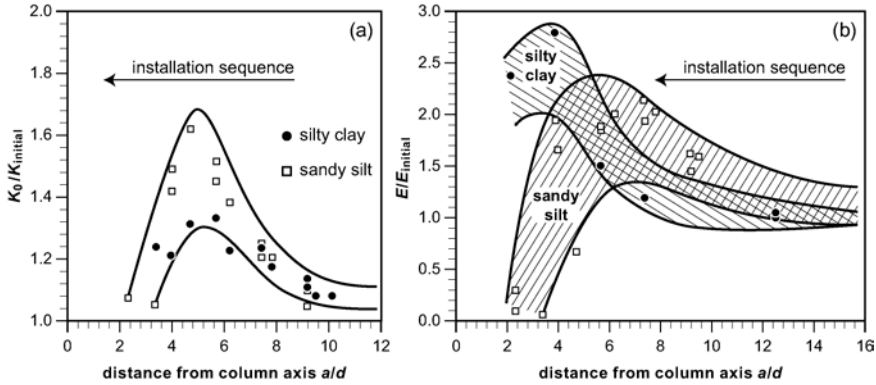


*Figure 4.25* (a) Horizontal stress increase and (b) development of ground stiffness, during installation of stone columns

axis. Figure 4.25(b) shows the modulus increase measured with the Menard pressure meter with a maximum of about 2.5 times the initial stiffness at distances of between 4 and 6 column diameters.

Both figures also show the stress relief due to remoulding caused by dynamic excitations in the vicinity of the columns, which will normally recover to original levels during reconsolidation of soils. The same paper also provides the results of a numerical analysis that simulates this installation effect on a foundation supported by 25 stone columns. Figure 4.26 summarises the findings and compares the load settlement behaviour of this footing, which is characterised by an area replacement factor (total stone column area/footing area) of $a_c = 0.28$, $\varphi_c = 45°$ and $l_c = 6$ m ($\lambda = 0.5$, "floating" situation), as derived from the numerical analysis with the results of standard analytical computations according to Priebe (2003) and Goughnour and Bayuk (1979b) (extended by Kirsch, 2004, to column groups).

It is interesting to see that the numerical method simulating the installation effect with groups of stone columns ties in well with the Priebe method (a) leading to improvement factors $\beta$ that are about 50% higher than those calculated without (b). This hidden reserve on the improvement factor as a result of the beneficial influence of the column installation in certain soils, as described above, indicates that the use of the standard analytical method after Priebe suffices for settlement estimation in such soils. Further studies to better define the characteristics of these soils in greater detail is nevertheless recommended.

Numerical simulations of the behaviour of stone column groups are helpful to better understand their performance under load and to provide useful recommendations for their design. Figure 4.27 gives a flow chart for the various steps necessary for the design based on settlement.

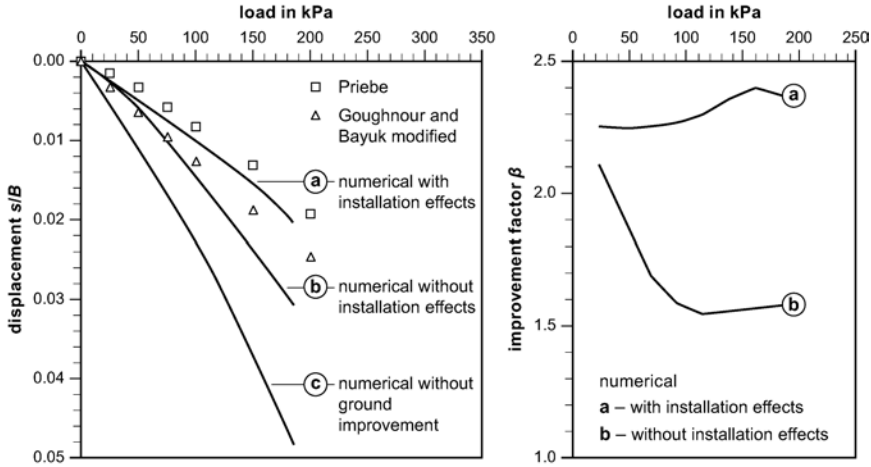


*Figure 4.26* Analytical and numerical results of the load settlement behaviour of a group of 25 stone columns ($a_c$ = 0.28, $\varphi_c$ = 45°, $\lambda$ = 0.5, settlement $s$ normalised with foundation width $B$) and influence of column installation on the improvement factor

The study has shown that only with sufficiently high replacement values ($a_c$ between 0.2 and 0.5), with a friction angle of the column material $\varphi_c$ of at least 45° and a relative stone column length $\lambda$ of more than 0.5, improvement factors $\beta$ between 1.5 and 2 can be achieved when dealing with column groups. Where the stone columns can be extended into a bearing stratum ($\lambda$ = 1) the improvement factor increases to $\beta$ = 2.5. Selection of a stone column material that, when properly compacted, allows friction angles $\varphi_c$ of over 45° to be used will further increase the improvement factors to values in excess of 3.

As a result of the study, it can be concluded that stone columns should preferably always be extended into a competent stratum, and only in exceptional cases, when the thickness of the layer needing improvement is large in comparison with the width of the foundation, floating columns should be executed. However, in these cases, the stone columns should always be longer than 1.5 times the smallest width of the footing. If $\beta$ needs to be increased further, it is more effective to achieve this by increasing the column length beyond $\lambda$ = 0.75. If, however, the thickness of the soft soil is very large in comparison with the dimensions of the footing, stone column lengths in excess of three times the footing width no longer contribute to the settlement reduction. Any chosen design must finally be checked with regard to its bearing capacity according to Section 4.3.3.

Generally, a load distribution layer consisting of gravel or crushed rock with a thickness of at least 300 mm is placed over the vibro stone column heads. This layer also serves to safeguard the drainage capability of the stone

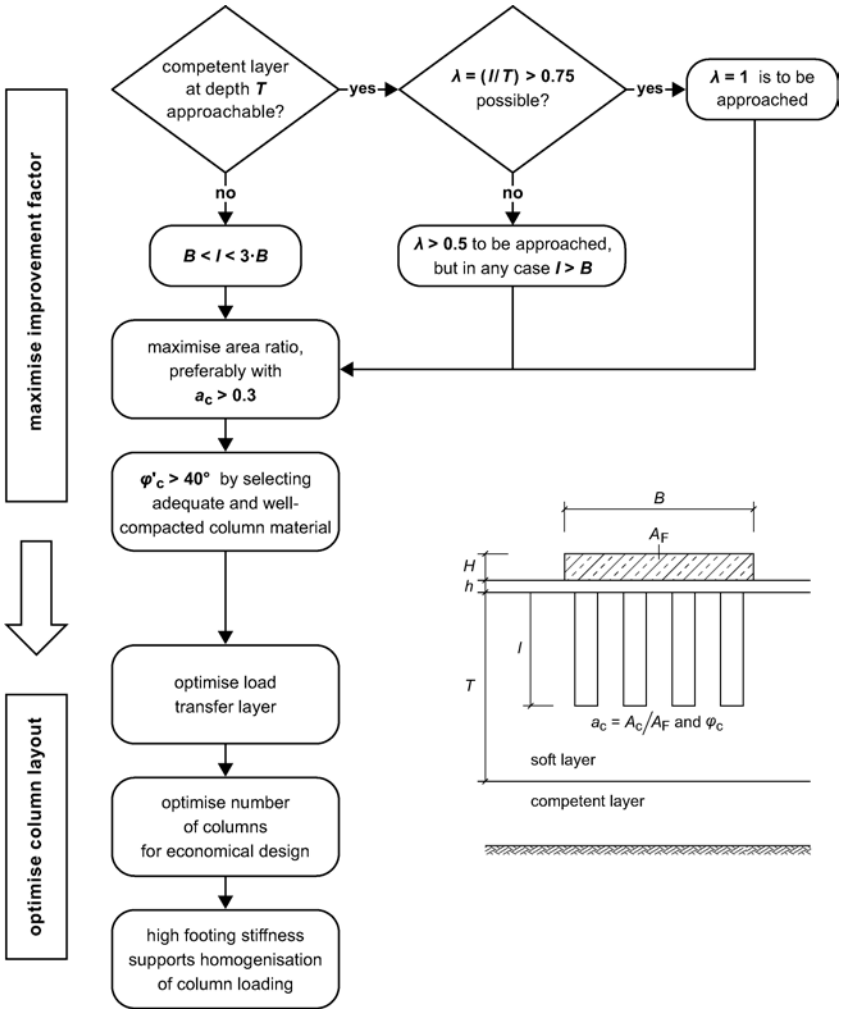


*Figure 4.27* Flow chart for the design of a group of stone columns

columns when loaded, but requires effective access to a working recipient. Thorough compaction of this layer is recommended before concreting work commences. Measurements and the above parametric study reveal that this layer helps to concentrate foundation loads into the stone columns. It helps to equalise the bearing stresses acting on the footing. However, the load distribution layer itself does not increase the improvement factor of the stone column reinforced strata any further.

Footing and slab stiffness help to evenly distribute foundation loads on the stone columns leading finally also to evenly distributed settlements. Stone columns should always be arranged directly below footings and

foundation slabs. Only when other criteria dictate – bearing capacity, slip failure or earthquake mitigation – do they also need to be placed outside.

For the prevention of liquefaction, it is also recommended to extend the stone columns outside the structure over a width which is equal to at least two-thirds of the soil improvement treatment depth.

## 4.4 Quality control and testing

In addition to the quality control measures that were discussed in Section 3.4 for the vibro compaction method, concerning assurance of the geometrical layout of the vibro stone column pattern and their treatment depth, verification of the column diameter $d$ is of prime importance. This geometrical relation is represented by the area replacement factor $a_c$, which significantly influences design and performance of the vibro stone column foundation.

Modern data acquisition systems for vibro replacement collect, store and display all relevant data of a stone column including column identification number and, as a function of real time, depth, AC current or hydraulic pressure of the vibrator motor, stone volume (measured directly or deduced from measured stone weight), air pressure and installation duration. All data are generally collected numerically and can be stored or used for graphical displays to support construction and supervision procedures or to serve for quantity surveying purposes (Bauldry *et al.*, 2008).

Where the stone backfill quantity cannot be measured directly versus depth and recorded by the monitoring device, a realistic estimate of the total volume of stone needs to be carried out. It should be correlated with the total length of stone columns executed during reasonable time intervals and calibrated with the delivered stone quantity. Material wastage and excessive heave developing at the working platform during column installation have to be considered.

Where heterogeneous site conditions prevail and compactable sand layers alternate with cohesive soil layers improvement can be achieved by a combination of the densification effect of vibro compaction with the reinforcement effect of stone columns. In these instances the degree of compaction can be measured in the sand layers by the methods described in Section 3.4. Improvement of the cohesive soils is then achieved in the first place by a sufficiently high area replacement value $a_c$ (i.e. column diameter $d$ and spacing) and the friction angle $\varphi_c$ of the stone column material.

The stiffness of the improved soil is controlled primarily by the shear strength of the stone column material. It is therefore recommended to verify, for each major site, the friction angle $\varphi_c$ of the stone backfill chosen in the design with suitable laboratory tests, if insufficient experience with the material exists. In exceptional cases, and if the size of the project merits the expenditure, the shearing resistance of the stone column alone or of stone column and tributary soil (i.e. the unit cell) can also be measured directly on site by full-scale shear tests (see Figure 2.15). Barksdale and Bachus (1983)

recommended these shear tests to be performed as double ring tests as described in the Jourdan Road Terminal Test Embankment report (Parsons-Brinkerhoff *et al*., 1980).

Suitability of the stone backfill material in terms of hardness and abrasion resistance may be controlled by relevant testing methods such as the Los Angeles Test following ASTM C131 designations or similar regulations such as the European standards EN 1097–2 and EN 13450.

When verification of the performance of single or strip foundations on column groups is needed, full-scale loading tests are recommended with actual footing dimensions because of the complex interaction between stone columns, footing size and stiffness. Alternatively, it may be possible to achieve sufficient confidence in some cases by performing tests with a footing on at least three columns.

For verification of the settlement performance of large column groups or infinite column grids, zone tests are necessary for modelling this loading scenario realistically. Load tests on single columns with the load only being applied directly on the column itself do not reflect actual stress conditions in these situations.

In cases where the soft soil to be improved is close to foundation level, say up to five times the unit cell diameter $d_e$, load tests on single columns are, however, indicative for the performance of an infinite column grid with the test footing size being equal to the unit cell area $A = 0.25 \cdot \pi \cdot d_e^2$. From the load-settlement curve of this unit cell loading test, an equivalent Young's modulus $E^*$ can be defined as the ratio of the uniform load $q$ multiplied by an equivalent column length $l^*$ and the measured settlement $s_m$. The uniform load $q$ on the infinite grid causes the settlement of the infinite grid $s_g$ with the actual column length $l$ and the equivalent modulus $E^*$ as follows:

$$\frac{q \cdot l^*}{s_m} = E^* = \frac{q \cdot l}{s_g} \tag{4.45}$$

In a parametric finite element analysis it was shown that the equivalent column length $l^*$, which is just a calculating unit, is essentially independent of the actual column length of the load test and of the stiffness ratio of column material and surrounding soil. It depends predominantly on the grid geometry as represented by the unit cell diameter $d_e$ and can be taken for different unit cell diameters from Figure 4.28(a).

These unit cell load tests on single columns to represent the load settlement performance of the infinite grid were developed from parametric studies and are, however, not yet verified in practice. In this context it is important, as with other load tests, to avoid any disturbing influence of the load application system on the settlement during their execution. It is therefore recommended to perform the load test with a setup such as that shown in Figure 4.28(b).

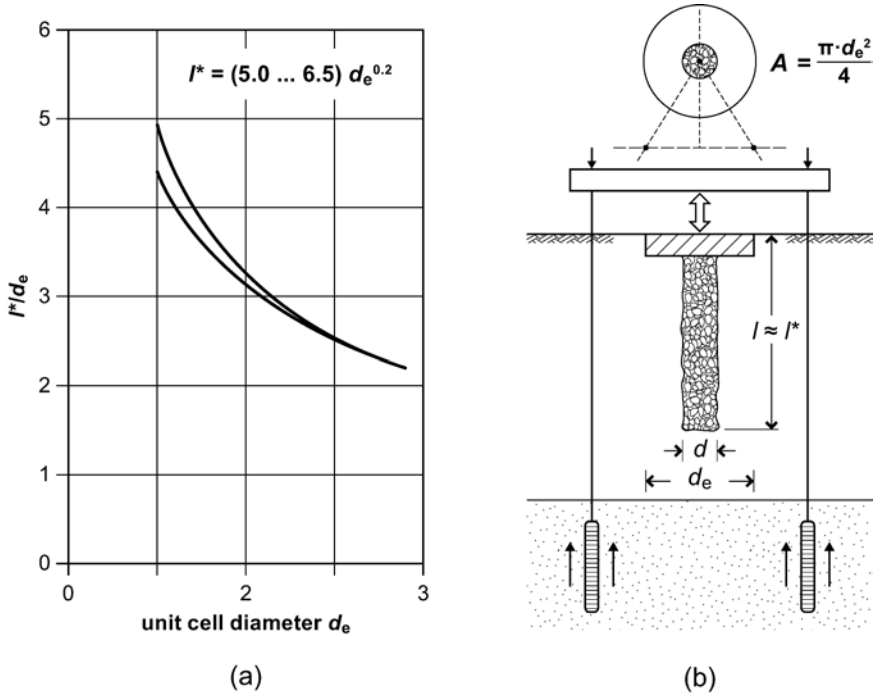


*Figure 4.28* Equivalent column length $l^*$ as a function of the unit cell diameter for determination of infinite column grid settlements from single column load tests (after Kirsch and Borchert, 2006)

Reports on the execution of load tests on groups of vibro stone columns are numerous, of which only a limited number of more recent publications are included in the references. These follow general ASTM or similar procedures for quick load tests on spread footings to indicate bearing capacity of the foundation applying test loads of at least 150% design load. For settlement control purposes long-term tests are required whereby it is necessary to allow a sufficient time span to elapse (generally 0.01 mm/min) before the next load increment is applied. Load test results need to be theoretically analysed to predict as realistically as possible the actual performance of the stone-column-reinforced ground under load. Unfortunately, field tests are expensive and very often for a true and realistic assessment of the effect of ground improvement certain elements – for instance the settlement performance of the untreated soil – are missing. It is therefore strongly recommended to carefully design all field measurements to reflect not only the relevant loading conditions as closely as possible but also the prevailing geotechnical conditions on site.

Occasionally, static cone or dynamic penetration tests are proposed to measure the density and continuity of the stone columns installed, although

test results obtained in this way are often questionable if not misleading and generally difficult to interpret. Very often, the steel rod of the testing equipment deviates from the vertical and leaves the relatively slender stone column without noticeable indication, thereby giving room for incorrect interpretations. Scrutiny in checking the printouts of the data collection system is the better, and most commonly used way to detect deviations from the specified geometry of the constructed stone columns.

## 4.5 Suitable soils and method limitations

In Figure 3.11 the application limits of the vibro compaction method are basically restricted to areas A and B. Soils with grain size distribution falling into areas C and D cannot be compacted anymore by vibratory motions, but their characteristics may be improvable by the vibro replacement stone column method, provided that their stiffness does not prevent the depth vibrator penetrating.

Degen (1997b) has provided useful comments for the applicability of the vibro stone column method in these soils using the USCS classification system (Table 4.3), which particularly take into account the plastic behaviour of these soils. To securely construct a stone column, the soils must have a minimum strength, expressed by their undrained cohesion, which should not fall below $c_u = 5$ kPa, since otherwise it cannot provide sufficient containing pressure for the column. If these soils extend to ground level, their softness generally requires a competent gravel blanket of about 0.5 m thickness to be placed as a working platform over the whole site. Into stiffer

*Table 4.3* Suitability assessment of fine-grained cohesive soils for vibro replacement (modified after Degen, 1997b)

| *Soil type* | *USCS* | *Comment on suitability for vibro replacement stone columns (VR)* |
|---|---|---|
| Silty sands | SM | VR necessary and suitable for silt content > 10% |
| Clayey sands | SC | VR with marginal overall compaction effect, very fast draining after treatment |
| Inorganic clays (low plasticity) | CL | $c_u \geq 5$ kPa recommended for upper 3 m, potential difficulties for vibrators to penetrate with $c_u > 50$ kPa (very stiff conditions) |
| Inorganic clays (high plasticity) | CH | As for CL, but not suitable when $w_n$ too close to $w_L$ |
| Silts and clays with $w_L < 50$ | ML | Pre-boring necessary when dry |
| Inorganic and organic silts and clays with $w_L < 50$ and high plasticity | MH<br>CH<br>OH<br>PT | Collapsing soils not suitable<br>Soils generally not or only marginally treatable<br>In excess of 1 m thickness not suitable |

soils at lower water content and cohesions of above $c_u$ = 50 kPa, even slender, powerful, high-frequency depth vibrators may not be able to penetrate. Although their characteristics may not need improvement, softer soils below may necessitate the stone columns to reach deep. In theses cases pre-drilling of the stiffer soils with suitable methods is advisable. Pre-drilling is often also necessary if a hard surface crust has developed by drying out or through site traffic, or when stone and weathered rock layers or other obstructions pose penetration problems.

In stiff soils with low water content, closely spaced vibro stone columns at distances below 3*d* can cause substantial heave at ground surface during their installation. It is important in these circumstances to avoid neighbouring columns causing mutual damage during construction. Should excessive heave be unavoidable, partial pre-boring can assist. After removal of the upper 0.5 m of surface soil following stone column installation, the site surface and stone column heads need to be recompacted before the load distribution layer is installed on top.

The practical depth range of vibro stone columns is 2–25 m. Exceptional cases may necessitate the installation of very deep stone columns, e.g. if stability or liquefaction requirements dictate. For these cases, crane-hung bottom feed systems have been developed with depth capability, both on and offshore, in excess of 50 m. These not only need careful planning and thorough site investigations but also execution should only be by very experienced contractors.

The vibro stone column method is often used to treat heterogeneous strata, sometimes with successive layers of very different characteristics or with imbedded lenses of soft, organic soil of inconsistent extent and thickness. Site investigation will not always detect these ground conditions. Although the method is no substitute for a site investigation, the regular and well-documented installation method is likely to detect unexpected ground irregularities. Engineer and contractor will then have to define ways and means of coping with the changed soil conditions, either by additional stone columns at closer spacing or by increasing the stone column diameter. In these circumstances stone columns may be able to bridge the soft layers if their thickness is not greater than about two column diameters. Any thicker layers will almost certainly have been detected by the site investigation and considered in the stone column design in the first place.

## 4.6 Case histories and computational examples

### *4.6.1 Analysis of settlement reduction*

The following analytical example is based on geometrical and material properties, which were slightly idealised from an existing ground improvement project for the foundation of a road embankment. The soil is characterised by very soft alluvial deposits. These soils make vibro stone columns

for infrastructural measures a very common technology, in order to reduce settlements. Figure 4.29 and Table 4.4 show the cross-section through the embankment and its foundation together with the necessary design parameters.

The settlement analysis is done first, using the Priebe method (Section 4.3.2) for the centre of the embankment, assuming unit cell conditions. The analysis requires the division of the soil mass into a sufficiently large number of horizontal layers. Here equidistant slices of 1 m thickness are chosen. The method of Priebe (1976) is based on a classical settlement analysis using stress distribution and the computation of a settlement improvement factor by which the calculated settlements are reduced.

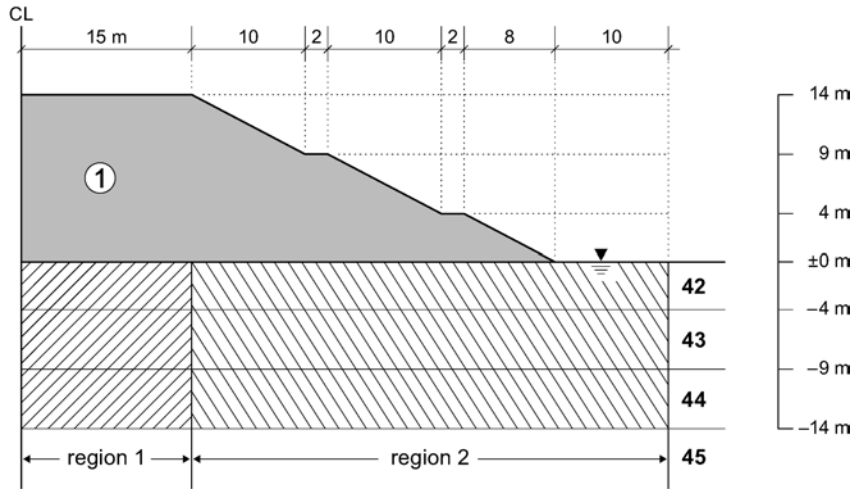


*Figure 4.29* Cross-section through embankment

*Table 4.4* (a) Soil properties and (b) stone column parameters chosen in the design

(a)

| *Soil layer* | *γ/γ′ (kN/m³)* | *$E_{oed}$ (MN/m²)* | *φ′ (degrees)* | *C (kN/m²)* | *μ(–)* |
|---|---|---|---|---|---|
| 1 embankment fill | 21.8/12 | – | 35 | 0 | 0.33 |
| 42 firm silt | 16/6 | 4 | 0 | 40 | 0.33 |
| 43 very soft silt | 14/4 | 0.6 | 0 | 6 | 0.33 |
| 44 soft silt | 14/4 | 0.8 | 0 | 8 | 0.33 |
| 45 hard silt | 18/8 | 20 | 0 | 200 | 0.33 |

(b)

| *Stone columns* | *Diameter (m)* | *Square grid spacing (m)* | *Area replacement ($a_c$–)* | *$E_{c,oed}$ (MN/m²)* | *γ/γ′ (kN/m³)* | *$φ'_c$ (degrees)* |
|---|---|---|---|---|---|---|
| Region 1 | 1.1 | 2.1 | 0.22 | 120 | 19/12 | 42 |
| Region 2 | 1.1 | 1.7 | 0.33 | 120 | 19/12 | 42 |

The basic improvement factor $\beta_0$, after Priebe, is calculated from

$$\beta_0 = 1 + \frac{A_c}{A} \cdot \left[ \frac{1/2 + f(\mu_s, A_c / A)}{K_{ac} \cdot f(\mu_s, A_c / A)} - 1 \right] \tag{4.46}$$

Where:

$$K_{ac} = \tan^2 (45° - \varphi_c / 2) \tag{4.47}$$

$$f(\mu_s, A_c / A) = \frac{1 - \mu_s^2}{1 - \mu_s - 2\mu_s^2} \cdot \frac{(1 - 2\mu_s) \cdot (1 - A_c / A)}{1 - 2\mu_s + A_c / A} \tag{4.48}$$

The basic improvement factor is usually reduced to account for the fact that a complete exchange of the soil by the column material should lead to a maximum improvement factor $\beta_{max}$ represented by the ratio of the modulus of column material and the modulus of the soil.

$$\beta_{max} = E_c / E_s \tag{4.49}$$

Hence the corrected improvement factor $\beta_1$ is calculated according to Priebe (1995) from

$$\beta_1 = 1 + \frac{\overline{A_c}}{A} \cdot \left[ \frac{1 / 2 + f(\mu_s, \overline{A_c / A})}{K_{ac} \cdot f(\mu_s, \overline{A_c / A})} - 1 \right] \tag{4.50}$$

where

$$f(\mu_s, \overline{A_c / A}) = \frac{1 - \mu_s^2}{1 - \mu_s - 2\mu_s^2} \cdot \frac{(1 - 2\mu_s) \cdot (1 - \overline{A_c / A})}{1 - 2\mu_s + \overline{A_c / A}} \tag{4.51}$$

$$\frac{\overline{A_C}}{A} = \frac{1}{A / A_c + \Delta(A / A_c)} \tag{4.52}$$

$$\Delta(A / A_c) = \frac{1}{(A_c / A)_1} - 1 \tag{4.53}$$

with $\mu_S = 0.33$

$$\left(\frac{A_c}{A}\right)_1 = -\frac{4 \cdot K_{ac} \cdot (\beta_{max} - 2) + 5}{2 \cdot (4 \cdot K_{ac} - 1)} \pm \frac{1}{2} \cdot \sqrt{\left[\frac{4 \cdot K_{ac} \cdot (\beta_{max} - 2) + 5}{4 \cdot K_{ac} - 1}\right]^2 + \frac{16 \cdot K_{ac} \cdot (\beta_{max} - 1)}{4 \cdot K_{ac} - 1}} \tag{4.54}$$

On the other hand, the improvement factor $\beta_1$ so calculated, which is mainly based on the assumption of a lateral support of the column by the surrounding soil, does not take into account the increasing support of the soil with depth $t$. Therefore the improvement factor is increased by introducing the depth factor $f_t$ to

$$\beta_2 = f_t \cdot \beta_1 \tag{4.55}$$

where

$$f_t = \frac{1}{1 + \dfrac{K_{0c} - 1}{K_{0c}} \cdot \dfrac{\Sigma(\gamma_s \cdot \Delta t)}{p_c}} \tag{4.56}$$

$$p_C = \frac{p}{\dfrac{\overline{A_c}}{A} + \dfrac{1 - \overline{A_c / A}}{p_c / p_s}} \tag{4.57}$$

$$\frac{p_c}{p_s} = \frac{1/2 + f(\mu_s, \overline{A_c / A})}{K_{ac} \cdot f(\mu_s, \overline{A_c / A})} \tag{4.58}$$

$$K_{0c} = 1 - \sin \varphi_c \tag{4.59}$$

The factor $f_t$ is limited by

$$f_t \leq \frac{E_c / E_s}{P_c / P_s} \tag{4.60}$$

and the improvement factor $\beta$ must not rise above $\beta_{lim}$ given by

$$\beta_2 \leq \beta_{lim} = 1 + \frac{A_c}{A} \cdot \left( \frac{E_c}{E_s} - 1 \right) \tag{4.61}$$

The above equations are best programmed, e.g. in a spreadsheet, together with the equations for classical settlement calculation under load.

The results of the Priebe analysis are presented in Table 4.5. Ground pressure in the middle of the embankment is calculated by using

$$p = 14m \cdot 21.8 \frac{kN}{m^3} = 305 \frac{kN}{m^2} \tag{4.62}$$

A second analysis shows the application of the method after Goughnour and Bayuk (1979b). It follows the flow chart as shown in Figure 4.15. As mentioned there, the algorithm consists of an iterative approach, which is best solved by using a computer routine.

*Table 4.5* Settlement analysis after Priebe (1995)

| *Depth (m)* | *Settlement without improvement (mm)* | *Improvement factor* $\beta_2$ – | *Settlement with stone columns (mm)* |
|---|---|---|---|
| 1 | 76 | 2.38 | 32 |
| 2 | 76 | 2.38 | 32 |
| 3 | 76 | 2.38 | 32 |
| 4 | 76 | 2.45 | 31 |
| 5 | 508 | 2.50 | 203 |
| 6 | 508 | 2.50 | 203 |
| 7 | 508 | 2.50 | 203 |
| 8 | 508 | 2.50 | 203 |
| 9 | 508 | 2.50 | 203 |
| 10 | 381 | 2.49 | 153 |
| 11 | 381 | 2.49 | 153 |
| 12 | 381 | 2.49 | 153 |
| 13 | 381 | 2.49 | 153 |
| 14 | 381 | 2.49 | 153 |
| 15 | 15 | 1 | 15 |
| 16 | 15 | 1 | 15 |
| Total: | 4783 | 2.47 | 1936 |

The analytical procedure of Goughnour and Bayuk requires the definition of the initial void ratio $e_0$ and the compression index $C_C$. In order to ensure comparability with the above analysis, $e_0$ and $C_C$ were chosen to fit the constrained modulus $E_{oed}$ as shown in Table 4.4(a) in terms of settlements of the unimproved ground. Therefore the compression index was calculated from an assumed initial porosity $e_0 = 1.2$ by

$$C_C = (1 + e_0)\, ln\, (10)\, \frac{\sigma_{v,0}}{E} \tag{4.63}$$

with the Young's modulus $E$ and the initial vertical stress $\sigma_{v,0}$. All other parameters and the geometry were kept identical.

The Goughnour and Bayuk method calculates total settlements of the improved ground to be approximately 2.70 m (see Table 4.6) which is about 140% of the settlements calculated with the Priebe method. With a fully three-dimensional finite element analysis of the situation, a maximum settlement of 2.40 m was calculated in the centre of the embankment (Kirsch and Sondermann, 2003).

### *4.6.2 Analysis of slope stability*

The example from Section 4.6.1 will now be analysed with respect to its stability. To this end, it is necessary to calculate the shear strength of the improved ground. Because the load is concentrated in the stone column

*Table 4.6* Settlement analysis after Goughnour and Bayuk (1979)

| *Depth (m)* | *Compression index* $C_C$ | *Initial void ratio* $e_0$ | *Settlement without improvement (mm)* | *Settlement with stone columns (mm)* |
|---|---|---|---|---|
| 1 | 0.03 | 1.2 | 24 | 16 |
| 2 | 0.05 | 1.2 | 36 | 23 |
| 3 | 0.08 | 1.2 | 47 | 29 |
| 4 | 0.10 | 1.2 | 56 | 34 |
| 5 | 0.80 | 1.2 | 402 | 241 |
| 6 | 0.91 | 1.2 | 436 | 257 |
| 7 | 1.03 | 1.2 | 467 | 272 |
| 8 | 1.14 | 1.2 | 497 | 285 |
| 9 | 1.26 | 1.2 | 524 | 298 |
| 10 | 1.03 | 1.2 | 413 | 232 |
| 11 | 1.11 | 1.2 | 431 | 239 |
| 12 | 1.20 | 1.2 | 449 | 246 |
| 13 | 1.29 | 1.2 | 466 | 252 |
| 14 | 1.37 | 1.2 | 482 | 258 |
| 15 | 0.06 | 1.2 | 21 | 21 |
| 16 | 0.07 | 1.2 | 22 | 22 |
| Total: | | | 4771 | 2726 |

material, it would be too conservative to compute average shear strength values only on the basis of the area ratio $a_c$, since allowable shear stresses in the column are governed by the stress-dependent inner friction. Therefore Priebe, 1995 suggests calculating the strength of the improved ground on the basis of ratio $m$ of the load carried by the column to the total load acting on the unit cell.

$$m = \frac{\sigma_c \cdot A_c}{\sigma \cdot A} \tag{4.64}$$

With equations (4.2) and (4.5), the above equation can be rewritten as

$$m = \frac{n \cdot a_c}{(1 + (n-1) \cdot a_c)} \tag{4.65}$$

Introducing equation (4.11), we get

$$m = \frac{n \cdot a_c}{\beta} = \frac{\beta - 1 + a_c}{\beta} \tag{4.66}$$

The above equation (4.66) denotes the maximum load ratio attributable to the stone columns. Conservatively $m$ can be reduced to $m'$ by simply

neglecting the area ratio $a_c$. The load ratio $m'_1$ may then be calculated from the settlement improvement factor $\beta_1$ according to Priebe (equation (4.50)) which includes the correction for column-compressibility by the equation

$$m'_1 = \frac{\beta_1 - 1}{\beta_1} \tag{4.67}$$

On the other hand, it might be unsafe to calculate the average shear strength based only on the load ratio of the stone columns, because doing so would apply the stress concentration also to the unit weight of the in-situ soil, which may not be conservative, especially with deep slip circles. In Kirsch and Sondermann (2003) it is therefore recommended to calculate the shear strength of the improved soil as the mean of the strength values on the basis of either the area ratio or the load ratio.

Priebe (2003) recommends modelling each individual stone column in a two-dimensional slip circle analysis with vertical slices, and factorising the load on top of the columns by the stress concentration factor and simultaneously reducing the load on the soil in between. This can, for example, be achieved by adjusting the unit weight of the embankment. With large systems, this approach can be quite laborious. Therefore Priebe alternatively proposes calculating average shear strength values on the basis of the load ratio but reducing them with depth by applying a reduction factor being the quotient of the load on top of the improved ground $Q_{top}$ and the total load $Q_{total}$ at the respective depth. The maximum reduction of the load ratio is reached when the columns are unloaded. In this case, the strength of the improved ground is the average of the strength of the soil and the columns, weighted by the area ratio according to Priebe adopted for the compressibility of the column material:

$$m''_1 = \overline{A_c / A} + (m'_1 - \overline{A_c / A}) \cdot \frac{Q_{top}}{Q_{total}} \tag{4.68}$$

With the adjusted load ratio $m'_1$ the average strength of the improved ground can be calculated by the following equations:

$$\varphi_{avg} = \arctan (m''_1 \cdot \tan \varphi_c + (1 - m''_1) \cdot \tan \varphi_s) \tag{4.69}$$

$$c_{avg} = (1 - m''_1) \cdot c_s \tag{4.70}$$

Calculating the average cohesion $c_{avg}$, also on the basis of the reduced load ratio $m'_1$ is on the safe side, since physically one could apply the area ratio, which would lead to higher cohesion values.

In order to calculate the corresponding shear strength values the system is divided into five vertical sections, A to E, in which the ground is improved by stone columns of different area ratios $a_c = 0.22$ in section A and $a_c = 0.33$ in

sections B to E. Additionally the four existing layers (Figure 4.29) are subdivided into sublayers of approximately 2 m thickness. The five sections A to E in Figure 4.30 are characterised by different loading conditions due to the different embankment heights which are averaged within the section for simplicity. Table 4.7 gives an overview of the resulting shear strength values. The soil properties of the unimproved ground (layers 42 to 45) and the embankment material (layer 1) are given in Table 4.4.

Figure 4.30 shows the embankment geometry with the different soil layers as chosen in the calculations, and the decisive slip circle, in this case with a minimum factor of safety of 2.08, together with the contours of equal safety.

*Table 4.7* Depth-dependent shear strength of the improved ground in sections A to E

| *Depth* | *A* | | | | | | *B* | | | | | |
|---|---|---|---|---|---|---|---|---|---|---|---|---|
| *(m)* | *layer* | $m'_1$ | $Q_{top}/Q_{total}$ | $m''_1$ | $\varphi_{avg}$ (°) | $c_{avg}$ *(kPa)* | *layer* | $m'_1$ | $Q_{top}/Q_{total}$ | $m''_1$ | $\varphi_{avg}$ (°) | $c_{avg}$ *(kPa)* |
| –2.0 | 2 | 0.58 | 0.96 | 0.57 | 27.00 | 17.36 | 10 | 0.70 | 0.95 | 0.68 | 31.56 | 12.71 |
| –4.0 | 3 | 0.58 | 0.93 | 0.55 | 26.47 | 17.88 | 11 | 0.70 | 0.91 | 0.67 | 30.95 | 13.36 |
| –5.5 | 4 | 0.59 | 0.91 | 0.56 | 26.63 | 2.66 | 12 | 0.72 | 0.89 | 0.68 | 31.41 | 1.93 |
| –7.0 | 5 | 0.59 | 0.89 | 0.55 | 26.39 | 2.69 | 13 | 0.72 | 0.87 | 0.67 | 31.14 | 1.97 |
| –9.0 | 6 | 0.59 | 0.87 | 0.54 | 26.07 | 2.74 | 14 | 0.72 | 0.85 | 0.66 | 30.79 | 2.03 |
| –10.5 | 7 | 0.59 | 0.86 | 0.54 | 25.84 | 3.70 | 15 | 0.72 | 0.83 | 0.66 | 30.54 | 2.76 |
| –12.0 | 8 | 0.59 | 0.84 | 0.53 | 25.62 | 3.74 | 16 | 0.72 | 0.82 | 0.65 | 30.29 | 2.81 |
| –14.0 | 9 | 0.59 | 0.83 | 0.53 | 25.34 | 3.79 | 17 | 0.72 | 0.80 | 0.64 | 29.98 | 2.87 |

| *Depth* | *C* | | | | | | *D* | | | | | |
|---|---|---|---|---|---|---|---|---|---|---|---|---|
| *(m)* | *layer* | $m'_1$ | $Q_{top}/Q_{total}$ | $m''_1$ | $\varphi_{avg}$ (°) | $c_{avg}$ *(kPa)* | *layer* | $m'_1$ | $Q_{top}/Q_{total}$ | $m''_1$ | $\varphi_{avg}$ (°) | $c_{avg}$ *(kPa)* |
| –2.0 | 18 | 0.70 | 0.92 | 0.67 | 31.08 | 13.22 | 26 | 0.70 | 0.78 | 0.62 | 29.01 | 15.37 |
| –4.0 | 19 | 0.70 | 0.86 | 0.64 | 30.09 | 14.26 | 27 | 0.70 | 0.64 | 0.56 | 26.82 | 17.54 |
| –5.5 | 20 | 0.72 | 0.83 | 0.65 | 30.41 | 2.09 | 28 | 0.72 | 0.59 | 0.56 | 26.80 | 2.63 |
| –7.0 | 21 | 0.72 | 0.80 | 0.64 | 29.99 | 2.15 | 29 | 0.72 | 0.55 | 0.54 | 26.08 | 2.74 |
| –9.0 | 22 | 0.72 | 0.76 | 0.63 | 29.47 | 2.23 | 30 | 0.72 | 0.50 | 0.52 | 25.26 | 2.86 |
| –10.5 | 23 | 0.72 | 0.74 | 0.62 | 29.10 | 3.05 | 31 | 0.72 | 0.47 | 0.51 | 24.74 | 3.91 |
| –12.0 | 24 | 0.72 | 0.72 | 0.61 | 28.76 | 3.12 | 32 | 0.72 | 0.44 | 0.50 | 24.27 | 3.99 |
| –14.0 | 25 | 0.72 | 0.69 | 0.60 | 28.33 | 3.21 | 33 | 0.72 | 0.41 | 0.49 | 23.72 | 4.10 |

| *Depth* | *E* | | | | | |
|---|---|---|---|---|---|---|
| *(m)* | *layer* | $m'_1$ | $Q_{top}/Q_{total}$ | $m''_1$ | $\varphi_{avg}$ (°) | $c_{avg}$ *(kPa)* |
| –2.0 | 34 | 0.70 | 0.00 | 0.31 | 15.60 | 27.60 |
| –4.0 | 35 | 0.70 | 0.00 | 0.31 | 15.60 | 27.60 |
| –5.5 | 36 | 0.72 | 0.00 | 0.33 | 16.55 | 4.02 |
| –7.0 | 37 | 0.72 | 0.00 | 0.33 | 16.55 | 4.02 |
| –9.0 | 38 | 0.72 | 0.00 | 0.33 | 16.55 | 4.02 |
| –10.5 | 39 | 0.72 | 0.00 | 0.33 | 16.55 | 5.36 |
| –12.0 | 40 | 0.72 | 0.00 | 0.33 | 16.55 | 5.36 |
| –14.0 | 41 | 0.72 | 0.00 | 0.33 | 16.55 | 5.36 |

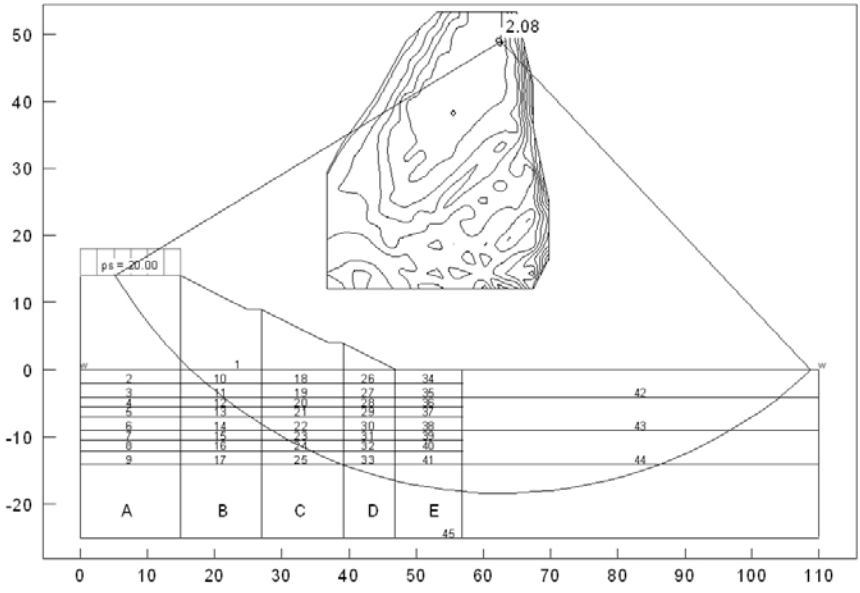


*Figure 4.30* Cross-section with soil layers as used in the computation and decisive slip circle

The analysis is performed using a standard stability analysis program and applying a division into 50 slices. The groundwater table was set equal to the ground surface. An additional loading of 20 kN/m$^2$ was applied on top of the embankment.

### *4.6.3 Bearing capacity calculation of single footings on stone columns*

The construction of a new steel framed industrial hall with a base area of 228 × 144 m and a height of 12 m makes ground improvement measures necessary, since the subsoil is unsuitable for carrying the high structural loads. Below a relatively old up-to-4.5-m-thick layer of fill consisting primarily of cohesive material follows soft marl with depths ranging to 15 m and more, which is underlain by dense sand. The foundation of the structure consists of single footings arranged in a regular pattern of 24 × 12 m, with footing areas between 3.5 × 3.5 m and 5.8 × 5.8 m depending on the applied loading.

The ground improvement is achieved by arranging vibro replacement stone columns below the structure with diameters of generally 0.7 m. Below the slab, the stone columns are arranged in a square pattern of 3 × 3 m, and underneath the footings groups of 9, 13 and 25 stone columns are constructed, depending on footing size and load to be carried.

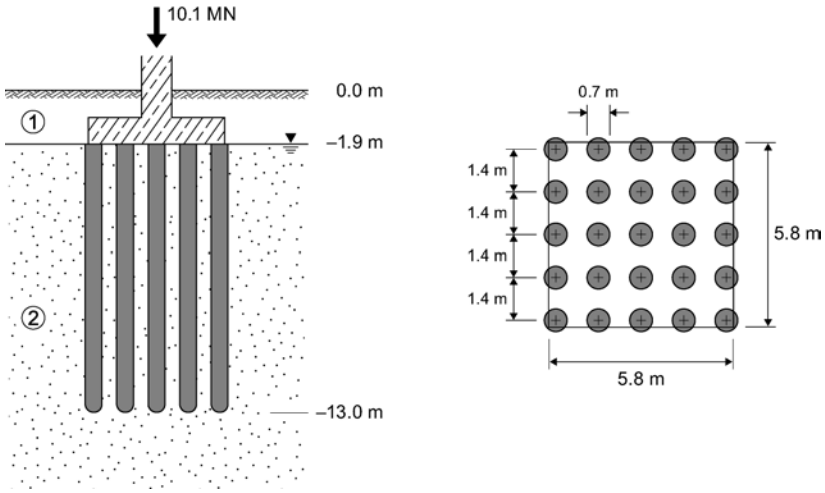


*Figure 4.31* Cross-section and plan view of single footing founded on 25 stone columns

*Table 4.8* Soil parameters

| | *Layer 1: fill* | *Layer 2: marl* | *Stone columns* |
|---|---|---|---|
| Unit weight $\gamma$ (kN/m$^3$) | 16 | 22 | 21 |
| Submerged unit weight $\gamma'$ (kN/m$^3$) | 6 | 10 | 11 |
| Constrained modulus $E_{oed}$ (MN/m$^2$) | – | 20 | 120 |
| Poisson's ratio $\mu$ | – | 0.45 | 0.33 |
| Young's modulus $E$ (MN/m$^2$) | – | 5.3 | 81 |
| Effective friction angle $\varphi'$ (degrees) | – | 27 | 40 |
| Effective cohesion $c'$ (kN/m$^2$) | – | 10 | 0 |
| Undrained shear strength $c_u$ (kN/m$^2$) | – | 25 | – |
| Coefficient of earth pressure at rest $K_0$ | – | 0.55 | – |

In the following, this project will also serve as an example to illustrate the way of assessing the bearing capacity of single footings founded on vibro stone columns. Figure 4.31 shows the soil profile and the plan view of a highly loaded 5.8 × 5.8 m footing carrying a maximum design load of 10.1 MN. Table 4.8 summarises the soil parameters necessary for this bearing capacity calculation. The settlement improvement factor $\beta_1$ according to Priebe (1995) can be calculated using, for example, equation (4.50):

$$\beta_1 = 2.3 \tag{4.71}$$

The assessment of the bearing capacity now follows the procedure as proposed by Barksdale and Bachus (1983) and as described in Section 4.3.3.

The area replacement ratio can be calculated as the sum of the stone column areas $A_c$ divided by the footing area $A_F$:

$$a_c = \frac{\Sigma A_c}{A_F} = \frac{25 \cdot \frac{\pi \cdot 0.7^2}{4}}{5.8^2} = 0.29 \tag{4.72}$$

The stress concentration factor $n$ can be computed from equation (4.11) with $\beta = \beta_1 = 2.3$:

$$n = \frac{\sigma_c}{\sigma_s} = \frac{\beta - 1}{a_c} + 1 = \frac{2.3 - 1}{0.29} + 1 = 5.5 \tag{4.73}$$

The stress concentration within the columns can thus be identified from equation (4.6):

$$n_c = \frac{n}{1 + (n - 1) \cdot a_c} = \frac{5.5}{1 + (5.5 - 1) \cdot 0.29} = 2.4 \tag{4.74}$$

Numerical analysis of the situation showed vertical stresses in the columns close to the footing between 500 kPa and 1 MPa depending on the position underneath the footing, which fits quite well to column stresses of

$$\sigma_c = n_c \cdot \sigma = 2.4 \cdot 300 = 720\ kPa \tag{4.75}$$

As described in Section 4.3.3, quick loading conditions are assumed with the undrained shear strength $c_u$ prevailing in the soil ($\varphi_s = 0°$). Therefore the composite shear strength can be computed from equations (4.25) and (4.27):

$$\tan \varphi_{avg} = n_c \cdot a_c \cdot \tan \varphi_c = 2.4 \cdot 0.29 \cdot \tan 40° = 0.58$$

$$\Rightarrow \varphi_{avg} = 30° \tag{4.76}$$

$$c_{avg} = c_u (1 - a_c) = 25 (1 - 0.29) = 18\ kPa \tag{4.77}$$

Therefore the inclination of the failure plane within the column group computes from equation (4.24) to

$$\delta = 45° + \frac{\varphi_{avg}}{2} = 45° + \frac{30°}{2} = 60° \tag{4.78}$$

The square column group in the soil is approximated by a composite material of circular shape. The equivalent diameter $B$ computes to

$$B = \sqrt{\frac{5.8^2 \cdot 4}{\pi}} = 6.5\ m \tag{4.79}$$

According to Figures 4.18 and 4.31 the depth of the failure wedge is

$$B \cdot \tan\delta + 1.9\ \text{m} = 6.5\ m \cdot \tan 60° + 1.9\ m$$
$$= 11.3\ m + 1.9\ m = 13.2\ m \tag{4.80}$$

The mean horizontal stress level $q$ is estimated from the initial stresses in the soil according to Figure 4.18:

$$q = K_0 \cdot \frac{\gamma_1 \cdot 1.9\ m + (\gamma_1 \cdot 1.9\ m + \gamma'_2 \cdot 11.3\ m)}{2} = 48\ kPa \tag{4.81}$$

The rigidity index $I_r$ of the soil can be computed from the Young's modulus $E$, the Poisson's ratio $\mu$, the mean stress level $q$ and the shear strength as

$$I_r = \frac{E}{2(1+\mu) \cdot (c' + q \cdot \tan\varphi')} \tag{4.82}$$

In case of undrained conditions, equation (4.82) can be reduced, with $\mu$ = 0.5 for deformations at constant volume, to

$$I_r = \frac{E}{3 \cdot c_u} = \frac{5300}{3 \cdot 25} \approx 70 \tag{4.83}$$

The Vesic cavity expansion factors $F'_c$ and $F'_q$ can be taken from Figure 4.19 or for undrained conditions ($\varphi_s = 0$) from the following equations:

$$F'_c = \ln(I_r) + 1 = 5.3$$
$$F'_q = 1.0 \tag{4.84}$$

The ultimate lateral stress in the surrounding soil can than be computed:

$$\sigma_3 = c_u \cdot F'_c + q \cdot F'_q = 25 \cdot 5.3 + 48 \cdot 1.0 = 181\ kPa \tag{4.85}$$

According to equation (4.21) the ultimate vertical stress on the column group then amounts to

$$q_{ult} = \sigma_3 \cdot \tan^2\delta + 2 \cdot c_{avg} \cdot \tan\delta$$
$$= 181 \cdot \tan^2 60° + 2 \cdot 18 \cdot \tan 60° = 605\ kPa \tag{4.86}$$

The overall factor of safety FS against ground failure in this case is

$$FS = \frac{605}{300} \approx 2.0 \tag{4.87}$$

### *4.6.4 Some results of a parametric study of stone column group behaviour*

Field measurements to study the group behaviour by investigating the interaction of load application, stone columns and soil for variable foundation stiffness, column pattern and length are almost prohibitive in view of the practical difficulties and costs. Alternatively, finite-element-based numerical analyses that are properly adjusted by accompanying field measurements can provide an interesting insight into vibro stone column behaviour under load.

Figure 4.32 shows details of such a study for a rectangular concrete foundation on stone columns of variable number and depth. The parametric 3-D study used APDL for the FEM ANSYS programming system (Kirsch, 2004). From the many parameters investigated, the following concentrates on the influence of the area replacement ratio $a_c$ (for column groups defined as the ratio between total area of stone columns $\Sigma A_c$ to footing area $A_F$ according to equation (4.88)), foundation stiffness and relative column length $\lambda$ (ratio of column length $l$ and depth $T$ of the soil to be improved according to equation (4.89)), on the improvement factor $\beta$ and on the stress

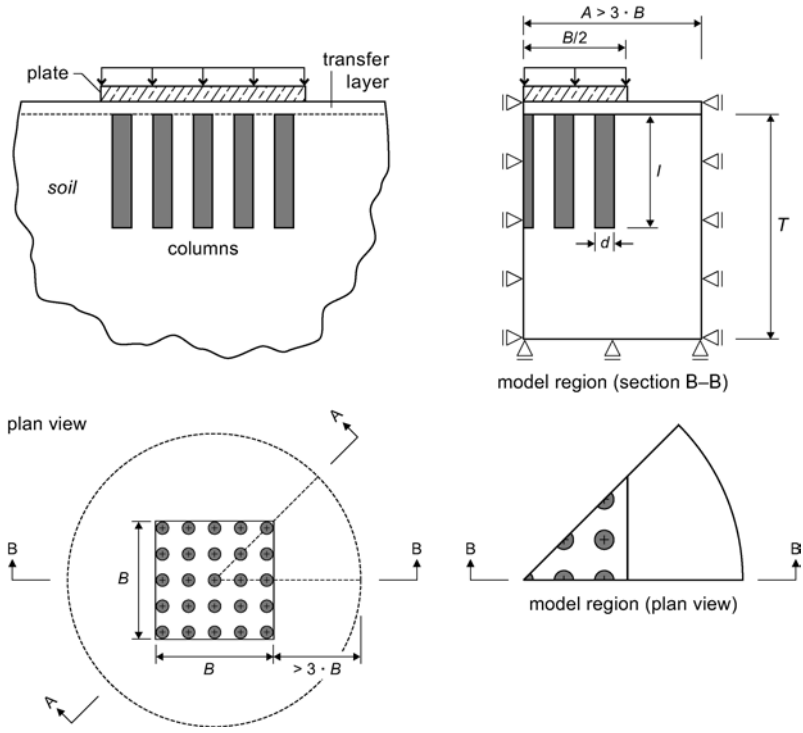


*Figure 4.32* System model and symmetries used in computations

concentration factor $n$. The study allowed computing groups of between 4 and 81 columns supporting a square foundation with a maximum width of $B = 20$ m. The friction angle $\varphi_c$ of the stone column material varied between 35° and 50°.

$$a_c = \frac{\Sigma A_c}{A_F} \tag{4.88}$$

$$\lambda = \frac{l}{T} \tag{4.89}$$

When looking at the influence of the area replacement ratio $a_c$ and the friction angle $\varphi_c$ of the stone column material on the improvement factor $\beta$, Figure 4.33 shows this relationship for rigid square footings founded on a variable number of stone columns with $\lambda = 1$ and $\lambda = 0.75$. In order to obtain an improvement factor of $\beta = 2$ for a foundation with stone columns extended to the bearing stratum $\lambda = 1$, the necessary replacement ratio is between an uneconomically high value of $a_c = 0.7$ for $\varphi_c = 35°$ and a realistic value of $a_c = 0.25$ for $\varphi_c = 50°$. The adjacent figure for $\lambda = 0.75$, whereby the columns reach only 75% of the necessary improvement depth, illustrates the importance extending the stone columns whenever possible into a competent bearing stratum, since the same configuration of stone columns with $a_c = 0.25$ achieves only improvement factors between $\beta = 1.3$ for $\varphi_c = 35°$ and $\beta = 1.9$ for $\varphi_c = 50°$ when the column is floating. For the same $a_c$ value, the improvement factor drops further with $\lambda = 0.5$ to $\beta = 1.3$ for $\varphi_c = 35°$ and $\beta = 1.7$ for $\varphi_c = 50°$.

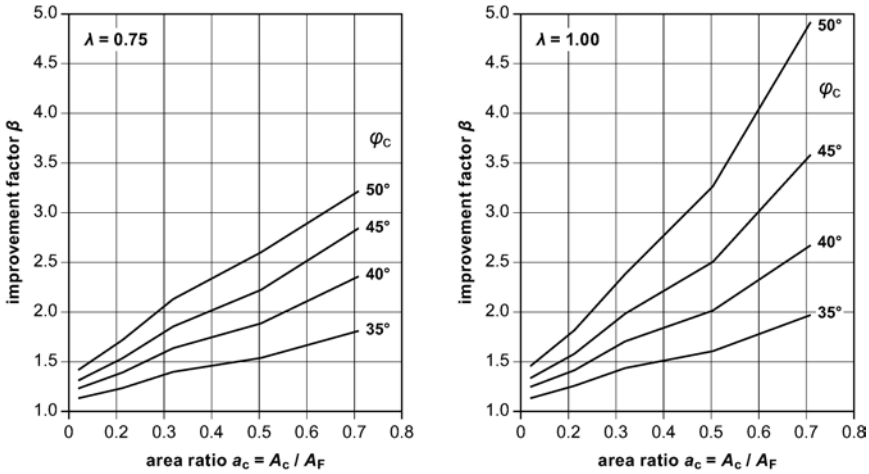


*Figure 4.33* Improvement factor $\beta$ as a function of replacement factor $a_c$ and stone column friction angle $\varphi_c$ for different relative column lengths $\lambda$

The study also revealed that the improvement factor $\beta$ is – within the a.m. limits – invariable for different foundation dimensions but equal foundation stiffness $K_S$.

$$K_S = \frac{E_F}{12 \cdot E_s} \left(\frac{H}{B}\right)^3 \frac{T}{B} \tag{4.90}$$

with

$E_F$ modulus of elasticity of footing in kPa
$E_s$ modulus of soil to be improved in kPa
$H$ thickness of footing in m
$B$ width of footing in m
$T$ thickness of soil layer to be improved in m.

Figure 4.34(a) gives the load settlement curves for different square footings founded on stone columns with identical area replacement values $a_c = 0.20$. As expected, settlement rises with increasing load and loaded area as a result of the different vertical stresses in the ground, which are shown in Figure 4.34(b) for a square footing ($B = 8$ m) founded on 25 stone columns with $a_c = 0.20$ in comparison with the infinite grid situation. Stress concentration within the stone columns results in stress relief in the soil as compared with the situation without stone columns ($a_c = 0$). Below the stone columns – here at a depth of 6.0 m – soil stresses of the improved and unimproved case are approaching each other again at about 7 m to 8 m depth.

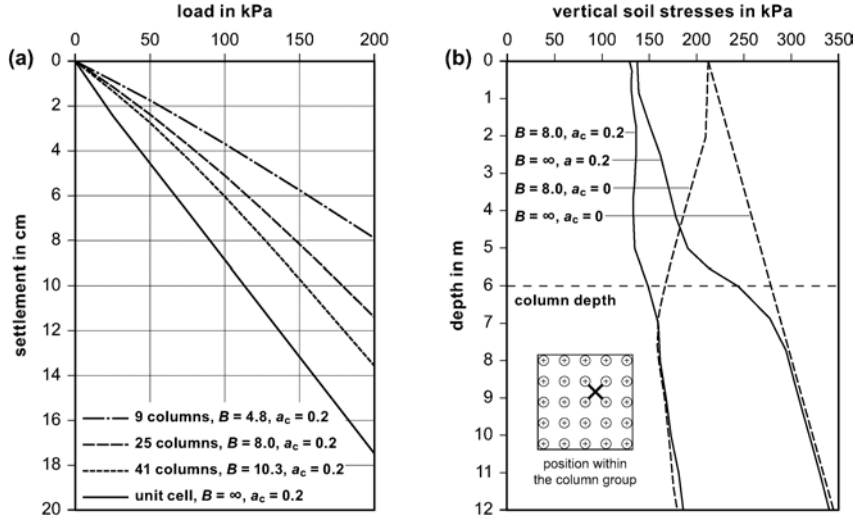


*Figure 4.34* Vertical deformations of square foundations and stress distribution in the soil for variable dimensions and constant $a_c$

The distribution of stresses between column and soil, which is in the first place responsible for the soil improvement, depends both on $a_c$ and $\varphi_c$, and also on the foundation situation of the stone column itself (founded in competent stratum with $\lambda = 1$ or floating with $\lambda < 1$). Figure 4.35 shows the situation of a square footing with $B = 8$ m founded on 25 stone columns with constant replacement ratio $a_c = 0.32$ but different lengths $l$ between 4 m

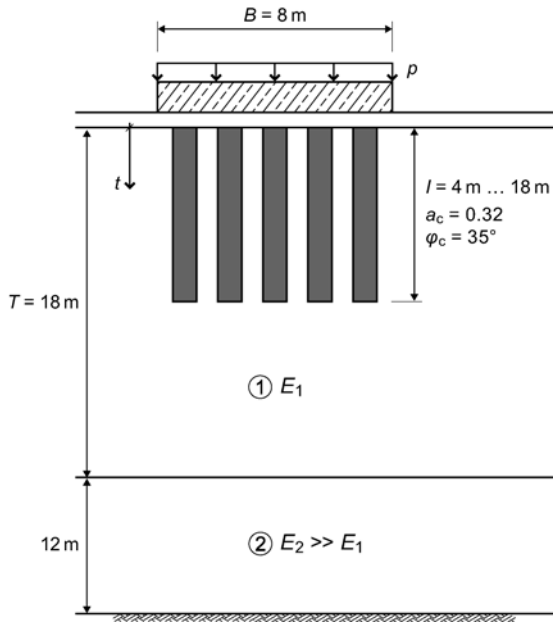


*Figure 4.35* Situation considered for study of column length influence

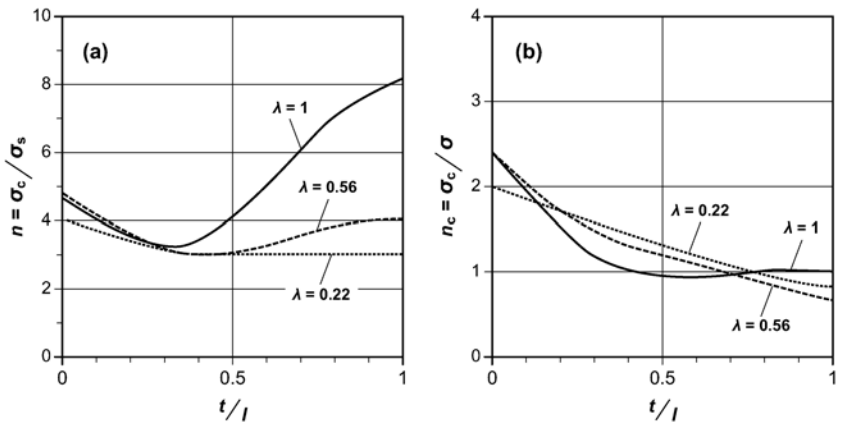


*Figure 4.36* Stress concentration factors $n$ and $n_c$ for a rigid square foundation ($B$ = 8 m) on 25 stone columns for $a_c = 0.32$ and $\varphi_c = 35°$

and 18 m. Layer 2 has a considerably higher modulus (factor 40) than layer 1 needing improvement.

The findings of the numerical analysis are presented in Figure 4.36 giving plots of (a) the stress concentration factors $n = \sigma_c/\sigma_s$ against depth for different relative stone column lengths $\lambda$, and (b) the column stress concentration factor $n_c = \sigma_c/\sigma$.

When looking at the $n_c$ development with depth for the square footing it is interesting to see that column stresses rise again even in very long columns ($\lambda = 1$) beyond a relative depth of about $t/l = 0.55$ to a level of $n_c = 1$ at the toe of the column. For floating columns, column stresses decrease gradually with column depth to $n_c$ levels of 0.8–0.6.

### *4.6.5 Wet vibro replacement stone columns for a thermal power plant*

For a new 1500 MW coal-fired thermal power plant in southern India all ancillary structures, such as cooling towers, service buildings and special storage tanks were founded on improved ground, since the original soil had insufficient characteristics to carry even moderate loads. It consists of soft clays to a depth of 7 m to 10 m followed by layers of silty sands and silts whose density increases with depth, and that is resting on dense sand at a depth of about 20 m below grade. The water table is generally close to ground surface. SPT *N*-values are between 0 and 2 in the upper 7 m rising to $N = 5$ at about 10 m depth and then gradually increasing to well over $N = 30$ at a depth of 20 m with values in excess of $N = 50$ below.

The vibro replacement scheme that was proposed for structures such as tanks, cooling towers and service buildings consisted of stone columns of lengths between 7 m and 10 m, which were arranged in triangular grids of 2 m and 2.5 m equal spacing. Table 4.9 provides details of the structures, their dimensions and loads and of the ground improvement scheme adopted.

Construction of the stone column foundation was in 2008 amounting to 285,000 lin.m for the whole project. The vibro stone columns were executed

*Table 4.9* Details of the structures founded on vibro stone columns

| | *Storage tanks* | *Cooling towers* | *Buildings* |
|---|---|---|---|
| Dimensions | 16.6 m diameter<br>11.5 m height | 144 m × 32 m | 11 m × 5 m |
| Loading | 135 kPa | 90 kPa | 55 kPa |
| Type of foundation | Raft | Raft | Strip footings |
| Allowable settlement | 100 mm | 75 mm | 40 mm |
| Triangular grid spacing | 2.5 m | 2.0 m | 2.5 m |
| Column length | 7.0 m | 11.0 m | 7.0 m |

with a diameter of 0.9 m by the wet vibro replacement method employing the Keller M vibrator and using 12/75 mm crushed stone aggregate as backfill material. Its gradation was characterised by $D_{60}/D_{10}$ value of 4, with less than 5% of the material passing the 12 mm sieve. Process water was channelled into silt ponds before it was released into a nearby creek. Quality control was performed with a standard data acquisition system measuring depth and amperage versus time of execution. In addition, numerous load tests were performed on single columns and on groups of three columns as proof of the load settlement performance of the structures. Figure 4.37 shows the stone column arrangement for a storage tank together with a cross-section through its foundation.

Acceptance tests for the vibro stone columns were carried out in accordance with the Indian Standard IS 15284, which require tests on single columns within a group of at least seven stone columns and load tests on a group of three columns out of a total of a minimum of 12 stone columns. Footing size required by the standard follows the unit cell principle in specifying it on the basis of "the effective tributary soil area of stone column for a single column test and three times the effective area of single column for a three column group test". The test footings were of circular shape, sufficiently rigid and centrally placed over a granular blanket of a minimum thickness of 0.30 m. At 150% design load, the single column settled generally not more than 15 mm with the three column group tests settling less than 25 mm. At the chosen design load of 300 kN per stone column, the settlements were only 8 mm or 8.5 mm respectively.

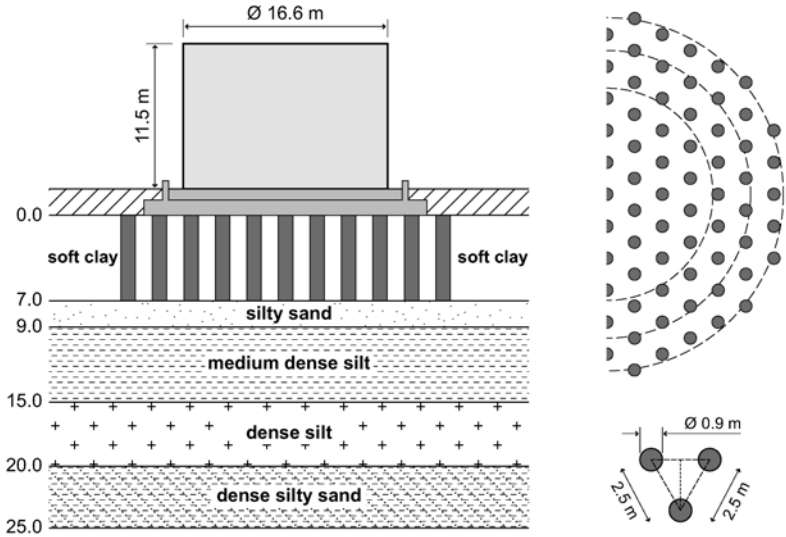


*Figure 4.37* Vibro stone column layout for and cross-section through tank foundation

### *4.6.6 Vibro replacement soil improvement for a double track railway project*

The Ipoh–Rawang and Ipoh–Padang Besar double track railway construction projects in Malaysia have been under way since 2001 and involve about 330 km of new line. The project crosses five states and encompasses the construction of a new track near, or next to, the existing railway track. Ground improvement works were necessary for about 32 km, where the new track crosses over poor soils. Some stretches of the track cut through valuable farmland. In such areas, stone column installation was restricted to the dry bottom feed method to avoid contamination of the neighbouring fields by the silt- and clay-loaded process water. The wet vibro replacement method was used when low headroom conditions below existing road bridges only allowed the execution of short columns of about 5 m length. As the soil improvement work had to be carried out as close as 2.5 m from the existing live track, very stringent safety measures were put in place to minimise the risks for passing trains and for the workmen and their rigs. Vibro stone columns were also used to support earth embankments and reinforced earth walls approaching new bridges crossing the railway tracks. Figure 4.38 shows a typical situation of a dry bottom feed vibrocat operating next to the existing track.

Where ground improvement was necessary the subsoil consisted generally of soft clay deposits to about a depth of 7 m and of firm clay to 10 m. At that elevation stiff clay was encountered whose stiffness increased at 15 m depth

*Figure 4.38* Vibrocat in operation next to existing railway track (by courtesy of Keller Group plc)

*Table 4.10* Idealised soil profile for stretches of the railway line needing ground improvement

| *Layer* | *Depth in m below GL* | *Soil type* | *Average SPT N-value* | *Undrained shear strength in kPa* | *Deformation modulus in kN/m²* |
|---|---|---|---|---|---|
| 1 | 0–4 | Soft clay | 0–1 | 10 | 1000 |
| 2 | 4–7 | Soft clay | 2 | 20 | 2000 |
| 3 | 7–10 | Firm clay | 4 | 30 | 3000 |
| 4 | 10–15 | Stiff clay | 10 | 60 | 18,000 |
| 5 | >15 | Very stiff clay | >15 | – | – |

and beyond considerably. Table 4.10 summarises the soil conditions in an idealised profile.

The design of the railway line had to fulfil the following performance criteria:

- 25 mm maximum settlement with a maximum deflection of 1:1000 of the track over 6 months from the certificate of acceptance;
- a minimum factor of safety against slope instability of 1.2 during construction and of 1.4 during service stage.

The vibro stone column scheme that was proposed and adopted consisted of a rectangular grid of 1.0 m diameter stone columns with lengths of generally 10 m, but in places up to 18 m. The distance between vibro probes within the grid was 2.25 m or 2.5 m, resulting in area replacement factors $a_c = 0.16$ and 0.13 respectively. In total an area of over 1 million $m^2$ covering unsuitable soil was improved by the vibro replacement method by the end of 2008 using M-type Keller bottom feed depth vibrators. The key element of the quality assurance programme was the standard data acquisition system recording depth and amperage over time, a conventional measurement of the stone consumption and frequent load tests on single columns. The load tests were performed with relatively small steel plates of 1.5 × 1.5 m or even only 1 m diameter as test footings. The regularity of the test result served as a good indicator for the steady execution of the stone columns and their performance under load.

In this context, it should be remembered that zone load tests, or at least tests with footing sizes equal to the unit cell area, would deliver more significant results, the latter at relatively low extra costs, to better interpret the load settlement performance of the structure.

### *4.6.7 Design and execution of a vibro replacement foundation*

The new international airport BBI for Berlin will go into operation with its first phase in 2011. For the construction of infrastructural measures to

connect the central terminal building with the highway and with high speed and regional rail traffic systems, ground improvement by vibro replacement was necessary. Subsoil at the site consists of marl and sand layers of glacial origin that are relatively soft to a depth of about 8 m below ground surface where generally stiff marl follows characterised by CPT cone resistance values typically well in excess of 15 MN/m$^2$. Design target of the ground improvement scheme was a reduction of the settlements deriving from the upper soft layers by a factor of 2 for single footings and a deformation modulus of 21 MN/m$^2$ below rafts and approach ramps. The necessary spacing of the vibro stone columns was determined by load tests on groups of four columns for structures and on single columns adopting the unit cell concept for area loads.

All single column load tests were performed with a test load of 200 kN/m$^2$ on square test footings of 1.25 × 1.25 m and 2 × 2 m, each supported by a 9 m long vibro stone column of 0.5 m or 0.6 m diameter. Figure 4.39 shows the load test setup together with a CPT diagram which is representative of the site. Table 4.11 gives details of the load tests which were evaluated by the method described in Section 4.4.

By adopting the unit cell concept the settlement of a single column determines the equivalent deformation modulus $E^*$ by introducing the equivalent column length $l^*$ from Figure 4.28 into equation (4.45). The necessary grid spacing for the target modulus can then be determined graphically, here by extrapolation according to Figure 4.40, where a necessary area $A_n$ = 7.4 m$^2$ for a square grid of 0.6 m diameter stone columns was obtained for the required design modulus $E_d$ = 21 MN/m$^2$. The ground improvement works were performed using conservatively a square grid of 0.6 m diameter stone columns of 9.0 m length with 2.5 m spacing.

While the necessary area replacement factor for the infinite grid was just $a_c$ = 0.05 to achieve a modulus of 21 MN/m$^2$, the evaluation of the column group tests resulted in a required $a_c$ = 0.09 for single footings to reduce settlements by 50%. Prior to the load tests, large shear box tests were

*Table 4.11* Evaluation of single column load tests

| *Test load 200 kN/m$^2$* | | *Test 1* | *Test 2* | *Test 3* | *Test 4* |
|---|---|---|---|---|---|
| Column dia. $d_c$ | m | 0.6 | 0.5 | 0.6 | 0.5 |
| Footing area $A$ | m$^2$ | 1.56 | 1.56 | 4.0 | 4.0 |
| $a_c = A_c/A$ | – | 0.18 | 0.13 | 0.07 | 0.05 |
| Settlement $s$ | mm | 8 | 11.4 | 15.7 | 23.9 |
| Equiv. diameter $d_e$ | m | 1.41 | 1.41 | 2.26 | 2.26 |
| Equiv. col. length $l^*$ | m | 5.36 | 5.36 | 5.88 | 5.88 |
| Equiv. modulus $E^*$ | MN/m$^2$ | 133.9 | 94.0 | 75.0 | 49.2 |
| Grid area $A$ ($d_c$ = 0.6 m) | m$^2$ | 1.56 | 2.17 | 4.0 | 5.65 |
| Grid spacing[1] ($d_c$ = 0.6 m) | m | 1.25 | 1.47 | 2.0 | 2.38 |

*Note:* 1 for square grid

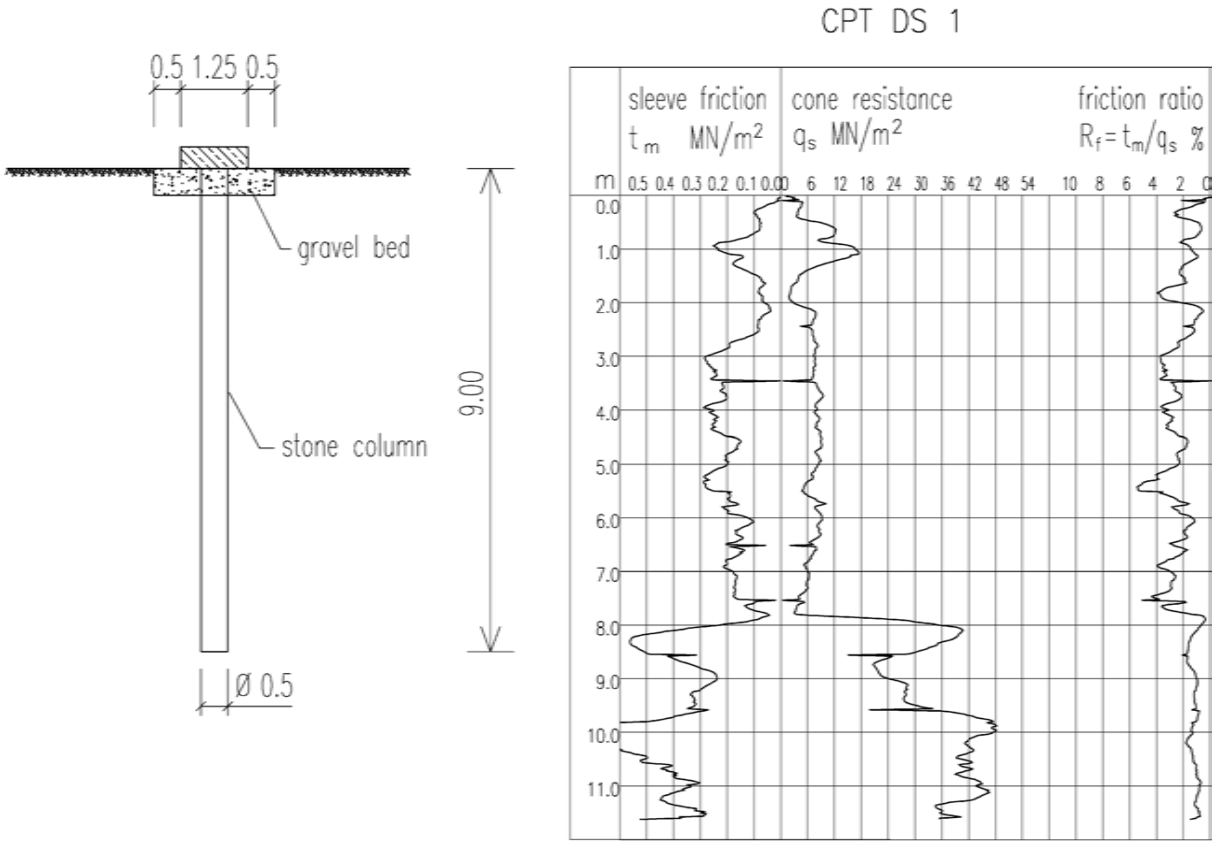


*Figure 4.39* Load test on single column and representative CPT result

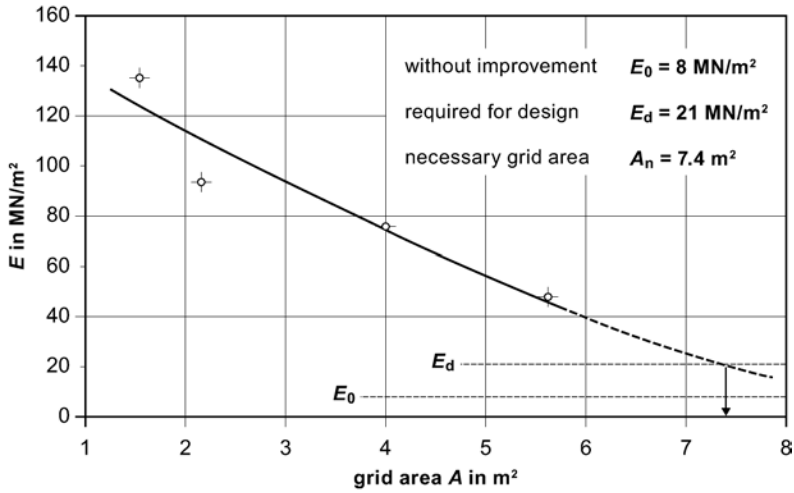


*Figure 4.40* Determination of grid spacing from single column load test results

performed in the laboratory with the stone column material anticipated for the ground improvement works. It consisted of crushed granite rock of 10–35 mm grain size. In the laboratory an average friction angle of 57° was determined for the backfill material at a density of 1.9 t/m$^3$, safely allowing the use of column friction angles of 45° in the design calculation.

An area of about 20,000 m$^2$ was improved by stone columns on this project in 2008 using Keller bottom feed M vibrators. Quality control measures included standard data acquisition systems to record the usual parameters including stone take. Early settlement measurements on the structures indicate that the performance is considerably better than expected and that the design criteria were met.

### *4.6.8 High replacement vibro stone columns for a port extension*

The majority of vibro stone column contracts are performed at area replacements of about 5–30%. It is feasible to provide higher replacement when higher bearing capacity, tighter settlement or higher effective angle of friction for slope stability are required. However, the vibrator when penetrating the ground induces lateral displacement of the soil. If the stone columns are constructed too close to each other, excessive heave can be generated. This can be overcome for treatment above the water table by preboring at each vibro stone column location, and in this way area replacements of up to 50–60% have been achieved.

Even higher replacement ratios were necessary for two port extension projects in the UK. Both involved sand fill being placed behind new quay walls where the presence of deep weak clays and silts required special design

considerations. While the specified short- and long-term settlement criteria could be achieved by soil improvement using vibro stone columns at about maximum 40% area replacement, the quay wall stability required the composite soil to be virtually wholly granular in character and replacement ratios of 80% and 75% had to be performed.

The first project was based on nominal 1.2 m diameter stone columns on 1.28 m triangular grid, resulting in a replacement ratio of $a_c = 0.8$. The larger-than-normal columns were achieved with the wet method by high pressure water flushing and using Keller S300 vibrators. Intensive investigations by CPT and piezocone had permitted the development of contours for the base and surface of the soft clays and silts across the area. The scheme was then designed for the vibrator to be lowered at least 1 m deeper than the contour base, with the stone columns to be performed to at least 2 m above contour surface of the soft soils. Vibro compaction was then performed to the overlying sands up to ground level.

About 50% of the soil improvement works were performed at lower level behind the tubular pile wall between high tides. It was noted that even when water-flushing was used to wash out the required soil volume, the piles were being displaced when the compaction was being applied to the stone to achieve the specified high angle of friction. A practical approach and sequence of construction combined with monitoring of the piles restricted these movements to within acceptable limits.

This project involved the construction of about 10,000 columns/compactions to depths of up to 20 m. Back-analysis of the stone consumption revealed that about 98.7% of the target area replacement ratio had been achieved.

The second project was more complex since there were real stability concerns and the vibro treatment had to be performed between tie bars to even more variable soils, the extensive and thick soft clays and silts sometimes being present to immediately beneath the working level above high tide. In view of the experience of the first project two advance trials were performed. The first was to confirm that the required stone column diameter of 1.2 m and hence replacement ratio of 75% could be achieved. The second was to examine the effect of the vibro stone column construction using high power vibrators to within 1 m of the sheet pile wall with external support bund.

The results of the second trial have been reported by Slocombe and Smith (2008), where analysis of in-situ earth pressure cells suggested that $K$ values of about 1 could be developed against the sheet piles during vibro compaction. Monitoring procedures were therefore put in place for the proposed main quay combi wall contract works, comprising large-diameter tubular piles with sheet pile infill. It was also concluded that "by installing stone columns away from the wall the peak earth pressures acting on the wall are lower than if the columns were installed towards the wall".

The works commenced with vibro treatment to the area in front and behind the proposed piled anchor wall to the proposed tie bars. The ties

were installed, and the area then filled using clean sand to about high tide level. Vibro stone columns were then constructed, with sand compaction above, between the buried tie bars at two levels and at about 3.65 m centres. Every column location was very carefully set out to avoid damaging the ties and, when the tie bars were subsequently exposed for tensioning, it was confirmed that no damage had been caused.

Again, about 10,000 vibro probes (stone columns/compactions) were constructed to depths of up to about 20 m on a triangular column grid of 1.32 m. Measurement of the stone take revealed that about 97.8% of the $a_c$ = 0.75 target replacement ratio had been achieved. As an illustration of the complexity of the works, the depths of treatment and elevations for the tops of the stone columns resulted in groups of no greater than six adjacent columns being of identical geometry and hence instruction.

A further phase of this port development is currently being built where the soft clay and silt was thin and easily removed by advance dredging. The area behind the tubular pile main quay wall was then filled by placing hydraulic sand fill in about 15 m depth of water. Vibro compaction was then performed prior to the installation of tie bars using Keller S340 vibrators to achieve the specified angle of friction and settlement performance. However, the quay wall design required that the $K$ value be limited to 0.5. Advance trials were therefore performed to confirm how far behind the wall both high- and lower-powered vibrators could be used. These revealed that better control of the wall movements could be achieved by installing the closest line of compaction using lower-power vibrators prior to using high power vibrators further away.

### *4.6.9 Vibro stone columns for settlement control behind bridge abutments*

In the course of the construction of an approach road to an existing highway in western Bavaria the necessary embankments were built well in advance to allow deformations to occur before any bridge and road building was due to commence. These embankments typically have a height of up to about 6 m and rest on soft tertiary silts and clays of about 4.5 m to 6.0 m thickness. Dense tertiary sand, gravel and marl form the competent bearing strata below. The silts and clays have a relatively low strength, $c_u$ = 15 kN/m$^2$, and a modulus between 5 MN/m$^2$ and 8 MN/m$^2$.

To reduce settlements of the embankment behind the bridge abutment, the soft silts and clays were improved by vibro stone columns over a length of about 35 m at both sides of the bridge. Settlement analysis was carried out using the method after Priebe, 1995, with area replacement values of $a_c$ = 0.22 for nine stone column rows immediately behind the pile raft representing the bridge foundation, and of $a_c$ = 0.13 for the remainder and below the embankment shoulders. These replacement values were achieved by 0.8 m diameter stone columns at square grid configurations with distances of

*Figure 4.41* Bauer TR 17 bottom feed vibrator operated from BG12 base machine (by courtesy of Bauer)

1.5 m and 2.0 m respectively. With a chosen angle of friction of $\varphi_c = 42°$ for the stone column material, modified improvement factors $\beta$ were calculated as 3.28 for the 1.5 m grid and 2.17 for the 2.0 m grid, safeguarding a smooth transition between bridge and embankment.

In total, 1680 stone columns with an average length of 5.0 m were carried out on this project in 2008 using Bauer TR 17 bottom feed vibrators operated from MBF 10 and BG 12 base machines. Figure 4.41 shows such a typical setup.

# 5 Method variations and related processes

Vibratory deep compaction as described in the previous chapters utilises, as its main tool, a depth vibrator creating horizontal vibrations when working in the ground. An alternate method using a top vibrator and vertical excitation to compact sand was developed in the late 1960s for the US market; it drove a 750 mm diameter steel pipe into the ground using a vibratory hammer. This so-called Terra Probe method was then, in Europe, modified by replacing the steel tube by steel H-beams and purposely built steel planks, known today as the vibro wing method or the Müller resonant compaction method (MRC). In contrast to vibro compaction, where the depth vibrator remains in the ground generating horizontal vibrations, the vibro wing or MRC methods both utilise vertical vibrations which are transmitted from the steel planks by shear stresses into the soil with the vibrator itself remaining outside the ground (see Section 3.2.1). These methods are restricted to compaction depths of up to about 15 m. Penetration of the vibratory Y- or double-Y-shaped planks is achieved at about 25 Hz whereas compaction is affected by considerably lower frequencies (16 Hz). To support the shearing effect in the soil, the plank has numerous apertures to support the lateral spread of the vibrations.

Process variations of the vibro replacement stone column method include both material and equipment variations. Concrete as backfill material instead of gravel is a key variant. When this is effected over the full length of the column a vibro concrete column, as it is known, is formed. When the stone backfill is replaced by concrete for only part of the column length, so-called hybrid columns are formed. This is done either at the column bottom, to prevent short circuiting of the groundwater, or at its upper part near the column head. Such columns act generally like a rigid soil reinforcement transmitting their vertical loads by end bearing and skin friction into the surrounding soil, in contrast to vibro stone columns. The displacement effect of the bottom feed vibrator which is generally used to construct these concrete columns results in closer bonding of column surface and soil, and enhanced skin friction leading to a higher bearing capacity of the vibro concrete column (Sondermann and Kirsch, 2009). Safe bearing capacities of vibro concrete columns are generally established by field load tests. These

process variants are frequently used when soils need improvements that are only marginally suitable for vibro replacement, such as organic silts and clays of high plasticity (see Table 4.3).

Other process variants use other tools than the depth vibrator to create a stone or sand column. These are, for example, the Compozer sand compaction pile method, the Franki gravel pile method, the controlled modulus column (CMC) method, the Geopier method and the dynamic replacement method.

The sand compaction pile method has been extensively used in the Far East for improving very soft marine clays, both in off-shore and on-shore applications to depths of about 20 m. The process uses closed-end steel pipes, with diameters between 0.5 m and up to 1.6 m, that are vibrated by vibratory hammers into the ground, and the process is largely automated including the sand backfill. Area replacement ratios are generally between 0.3 and 0.5, and settlement improvement is based on experience, with an empirical stress concentration factor $n = 3$ (Tanimoto, 1973). To reduce the settlements of large diameter replacement sand columns a method has been introduced in Germany whereby a geotextile liner encases the sand (Raithel and Kempfert, 1999). Considerable vertical deformations activate the tensile forces of the geotextile before, ultimately, horizontal deformations of the column generate supporting stresses of the surrounding soil (Raithel, 1999).

In the Franki gravel pile method, which is similar to the well-known piling method, a steel pipe is driven, after a gravel plug was formed at its base, to the required depth and is then gradually withdrawn while the coarse fill material is rammed out by means of an internal drop weight.

From a multitude of similar small diameter piling methods being installed for ground improvement purposes in soft soils at relatively close spacing, the CMC method utilises a special displacement auger that penetrates the ground to the predesigned depth essentially without spoil. Grouting of the pile shaft is carried out through the hollow auger stem. If necessary, this process can be repeated to push the grout into the soil thereby increasing contact with it to enhance skin friction at the pile perimeter. In contrast to the vibro concrete columns, end bearing of these columns is generally avoided and their design is based on the equal strain concept of soil and columns whereby column strength can be selected to keep the ratio of soil and column modulus within reasonable limits.

By contrast with the CMC method, which is used to improve soils at considerable depths, the dynamic replacement method is restricted to moderate depths ranges of about 5 m to 7 m. With the dynamic replacement method, a large diameter gravel column is formed in cohesive soils by hammering crushed stone into the ground in a controlled way applying a similar procedure to the well-known dynamic compaction method, but using moderate weights and drop heights. The heavy impact of the drop weight is accompanied by very severe shearing in soft cohesive soils generally without any compaction. To avoid unwanted heave and to

increase column depths pre-excavation may be necessary. Generally, the method requires experience during its execution and close supervision of the development of the imprints and their filling with coarse backfill material (Varaksin, 1990; Luongo, 1992).

The Geopier method constructs impact stone columns in soft cohesive soils by driving a steel tube of approximately 0.5 m diameter into the ground using a special vibratory hammer. After excavating, coarse backfill is placed in small quantities that are compacted utilising an internal mandrill compactor. In stiffer soils the necessary hole, generally 0.75 m in diameter, can be drilled out using standard augers. Material backfill and compaction is then performed in the same way, employing a special compactor (White *et al.*, 2002).

It is obvious that the design approaches that are valid for vibro replacement stone columns can also be applied to all types of columns that are installed by full or partial displacement of the surrounding soil and by subsequent insertion and compaction of granular material. With similar load-carrying mechanisms the key design parameter is the strength of the compacted coarse backfill which is controlled by the compaction energy employed. The adequate choice of the friction angle $\varphi_c$ is decisive for a realistic prediction of bearing capacity and deformation of these foundation methods.

All types of columns that consist of materials whose higher strength is controlled by hardening substances such as cement or other types of hydrating binder act as piles that develop their bearing capacity from skin friction and end bearing.

# 6 Environmental considerations

## 6.1 General remarks

When not appropriately applied and executed, deep vibratory methods, vibro compaction and vibro replacement are potential sources of annoyance and nuisance to people and environment. They may also cause damage to adjacent structures if certain rules are ignored.

It should be appreciated that the vibro methods generate considerably lower greenhouse gases, notably carbon dioxide, than the common conventional foundation solutions.

## 6.2 Noise emission

Most countries have issued national laws or regulations for noise emission of construction sites to protect residents living in the vicinity – for example, in the UK BS 5228, and in Germany DIN EN ISO 3744. These regulations generally contain permitted values of noise levels for different types of neighbourhood: commercial and industrial areas, housing areas, and hospitals and nursing homes. Allowable sound levels are generally specified in dB(A) and are based on the well-established fact that human mental and physical wellbeing is negatively influenced if continuous sound levels are in excess of (Maurer, 2008b):

50–55 dB(A) outside buildings during the day
35–45 dB(A) outside buildings by night

30–35 dB(A) inside buildings during the day
25–30 dB(A) inside buildings by night

The perception of the noise intensity, generally expressed by its rate of decay with distance $\Delta L$, measured in dB(A), is proportional to the logarithm of the distance ratio $r_1/r_2$ according to

$$\Delta L = 20 \cdot \log\left(\frac{r_1}{r_2}\right) \tag{6.1}$$

With $r_1$ and $r_2$ being the distances from the source of the noise, any doubling of the distance results in a sound level reduction of 6 dB(A).

Numerous noise level measurements conducted with the typical vibro replacement equipment, consisting of vibrocat, depth vibrator, generator and air compressor including the pay loader for the gravel backfill, indicate, at the source ($r_1$ = 1 m), a sound level of about 85 dB(A), which drops to about 60 dB(A) at a distance of 100 m. During filling of the gravel container, noise levels may rise by about 10 dB(A) for a relatively short period of time. Sound absorbing elements around diesel engines and inside gravel containers can reduce noise levels at the source by about 5 dB(A), rendering the vibro replacement method a relatively noise-nuisance-free ground engineering construction method (see Figure 6.1).

When vibro compaction work is carried out, typically using crawler cranes as base machines and water as flushing medium, the noise levels at the source will be considerably below those measured for the dry vibro replacement method.

Predicted noise level graphs such as given in Figure 6.1 allow engineers to make a prediction and appraisal of the acceptability of a chosen foundation method on the projected foundation site. In particular cases, the direct measurement and review of noise levels and their propagation into the neighbourhood may become necessary and will help increasing acceptability of a valued foundation engineering solution (O'Hara and Davison, 2004).

## 6.3 Vibration nuisance and potential damages to adjacent structures

Vibration nuisance is generally measured by the peak particle velocity (PPV) of the shear waves emanating from the depth vibrator where potential damage to structures in the vicinity of the compaction works is concerned.

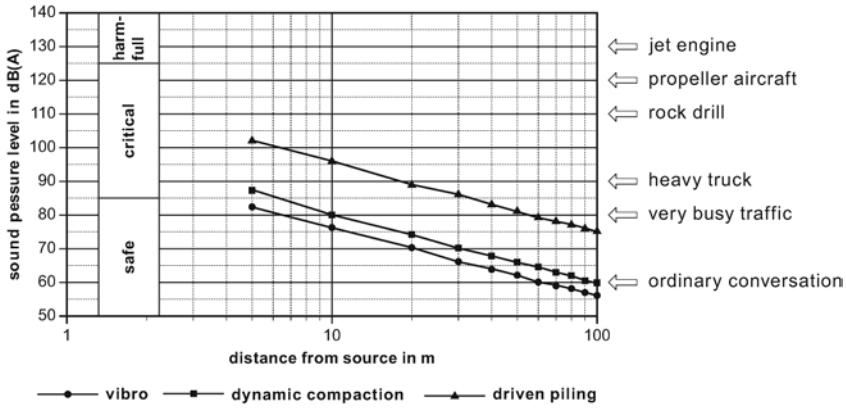


*Figure 6.1* Noise levels for different ground engineering construction methods (O'Hara, 2003)

Such structures can be normal buildings at ground surface but also infrastructure facilities below ground. As we saw in Section 3.2.1 these vibrations may also have a direct influence on the density of granular, non-cohesive soils depending on the generated ground acceleration, which can cause settlement and subsequent damage to the structure. Loose sands below groundwater are particularly sensitive to this effect if a critical acceleration of 0.3 g to 0.5 g is exceeded.

For a steady-state vibration with a frequency $f$, peak particle velocity ($PPV$) and peak particle acceleration ($PPA$) are connected with each other by the following expression:

$$PPA = 2\pi \cdot f \cdot PPV \tag{6.2}$$

Different national codes and regulations, such as the German DIN 4150–3 and the Swiss SN 640312a, provide maximum horizontal or resultant $PPV$ values, respectively, for different types of structures (Tables 6.1 and 6.2).

In a recent study, Achmus *et al.* (2007) have investigated the impact of various depth vibrators on adjacent buildings by evaluating $PPV$ measurements. In total, over 200 vibration measurements on over 20 different

*Table 6.1* Design values for the maximum horizontal $PPV$ at the top floor level of a building due to steady state vibration (according to DIN 4150–3, from Achmus *et al.*, 2007)

| *Building type* | *Design values for the horizontal PPV of construction elements at the top floor level, $DPPV_h$ in mm/s* |
|---|---|
| Industrial buildings | 10 |
| Residential buildings | 5 |
| Very sensitive buildings | 2.5 |

*Table 6.2* Design values for the maximum resultant $PPV$ for construction elements of buildings (according to SN 640312a, from Achmus *et al.*, 2007)

| *Sensitivity classes* | *Frequency class* | *Design values for the resultant PPV of construction elements, $DPPV_{res}$ in mm/s* | | |
|---|---|---|---|---|
| Normal sensitivity | | f < 30 Hz | f = 30–60 Hz | f > 60 Hz |
| (e.g. usual residential | occasional | 15 | 20 | 30 |
| Buildings, office | frequent | 6 | 8 | 12 |
| buildings) | permanent | 3 | 4 | 6 |
| Little sensitivity (e.g. industrial buildings) | | up to two times the respective values for normally sensitive buildings | | |
| Increased sensitivity (e.g. new residential and historic buildings) | | between 100% and 50% of the respective values for normally sensitive buildings | | |

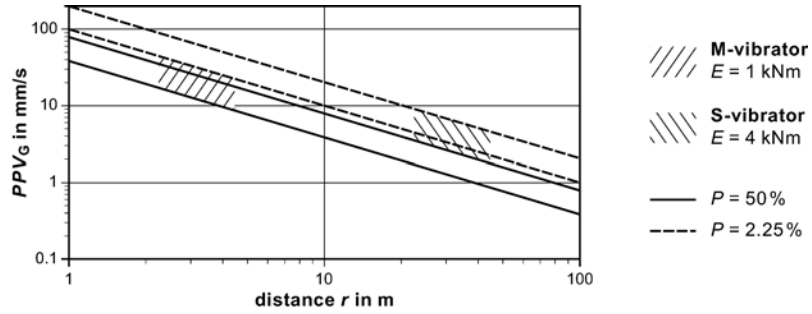


*Figure 6.2* Ground *PPV*-values induced by Keller M- and S-vibrators for 50% and 2.25% probabilities (from Achmus *et al*., 2007)

construction sites using four different Keller depth vibrators were analysed. Vibrator data were according to Table 3.1 and a typical ground peak particle velocity relationship versus distance from the vibrator is given in Figure 6.2 for the M- and S-vibrators, which are characterised by the nominal vibratory energy $E$ according to equation (6.3) and ground peak particle velocity $PPV_G$ from equation (6.4). The factor $K$ in equation (6.4) is an empirical correlation factor developed from a multitude of vibration measurements of different ground engineering methods and can be found in Vrettos (2009).

$$E = \frac{W}{f} \qquad \text{in kNm} \tag{6.3}$$

with

$f$ vibrator frequency in Hz
$W$ nominal vibrator power in kW.

$$PPV = \frac{K\sqrt{E}}{r} \qquad \text{in mm/s} \tag{6.4}$$

with

$K$ factor evaluated by field vibration measurements
$r$ distance from vibrator in m.

From Figure 6.2, for a building at a distance of 6 m from the vibrator position of the S-vibrator, we get a ground peak particle velocity (*PPV*) of 13 mm/s and for the M-vibrator 6 mm/s, when assuming a 50% (exceeding) probability. The corresponding ground peak particle accelerations (*PPA*) follow from equation (6.2) with 2.5 m/s$^2$ for the 30 Hz S-vibrator and 1.9 m/s$^2$ for the M-vibrator, operating at 50 Hz, both values being well

below the 0.3 g to 0.5 g threshold. When considering, more appropriately, a probability of 2.25% (exceeding) only, *PPA* values rise to 6.6 m/s$^2$ for the S-vibrator and to 5.3 m/s$^2$ for the M-vibrator, which both are in excess of the above limit. Should the structure be founded on loose to medium dense, saturated sand, the resulting accelerations are marginally within acceptable limits for the M-vibrator at the 6 m distance but are not tolerable should the S-vibrator be used, since it could result in intolerable induced settlements of the structure. Based upon a tolerable ground *PPA* value of 0.5 g, the necessary distance from the building, not to cause vibration-induced settlements to it, should be about 8 m for this more powerful vibrator. When the influence of other types of depth vibrators are concerned, their vibratory energy $E$ can be calculated using the data from Table 3.1 allowing a sensible comparison with the results as given in Figure 6.2.

Achmus *et al*. have developed from these data a risk assessment method for potential building damage resulting from the impact of the vibratory deep compaction.

In a first step (Table 6.3), the peak particle velocity values (*PPV*) can be predicted for the average (50%) and the worst case (2.25%) using the

*Table 6.3* Risk assessment method for potential building damages due to vibratory deep compaction (Achmus *et al*., 2010)

| *Step* | *Description/equation* |
|---|---|
| **1** | *Prediction of foundation and ground vibration intensities:*<br>foundation, horizontal:<br>for $P = 50\%$: $PPV_{F,h} = 10.3(E^{1/2})/r$<br>for $P = 2.25\%$: $PPV_{F,h} = 23.1(E^{1/2})/r$<br>foundation, vertical:<br>for $P = 50\%$: $PPV_{F,z} = 7.3(E^{1/2})/r$<br>for $P = 2.25\%$: $PPV_{F,z} = 17.0(E^{1/2})/r$<br>foundation, resultant:<br>$PPV_{F,res} = (PPV_{F,z}^2 + 2PPV_{F,h}^2)^{1/2}$<br>ground, resultant:<br>for $P = 50\%$: $PPV_{G,res} = 37.2(E^{1/2})/r$<br>for $P = 2.25\%$: $PPV_{G,res} = 95.2(E^{1/2})/r$<br>$PPA_{G,res} = 2\pi f\, PPV_{G,res}$ |
| **2** | *Transfer coefficient* $TC = PPV/PPV_F$:<br>for horizontal vibrations of walls and floors:<br>$TC_h = 1.0$<br>for vertical vibrations of floors and slabs, if no resonance is to be expected:<br>$TC_z = 2$<br>$PPV_h = TC_h\, PPV_{F,h}$<br>$PPV_z = TC_z\, PPV_{F,z}$ |
| **3** | *Comparison with design values/assessment:*<br>$PPV_{F,res} \le DPPV_{F,res}$ for $P = 2.25\%$ and $P = 50\%$<br>$PPV_h \le DPPV_h$ for $P = 2.25\%$ and $P = 50\%$<br>$PPV_z \le DPPV_z$ for $P = 2.25\%$ and $P = 50\%$<br>$PPA_{G,res} \le DPPA_{G,res}$ for $P = 2.25\%$ and $P = 50\%$ |

appropriate vibrator energy $E$ and distance $r$. With the resultant ground $PPV_{G,res}$ the peak particle accelerations $PPA_{G,res}$ follow using equation (6.2). In a second step, the propagation of the vibrations within the building need to be estimated. Neglecting unlikely resonance effect, the maximum vertical *PPV* for floor slabs can be roughly estimated by applying a transfer coefficient *TC* of 2 to the vertical foundation *PPV*. The horizontal *PPV* at the top floor level can be assumed equal to the horizontal *PPV* at foundation level. The third step compares *PPV*s so established with design values from relevant regulation, such as given in Tables 6.1 and 6.2. Whenever worst case values are below design values, no building damage is likely to occur. However, if predicted values, particularly the average values, exceed the design values, caution is necessary. Direct vibration measurements should be carried out, which could necessitate increasing the distance from the closest vibro probe, or alternatively usage of a less powerful depth vibrator or a modification of the foundation method would have to be considered. Vibration measurement can, by all means, serve as preservation of evidence in order to prove the admissibility of vibrations.

When vibro compaction works are performed in granular soil behind retaining structures or inside cofferdams, to make use of the high friction angle attained from increased density, the design has to take into account different loading conditions. Initially, the wall has to support a high earth pressure that derives from a lower density but considerably higher earth pressure coefficient. Ultimately the wall is subjected to a reduced earth pressure resulting from the much reduced earth pressure coefficient and in spite of the higher density.

In the direct vicinity of the wall with a vibro probe, the soil liquefies during compaction and local stresses rise to hydrostatic pressures with densities of approximately 2.25 t/m$^3$ for saturated sand. Stress attenuation follows as pore water pressure declines (Dücker, 1957, 1968). These temporary local stress peaks have to be considered in the design, particularly where steel sheet piles are concerned.

We have seen that the vibro compaction process leads to a densification of granular soils, which is accompanied by a volume reduction manifesting itself in a ground surface lowering. Whenever adjacent structures are within reach of this deformation that develops during compaction, the structure may undergo intolerable settlements particularly when its foundations are situated close to ground surface resting on loose sandy soil. Although such foundation settlements generally do not occur, except within a distance from the depth vibrator equal to the probe depth, care should be exercised, particularly when very powerful machines are being used (cf. e.g. DIN 4150–3, Appendix C).

In general, deformation can be minimised by performing the compaction work in the direction towards the structure concerned, and by adopting an effective control of the material backfill during vibro probe execution or, more effectively, by keeping a safe distance from the nearest vibro probe

equal to its penetration depth. Whatever the protective measures, sensitive structures must be well monitored, with regard to induced vibration and settlement throughout the vibro compaction works carried out in their vicinity.

To avoid unwanted horizontal loads developing during dry stone column installation in cohesive soils as a result of soil displacement, pre-boring is recommended to partial or full depth at the column locations close to sensitive structures. It is also recommended to start with the nearest row of stone columns and to work away from the structure needing protection. Generally not more than three rows of stone columns should be carried out in this way until normal production can be resumed again at larger distances.

## 6.4 Carbon dioxide emission

The environmental advantages of the deep vibratory ground improvement methods are evident when looking at the nature and amount of the materials used in the processes and their neutral impact on the ground and the groundwater in which they are used. However, this view would be short-sighted if their carbon dioxide emissions were not addressed. Since researchers, most prominently Stern (2006), published reports on the impact of climate change on the world economy, strategies have been developed in some countries for the abatement of carbon dioxide emission, setting targets for 2050 by which global concentration of greenhouse gases could be stabilised at a level to avoid further dramatic global temperature rises.

Although buildings, including their construction and maintenance, account for almost half of a European country's total $CO_2$ emission (Egan and Slocombe, 2010) only a few countries have introduced regulatory rules that could help to reduce the environmental impact of the construction industry by controlling the energy demand, the generation of greenhouse gases and the production of waste on construction projects. Egan and Slocombe show in their investigation the environmental advantages of the deep vibratory methods over conventional piling methods by applying the principle of Reduce, Reuse and Recycle, not only qualitatively to a number of real construction projects but quantitatively by calculating the embodied $CO_2$ for different foundation solutions.

The comparison was made on a like-for-like basis for ground conditions that allowed both the execution of a standard piling solution and a vibro replacement stone column foundation with specifications for total settlements of 10 mm for piling and between 15 mm and 30 mm for the stone column alternative. The embodied $CO_2$ was calculated with values given in Table 6.4 which followed the principles of PAS2050 (Specification for the assessment of the lifecycle greenhouse gas emissions of goods and services) which is consistent with the approach described in EN ISO 14040.

*Table 6.4* Embodied $CO_2$ for construction materials and services (from Egan and Slocombe, 2010)

| *Materials and services* | *Embodied $CO_2$* | *Remarks* |
|---|---|---|
| Concrete (300 kg/m$^3$ cement) | 225 kg/m$^3$ | UK data average |
| Concrete (340 kg/m$^3$ cement) | 255 kg/m$^3$ | The Concrete Centre |
| Reinforcing steel | 420 kg/t | recycled steel |
| Stone aggregate (quarried) | 8.0 kg/t | |
| Stone aggregate (recycled) | 3.7 kg/t | |
| Stone aggregate (virgin) | 5.0 kg/t | |
| Diesel fuel | 2.6 kg/t | |
| 20 t truck | 4.4 kg/km | |

Egan and Slocombe conclude that ground improvement foundation alternatives (vibro replacement and dynamic compaction – and vibro compaction can be added, although not specifically mentioned) account for a $CO_2$ saving of about 90% compared with conventional piling. Typically the carbon footprint of a normal piling project is made up of 67% embodied $CO_2$ for the concrete, of 27% for the reinforcing steel and of 6% for the works execution and other supporting services. This picture changes completely for a typical vibro stone column site for which 68% of the embodied $CO_2$ is consumed by the stone backfill material and 32% by the works execution and transport, all this however on a much reduced overall total $CO_2$ emission.

Although valid European law and regulations already allow awarding public work based upon comprehensive standards of values, i.e. including the cost of $CO_2$ emissions, and although the Stern review proposes valuing $CO_2$ emission at 85 EUR/t, in reality public submissions in construction continue to be assessed solely on the basis of traditional economical advantages of cost and time. Within the time horizon of the Stern review to 2050 it is not yet too late to educate decision makers in construction of the advantages of $CO_2$ valuation in general and of the environmental benefits which can be gained when adopting the deep vibratory ground improvement methods in particular.

We have seen that vibro compaction in its ideal form does not require any raw material for its execution, and that vibro replacement uses only stone aggregate as backfill material, in this way significantly reducing greenhouse gas emission. Both ground improvement methods do not leave behind troublesome obstructions in the ground encouraging in this way the unhindered reuse of the building site after demolishing of the structures. We have also seen that recycled aggregate can be used as backfill material for the stone columns provided that their physical properties are assessed properly for the purpose.

# 7 Contractual matters

In the traditional way to execute a contract, the employer or owner engages a consulting engineer to do the design work, prepare the tender documents and generally also to supervise the works during construction. After selecting a contractor, he would normally work under a direct contract for the employer. In this role he is responsible for the execution of the works according to the contract conditions and specifications, and to instructions of the engineer who supervises the works.

In other contract forms, such as BOT (build, operate, transfer) contracts, the traditional role of the engineer has changed. The employer is often a group of private companies that are willing to finance a specific project on behalf of the government. Following a bidding procedure, it would order a contractor or joint venture of different contractors to realise the project, often on a turnkey basis, according to their own design which would normally be subcontracted to an engineer who might also supervise the construction works. It is quite obvious that there has been a change in the responsibilities of the engineer and particularly the key risk of the employer, i.e. the responsibility for unexpected, unknown and unforeseen ground conditions.

Traditionally the engineer, working directly for the employer, would provide the contractor also with the results of the geotechnical investigations and would base his design on his own interpretation of these findings, which will also direct any contractor's own design work. Accordingly, it is the risk of the employer and his engineer if a substantial change of the geological conditions requires changes in the design or the work procedure. In these circumstances, it is the contractor's responsibility to notify the engineer of these changed conditions and, ultimately, the employer would have to reimburse the contractor for any additional work resulting from these changes. This principle should also apply if a contract was executed on a lump sum basis with warranted dimensions and properties.

Where BOT contracts are concerned the employer's risk for the geotechnical conditions is passed on to the contracting consortium, which has to carry out all necessary investigations for the design and execution of the works and which employs therefore its own engineer.

In the majority of contracts any necessary ground improvement work will be carried out by specialist contractors working as subcontractors. With both types of contracts, the geotechnical investigation and its competent interpretation by the engineer (either working on behalf of the employer or for the turnkey contractor) is essential for a successful execution of the foundation works. Regardless of who ultimately will bear the risk for the subsoil conditions, it is in the best interest of geotechnical engineers to help to make specialist foundation works such as ground improvement by deep vibratory compaction a technically and scientifically accepted method.

Contract conditions will also contain a project description including a time schedule to allow the specialist contractor to define the amount of the required plant and equipment. A bill of quantities with payment and legal conditions are the key elements of the contract which is generally complemented by technical specifications. The rules of the contract have to reflect the employer's right to have all works done according to the current state-of-the-art.

The increasing importance of ground improvement in general, and the rising demand for the deep vibratory methods of vibro compaction and vibro replacement stone columns in particular, prompted engineering societies in many countries to work out standards, specifications and notes of guidance to support good practice in this specialised field in the construction industry (ICE, 1987, BRE, 2000 and CFMS, 2005 or codes such as DIN EN 14731). In the USA, preference is given to case-by-case specifications which often can better reflect the needs of the specific project. These and the guideline specifications generally reflect experts' knowledge in the technical field as well as in contractual affairs and serve for both design-and-build and for measured contracts.

The previous chapters have highlighted the importance of a comprehensive soil report which is prerequisite for the ground improvement design. It should contain all information on the soil which is generally necessary for bearing capacity and settlement calculations under the loading conditions of the project. When vibro compaction of loose granular soils is envisaged the soil investigation has to include, apart from general information on in-situ densities and water table, stratification, sieve analyses and mineralogical composition of the sand layers. We have seen that unsuitable cohesive soils are not just bypassed with the vibro stone column method. Their strength and deformation characteristics are essential information for the design. Equally important are the contractual regulations to cope with non-conformance situations when assessing the effectiveness of the ground improvement method. Whenever the deviations from the performance requirements are not caused by the quality of the works, specialist contractor and engineer together have to work out a solution to remedy this situation which will have to rely on an accurate description and of soil properties and their meaningful interpretation.

On vibro compaction contracts performance checks are normally by

comparison of pre- and post-compaction in-situ density measurements, such as CPT or SPT, with specified values. Depending on the size of the projects, in-situ testing should be carried out at a frequency of between 400 $m^2$ and 900 $m^2$ per test, with a time lapse for the post-treatment test of two weeks for silica and of at least three weeks for calcareous sand. Although the location of the post-compaction test is generally chosen as the "weakest" point of the vibro compaction probe grid, other criteria for the location of the verification testing, particularly for large grid spacing in calcareous soils, were found to be more appropriate. To cope with the relatively sharp density attenuation in these soils with increasing distance from the compaction centre the weighted average $q_{c(wa)}$ of two CPTs carried out at the "third point", being representative for 40% of the grid area, and at the "mid point", representing 60% of the area, of the distance between two compaction probes were found to be more appropriate (see equation (7.1) and Figure 7.1).

$$q_{c(wa)} = 0.4 \cdot q_{c(1/3)} + 0.6 \cdot q_{c(1/2)} \tag{7.1}$$

In addition to this approach, it is recommended to smooth the $q_c$ values by averaging the measurements over a depth increment of 0.3–0.5 m. The curve so developed can then be compared with performance criteria of the contract. A failed test would generally trigger verification procedures which ultimately could require remedial measures. Verification should be generally by two additional CPTs which, when one of these fails again, would require remedial action, which could be recompaction or, in the case of adverse soil conditions, a detailed geotechnical analysis necessitating other ground improvement measures (vibro stone columns, compaction grouting, etc.).

The technical specifications should also contain detailed requirements for the compaction probe records, information on adjacent structures needing protection (underground services, seawalls, quays and other buildings), details for the post-treatment surface grading and compaction, and a survey of the site levels before and after compaction, which is an excellent indicator of the effectiveness of the vibro compaction method.

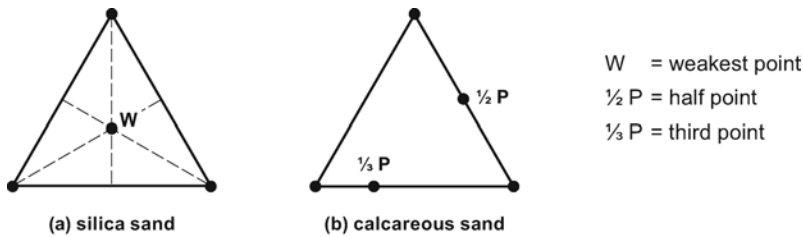


*Figure 7.1* Location of CPT in triangular grids (a) silica sand (b) calcareous sand

Where vibro replacement stone columns are concerned, the specifications should not give too much detail unless trial stone columns have been constructed beforehand, allowing the specialist contractor sufficient latitude in choosing the appropriate equipment and in the detailed construction procedure (Barksdale and Bachus, 1983). This philosophy is particularly valid when looking at the range of depth vibrators in use today. End result specifications therefore appear to be preferable restricting the key requirements to a certain design bearing pressure and providing limits for the total and differential settlement.

The construction process will, in the majority of projects, involve the dry bottom feed method since the use of jetting water necessary for wet stone columns requires special considerations in their construction (sludge handling and disposal of process water), and this is only rarely possible due to environmental restrictions. In the case of soft ground extending to ground surface, the owner and the engineer need to address the requirement of a granular working platform which is necessary for the safe operation of the heavy equipment and the efficient execution of the work.

An effective data acquisition system recording all relevant process parameters, in particular the actual amount of stone backfill used, is indispensable for all vibro stone column projects. A realistic measurement of the stone volume over depth, currently state-of-the-art with the bottom feed method, enables determination of the stone column diameter. Together with the friction angle of the stone column material, these are the key parameters determining their behaviour under load. Stone consumption is therefore an essential element of quality control procedure and a key assumption made in the design. Measurement and control of the stone quantity is particularly important in very soft soils in which an overtreatment is to be avoided which otherwise may lead to an unwanted reduction of local strength of the surrounding soil by remoulding. Similarly important are measures to avoid excessive heave, particularly in the final stage of column construction. Pre-boring, which can also become necessary to penetrate obstructive layers, is an effective measure in these instances.

Load testing will not be required when the performance of stone columns can be assessed with sufficient confidence from similar projects with comparable ground and loading conditions. In all other cases, and particularly for large contracts, load test on single columns, or on groups of columns – known as zone tests – is recommended and will help to verify bearing capacity and settlement performance requirements. Procedures for testing and instrumentation need to be specified together with the observation of the pore water pressure development in the ground to allow time to elapse before commencing the load test procedures.

Measurement of vibro compaction is generally by the volume in $m^3$ of sand to be compacted to a specified density. Pre- and post-testing at specified frequencies can also be included in this item. The compaction work includes rough site levelling. It may or may not include surface compaction of the

upper 0.5 m. The engineer may specify a depth vibrator with a certain power rating, although this selection sis better left to the specialist contractor and will be reflected in his proposal by the probe pattern, method statement and execution time necessary for the volume of works. For preliminary assessment of the time to compact sand from loose to medium density an average production rate of about 7500 $m^3$ for a 10-hour shift of a single depth vibrator is reasonable. Production and unit price depend, of course, on many parameters and conditions described in previous chapters.

For vibro stone columns the proposed unit for measurement is lin.m of stone column with specified diameter, length and quality of gravel backfill, which the contractor has to identify with appropriate data acquisition, calibrated before starting the work and at suitable intervals during the contract. The specifications will indicate which method of execution (wet, dry top or bottom feed system) should be used. It is advisable to specify a minimum power rating for the depth vibrator to be used to ensure proper densification of the stone backfill. The decision to pre-bore through hard layers should be left with the specialist contractor, provided their strength can be described sufficiently accurately. For normal conditions an average production rate of 300 lin.m of 0.5 m diameter dry bottom feed stone columns can be assumed for a 10-hour shift and one machine operating.

The main item for the execution of stone columns is occasionally split in an item for the column construction in lin.m and a second item for the delivery and placement of the stone backfill in $m^3$ or per ton. To underline the importance of the stone column diameter, the authors do recommend always specifying the stone columns together with a minimum diameter according to the design which has to be verified during execution of the works. Price of the backfill stone can be decisive for the cost of a vibro replacement project. It is therefore important to find suitable material at economic prices. The use of sand or recycled material is often a worthwhile compromise, even if the stone column design needs amending for reduced shear properties.

In all cases in which the works are being executed according to the specialist subcontractor's design, the employer or turnkey contractor will base his decision for the contract award on price, time of execution and a warranted design. Resolution of disputes on the extent of the treatment (probe spacing and depth, column diameter, depth and distance) will be on the basis of a comprehensive geotechnical report.

# Bibliography


Aboshi, H. *et al*. (1979) The compozer: a method to improve characteristics of soft clays by inclusion of large diameter sand columns. *Colloque International sur le Renforcement des Sols*. ENPC-LCPC. Paris.

Achmus, M. *et al*. (2007) Untersuchung zu Bauwerks – und Bodenerschütterungen infolge Tiefenrüttlung. TU Berlin. *3. Hans Lorenz Symposium*. Grundbauinstitut H. 41.

Achmus, M. *et al*. (2010) Building vibrations due to deep vibro processes. 7th Conference on Ground Improvement Techniques. Seoul, June 2010.

Adalier, K. *et al*. (2003) Stone columns as liquefaction counter measure in non-plastic silty soils. *Soil Dynamics and Earthquake Engineering*, Vol. 23, No. 7.

Ahrens, W. (1941) Die Bodenverdichtung bei der Gründung für die Kongresshalle in Nürnberg. *Die Bauindustrie*, Vol. 9, No. 35.

Arnold, M. *et al*. (2008) Comparison of vibrocompaction methods by numerical simulations. In Karstanen *et al*. (eds), *Geotechnics of Soft Soil: Focus on Ground Improvement*. Second International Workshop on Geotechnics of Soft Soils. University of Strathclyde, Glasgow.

Avalle, D. (2007) *Trials and Validation of Deep Compaction Using the "Square" Impact Roller.* Australian Geomechanics Society: Advances in Earthwork.

Baez, J.I. (1995) A design model for the reduction of soil liquefaction by vibro stone columns. PhD Thesis, University of Southern California, USA.

Baez, J.I. and Martin, G.R. (1993) Advances in the design of vibro systems for the improvement of liquefaction resistance. *Proc. Symposium on Ground Improvement*. Vancouver Geotechnical Society. Vancouver, Canada.

Baez, J.I. *et al*. (1998) Liquefaction mitigation of silty dam foundation using vibro stone columns and drainage wick drains: A test section case history at Salmon Lake Dam. *Proceedings of Dam Safety 1998*, Association of State Dam Safety Officials Annual Conference, Las Vegas, Nevada.

Baez, J.I. *et al*. (2000) Comparison of SPT-CPT liquefaction evaluations and CPT interpretations, innovations and applications in geotechnical site characterization. *Proceedings of Sessions of Geo-Denver 2000*. ASCE GSP 97.

Balaam, N.P. and Booker, J.R. (1981) Analysis of rigid rafts supported by granular piles. *Int. J. for Numerical and Analytical Methods in Geomechanics*, Vol. 5.

Balaam, N.P. and Booker, J.R. (1985) Effect of stone column yield on settlement of rigid foundations in stabilized clay. *Int. J. for Numerical and Analytical Methods in Geomechanics*, Vol. 9.

Balaam, N.P. and Poulos, H. G. (1983) The behaviour of foundations supported by clay stabilised by stone columns. *Proc. VIIIth ICSMFE*, Helsinki.

Balaam, N.P. *et al.* (1977) Settlement analysis of soft clays reinforced with granular piles. The University of Sidney, School of Engineering.

Barksdale, R.D. and Bachus, R.C. (1983) Design and construction of stone columns. Georgia Institute of Technology. US Department of Transportation. FHWA/RD-83/026.

Barksdale, R.D. and Bachus, R.C. (1984) Vertical and lateral behaviour of model stone columns. *Proc. Int. Conf. on In-situ Soil and Rock Reinforcement*. Paris: Presses de l'ecole nationale des ponts et chausses.

Barron, R.A. (1948) Consolidation of fine-grained soils by drain wells. *Trans. ASCE*, 2346.

Bauldry, B.D. *et al.* (2008) Monitoring for successful site improvement. *Geotechnical Earthquake Engineering and Soil Dynamics IV*. ASCE GSP 181.

Bell, A.L. (1915) The lateral pressure and resistance of clay and the supporting power of clay foundations. *Proc. of the Institution of Civil Engineers*, Vol. 199.

Bellotti, R. and Jamiolkowski, M. (1991) Evaluation of CPT and DMT in crushable and silty sands. Third interim report ENEL CRIS, Milano.

Bergado, D.T. *et al.* (1994) *Improvement Techniques of Soft Ground in Subsiding and Lowland Environment*. Balkema, Rotterdam.

Boley, C. (2007) Filter stability of stone columns. Universität der Bundeswehr München. Commissioned by Keller. Unpublished.

Borchert, K.-M. *et al.* (2005) Berechnung und Ausführung einer Rüttelstopfverdichtung in weichem Geschiebemergel. Beitrag zum *4. Geotechniktag München.* Schriftenreihe des Lehrstuhls für Bodenmechanik und Felsmechanik der TU München, 37.

Borchert, K.-M. *et al.* (2005) Betonsäulen als pfahlartige Tragglieder – Herstellungsverfahren, Qualitätssicherung, Tragverhalten und Anwendungsbeispiele. *Pfahl-Symposium 2005*. Mitteilungen des Instituts für Grundbau und Bodenmechanik der TU Braunschweig, 80.

Brauns, J. (1978) Die Anfangstraglast von Schottersäulen im bindigen Untergrund. *Die Bautechnik*, Vol. 8.

Brauns, J. (1980) Untergrundverbesserung mittels Sandpfählen oder Schottersäulen. *Tiefbau, Ingenieurbau, Straßenbau 8*.

BRE Building Research Establishment (2000) *Specifying Vibro Stone Columns*. CRC, London.

Breitsprecher, G. *et al.* (2009) Flughafen Berlin Brandenburg International-Dimensionierung und Ausführung einer Baugrundverbesserung für Bauwerke und Verkehrsflächen der landseitigen Anbindung. TU Berlin. 5. Hans Lorenz Symposium.

Bremer, K. and Hofmann, O.E. (1976) Tiefenverdichtung von gleichförmigen Sanden mit Tauchrüttlern. *Tiefbau, Ingenieurbau, Strassenbau*, Juli.

Breth, H. (1973) Die Verflüssigung wassergesättigter Sande die Möglichkeit, ihrer zu begegnen; ein Beitrag zur Reaktorsicherheit. Festschrift zum 60. Geburtstag von Professor Börnke, Essen.

Brown, R.E. (1977) Vibroflotation compaction of cohesionless soils. *Journal of Geotechnical Engineering*, ASCE 103, GT12.

BSI British Standards Institution (2008) *PAS2050: 2008-Specifications for the Assessment of the Lifecycle Greenhouse Gas Emissions of Goods and Services*.

Bureau of Reclamation (1948) Vibroflotation experiments at Enders Dam. Denver Colorado, July 20.

Casagrande, A. (1936) Characteristics of cohesionless soils affecting the stability of slopes and earthfills. *Journal of the Boston Society of Civil Engineers*, Vol. 23.

CFMS Comite Francais de Mecanique des Sols (2005) Recommandations sur la conception, le calcul, l'execution et le controle des colonnes ballastees sous batiments et ouvrages sensibles au tassement. *Revue Francaise de Geotechnique*, No. 111.

Charlie, W.A. *et al*. (1992) Time-dependent cone penetration resistance due to blasting. *Journal of Geotechnical Engineering*, ASCE, 118, No. 8.

Committe on Placement and Improvement of Soils (1978) *Soil Improvement: History, Capabilities and Outlook*. GED of the ASCE, New York.

Cudmani, R.O. (2001) Statische, alternierende und dynamische Penetration in nicht bindigen Böden. Dissertation, Karlsruhe University.

CUR (1996) *Building on Soft Soils*. Centre for Civil Engineering Research and Codes. Balkema, Rotterdam.

D'Appolonia, E. (1954) *Loose Sands: Their Compaction by Vibroflotation*. Special Technical Publication, ASTM No. 156.

Das, B.M. (1993) *Principles of Soil Dynamic*. PWS-Kent Publishing Company. Boston.

Debats, J.M. *et al*. (2003) Soft soil improvement due to vibro compacted columns installations. In Vermeer, Schweiger, Karstunen, Cudny (eds), *Int. Workshop on Geotechnics of Soft Soils: Theory and Practice*. Essen: VGE.

Degebo (1940) Versuchsbericht (unpublished).

Degebo (1942) Gutachten über die Tragfähigkeit des nach dem Kellerverfahren verfestigten Untergrundes in Rolingheten/Heroen (unpublished).

Degen, W. (1997a) 56 m Deep vibro-compaction at German lignite mining area. *Proc. 3rd Intl. Conf. on Ground Improvement Geosystems*. London.

Degen, W. (1997b) Vibroflotation Ground Improvement (unpublished).

Dücker, F.-J. (1957) Über Erddruckmessungen an einem Brückenwiderlager, *Die Bautechnik*, Vol. 11.

Dücker, F.-J. (1968) Bodenverdichtung und Gründungen unter Verwendung von Kellerschen Grossrüttlern. 5. int. Hafenkongress, Antwerpen.

Egan, D. and Slocombe, B. (2010) Demonstrating the environmental benefits of ground improvement. Ground improvement. *Proceedings of the Institution of Civil Engineers*, Vol. 163, No. 1.

Engelhardt, K. and Golding, H. C. (1973) Field testing to evaluate stone column performance in a seismic area. *Geotechnique*, Vol. 25, No. 1.

Fellin, W. (2000) Rütteldruckverdichtung als plastodynamisches Problem. *Advances in Geotechnical Engineering and Tunnelling*, Vol. 3, Feb.

Frankipile Australia (1974) Grainterminal Kwinana, Western Australia. Foundation Works. *Contracting and Construction Engineer*, November.

Gibson, R.E. and Anderson, W.F. (1961) In-situ measurement of soil properties with the pressuremeter. *Civil Engineering and Publics Work Review*, Vol. 56, No. 658.

Goughnour, R.R. (1983) Settlement of vertically loaded stone columns in soft ground. *Proc. 8th ECSMFE. Helsinki*, Vol. 1.

Goughnour, R.R. and Bayuk, A.A. (1979a) A field study of long-term settlements of loads supported by stone columns in soft ground. *Coll. Int. Renforcement des Sols*. Paris.

Goughnour, R.R. and Bayuk, A.A. (1979b) Analysis of stone column–soil matrix interaction under vertical load. *Coll. Int. sur le Renforcement des Sols*. Paris.

Greenwood, D.A. (1970) Mechanical improvement of soils below ground surface. Ground engineering. The Institution of Civil Engineers, London.

Greenwood, D.A. (1976) Discussion. Ground treatment by deep compaction. The Institution of Civil Engineers, London, 123.

Greenwood, D.A. (1991) Load tests on stone columns. In Esrig, Bacchus (eds), *Deep Foundation Improvements: Design, Construction and Testing*. ASTM STP 1089.

Greenwood, D.A. and Kirsch, K. (1984) *Specialist Ground Treatment by Vibratory and Dynamic Methods. Piling and Ground Treatment*. The Institution of Civil Engineers, Thomas Telford, London.

Gruber, F.J. (1994) Verhalten einer Rüttelstopfverdichtung unter einem Straßendamm. Dissertation, TU Graz.

Herle, I. *et al*. (2007) Einfluß von Druck und Lagerungsdichte auf den Reibungswinkel des Schotters in Rüttelstopfsäulen. *Pfahl Symposium 2007*. Institut für Grundbau und Bodenmechanik. TU Braunschweig, 84.

Hoffmann, R. and Muhs, H. (1944) Die mechanische Verdichtung sandigen und kiesigen Baugrundes. *Die Bautechnik*, Vol. 33/36.

Hu, W. (1995) Physical modelling of group behaviour of stone column foundations. Dissertation, University of Glasgow.

Hughes, J.M. and Withers, N.J. (1974) Reinforcing of soft cohesive soils with stone columns. *Ground Engineering*, Vol. 7, No. 3.

Hughes, J.M. *et al*. (1975) A field trial of the reinforcing effect of a stone column in soil. *Geotechnique*, Vol. 25, No. 1.

ICE Institution of Civil Engineers (1987) *Specification for Ground Treatment*, Thomas Telford, London.

Jebe, W. and Bartels, K. (1983) Entwicklung der Tiefenverdichtungsverfahren mit Tiefenrüttlern von 1976–1982. *VIIIth ECSMFE* Helsinki.

Johann Keller GmbH (1935) Der Rütteldruck. Die neue Technik des Erd- und Betonbaus. Company Publication.

Johann Keller GmbH (1936) Der Rütteldruck. Die neue Technik des Erd- und Betonbaus in Anwendung auf die Verdichtung des Baugrundes beim Kongressbau Nürnberg. Company Publication.

Johann Keller GmbH (1938) Bodenverfestigung nach dem Rütteldruckverfahren (DRP und Auslandspatente). Company Publication.

Johann Keller GmbH (1958) Verdichtungsversuche für den Bau des Hochdammes bei Assuan. Unpublished report for the Sadd el Aali Authority, Cairo.

Kirsch, K. (1979) Erfahrungen mit der Baugrundverbesserung durch Tiefenrüttler. *Geotechnik*, Vol. 1.

Kirsch, K. (1985) Application of deep vibratory compaction in harbour construction. Egyptian-German Seminar on Foundation Problems in Egypt and Northern Germany.

Kirsch, K. (1985) Over 50 years of deep vibratory compaction: milestones of German geotechnique. *Geotechnik, Special Issue*.

Kirsch, K. (1993) Die Baugrundverbesserung mit Tiefenruettlern. Englert, K. and Stocker, M. (eds) *40 Jahre Spezialtiefbau 1953–1993: Technische und rechtliche Entwicklungen*. Werner Verlag, Düsseldorf.

Kirsch, F. (2004) Experimentelle und numerische Untersuchungen zum Tragverhalten von Rüttelstopfsäulengruppen. Dissertation, Technische Universität Carolo-Wilhelmina zu Braunschweig.

Kirsch, F. (2006) Vibro stone column installation and its effect on ground improvement. In Triantafyllidis, Th. (ed.), *Numerical Modelling of Construction Processes in Geotechnical Engineering for Urban Environment*. Taylor & Francis, London.

Kirsch, F. (2008) Evaluation of ground improvement by groups of vibro stone columns using field measurements and numerical analysis. In Karstunen *et al*. (eds), *Geotechnics of Soft Soils-Focus on Ground Improvement*, Proceedings of the Second International Workshop on Geotechnics of Soft Soils, Glasgow, CRC Press/Balkema.

Kirsch, F. and Borchert, K.-M. (2006) Probebelastungen zum Nachweis der Baugrundverbesserungswirkung. 21. *Chr. Veder Kolloquium: Neue Entwicklungen der Bodenverbesserung*. TU Graz.

Kirsch, F. and Sondermann, W. (2001) Ground improvement and its numerical analysis. *Proc. XVth ICSMFE*, Istanbul 2001, Balkema.

Kirsch, F. and Sondermann, W. (2003) Field measurements and numerical analysis of the stress distribution below stone column supported embankments and their stability. In Vermeer *et al*. (eds), *Geotechnics of Soft Soils: Theory and Practice*. VGE, Essen.

Kirsch, F. *et al*. (2004) Berechnung von Baugrundverbesserungen nach dem Rüttelstopfverfahren. *Vorträge der Baugrundtagung 2004 in Leipzig*. Hrsg. DGGT. VGE.

Kolymbas, D. and Fellin, W. (2000) *Compaction of Soils, Granulates and Powders: Advances in Geotechnical Engineering and Tunnelling*. A.A. Balkema, Rotterdam.

Kutzner, C. (1996) *Grouting of Rock and Soil*. A.A. Balkema, Rotterdam.

Lackner, E. (1966) Schwierige Gründungen in Verbindung mit Bodenverbesserungen. *Der Bauingenieur*, Vol. 41, No. 9.

Lee, J.S. and Pande, G.N. (1998) Analysis of stone column reinforced foundations. *Int. J. Num. Anal. Meth. Geomech*, Vol. 22.

Lee, J.S. *et al*. (1999) Elasto-plastic analysis of composite material using a macro level yield function. In Pande, Pietruszcak, Schweiger (eds), *Numerical Models in Geomechanics – NUMOG VII*. Balkema, Rotterdam.

Liquefypro (2008) *Liquefaction and Settlement Analysis*. Software Manual.

Lopez, R.A. and Shao, L. (2008) Use of the static and seismic deformation criteria for vibro replacement stone columns: A case history. *ASCE GSP 172 Soil Improvement*.

Lunne, T. and Christophersen, H. P. (1983) Interpretation of cone penetrometer data for offshore sands. *Proceedings of the Offshore Technology Conference*, Richardson, Texas, Paper No. 4464.

Lunne, T. *et al*. (1997) *Cone Penetration Testing in Geotechnical Practice*. Blackie Academic & Professional, Glasgow.

Luongo, V. (1992) *Predicting Depth of Improvement in Grouting, Soil Improvement and Geosynthetics*, ASCE Geotechnical Special Publication No. 30.

Massarsch, K.R. (1991) *Deep Soil Compaction Using Vibratory Probes in Deep Foundation Improvement*, STP 1089, ASTM.

Massarsch, K.R. (1994) Design aspects of deep vibratory compaction, *Proceedings Seminar on Ground Improvement Methods*, Hong Kong Inst. Civ. Eng.

Maurer, C. (2008a) Influence of vibrations on adjacent buildings and soil as a result of deep vibro processes. Keller Holding GmbH, internal report.

Maurer, C. (2008b) Sound measurements during vibro replacement in Germany and England. Keller Holding GmbH, internal report.

Mitchell, J.K. (1984) Practical problems from surprising soil behaviour. 12th Terzaghi Lecture. *Journal of Geotechnical Engineering*, ASCE, Vol. 112, No. 3.

Mitchell, J.K. and Katti, R.K. (1981) Soil Improvement: State of the Art Report. *Xth ICSMFE*, Stockholm.

Mitchell, J.K. and Solymar, Z.V. (1984) Time-dependent strength gain in freshly deposited or densified sand. *Journal of Geotechnical Engineering*, ASCE, Vol. 110, No. 11.

Moseley, M.P. and Priebe, H. J. (1993) Vibro techniques. In Moseley (ed.) *Ground Improvement*. Blackie Academic & Professional, Glasgow.

Muir Wood, D. *et al*. (2000) Group effects in stone column foundations: model tests. *Geotechnique*, Vol. 50, No. 6.

Nahrgang, E. (1976) Untersuchung des Tragverhaltens von eingerüttelten Schottersäulen an Hand von Modellversuchen. *Baumaschine + Bautechnik*. Heft 8.

NCEER (1997) *Proceedings of the NCEER Workshop on Evaluation of Liquefaction Resistance*. Youd, T.L. and Idriss, I.M. (eds) Technical Report NCEER-97-0022.

Nendza, M. (2007) Untersuchungen zu den Mechanismen der Dynamischen Bodenverdichtung bei Anwendung des Rütteldruckverfahrens. Dissertation, Technische Universität Carolo – Wilhelmina zu Braunschweig.

O'Hara, V. (2003) Vibration and noise levels on ground improvement sites. Guidance Notes for Engineers. Keller Ground Engineering (unpublished).

O'Hara, V. and Davison, A. (2004) Noise propagation from driven piling. Noise control engineering. *Inter-Noise 2004*. Prague.

Parsons-Brinkerhoff *et al*. (1980) Jourdan Road Terminal Test Embankment, report prepared for Board of Commissioners of the Port of New Orleans.

Plannerer, A. (1965) Das Rütteldruckverfahren. Seine Weiterentwicklung und Anwendung für Gründungsaufgaben. Report of the Institute for Soil Mechanics and Foundation Engineering, Technical University Vienna.

Priebe, H. J. (1976) Abschätzung des Setzungsverhaltens eines durch Stopfverdichtung verbesserten Baugrundes. *Die Bautechnik*, Vol. 53, No. 8.

Priebe, H. J. (1987) Abschätzung des Scherwiderstandes eines durch Stopfverdichtung verbesserten Baugrundes. *Die Bautechnik*, Vol. 55, No. 8.

Priebe, H. J. (1988) Zur Abschätzung des Setzungsverhaltens eines durch Stopfverdichtung verbesserten Baugrundes. *Die Bautechnik*, Vol. 65, No. 1.

Priebe, H. J. (1995) Die Bemessung von Rüttelstopfverdichtungen. *Die Bautechnik*, Vol. 72, No. 3.

Priebe, H. J. (2003) Zur Bemessung von Rüttelstopfverdichtungen – Anwendung des Verfahrens bei extrem weichen Böden, bei schwimmenden Gründungen und beim Nachweis der Sicherheit gegen Gelände – oder Böschungsbruch. *Die Bautechnik*, Vol. 80.

Raithel, M. (1999) *Zum Trag- und Verformungsverhalten von geokunststoffummantelten Sandsäulen*, Schriftenreihe Geotechnik, Univ. Kassel, No. 6.

Raithel, M. and Kempfert, H.-G. (1999) Bemessung von geokunststoffummantelten Sandsäulen, *Die Bautechnik*, Vol. 76, No. 11.

Raju, V.R. *et al*. (2004) Vibro replacement for the construction of a 15 m high

highway embankment over a mining pond. *Malaysian Geotechnical Conference*. Kuala Lumpur.

Raju, V.R. and Hoffmann, G. (1996) Treatment of tin mine tailings in Kuala Lumpur using vibro replacement. *Proc. 13th Southeast Asian Geotechnical Conference*. Kuala Lumpur.

Raju, V.R. and Wegner, R. (1998) Ground improvement using vibro techniques: Case histories from South East Asia. *Ground Improvement Conference*, Singapore.

Rappert, C. (1952) Die Entwicklung von Großrüttlern und ihre Einsatzmöglichkeiten im Talsperrenbau. *Die Wasserwirtschaft*, Vol. 4.

Robertson, P.K. (1990) Soil classification using CPT. *Canadian Geotechnical Journal*, Vol. 27, No. 1.

Robertson, P.K. and Campanella, R.G. (1983) Interpretation of cone penetrometer tests. *Canadian Geotechnical Journal*, Vol. 20, No. 4.

Robertson, P.K. *et al*. (1983) SPT-CPT correlations. *Journal of Geotechnical Engineering*. Vol. 109, No. 11.

Rodger, A.A. (1979) Vibrocompaction of cohesionless soils. Cementation Research Limited, Internal Report, R.7/79.

Rodger, A.A. and Littlejohn, G.S. (1980) A study of vibratory driving in granular soils. *Géotechnique*, Vol. 30.

Saito, A. *et al*. (1987) A countermeasure for sand liquefaction, "gravel drains method". Nippon Kokan Technical Report Overseas No. 51.

Savidis, S. (2007) *Grundbau-Dynamik*. Technische Universität Berlin. FG Grundbau und Bodenmechanik-Degebo.

Scheidig, A. (1940) Speichergründung auf Rüttelfusspfählen. *Die Bautechnik*, Vol. 25.

Schmertmann, J.H. (1970) Static cone to compute static settlement over sand. *ASCE Journal of the SMFD*.

Schmertmann, J.H. (1978) Guidelines for cone penetration test, performance and design. US Federal Highway Administration, Washington, DC, Report FHWA-TS-78-209, 145.

Schmertmann, J.H. (1991) The mechanical aging of soils. *Journal of Geotechnical Engineering*, ASCE, Vol. 117, No. 12.

Schneider, H. (1938) Das Rütteldruckverfahren und seine Anwendung im Erd- und Betonbau. *Beton und Eisen*, 37. Jahrgang, Heft 1.

Schultze, E. and Moussa, A. (1961) Factors affecting the compressibility of sand. *Proceedings of the 5th ICSMFE*, Paris, Vol. 1.

Schweiger, H.F. (1989) Finite element analysis of stone column reinforced foundations. Dissertation, University of Swansea. Mitteilungen des Inst. für Bodenmechanik, Felsmechanik und Grundbau TU Graz. Heft 8.

Schweiger, H.F. (1990) Finite Element Berechnung von Rüttelstopfverdichtungen. *5. Chr. Veder Kolloquium*. TU Graz.

Seed, H.B. and Booker, J.R. (1976) Stabilization of potentially liquefiable sand deposits using gravel drain systems. Report No. EERC 76-10. University of California. Berkeley, California.

Seed, H.B. and Booker, J.R. (1977) Stabilization of potentially liquefiable ground deposits using gravel drains. *Journal of Geotechnical Engineering, Div.* ASCE, Vol. 103, GT 7, July.

Seed, H.B. and Idriss, I.M. (1971) Simplified procedure for evaluating soil liquefaction potential. *Journal of the SMFD*, ASCE, Vol. 97, No. SM9.

Seed, H.B. and Idriss, I.M. (1982) *Ground Motions and Soil Liquefaction during Earthquakes*. Earthquake Engineering Research Institute Monograph.

Seed, H.B. *et al*. (1985) The influence of SPT procedures in soil liquefaction resistance evaluations. *Journal of Geotechnical Engineering*, ASCE, Vol. 111, No. 12.

Sehn, L.S. (2003) Shear strength of vibro replacement stone and how it affects deformation. Hayward Baker Engineering Conference.

Shake (2000) A computer program for the 1-D analysis of geotechnical earthquake engineering problems.

Sidak, N. (2000) Soil improvement by vibro compaction in sandy gravel for ground water reduction. Compaction of soils, granulates and powders. In Kolymbas, D. and Fellin, W. (eds), *Advances in Geotechnical Engineering and Tunnelling*. A.A. Balkema, Rotterdam.

Silver, M.L. and Seed, H. B. (1971) Volume changes in sands during cyclic loading. *Journal Soil Mech. Found. Div.*, ASCE, Vol. 97, No. 9.

Slocombe, B.C. and Smith, P. (2008) The impact of vibro compaction adjacent to large vertical maritime retaining structures. *Proceeding of the 33rd Annual & 11th International Conference on Deep Foundations*. New York.

Smoltczyk, H.-U. (1966) Unterschätzen wir die Festigkeit des Sandes? *Wasser und Boden*. N.9.

Solymar, Z.V. *et al*. (1984) Earth foundation treatment at Jebba Dam site. *Journal of Geotechnical Engineering*, Vol. 110, No. 10.

Sondermann, W. and Kirsch, K. (2009) Baugrundverbesserung. *Grundbautaschenbuch, 7. Auflage. Teil 2: Geotechnische Verfahren*. Hrsg.: Witt, K. J., Ernst & und Sohn, Berlin.

Sondermann, W. and Wehr, W. (2004) Deep vibro techniques. In Moseley, M.P. and Kirsch, K. (eds), *Ground Improvement*, 2nd edition. Spon Press, London and New York.

Soyez, B. (1987) Bemessung von Stopfverdichtungen. *BMT*, April.

Stern, N. (2006) Review of the economic challenges of climate change. OCC Analytical Audit. Executive Summary. www.sternreview.org.uk.

Steuermann, S. (1939) A new soil compaction device. *ENR*, July 20.

Tanimoto, K. (1973) Introduction to the sand compaction pile method as applied to stabilisation of soft foundation grounds. Commonwealth Scientific and Industrial Research Organisation. Australia.

Terzaghi, K. and Peck, R.B. (1961) *Die Bodenmechanik in der Baupraxis*. Springer Verlag, Berlin.

Thorburn, S. (1975) Building structures supported by stabilized ground. *Geotechnique*, Vol. 25.

Thorburn, S. *et al*. (1968) Soil stabilization employing surface and depth vibrators. *The Structural Engineer*, Vol. 46, No. 10.

Tokimatsu, K. and Seed, H.B. (1987) Evaluation of settlements in sand due to earthquake shaking. *ASCE Journal of Geotechnical Engineering*, Vol. 113.

Topolnicki, M. (2004) In situ soil mixing. In Moseley, M.P. and Kirsch, K. (eds), *Ground Improvement*, Spon Press, London and New York.

University Karlsruhe (2006) CPT calibration testing on calcareous sands. Commissioned by Keller Grundbau. Unpublished.

van Impe, W.F. (2001) About the effectiveness of stone columns. *Proc. 15th. ICSMGE*. Istanbul. Vol. 4

van Impe, W.F. and Debeer, E. (1983) Improvement of settlement behaviour of soft layers by means of stone columns. *Proc. 8th ECSMFE*. Helsinki. Vol. 1.

van Impe, W.F. and Madhav, M.R. (1992) Analysis and settlement of dilating stone column reinforced soil. *Österreichische Ingenieur- und Architekten-Zeitschrift (ÖIAZ)*, Vol. 137, No. 3.

van Impe, W.F. *et al*. (1994) Recent experiences and developments of the resonant vibrocompaction technique. *XIII ICSMFE*, New Delhi.

Varaksin, S. (1990) Neuere Entwicklungen von Bodenverbesserungsverfahren und ihre Anwendung, *5.Chr. Veder Kolloquium*, TU Graz.

Vesic, A.S. (1965) Ultimate loads and settlements of deep foundations in sand. *Proceedings of the Symposium on bearing capacity and settlement of foundations in sand*. Duke University, Durham.

Vesic, A.S. (1972) Expansion of cavities in infinite soil mass. *JSMFD. ASCE*, Vol. 98.

Vrettos, C. (2009) Erschütterungsschutz. In Witt, K.J. (ed.) *Grundbau-Taschenbuch, Teil 3, 7. Aufl.*, Ernst & Sohn, Berlin.

Vrettos, C. and Savidis, S. (2004) Seismic design of the foundation of an immersed tube tunnel in liquefiable soil. *Rivista Italiana di Geotechnica*.

Watts, K.S. *et al*. (2000) An instrumented trial of vibro ground treatment supporting strip foundations in variable fill. *Geotechnique*, Vol. 50, No. 6.

Wehr, W. (1999) Schottersäulen – das Verhalten von einzelnen Säulen und Säulengruppen, *Geotechnik*, Vol. 22.

Wehr, W. (2005a) Influence of the carbonate content of sand on vibro compaction. *6th Int. Conf. on Ground Improvement Techniques*. Coimbra.

Wehr, W. (2005b) Variation der Frequenz von Tiefenrüttlern zur Optimierung der Rütteldruckverdichtung. 1. Hans Lorenz Symposium. Grundbauinstitut der TU Berlin. Heft 38.

Wehr, W. (2007) Rütteldruckverdichtung von karbonathaltigen Sanden. Geotechnik-Kolloquium Freiberg.

Wehr, W. *et al*. (2008) Stone columns in very soft clays in Sweden. 11th Baltic Sea *Geotechnical Conference "Geotechnics in Maritime Engineering"*. Gdansk.

West, J.M. (1976) *The Role of Ground Improvement in Foundation Engineering: Ground Treatment by Deep Compaction*. The Institution of Civil Engineers. London.

White, D. *et al*. (2002) Constitutive equations for aggregates used in Geopier foundation construction. Iowa State University, Department of Civil Construction Engineering.

Yoshimi, Y. (1980) Protection of structures from soil liquefaction hazards. *Geotechnical Engineering*, Vol. 11.

# Index